MECHANISMS OF MODULATION OF N-METHYL-D-ASPARTATE (NMDA) RECEPTORS BY MUTANT HUNTINGTIN

by

MANNIE MAN YEE FAN

B.Sc., McGill University, 1998
M.Sc., The University of British Columbia, 2001

A THESIS SUBMITTED IN PARTIAL FULFILLMENT OF
THE REQUIREMENTS FOR THE DEGREE OF

DOCTOR OF PHILOSOPHY

in

THE FACULTY OF GRADUATE STUDIES

(Neuroscience)

THE UNIVERSITY OF BRITISH COLUMBIA

April 2007

© Mannie Man Yee Fan, 2007

ABSTRACT

Evidence supports a role for neuronal damage arising from excessive activation of glutamate receptors (especially the NMDA subtype) in the pathogenesis of Huntington's disease (HD), although clinical trials involving NMDA receptor inhibition have mostly failed. Further understanding of the underlying molecular mechanisms is therefore needed to refine therapeutic approaches. My work has focused on the elucidation of molecular pathways linking huntingtin (htt) to NMDA receptors (NMDARs).

I found that NMDAR subunits NR1/NR2B are shifted from internal pools to the plasma membrane, with faster NMDAR insertion to the surface in striatal neurons from YAC72 HD mice. YAC72 striatum shows a relative enrichment of NR1 C2' isoforms in the vesicle/microsome-enriched fraction and preferential association of these isoforms with NR2B subunits, suggesting alternative splicing of NR1 may favour faster forward trafficking of receptors to potentiate NMDAR current and toxicity in this HD mouse model.

I demonstrated co-localization and interaction of the htt-interacting protein HIP-1 and actin-crosslinking α-actinin proteins, together in a complex with NMDARs in mouse striatal neurons and forebrain tissue. In fact, HIP-1 can directly interact with α-actinin, thus providing a physical link between htt and NMDARs.

To broaden the search for candidate proteins mediating the effects of mutant htt (mhtt) on NMDAR function, I collaborated with Kinexus Bioinformatics Corp. to examine expression patterns of a variety of protein kinases, phosphatases, and heat shock/stress proteins, in HEK cells over-expressing NR1/NR2B-type NMDARs and wild-type or mutant htt. Multiple proteins involved in the heat shock response pathway, including Hsp-70 and CK2, show altered subcellular distribution with co-expression of mhtt and NR1/NR2B, an

effect potentiated by NMDAR stimulation. CK2 expression is also elevated in striatal tissue from YAC HD mice, and its activity plays a protective role against NMDAR toxicity. Altered expression of stress response proteins in the presence of mhtt and NR1/NR2B may reflect an attempt to mitigate mhtt-induced sensitivity to excitotoxicity.

Findings from this thesis provide additional insight into the molecular mechanisms underlying increased NMDAR-mediated excitotoxicity in the YAC mouse model of HD. Target molecules and pathways identified in this work may contribute to the optimization of strategies for the treatment of HD.

TABLE OF CONTENTS

Abstract ii

Table of Contents iv

List of Tables x

List of Figures xi

List of Abbreviations xv

Acknowledgments xxiii

Dedication xxiv

CHAPTER 1. Introduction 1

1.1. Huntington's Disease 1

1.1.1. Clinical Presentation 1

1.1.2. Neuropathology 2

1.1.3. Molecular Pathology 3

1.1.3.1. Toxic Effects of Aggregated versus Soluble mHtt 4

1.1.3.2. Other Toxic Actions of mHtt 6

1.1.4. Normal Functions and Interactions of Htt 8

1.1.4.1. Role of Htt in Vesicular/Mitochondrial Transport and Energy Production 8

1.1.4.2. Binding Partners of Htt Provide Clues to Its Functions 9

1.1.4.3. Domain Structure of Htt Provides Clues to Its Functions 10

1.1.5. Gains and Losses of Htt Function in HD 11

1.1.6. Selective Neuronal Degeneration 14

1.1.7. Animal Models of HD 14

1.2. Excitotoxicity Hypothesis 16

1.2.1. What is Excitotoxicity? 16
1.2.2. Classes of Glutamate Receptors 17
1.2.3. Structure and Functional Characteristics of NMDARs 18
1.2.4. Trafficking of NMDARs 21
1.2.5. Striatal Expression of NMDARs in HD-Affected Individuals and Mouse Models 24
1.2.6. Chemical Models of HD 26
1.3. Aberrant NMDAR Activity in HD 29
1.3.1. Synaptic Abnormalities in HD Models 29
1.3.1.1. Alterations in NMDA-LTP and NMDA-LTD in HD Models 30
1.3.2. Enhanced Sensitivity to NMDA in HD Mouse Models 32
1.4. Signaling Downstream of Altered NMDAR Activity 34
1.4.1. Loss of Calcium Homeostasis 34
1.4.2. Mitochondrial Dysfunction in HD and Models of HD 36
1.4.3. Caspase Activation 40
1.4.4. Cellular Toxicity and Involvement of NR1/NR2B-Type NMDARs 41
1.5. Mechanisms Underlying mHtt-Induced Alterations in NMDAR Signaling 44
1.5.1. Interactions of NMDARs with the Actin CSK and PSD-Associated Proteins 44
1.5.2. Interaction of NMDARs and mHtt via PSD-95 45
1.5.3. Phosphorylation of NMDARs 47
1.5.4. Other Possible Mechanisms of Modulation of NMDAR Activity by mHtt ..50
1.6. Hypothesis and Rationale 51
CHAPTER 2. Materials and Methods 57
2.1. Transgenic Mice 57

2.1.1. Breeding and Maintenance of Mice 57
2.1.2. Primary Culture of Mouse Striatal MSNs 57
2.1.2.1. Transfection of Cultured Striatal MSNs with Plasmid DNA 58
2.1.2.2. Immunofluorescent Staining and Quantification 59
2.1.2.3. Chymotrypsin Assay 62
2.1.2.4. Biotinylation Assays 63
2.1.2.4.1. To Examine NR1/NR2B Surface Expression 63
2.1.2.4.2. To Examine Loss of NR1/NR2B from the Cell Surface 64
2.1.2.4.2.1. Blocking Degradation by Lysosomal Inhibition 65
2.1.2.4.3. To Examine NR1/NR2B Insertion Using Chlorpromazine to Block Endocytosis and Recycling 65
2.1.2.5. NMDAR-Dependent Toxicity Assay 66
2.1.2.5.1. Induction of Toxicity 66
2.1.2.5.2. Analysis of Apoptotic Death 67
2.1.3. Harvesting Tissue 68
2.1.3.1. Immunoblot Analysis 68
2.1.3.2. Examination of NR1/NR2B Expression in Mice of Different Ages 68
2.1.3.3. Examination of Protein Expression in Mouse Tissue to Follow Up on Kinetworks™ Results 69
2.1.3.4. Subcellular Fractionation 70
2.1.3.5. Immunoprecipitation 71
2.1.3.5.1. From Mouse Forebrain Tissue 71
2.1.3.5.2. From Mouse Striatal Tissue 72
2.2. HEK293 Cell Line 73
2.2.1. Passaging and Maintaining Cell Line 73

2.2.2. Transfection of Cell Line with Plasmid DNA 73
2.2.2.1. β-Galactosidase Staining to Determine Transfection Efficiency 74
2.2.3. Immunoprecipitation 75
2.2.4. NMDAR Stimulation of Transfected Cells 76
2.2.5. Harvesting Cells for Kinetworks™ or Immunoblotting Analysis 76
2.3. *E. Coli* Bacteria 78
2.3.1. Transformation with Plasmid DNA 78
2.3.2. Purification of Plasmid DNA 79
2.3.3. Purification of GST-Fusion Proteins from Bacteria 80
2.4. Plasmid DNA 81
2.5. Antibodies 82
2.6. Gel Overlay Assay 84
2.7. Materials 85
2.8. Data Analysis 85
CHAPTER 3. Altered NMDAR Trafficking in YAC72 Transgenic HD Mouse Model 90
3.1. No Change in NR1/NR2B Total Expression in Striatal Tissue from YAC46 or YAC72 Mice 90
3.2. Increased NMDAR Surface Expression in YAC72 MSNs 91
3.2.1. By Immunofluorescent Staining 91
3.2.2. By Chymotrypsin Assay 92
3.2.3. By Biotinylation Assay 93
3.3. Increased Rate of NMDAR Trafficking in YAC72 MSNs 94
3.3.1. Increased Rate of Receptor Loss from the Cell Surface 94
3.3.2. Increased Rate of Receptor Insertion to the Cell Surface 95
3.4. Altered Splicing of NR1 Isoform in YAC72 Striatal Tissue 97

3.5. Differential Interaction of NR1 C2' Splice Isoform with NR2 Subunits in YAC72 Striatal Tissue 99
3.6. Summary 100
CHAPTER 4. HIP-1 and α-Actinins Link Huntingtin with NMDARs 120
4.1. Role for HIP-1 in Receptor Trafficking 120
4.2. Role for Actin-Binding Proteins in Regulating NMDARs 121
4.3. Interaction of HIP-1 and α-Actinin with NMDARs 122
4.3.1. Co-Localization of HIP-1 with α-Actinin 4 in Mouse Striatal MSNs 122
4.3.2. HIP-1 and α-Actinin 4 Interact with NMDARs by Co-Immunoprecipitation 123
4.3.3. HIP-1, α-Actinin 4, and NMDARs Co-Fractionate 124
4.3.4. Direct Interaction between HIP-1 and α-Actinin 125
4.4. HIP-1 Over-Expression Increases NR1 Surface Expression in Striatal MSNs 126
4.5. Summary 127
CHAPTER 5. Kinetworks™ Profiling of Protein Expression Changes in Cells Expressing mHtt 137
5.1. Introduction to Kinetworks™ Screening Technique 137
5.2. Results from KPKS Protein Kinase Screens 139
5.3. Results from KPPS Protein Phosphatase Screens 140
5.4. Results from KHSP Heat Shock Protein Screens 141
5.5. NMDAR Expression- and Activity-Dependent Increase in Cytosolic Hsp70 142
5.6. Analyzing Total Expresson of Selected Protein Targets 144
5.7. Role of Increased CK2 Expression in Membrane Compartments 145

5.7.1. Increased CK2 Expression in Particulate Fraction from YAC Mouse Striatum 145
5.7.2 CK2 Activity Protects Against NMDAR-Mediated Apoptotic Death in mHtt-Expressing Cells 146
5.8. Summary 147
CHAPTER 6. Conclusions 166
6.1. Mechanisms of Modulation of NMDAR Activity/Trafficking by mHtt 166
6.1.1. Limitations of Methods Available for Measuring Forward Trafficking 168
6.1.2. Enhanced Trafficking of NMDARs Composed of NR1 C2' and NR2B 171
6.1.3. Implications for YAC128 HD Mice 172
6.2. Physical Link between NMDARs and Htt 176
6.2.1. Modulation of NMDARs by HIP-1 177
6.3. Effect of Htt PolyQ Expansion on Expression and/or Distribution of Signaling Proteins 179
6.3.1. Modulation of NMDAR Activity by CK2 in the Context of HD 181
6.4. Selective Vulnerability of Striatal MSNs in HD 183
6.5. Future Directions 185
Bibliography 190

LIST OF TABLES

Table 1. Summary of Referenced HD Mouse Models 53

Table 2. List of Protein Kinases Examined in Kinetworks™ KPKS Screen 148

Table 3. List of Protein Phosphatases Examined in Kinetworks™ KPPS Screen 149

Table 4. List of Stress/Heat Shock Proteins Examined in Kinetworks™ KHSP Screen 150

Table 5. Expression Levels of Selected Proteins from KPKS, KPPS, and KHSP Screens 151

Table 6. Summary of Changes in Expression Levels of Selected Proteins from KPKS, KPPS, and KHSP Screens 152

Table 7. Quantification of Results from Immunoblot Analysis of Selected Protein Targets as Shown in Figure 39B 153

LIST OF FIGURES

Figure 1. Cartoon of Possible Points Along the Corticostriatal Pathway Where Dysfunction May Contribute to Excitotoxicity 54

Figure 2. Cartoon of NR1 Membrane Topology and C-Terminal Splice Variants 55

Figure 3. Cartoon of Possible Mechanisms Underlying Potentiation of NMDAR Activity by mHtt 56

Figure 4. Schematic of Biotinylation Assay to Examine Loss of Receptors from the Cell Surface 87

Figure 5. Schematic of Biotinylation Assay to Examine Surface Protein Insertion 88

Figure 6. Schematic of Subcellular Fractionation Protocol 89

Figure 7. NR1/NR2B Total Expression is not Different in Striatal Tissue from 2 Month-Old FVB/N WT, YAC46, or YAC72 Mice 102

Figure 8. NR1/NR2B Total Expression is not Different in Striatal Tissue from FVB/N WT or YAC72 Mice at 2, 6, 9, or 12 Months of Age 103

Figure 9. Plots Comparing NR1 and NR2B Expression Levels in Striatal Tissue from WT and YAC72 Mice, Grouped by Age 104

Figure 10. Immunofluorescent Staining Demonstrates Increased Proportion of Surface NR1 in MSNs from YAC72 Mice 105

Figure 11. Representative Immunoblot of NR1/NR2B Levels in 9-10 d.i.v. MSNs from YAC72 versus WT Mice With or Without Chymotrypsin Treatment 106

Figure 12. Biotinylation Assay Demonstrates Increased Proportion of Surface NR1 in MSNs from YAC72 Mice 107

Figure 13. Biotinylation Assay Demonstrates Increased Proportion of Surface NR2B in MSNs from YAC72 Mice 108

Figure 14. Biotinylation Assay Demonstrates Unchanged Proportion of Surface GluR1 in MSNs from YAC72 Mice 109

Figure 15. Representative Immunoblots Illustrating Loss of Biotin-Tagged NR1 Over Time in MSNs from WT and YAC72 Mice 110

Figure 16. Enhanced Rate of Loss of Surface-Labeled NR1/NR2B in MSNs from YAC72 Mice 111

Figure 17. Plots Comparing Loss of Surface-Labeled GluR1 in MSNs from WT and YAC72 Mice 112

Figure 18. Representative Immunoblots Illustrating Insertion of NR1 to the Cell Surface Over Time in MSNs from WT and YAC72 Mice 113

Figure 19. Insertion of NR1/NR2B to the Cell Surface Proceeds More Rapidly in MSNs from YAC72 Mice 114

Figure 20. Plots Comparing Insertion of GluR1 in MSNs from WT and YAC72 Mice ..115

Figure 21. NR1 C2 and NR1 C2' Expression is Not Different in Striatal Tissue from 2 Month-Old FVB/N WT or YAC72 Mice 116

Figure 22. Increased YAC72/WT Ratio of NR1 C2'-to-C2 Expression in Microsome-Enriched Fraction 117

Figure 23. Representative Immunoblots Illustrating Co-Immunoprecipitation of NR1 or NR1 C2' with NR2 Subunits in Striatal Tissue from 2 Month-Old WT or YAC72 Mice 118

Figure 24. Plots Comparing Fraction of Immunoprecipitated NR1 C2' Normalized to NR1 in Anti-NR2 Precipitates from Striatal Tissue of 2 Month-Old WT or YAC72 Mice 119

Figure 25. Schematic of Selected Modular Domains in HIP-1 and α-Actinin Proteins 129

Figure 26. HIP-1 and α-Actinin 4 Co-Localize by Immunostaining in Mouse Striatal MSNs 130

Figure 27. HIP-1 and α-Actinin 4 Interact with NMDARs in Transfected HEK293 Cells by Co-Immunoprecipitation 131

Figure 28. HIP-1 and α-Actinin 4 Interact with NMDARs in Mouse Forebrain Tissue by Co-Immunoprecipitation 132

Figure 29. HIP-1, α-Actinin 4, and NMDARs Co-Fractionate in Mouse Striatal Tissue 133

Figure 30. HIP-1 Binds Directly to α-Actinin by Gel Overlay Assay 134

Figure 31. Cartoon of Hypothesized HIP-1/α-Actinin Interactions in Linking Htt to NMDARs 135

Figure 32. Immunofluorescent Staining Demonstrates Increased Proportion of Surface NR1 in MSNs Over-Expressing HIP-1 136

Figure 33. Sample Kinetworks™ KPKS Screen Results 154

Figure 34. Plots of Quantified Kinetworks™ KPKS Screen Results 155

Figure 35. Sample Kinetworks™ KPPS Screen Results 156

Figure 36. Plots of Quantified Kinetworks™ KPPS Screen Results 157

Figure 37. Sample Kinetworks™ KHSP Screen Results 158

Figure 38. Plots of Quantified Kinetworks™ KHSP Screen Results 159

Figure 39. Up-Regulation of Cytosolic Hsp70 Expression by mHtt Depends on Co-Expression of NMDARs and is Enhanced by NMDAR Activity 160

Figure 40. Immunoblots for Total Cellular Expression of Selected Proteins from Transfected HEK293 Cells With or Without NMDAR Stimulation 161

Figure 41. Quantification of Total Cellular Expression of Selected Proteins from Transfected HEK293 Cells With or Without NMDAR Stimulation 162

Figure 42. Particulate CK2 Expression is Up-Regulated in Striatal Tissue from Mice Expressing mHtt 163

Figure 43. NMDA-Induced Apoptosis in MSNs from FVB/N WT, YAC72, or YAC128 Mice in the Presence or Absence of CK2 Inhibition 164

Figure 44. Blockade of CK2 Activity in Mouse Striatal MSNs Exacerbates NMDAR-Mediated mHtt-Induced Apoptosis 165

Figure 45. Flowchart Illustrating Cellular Processes Affected by Expression of mHtt ...188

Figure 46. Cartoon of Possible Mechanisms Underlying Potentiation of NMDAR Activity by mHtt at Non-Synaptic Sites 189

LIST OF ABBREVIATIONS

3-NP, 3-nitropropionic acid

Ab, antibody

AMPA, α-amino-3-hydroxy-5-methyl-4-isoxazole-propionic acid

AMPAR, AMPA receptor

ANOVA, analysis of variance

AP-2, adaptor protein-2

ATP, adenosine 5'-triphosphate

BCA, bicinchoninic acid

BDNF, brain-derived neurotrophic factor

BES, N,N-Bis-(2-hydroxyethyl)-2-aminoethanesulfonic acid

Biot Eluate, biotinylation eluate

BSA, bovine serum albumin

BSS, balanced salt solution

BTK, Bruton agammaglobulinemia tyrosine kinase

Calnxn, calnexin

CaMK1, calmodulin-dependent kinase 1

CaMK4, calmodulin-dependent kinase 4

cAMP, cyclic adenosine 5'-monophosphate

CaP, calcium phosphate

CBP, CREB-binding protein

CDK2, cyclin-dependent kinase 2

CDK4, cyclin-dependent kinase 4

CDK5, cyclin-dependent kinase 5

cDNA, complementary DNA

CK1ε, casein kinase 1 epsilon

CK2, casein kinase 2

CMV, cytomegalovirus

CNS, central nervous system

Cox-2, cyclo-oxygenase 2

CRE, cAMP response element

CREB, CRE-binding protein

CSF, cerebrospinal fluid

CSK, cytoskeleton

cyto, cytosolic

DED, death effector domain

DF, detergent-free buffer

d.i.v., days *in vitro*

DMSO, dimethyl sulfoxide

DNA, deoxyribonucleic acid

DNAse, deoxyribonuclease

DRB, 5,6-dichlorobenzimidazole riboside

ECL, enhanced chemiluminescence

E. coli, *Escherichia coli*

eIF2α, eukaryotic translation initiation factor 2 alpha

EPSC, excitatory post-synaptic current

ER, endoplasmic reticulum

ERK1, extracellular-regulated kinase 1

ERK2, extracellular-regulated kinase 2

ERp57, 57 kDa ER protein

ERp72, 72 kDa ER protein

EtOH, ethanol

FBS, fetal bovine serum

FVB/N, friend leukemia virus strain B NIH

GABA, γ-aminobutyric acid

GAPDH, glyceraldehyde-3-phosphate dehydrogenase

GCK, germinal centre kinase

GEB, Glutathione Elution Buffer

GFP, green fluorescent protein

GPe, external globus pallidus

GPi, internal globus pallidus

GroEL, chaperonin heat shock 60 kDa protein 1

Grp94, 94 kDa glucose-regulated protein

GST, glutathione-S-transferase

GTP, guanosine 5'-triphosphate

HAP-1, huntingtin-associated protein 1

HB, Harvest Buffer

HBSS, Hanks' balanced salt solution

HD, Huntington's disease

Hdh, Huntington's disease homologue

HEAT, Htt/Elongation factor 3/PP2A Regulatory A subunit/TOR1

HEK, human embryonic kidney

HIP-1, huntingtin-interacting protein 1

HIPPI, HIP-1 protein interactor

hnRNA, heteronuclear RNA

HO2, heme oxygenase 2

HPK1, hematopoietic progenitor kinase 1

HSF4, heat shock transcription factor 4

Hsp60, Heat shock 60 kDa protein 1

Hsp70, heat shock 70 kDa protein 1A

Hsp90, heat shock 90 kDa protein

Hsp105, heat shock 105 kDa protein

HspBP1, Hsp70-binding protein 1

htt, huntingtin

IB, immunoblot

iGluR, ionotropic glutamate receptor

IKKα, inhibitor NFκB kinase alpha

IMM, inner mitochondrial membrane

IP, immunoprecipitation; immunoprecipitate

IP3, inositol 1,4,5-trisphosphate

IP3R, IP3 receptor

IPTG, isopropyl thiogalactoside

JAK2, Janus kinase 2

JNK, Jun N-terminal kinase

KHSP, Kinetworks™ heat shock protein screen

KI, knock-in

KO, knock-out

KPKS, Kinetworks™ protein kinase screen

KPPS, Kinetworks™ protein phosphatase screen

LB, Luria broth

Lck, lymphocyte-specific protein tyrosine kinase

leup, leupeptin

LTD, long-term depression

LTP, long-term potentiation

Lys, lysate

MAGUK, membrane-associated guanylate kinase

MEM, minimum essential medium

MEM+, MEM supplemented with 10% FBS, 2 mM glutamine, 1 mM sodium pyruvate, and 100 units/ml penicillin-streptomycin

mGluR, metabotropic glutamate receptor

mhtt, mutant htt

MKK7, MAP kinase kinase 7

Mnk2, MAP kinase-interacting kinase 2

mPT, mitochondrial permeability transition

mRNA, messenger RNA

MSN, medium-sized spiny neuron

MW, molecular weight

myr-Dyn, myristoylated dynamin-derived peptide

Nek2, NIMA-related kinase 2

NES, nuclear export signal

NBM, neurobasal medium

NGS, normal goat serum

NII, neuronal intranuclear inclusion

NMDA, N-methyl-D-aspartate

NMDAR, NMDA receptor

NP-40, Nonidet P-40

N.R., not reported

NSE, neuron-specific enolase

NSF, N-ethylmaleimide-sensitive fusion protein

OD, optical density

PACSIN, PKC and Casein Kinase Substrate in Neurons

PAK1, p21-activated kinase 1

PAK3, p21-activated kinase 3

partic, particulate

PBS, phosphate-buffered saline

PDK1, 3-phosphoinositide-dependent protein kinase 1

PDL, poly-D-lysine

PDZ, PSD-95/Discs large/Zona occludens-1

PFA, paraformaldehyde

PI, propidium iodide

PI3K, phosphoinositide 3-kinase

PKA, protein kinase A

PKB, protein kinase B

PKC, protein kinase C

PKCα, protein kinase C alpha

PKCε, protein kinase C epsilon

PKCγ, protein kinase C gamma

PKCλ, protein kinase C lambda

PKCθ, protein kinase C theta

PKCζ, protein kinase C zeta

PKR, dsRNA-dependent kinase

PMSF, phenylmethylsulfonylfluoride

PolyP, polyproline

PolyQ, polyglutamine

PP2A/Aα/β, protein phosphatase 2A – A regulatory subunits (alpha/beta isoforms)

PP5, protein phosphatase 5

PPV/C, protein phosphatase 6 catalytic subunit

PSB, protein sample buffer

PSD, post-synaptic density

PSD-95, post-synaptic density protein 95 kDa

PTP-1B, protein tyrosine phosphatase 1B

PVDF, polyvinylidene difluoride

PYK2, protein tyrosine kinase 2

QA, quinolinic acid

RIPA, radioimmunoprecipitation

RNA, ribonucleic acid

ROS, reactive oxygen species

RSK1, ribosomal S6 kinase 1

RSK2, ribosomal S6 kinase 2

SAP-97, synapse-associated protein 97 kDa

SAP-102, synapse-associated protein 102 kDa

SAPKb, stress-activated protein kinase beta

SB, Solubilization Buffer

SDS, sodium dodecyl sulfate

SDS-PAGE, sodium dodecyl sulfate-polyacrylamide gel electrophoresis

SEM, standard error of the mean

SFK, Src family kinase

SH3, Src homology region 3

SH3GL3, SH3-domain-containing Grb-2-like protein-3

SNARE, soluble NSF (N-ethylmaleimide-sensitive fusion protein) attachment protein receptor

SNc, substantia nigra pars compacta

SPN, supernatant

STN, subthalamic nucleus

Syp, synaptophysin

TBS, Tris-buffered saline

TBS-T, TBS 0.5% Tween-20

TE, Tris-EDTA

tg, transgenic

TrkB, tyrosine receptor kinase B

TUNEL, terminal deoxynucleotidyl transferase (TdT)-mediated dUTP nick end labeling

TWB, Tris wash buffer

TX, DF buffer containing 1% Triton X-100

UPS, ubiquitin/proteasome system

UT, untransfected

WT, wild-type

YAC, yeast artificial chromosome

ACKNOWLEDGMENTS

Many thanks go first and foremost to my research supervisor, Dr. Lynn Raymond, for her tireless support during the past several years. Amazingly generous with her time, Lynn is always there for her students. Not only does she provide exceptional experimental and conceptual guidance for my research, but she is very much a good friend and mentor as well. Working with Lynn has been a thoroughly enjoyable and intellectually stimulating experience; I thank her for giving me the opportunity to pursue my Ph.D. studies in her lab.

I would also like to thank all the members of the Raymond lab, past and present, for being good friends and colleagues: Herman, Jackie, Melinda, Carolyn, Lavan, Austen, and Cristina... Special thanks go to Esther and Lily for putting up with my endless requests for 60mm dishes, Jing and Cath for listening to me complain about blots that don't work, and Tulin and Christine for sharing amusing tales of choral practise. Tao, life in the Raymond lab would've been very different for me if you hadn't been there; and Bo, thank you for being my good friend and role model.

Thanks also to Helen, Andy, Ping, Kun, and Rujun, for making Kinsmen an even more interesting place!

Last but not least, I would like to extend thanks to my supervisory committee members Drs. Alaa El-Din El-Husseini, Steven Pelech, and Yu-Tian Wang for always providing thoughtful suggestions at my committee meetings. Thank you Steve for sharing your immense knowledge during our collaborative efforts, and Yu-Tian for critical reading of this thesis on such short notice! Collectively, your guidance has been indispensable and your advice most invaluable. A big "thank you" to you all!

DEDICATION

I would like to dedicate this work to my mom and dad, my sisters, and Allan Chak Man Kwan. Dad, I know you would've been proud of the first Ph.D. in the family. Mom, thank you for putting up with my always-changing experiment schedule. Lilian and Tania, thanks for getting out of bed for those insanely early morning carpools! Allan, thank you so much for being my "pillar of support" in every sense of the term for the past three years, especially during the last several months as I inevitably became a fixture in the lab or in front of the computer screen in order to finish writing what you are now reading...

CHAPTER 1. INTRODUCTION

Given a relative paucity of knowledge concerning the molecular pathways leading to cell death by over-excitation of glutamate receptors in Huntington's disease (HD) and in models mimicking the disease, my goal was to investigate the underlying mechanisms using a variety of biochemical and molecular biological techniques. Immunostaining and receptor-tagging assays were performed to assess receptor surface expression and the kinetics of receptor trafficking, while co-localization of receptors and other proteins of interest were demonstrated using immunoprecipitation, subcellular fractionation, and gel overlay assays. Moreover, a high-throughput screen is described in this thesis where candidate target proteins with altered expression and/or distribution were initially surveyed in a cell line model of the disease. The specific aims of this thesis are discussed in further detail in section 1.6 of this Introduction under "Hypothesis and Rationale", and I begin this Introduction with a description of HD in the following sections.

1.1. Huntington's Disease

1.1.1. Clinical Presentation

Huntington's disease (HD) is one of eight neurodegenerative diseases identified as resulting from expansion of the CAG repeat in the coding region of their respective genes leading to polyglutamine (polyQ) expansion in the protein products (reviewed in Zoghbi and Orr, 2000). As with all diseases in this group, HD is progressive, with symptom onset typically in mid-life but varying inversely with length of the polyQ repeat

such that the larger the number of repeats, the earlier the onset of symptoms (Brinkman et al., 1997; Gusella and MacDonald, 2000). These symptoms worsen over time, and death of the individual invariably follows, generally some 10-20 years after disease presentation.

HD is dominantly heritable, and patients present with deficits in motor function and memory as well as an affective disturbance (Hayden et al., 1981; Harper, 1991; Paulsen et al., 2001). Even though subtle changes in personality, mood, and cognition generally precede dementia and motor symptoms, development of choreic, dance-like movements is by far the most common and tell-tale symptom in individuals carrying the HD gene at the time of clinical presentation. At later stages of the disease, chorea is replaced by parkinsonism and akinesia. In the case of patients carrying HD allele(s) with extreme expansions of the CAG repeat (>70), they develop the juvenile version of the disease presenting with a more aggressive phenotype and a different symptomatic profile including bradykinesia, rigidity, epilepsy, and severe dementia (Bittenbender and Quadfasel, 1962; Van Dijk et al., 1986).

1.1.2. Neuropathology

The neuropsychiatric manifestations of HD result from the dysfunction and/or demise of specific neuronal populations and regions of the brain, with the GABAergic projection medium-sized spiny neurons (MSNs) of the neostriatum being most severely affected leading to striatal atrophy and/or neuronal loss (Vonsattel et al., 1985; Vonsattel and DiFiglia, 1998). MSNs receive glutamatergic input from the cortex and parts of the thalamus, as well as dopaminergic transmission from the substantia nigra pars compacta (SNc). One population of GABA-containing MSNs, those that are enriched in dopamine

D2 receptor and enkephalin expression, project to the internal globus pallidus (GPi) via an indirect pathway involving the external globus pallidus (GPe) and the subthalamic nucleus (STN). The other population of MSNs, which express the dopamine D1 receptor, dynorphin, and substance P, project directly to the GPi. In HD, those MSNs of the indirect pathway are lost before those projecting in the direct pathway (Reiner et al., 1988; Albin et al., 1992; Richfield et al., 1995; Sapp et al., 1995), thus leading to a net reduction of GPi inhibitory output to the thalamus, causing enhanced initiation of cortical motor programs that manifest as choreic movements. Because both pathways are later impaired, neostriatal output to the GPi is lost; as a result, inhibitory drive from the GPi to the thalamus is increased and the hyperkinetic phenotype gives way to rigidity and bradykinesia. As disease progresses, other parts of the brain including parts of the cortex, globus pallidus, and the hippocampus, may become affected as well.

1.1.3. Molecular Pathology

Much research in recent years has been directed towards elucidation of the pathogenic mechanisms underlying development and progression of HD. With the identification of the *HD* gene and its protein product huntingtin (htt) in the early 1990's (Huntington's Disease Collaborative Research Group, 1993), the genetic mutation leading to the development of HD has been determined as the expansion of a polymorphic CAG repeat (>35) in the *HD* gene. Much attention has since focused on the cellular functions of htt in both its normal and mutant forms.

1.1.3.1. Toxic Effects of Aggregated versus Soluble mHtt

Htt is predominantly a cytoplasmic protein (DiFiglia et al., 1995; Sharp et al., 1995; Trottier et al., 1995). It is a known substrate for a variety of proteases, and proteolytic cleavage of polyQ-expanded forms of htt is associated with loss of the C-terminal nuclear export signal (NES) (Xia et al., 2003). Coupled with an inhibition of its own nuclear export by polyQ expansion within the mutant htt (mhtt) protein (Cornett et al., 2005), retention of the N-terminal cleavage products in the nucleus is favoured (Davies et al., 1997; DiFiglia et al., 1997; Becher et al., 1998; Wheeler et al., 2000).

In tissue from HD brains, N-terminal fragments of mhtt were found aggregated in neuronal intranuclear inclusions (NIIs) and dystrophic neurites of the cortex or striatum, while such fragments were absent from nuclear extracts in brain tissue from normal individuals (DiFiglia et al., 1997; Sieradzan et al., 1999). Formation of NIIs was proportional to the length of the htt polyQ repeat (DiFiglia et al., 1997; Becher et al., 1998) and generally coincided with the onset of symptoms in mouse models of HD, suggesting cleavage products of mhtt that undergo translocation to the nucleus may be the species responsible for exerting the toxic effects of mhtt expression (DiFiglia et al., 1997; Becher et al., 1998; Sapp et al., 1999). Indeed, targeting of N-terminally truncated mhtt to the nucleus in a neuronal cell line was found to increase the extent of cell loss as well as the number of cells with nuclear aggregates, while cytoplasmic targeting of these mhtt fragments had the opposite effect (Saudou et al., 1998; Peters et al., 1999).

There is evidence that the cytoplasmic population of aggregated N-terminally truncated mhtt also contributes to toxicity (Cooper et al., 1998; Hackam et al., 1999a, 1999b). Additionally, soluble and protofibril forms of mhtt (as monomers or small oligomers) have been shown to play a role in causing cellular toxicity. Neurons that later

degenerated first exhibited diffuse nuclear immunostaining for htt, at a time when symptoms began to develop and well before formation of NIIs (Hodgson et al., 1999; Wheeler et al., 2000; Slow et al., 2003; Van Raamsdonk et al., 2005). These non-aggregated forms of mhtt are believed to mediate toxicity in part by sequestering essential proteins such as nuclear transcription factors and components of the ubiquitin/proteasome system (UPS) away from their normal functions (Schaffar et al., 2004).

Intriguingly, a number of molecular chaperones have been shown to successfully protect against N-terminal mhtt fragment-induced toxicity without reducing mhtt aggregation, suggesting the two phenomena (toxicity and aggregation) can be dissociated (Zhou et al., 2001). In fact, the presence of aggregates does not always predict cell death, nor does cell death necessarily occur in those neurons that contain visible aggregates (Kuemmerle et al., 1999; reviewed in Sisodia, 1998). As further evidence against the two phenomena being necessarily related by cause and effect, NIIs were found generally not to be abundant in the most vulnerable population of neurons (projection MSNs) within the striatum (Kuemmerle et al., 1999). The relative paucity of nuclear or neuropil aggregates in the striatum, relative to other parts of the brain, also argues against a direct role for aggregate formation in pathogenesis (DiFiglia et al., 1997; Gutekunst et al., 1999; Sieradzan et al., 1999).

Evidence indicating a protective role for aggregate formation came from studies showing exacerbation of neuronal death by manipulations or genetic mutations that inhibited aggregate formation, through either a decrease in ubiquitination or an increase in SUMOylation of mhtt (Saudou et al., 1998; Steffan et al., 2004). Also, neurons containing NIIs were found to have lower levels of cell death in comparison to those neurons that lacked NIIs (Arrasate et al., 2004). In mouse models of HD where truncated

N-terminal fragments of mhtt were expressed, NIIs were always formed while development of HD-like symptoms and neuropathology was variable depending on the exact fragment that was expressed (Slow et al., 2005), suggesting that not all NIIs or N-terminal fragments of mhtt are necessarily equally toxic. Hence it remains an issue of debate as to whether formation of aggregates in the human brain contributes to pathology, plays a protective role against mhtt-mediated toxicity, or is merely coincidental with neurodegeneration.

1.1.3.2. Other Toxic Actions of mHtt

Among the toxic effects of mhtt expression are roles for the protein in exacerbating oxidative stress, metabolic failure and mitochondrial dysfunction, which will be discussed in a later section. Fragments of polyQ-expanded htt also interact with lipid membranes thereby disrupting phospholipid bilayer structure (Suopanki et al., 2006). Moreover, mhtt perturbs ubiquitin/proteasomal function and leads to aberrant axonal transport and endocytosis, as well as participates in abnormal interactions with other proteins, some of which lead to dysregulation of the transcriptional machinery and hence altered gene expression (reviewed in Cha, 2000; Tobin and Signer, 2000; Davies and Ramsden, 2001; Menalled and Chesselet, 2002; Ross, 2002; Rubinsztein, 2002; Harjes and Wanker, 2003; Sugars and Rubinsztein, 2003; Li and Li, 2004).

There is evidence to indicate increased association of mhtt-containing aggregates with components of the UPS. However, longer polyQ tracts appear to be associated with a slower rate of proteolysis of the mutant protein (Dyer and McMurray, 2001; Jana et al., 2001), suggesting an impairment of the UPS function likely via sequestration into aggregates. Because the function of a number of transcription factors depends on

proteosomal processing (reviewed in Ciechanover, 1994; Pahl and Baeuerle, 1996), mhtt may impair the function of these factors in part by sequestration of UPS components. Other transcription factors contain regulatory glutamine-rich regions (Courey et al., 1989; Gerber et al., 1994), and because polyQ tracts can interact not only with DNA but also with one another via transglutamination (Green, 1993) and/or polar-zipper formation (Perutz et al., 1994; Perutz, 1996), these glutamine-rich regions can aberrantly interact with the mhtt polyQ stretch thereby trapping these transcriptional factors within htt-containing aggregates and preventing them from carrying out their normal function (Huang et al., 1998). Alternatively, by binding DNA or transcriptional factors such as p53 and cAMP response element (CRE)-binding protein (CREB)-binding protein (CBP), the expanded polyQ tract of mhtt may directly repress transcription by forming inactive transcriptional complexes (Boutell et al., 1999; McCampbell et al., 2000; Steffan et al., 2000; reviewed in Cha, 2000).

Altered transcription resulting from expression of N-terminal fragments of mhtt has been reported in both cell line and mouse models, including down-regulation of mRNAs for various neurotransmitter receptors (Cha et al., 1998, 1999; Li et al., 1999). DNA microarray studies in striatal tissue from R6/2 mice revealed additional classes of genes that were down-regulated, such as those involved in regulation of Ca^{2+} homeostasis and intracellular signaling (Luthi-Carter et al., 2000).

Interestingly, induction and maintenance of the progressive HD phenotype is entirely dependent on continued expression of the mutant protein product, as studies from a conditional transgenic mouse model indicated that shutting off transgene expression at a time well after symptom onset was able to reverse the symptoms and neuropathological changes associated with HD (Yamamoto et al., 2000).

1.1.4. Normal Functions and Interactions of Htt

1.1.4.1. Role of Htt in Vesicular/Mitochondrial Transport and Energy Production

While numerous neurotoxic processes have been related to htt polyQ expansion, the physiological functions of the protein in its normal form are far from clearly defined. Htt expression is widespread throughout the brain, with no particular enrichment in the striatum (DiFiglia et al., 1995; Trottier et al., 1995). The 350 kDa protein is primarily cytoplasmic but may also be found associated with clathrin-coated vesicles, microtubules, and the endoplasmic reticulum (ER)/Golgi membranes, indicative of possible roles in trafficking and fast axonal transport of membranous organelles and/or proteins to regulate such neuronal processes as neurotransmitter release (Sharp et al., 1995; Strehlow et al., 2006; reviewed in Truant et al., 2006).

Demonstration of a physical interaction between htt and the outer mitochondrial membrane (Gutekunst et al., 1998; Choo et al., 2004) provides support for a normal role of this protein in mitochondrial functions and may represent one route through which polyQ-expanded htt could act to impair metabolic energy production and/or Ca^{2+}-buffering ability in various models of HD. The neuronal capacity for generating energy in the form of ATP appeared to be inversely correlated with polyQ repeat length, for repeat lengths in both the normal (<35) and pathological (>35) ranges (Seong et al., 2005), consistent with a role for htt in regulating ATP generation in normal physiology and in HD. Further evidence implicating htt in the regulation of energy production came from examination of proteins that interact with htt, one of which was found to be the metabolic enzyme glyceraldehyde-3-phosphate dehydrogenase (GAPDH) (Burke et al., 1996).

Additionally, htt has been shown to be essential for fast axonal trafficking, based

on studies in both invertebrates (Gunawardena et al., 2003; Szebenyi et al., 2003) and mammals (Trushina et al., 2004). Reduced expression or polyQ-expansion of htt led to axonal transport defects (Gunawardena et al., 2003; Szebenyi et al., 2003), and mhtt-induced impairments in vesicular and mitochondrial trafficking were demonstrated in mammalian neurons both *in vitro* and *in vivo* (Trushina et al., 2004). Importantly, aggregate formation by mhtt blocked the trafficking of mitochondria along neuronal processes, causing these organelles to become immobilized and to accumulate at sites containing aggregates (Chang et al., 2006). Mitochondrial motility is also directly impaired by glutamate (Rintoul et al., 2003), and presumably mitochondria which are unable to traffick normally then become trapped and damaged with time, adding to the other toxic effects of glutamate receptor over-activation. All of these findings point to a likely involvement of aberrant mitochondrial movement in HD pathophysiology, where the *HD* mutation would couple with excitotoxic pathways to inhibit normal mitochondrial trafficking and function.

1.1.4.2. Binding Partners of Htt Provide Clues to Its Functions

Identification of other interactors of htt provides additional clues as to its normal functions under physiological conditions, and the diverse functions these proteins assume implicate htt in a number of cellular processes ranging from endocytosis to vesicular transport to non-receptor signaling to mRNA biogenesis (Goehler et al., 2004; reviewed in Harjes and Wanker, 2003; Li and Li, 2004; Giorgini and Muchowski, 2005). One of these binding partners, huntingtin-interacting protein 1 (HIP-1), is the human homologue of the yeast protein Sla2p which is involved in regulation of the cytoskeleton (CSK) (Kalchman et al., 1997; Wanker et al., 1997). As will be discussed in a later section

(see section 4.1), HIP-1 appears to be involved in clathrin-mediated endocytosis (Metzler et al., 2001) and has pro-apoptotic functions (Hackam et al., 2000; Gervais et al., 2002). Interestingly, HIP-1-mediated toxicity was abolished by concurrent expression of wild-type (WT) htt (Hackam et al., 2000), and striatal cells expressing WT htt were protected from apoptotic stimuli and N-methyl-D-aspartate (NMDA) receptor (NMDAR)-mediated excitotoxicity (Rigamonti et al., 2000; Ho et al., 2001; Leavitt et al., 2006), suggesting an anti-apoptotic role for the protein.

Htt also binds post-synaptic density (PSD) protein 95 kDa (PSD-95), and the implication of this interaction in the modulation of NMDAR function will be addressed in a subsequent section (see section 1.5.2), in the context of discussing the contribution of PSD-95 function to excitotoxic cell death in HD.

1.1.4.3. Domain Structure of Htt Provides Clues to Its Functions

As is true for many large proteins, htt consists of a number of repeated structures and modular domains, the analysis of which provides additional insight into the functions of the protein. The N-terminus of the htt protein is followed closely by the polyQ tract and then a polyproline (polyP) region. Proline-rich domains mediate binding to other proteins containing the Src homology region 3 (SH3) or tryptophan (WW) domain, and htt binds via its polyP region to the SH3-domain-containing Grb-2-like protein-3 (SH3GL3) (Sittler et al., 1998), thereby linking htt with Grb2/Sos and the downstream Ras-Raf-MEK-MAPK signaling cascade. As well, htt appears to be a key player in the phosphoinositide 3-kinase (PI3K)-protein kinase B (PKB/Akt) signaling pathway, as a direct substrate of the serine/threonine kinase Akt (Humbert et al., 2002). Endogenous levels of Akt-mediated phosphorylation on htt S421 appeared significantly reduced in the presence of an

expanded polyQ tract (Warby et al., 2005), and phosphorylation (or inhibition of dephosphorylation) of htt at S421 was found to protect the cell against mhtt-mediated toxicity (Humbert et al., 2002; Rangone et al., 2004; Pardo et al., 2006). Palmitoylation of htt on C214 was likewise significantly decreased by htt polyQ expansion, and the propensity of mhtt to form NIIs appeared to be inversely correlated with the extent of htt palmitoylation (Yanai et al., 2006). Together, these findings are suggestive of a role for post-translational modifications in the regulation of WT htt under normal circumstances, and of mhtt in HD.

Within the modular structure of htt, there are also ten ~40 amino acid-long Htt/Elongation factor 3/PP2A Regulatory A subunit/TOR1 (HEAT) repeats (Andrade and Bork, 1995), domains which are commonly found in transcription factors as well as proteins involved in chromosomal regulation, cytoplasmic and nuclear transport pathways (Cingolani et al., 1999; Neuwald and Hirano, 2000; reviewed in Andrade et al., 2001; Truant et al., 2007). The presence of these motifs implicates htt in the regulation of protein and/or nucleic acid transport to or from the nucleus. Interestingly, htt was shown to bind acidic phospholipids via these HEAT domains, providing further evidence in support of a physiological role for htt in the regulation of vesicular trafficking and/or structure of membranous organelles (Kegel et al., 2005).

1.1.5. Gains and Losses of Htt Function in HD

Thus far the data from human patients and findings based on studies in animal models of HD would suggest that polyQ expansion confers a deleterious gain in protein function, where mutation of the gene causes the resulting protein to assume an altered conformation and/or novel functions. PolyQ is in itself toxic, as ectopic expression of a

long polyQ tract in the context of an otherwise innocuous protein leads to a progressive neurological phenotype accompanied by neuropathological changes and neuronal death (Ordway et al., 1997). HD patients homozygous for the mutant allele exhibit similar disease phenotype and severity as those who are heterozygous for the allele (Wexler et al., 1987), and mouse embryos lacking both copies of the gene do not develop HD (Duyao et al., 1995; Nasir et al., 1995; Zeitlin et al., 1995). Instead, these mice die in gestation, in complete contrast with HD mice which develop normally suggesting that the developmental role played by normal htt is maintained in mutant forms of the protein containing expanded polyQ tracts.

So-called "gains" in both structure and function due to polyQ expansion lead not only to an acquired resistance against degradation of the mutant protein by normal proteolytic processing (reviewed in Cummings and Zoghbi, 2000; Sieradzan and Mann, 2001), but also novel or perturbed interactions with other intracellular molecules or organelles. In recent years, however, increasing evidence indicates that losses in certain aspects of normal htt function may be implicated in HD as well (reviewed in Cattaneo et al., 2001; Cattaneo, 2003).

Striatal MSNs rely on brain-derived neurotrophic factor (BDNF) from cortical afferents in order to survive, since they themselves do not express this growth factor. WT htt has been shown to promote BDNF expression via sequestration of a transcriptional repressor (Zuccato et al., 2001), while BDNF expression levels were found to be reduced in the striatum of HD patients (Ferrer et al., 2000), suggesting loss of htt-mediated transcription of BDNF likely contributes to striatal neuronal dysfunction in HD. The regulation of trophic support for striatal neurons by mhtt is not only limited to regulation at the transcriptional level, but also encompasses delivery of this trophic factor to the striatum; several recent studies revealed impairments in post-Golgi trafficking of BDNF in

striatal knock-in (KI) cells expressing full-length mhtt (Del Toro et al., 2006), as well as deficiencies in BDNF transport along cortical axons due to decreased binding of the htt-associated protein HAP-1 with microtubule molecular motors resulting from enhanced mhtt/HAP-1 interactions (Gauthier et al., 2004). Related to these findings, expression of the endogenous BDNF receptor, TrkB, was also shown to be down-regulated by mhtt both in mouse models of HD and in post-mortem brain tissue from human patients, independent of changes in BDNF levels (Gines et al., 2006). Together, these results indicate a role for htt in the regulation at many steps of a pathway that normally supplies striatal neurons with a source of trophic growth factors, suggesting HD pathology may result in part from loss of specific WT htt functions, in this case related to the provision of trophic support, due to polyQ expansion.

Adding to the pro-survival role of htt in mediating BDNF transcription and/or transport is its anti-apoptotic role as discussed in previous sections (see sections 1.1.4.2 and 1.1.4.3), where WT htt plays a protective role against toxic stimuli (Rigamonti et al., 2000; Cattaneo et al., 2001; Ho et al., 2001; Leavitt et al., 2006), sequesters toxic molecules such as HIP-1 (Hackam et al., 2000), and participates in the PI3K/Akt survival signaling pathway (Humbert et al., 2002). Given these important functions ascribed to normal WT htt, replacement of one WT *HD* allele with the mutant form may increase cell vulnerability in two ways – firstly by generating a molecule with toxic properties and secondly by a reduction of cellular protection otherwise afforded by the product from the WT allele. Not only is expression of WT htt reduced in this case, but because mhtt-containing aggregates are capable of recruiting polypeptides with shorter polyQ repeats (Chen et al., 2001), the little that is expressed for WT htt may well be depleted by sequestration into these pre-formed aggregates.

1.1.6. Selective Neuronal Degeneration

Both gain and loss of functions of the mutant and WT forms of the htt protein, respectively, have been identified as potential contributors to neuronal dysfunction or death in HD as outlined above. The reasons for selective neuronal degeneration remain elusive however. Expanded polyQ tracts are toxic to cells of both neuronal and non-neuronal origins, while the htt protein is widely expressed in both the central nervous system (CNS) and peripheral tissues (Aronin et al., 1995; Trottier et al., 1995) regardless of polyQ length. Not only is there no enrichment for mhtt expression in the striatum (Aronin et al., 1995; Sharp et al., 1995), but the projection MSNs in fact express lower levels of mhtt than do interneurons which are spared in HD (Fusco et al., 1999). Additionally, none of the proteins identified as interactors of htt is selectively expressed or altered in striatal MSNs expressing mhtt, therefore failing to provide an adequate explanation as to how mhtt selectively targets striatal MSNs for cellular demise (Graveland et al., 1985; Ferrante et al., 1985, 1987). In the rest of this Introduction, then, we review evidence accumulated over the past two decades in support of a role for altered NMDAR signaling in mediating the region-selective pathogenic effects of mhtt in the course of HD pathogenesis.

1.1.7. Animal Models of HD

Identification of mechanisms promoting neuronal dysfunction and degeneration in HD has been greatly aided by the development of numerous mouse models of the disease. Some features of these models that are relevant to the current study are summarized in Table 1. Mouse models expressing short, truncated forms of human mhtt,

such as the R6/1, R6/2, and N171 mice, present with an early phenotype with motor symptoms characteristic of HD and progress to death by 4 to 5 months of age (Mangiarini et al., 1996; Schilling et al., 1999). Distribution of neuronal aggregates containing truncated N-terminal mhtt fragments is widespread in dense NIIs (Davies et al., 1997), despite scant evidence for selective neuronal loss. This accelerated phenotype makes these animals especially suitable for therapeutic trials targeting the proximate causes of neuronal dysfunction in the symptomatic stages of disease.

Transgenic mice that express full-length human mhtt, including YAC46 and YAC72 mice, develop progressive motor deficits consistent with adult-onset HD at 3-6 months or later, depending on polyQ length and expression levels (Hodgson et al., 1999). Death ensues more quickly only in a subgroup of the most extreme model, the YAC128 mice (Slow et al., 2003; Van Raamsdonk et al., 2005). These mice exhibit selective neuronal degeneration and therefore represent a good model for investigating mechanisms that target specific neuronal populations in HD. Another full-length HD mouse model, which expresses the *HD* cDNA with various polyQ lengths under the control of the CMV promoter (Reddy et al., 1998, 1999), also displayed a progressive phenotype including eventual hypokinesia coincident with selective neuronal loss and gliosis within the striatum. The relative absence of prominent aggregates in the region most severely affected by neurodegeneration argues against a role for aggregated mhtt in the initiation of disease pathogenesis. Additionally, because striatal neuronal loss is observed in the full-length models but not in those that express shorter fragments of mhtt, the context of the full-length mhtt protein appears to be implicated in mediating the selectivity of neuronal degeneration seen in HD.

KI mouse models, such as the CAG80 and 94 (Shelbourne et al., 1999; Levine et al., 1999) as well as the *Hdh*Q92 and Q111 mice (Wheeler et al., 2000), may well be the

most accurate genetic model of HD since these mice carry a CAG-expanded version of the endogenous murine *Huntington's disease homologue (Hdh)* gene and therefore express normal levels of htt. These animals display a very mild phenotype and do not develop neurodegeneration, and all but the CAG94 model exhibited formation of NIIs and neuritic aggregates similar to those found in human HD brains (Albin et al., 1990, 1992; Li et al., 2001). These features coupled with the genetically accurate expression of mhtt in these mice make them excellent models with which to examine the mechanisms of neuronal dysfunction in HD.

1.2. Excitotoxicity Hypothesis

1.2.1. What is Excitotoxicity?

Excitotoxicity refers to a mode of cell death resulting from the toxic effects of excitatory amino acids (Lucas and Newhouse, 1957; Rothman and Olney, 1995). Because glutamate is the principal neurotransmitter responsible for mediating excitatory synaptic transmission in the mammalian CNS (reviewed in Hebb, 1970; Engelsen, 1986), neuronal excitotoxicity typically refers to the cellular death arising from exposure to glutamate at high concentrations and/or for prolonged periods of time, which leads to massive influx of ions and water thus causing the cell to swell. This is accompanied by an accumulation of excessive amounts of Ca^{2+}, triggering secondary messenger pathways that are toxic to the neuron including activation of catabolic enzymes to degrade proteins, nucleic acids, and other cellular components (reviewed in Berliocchi et al., 2005).

One major hypothesis to explain the exquisite sensitivity with which MSNs in the striatum undergo selective degeneration in HD is the "excitotoxicity hypothesis".

Excessive activation of glutamate receptors could result from enhanced glutamate release from cortical and thalamic afferents, diminished glial uptake of glutamate, increased sensitivity of post-synaptic glutamate receptors on striatal projection neurons, or a combination of these. In the context of HD, the excitotoxicity hypothesis proposes that over-activation of glutamate receptors by one or more of the aforementioned mechanisms, in combination with impaired mitochondrial function, compromised intracellular Ca^{2+} homeostasis, and the associated pathological downstream signaling, would activate cytotoxic pathways leading to MSN dysfunction and death (Schwarcz et al., 1977; DiFiglia, 1990) (see Figure 1). Here we present evidence from HD mouse models (summarized in Table 1) and post-mortem brain tissue that incriminates altered glutamate receptor signaling and mitochondrial function in HD pathogenesis.

1.2.2. Classes of Glutamate Receptors

Glutamate-binding post-synaptic receptors belong to one of two broad classes: the metabotropic glutamate receptors (mGluRs) (reviewed in Conn and Pin, 1997), which initiate secondary signaling pathways to activate or inhibit effector systems through GTP-binding proteins; and ionotropic glutamate receptors (iGluRs) (reviewed in Dingledine et al., 1999), which form ion channel pores upon ligand binding to facilitate cationic influx. This latter class of glutamate receptors, the iGluRs, includes the α-amino-3-hydroxy-5-methyl-4-isoxazole-propionic acid (AMPA) receptors (AMPARs), kainate receptors, and NMDARs. AMPA and kainate receptors mediate fast synaptic transmission with relatively low Ca^{2+} permeability. The NMDARs are of special importance to our discussion of excitotoxicity because of their high permeability to Ca^{2+} and slow gating kinetics. NMDARs are also remarkably sensitive to voltage-dependent

block by Mg^{2+} in the extracellular milieu (Mayer et al., 1984; Nowak et al., 1984; Monyer et al., 1992; reviewed in Cull-Candy et al., 2001). Under normal physiological conditions, Ca^{2+} influx through NMDARs is crucial not only for the formation and stabilization of new synapses but also for the induction and maintenance of synaptic plasticity (Bliss and Collingridge, 1993; Maren and Baudry, 1995; Asztely and Gustafsson, 1996). In certain pathological conditions, activity of these same receptors is altered leading to increased oxidative stress and excitotoxicity (Lucas and Newhouse, 1957; Rothman and Olney, 1995; Michaelis, 1998).

1.2.3. Structure and Functional Characteristics of NMDARs

Functional NMDARs are heteromeric complexes composed of different subunits from the NR1, NR2, and NR3 subtypes (reviewed in Cull-Candy and Leszkiewicz, 2004; Paoletti and Neyton, 2006). (A cartoon illustrating the membrane topology and C-terminal splice cassettes of the NR1 subunit is shown in Figure 2.) Although the stoichiometry of NMDARs has not been unequivocally defined, most functional receptors in neurons are widely believed to be tetrameric structures (Laube et al., 1998) composed of two glycine-binding NR1 subunits and two glutamate-binding NR2 subunits that assemble in the ER (Monyer et al., 1994; McIlhinney et al., 1998; reviewed in Ozawa et al., 1998; Dingledine et al., 1999). While the relatively large C-terminal tails of these receptors are intracellularly located and are involved in binding to cytoplasmic signaling molecules, synaptic scaffolds, and structural proteins, subunit assembly is thought to be mediated by the extracellular portion of each subunit (Meddows et al., 2001). The re-entrant pore loops (M2) from all subunits dip into the membrane from the cytoplasmic side to form the channel-lining region (Figure 2) and as such define permeation properties of the receptor.

Importantly, NMDARs are permeable to cations including Ca^{2+}, which acts as a second messenger to initiate numerous intracellular signaling pathways and to activate a multitude of protein kinases and phosphatases. This property of the NMDAR underscores its importance in the induction of synaptic plasticity (reviewed in Bliss and Collingridge, 1993), as well as in mediating excitotoxic damage resulting from receptor over-stimulation (Lucas and Newhouse, 1957; Rothman and Olney, 1995).

Receptors comprising NR1 and NR2 subunits are activated only when two conditions are met simultaneously: (1) coincident binding of glycine (or serine) to each NR1 subunit, and glutamate to each NR2 subunit; and (2) relief of voltage-dependent block by extracellular Mg^{2+} either by artificially removing Mg^{2+} from the extracellular solution or by post-synaptic depolarization of the neuron. Because of these unique requirements, NMDARs essentially act as coincidence detectors under physiological conditions and are activated to permit ion flux only when both pre- and post-synaptic neurons are excited at the same time.

The transcript encoding NR1 can undergo alternative splicing at three independent sites giving rise to a total of eight possible isoforms of the NR1 protein (Hollmann et al., 1993). One such splice site determines the inclusion or exclusion of exon 5 at the 5'-end of the mRNA which corresponds to the extracellular N-terminus of the translated protein. The exon 5 portion forms a surface loop similar in structure to polyamine, which is believed to shield the proton sensor of the receptor. Hence exon 5-containing NR1 isoforms are insensitive to regulation by protons, Zn^{2+} (which at low concentrations selectively inhibits NR1/NR2A-subtype of NMDARs), and polyamines. In contrast, the major splice variant of NR1 expressed in most neurons lacks exon 5 and as such, most NMDARs are subjected to inhibition by Zn^{2+} (for NR1/NR2A) and protons, as well as potentiation by polyamines (reviewed in McBain and Mayer, 1994; Cull-Candy et al.,

2001; Cull-Candy and Leszkiewicz, 2004). The characteristics of other NR1 splice variants will be discussed in section 1.2.4 in the context of receptor trafficking.

In addition to the role that NR1 subunits play in influencing regulation of the NMDAR complex by allosteric modulators, NR2 subunits play a critical role in conferring the biophysical and pharmacological properties of the receptor. Four different genes encode for the NR2 subunit (NR2A, B, C and D), and the different NR2 subunits and NMDAR subtypes are expressed not only in a developmentally and regionally regulated manner (Ishii et al., 1993; Akazawa et al., 1994; Monyer et al., 1994; Laurie et al., 1997), but also in an activity-dependent fashion (Philpot et al., 2001; Barria and Malinow, 2002).

During development, some regions of the brain also express NR3A or NR3B subunits. These glycine-binding subunits, when expressed as a triheteromeric receptor with NR1 and NR2 subunits, greatly decrease both the current flow and Ca^{2+} permeability of the receptor. When expressed as NR1/NR3 diheteromers, on the other hand, it forms a cation-permeable glycine receptor that is unresponsive to glutamate receptor agonists or antagonists, and is neither sensitive to voltage-dependent blockade by Mg^{2+} nor permeable to Ca^{2+} (Perez-Otano et al., 2001; Chatterton et al., 2002). The multitude of different NR1 splice variants along with the many NR2 and NR3 subunit choices available therefore allow the formation (at least in theory) of an impressive repertoire of NMDARs, each of which differs from others in such functional characteristics as affinity for receptor agonists and antagonists, sensitivity to Mg^{2+}, single channel conductance, and channel kinetics (Ishii et al., 1993; Monyer et al., 1994; Chen et al., 1999a; reviewed in Cull-Candy et al., 2001; Cull-Candy and Leszkiewicz, 2004; Waxman and Lynch, 2005).

Most NMDARs in the adult mammalian forebrain are composed of NR1 with NR2A and/or NR2B subunits. These receptors, regardless of NR2A/NR2B content (i.e., two subunits of NR2A, two subunits of NR2B, or one subunit each of NR2A and NR2B forming

triheteromeric receptors), display comparable permeability to Ca^{2+}, sensitivity to voltage-dependent Mg^{2+} block, and similarly high single channel conductances in the range of ~40-50 pS. However, NR2A- and NR2B-containing NMDARs exhibit differences in channel gating properties in response to known NMDAR agonists and antagonists (Vicini et al., 1998; reviewed in Dingledine et al., 1999; Kew and Kemp, 2005; Waxman and Lynch, 2005). In this way, pharmacological tools and differences in channel gating kinetics help to identify the subunit composition within a given population of functional NMDARs.

1.2.4. Trafficking of NMDARs

In addition to roles for different NMDAR subunits and isoforms in conferring unique biophysical and pharmacological properties upon the receptor, NMDAR complexes containing different complements of receptor isoforms and subunits also behave differently with respect to how they are transported, targeted, and anchored at the cell surface (Rumbaugh and Vicini, 1999; Tovar and Westbrook, 1999; Barria and Malinow, 2002; Prybylowski et al., 2005; Mauceri et al., 2007; reviewed in Prybylowski and Wenthold, 2004).

Of the three alternative splice sites in NR1, two are located intracellularly close to the C-terminus of the protein (Figure 2). The more membrane-proximal one of these, involving deletion or retention of exon 21, gives rise to the inclusion of a C1 cassette when exon 21 is not spliced out from the hnRNA. Within the C1 cassette exists an RXR motif which acts as a consensus sequence mediating retention of the newly synthesized protein within the ER. Therefore C1-containing NR1 isoforms do not get trafficked to the Golgi apparatus until the ER retention signal is masked, generally via assembly with NR2

subunits as well as phosphorylation of nearby serine residues at amino acid positions 896 and 897 (McIlhinney et al., 1996, 1998; Xia et al., 2001; Scott et al., 2001, 2003; reviewed in Carroll and Zukin, 2002; Wenthold et al., 2003; Prybylowski and Wenthold, 2004).

The third splice site in NR1 is positioned close to the 3'-end of the hnRNA and involves differing splice acceptor sites within exon 22. With the use of the normal splice acceptor site, the NR1 isoform generated contains what is referred to as the C2 cassette. Use of the alternate splice acceptor site gives rise to a truncated version, the C2' cassette, which contains a PSD-95/Discs large/Zona occludens-1 (PDZ) ligand motif located at the C-terminal end. Interestingly, C2'-containing NR1 isoforms are able to egress from the ER and reach the surface in the absence of assembly with NR2 subunits, and regardless of whether the RXR motif-containing C1 cassette is present or not (Standley et al., 2000; reviewed in Carroll and Zukin, 2002; Wenthold et al., 2003). The presence of the PDZ ligand motif appears to have a dominant effect, and forward trafficking of these NR1 C2' isoforms is postulated to be mediated in part by interactions of the C-terminal tail with PDZ domain-containing proteins such as PSD-95. As with NR2 subunit expression, alternative splicing of NR1 isoforms appears to be modulated by activity; C2 splice isoforms are favoured by high levels of neuronal activity, whereas C2' variants are up-regulated during periods of low activity, leading to formation of NMDAR complexes with distinct ER export and surface delivery kinetics (Mu et al., 2003)

NR2 subunits, unlike NR1, do not traffick to the cell surface unless pre-assembled in the ER with NR1 subunits into the tetrameric complex (McIlhinney et al., 1998; reviewed in Wenthold et al., 2003). Like the NR1 C2' isoforms, however, C-terminal tails of NMDAR NR2 subunits contain PDZ ligand motifs that permit interaction with scaffolding proteins of the membrane-associated guanylate kinase (MAGUK) family, such as PSD-95 and the 102 kDa synapse-associated protein (SAP-102) (Kornau et al., 1995;

Sans et al., 2000; Lin et al., 2004; reviewed in Wenthold et al., 2003). These interactions serve to promote surface delivery and/or stabilize surface expression of the NMDARs, and affinities for binding different MAGUKs are relatively NR2 subunit-specific. While interaction of NR2A with the MAGUK family member synapse-associated protein 97 kDa (SAP-97) controls forward trafficking and insertion of NR2A-containing NMDARs (Mauceri et al., 2007), NR2B subunits interact with SAP-102 and the exocyst protein Sec8 to facilitate trafficking of NR2B-containing receptors to the cell surface membrane (Sans et al., 2000, 2003; reviewed in Prybylowski and Wenthold, 2004). The presence of a YEKL motif near the C-terminus of NR2B, on the other hand, allows binding to components of the clathrin-dependent endocytic machinery (Roche et al., 2001) to regulate internalization of NR2B-containing NMDARs. Similarly, a tyrosine-enriched "ring" of amino acids in the membrane-proximal region of the NR2A C-terminus regulates internalization for this subtype of receptor, where agonist binding to NR2A-containing NMDARs leads to dephosphorylation of these tyrosine residues and subsequent receptor internalization, independent of current flow through the receptor (Vissel et al., 2001). Regulation of NMDAR activity by phosphorylation, especially in the context of mhtt expression, will be discussed in a later section of this Introduction (section 1.5.3).

As with other properties of the receptors, targeting of NMDARs also appears to be distinctly regulated in an NR2 subunit-dependent manner, with increasing evidence to suggest differential subcellular localization of NR2A- versus NR2B-containing NMDARs. While the former are abundantly expressed at synaptic membranes, the latter preferentially target to extra-synaptic regions of the plasma membrane (Li et al., 1998; Stocca and Vicini, 1998; Tovar and Westbrook, 1999; Barria and Malinow, 2002) although this distinction is not absolute (Thomas et al., 2006). The relative contribution of each subunit to the total NMDAR pool and differences in subcellular distribution are

important in the control of neuronal survival, as well as in the determination of cellular responses to plasticity-inducing stimuli in forebrain regions such as the hippocampus (Hardingham et al., 2002; Hardingham and Bading, 2003; Liu et al., 2004; Massey et al., 2004; Berberich et al., 2005, 2006; Bartlett et al., 2006; Morishita et al., 2006, Soriano et al., 2006).

The human striatum is notable for its remarkably high levels of NMDARs containing the NR2B subunit relative to other subunits, in comparison to other parts of the forebrain. This enrichment appears to be conserved in other mammalian species, as striatal tissues from rodents such as rat and mouse also display increased NR2B expression (Landwehrmeyer et al., 1995; Ghasemzadeh et al., 1996; Rigby et al., 1996; Standaert et al., 1999; Christie et al., 2000; Kuppenbender et al., 2000; Li et al., 2003). Additional evidence supporting a role for the NR1/NR2B subtype of NMDARs in HD pathogenesis will be presented in section 1.4.4 of this Introduction.

1.2.5. Striatal Expression of NMDARs in HD-Affected Individuals and Mouse Models

Early studies involving radioligand-binding of NMDARs in post-mortem brain tissue from HD patients demonstrated a disproportionate loss of NMDARs from the striatum of patients at pre-symptomatic stages of the disease, even though these patients exhibit only relatively small amounts of neuronal loss at this point (Young et al., 1988; Albin et al., 1990). Because the amount of NMDARs lost greatly exceeds the expected amount based on the extent of neuronal loss, these findings suggest that striatal neurons with high expression of NMDARs may be preferentially lost even from the earliest stages of disease, revealing an exquisite vulnerability in these cells.

More recently, scrutiny of expression of the different NMDAR subunits in

transgenic mouse models of HD have yielded sometimes conflicting results, depending on the model used and whether mRNA or protein levels were examined. As discussed earlier, R6/2 mice express an exon 1 fragment of mhtt containing ~150Q (Mangiarini et al., 1996). These mice at symptomatic ages displayed enhanced striatal NR1 expression but reduced NR2A and NR2B expression, as revealed by immunohistochemical staining of brain slices (Cepeda et al., 2001a). In contrast, Cha and colleagues (1999) reported no changes in NR1 protein levels from 12-week old symptomatic R6/2 mice, either in the striatum (as revealed by receptor binding assays) or in whole brain homogenates (by immunoblot analysis). A different study investigating changes at the mRNA level, using mice of the same model from both early (6-week) and late (12-week) symptomatic stages, found no change in striatal NR1 mRNA expression relative to WT littermates regardless of stage of disease progression (Luthi-Carter et al., 2000, 2003). These findings were corroborated by Ali and Levine in a recent study (2006) examining striatal MSNs from pre-symptomatic and early symptomatic R6/2 mice, which once again confirmed unaltered NR1 mRNA levels. Moreover, the same study showed NR2B mRNA expression to be unchanged while NR2A mRNA levels were reduced.

NMDAR subunit expression has been investigated in other HD mouse models as well. In the YAC transgenic mouse model, which expresses full-length human mhtt under the control of human promoter and regulatory sequences (Hodgson et al., 1999), analysis of NR1 and NR2B protein expression revealed no polyQ length-dependent differences in striatal tissues of pre-symptomatic YAC46 or YAC72 mice at 2 months of age, relative to FVB/N WT littermates (Li et al., 2003; also see Figure 7). The YAC128 mice, which express full-length mhtt with a more extreme expansion of 128Q, showed reduced striatal NR2B expression at 12 months of age (J. Shehadeh and L.A. Raymond, unpublished results), a time when the animals are symptomatic and display significant striatal

degeneration (Slow et al., 2003). Studies in the N171-82Q mouse model (Schilling et al., 1999) revealed unaltered levels of striatal NR1 or NR2B protein expression regardless of disease stage (pre-symptomatic versus symptomatic), with the exception of a transient reduction in NR2A subunit expression in the striatum of pre-symptomatic animals (Jarabek et al., 2004).

Despite some notable differences in findings from the different animal models, most of them seem to indicate diminished NR2A and/or NR2B subunit expression while NR1 levels remain unaltered. Because NMDAR complexes require both NR1 and NR2 subunits to form functional channels, these data collectively suggest that a reduction in numbers of active NMDARs and/or changes in NMDAR subunit composition may occur with disease progression in a number of these transgenic mouse models for HD. Importantly, findings from studies in transgenic mice in general appear consistent with results from receptor ligand-binding studies in post-mortem human HD brains as described above, although direct correlations between these studies are difficult to draw due to differences in the experimental approaches that were used.

1.2.6. Chemical Models of HD

Before the advent of transgenic models, some of the earliest systems used to model HD involved injection of a variety of toxins into the striatum of animals. Specifically, injection of NMDAR agonists such as quinolinic acid (QA) into the striatum of rodents or primates caused lesioning of the striatum and reproduced several behavioural and neuropathological characteristics of HD, including selective loss of projection MSNs from the striatum while interneurons were not affected (Schwarcz et al., 1984; Beal et al., 1986, 1991; Sanberg et al., 1989; Hantraye et al., 1990; Ferrante et al., 1993). Endogenously,

QA is generated from the kynurenine pathway of tryptophan degradation, which was shown to be perturbed in HD patients as well as in R6/2 and YAC128 mice. Among the metabolites produced in this pathway, those that led to an increase in oxidative stress (such as 3-hydroxykynurenine) or directly activated NMDARs (such as QA) were found at abnormally high levels in cortical and/or striatal tissue in the early symptomatic stages (Guidetti et al., 2004, 2006). These findings would therefore suggest that excitotoxic damage as a result of exposure to metabolites of the kynurenine pathway may contribute to NMDAR-mediated toxicity in HD.

Another excitotoxin used in those early days was the non-NMDAR agonist kainic acid, which also caused death of striatal neurones but did not selectively target projection MSNs (Coyle and Schwarcz, 1976; McGeer and McGeer, 1976). Both kainate- and QA-induced neuronal toxicity in the striatum were abolished when synaptic input from the cortex via corticostriatal glutamatergic afferents was removed by decortication, indicating a role for cortically released glutamate in contributing to excitotoxin-mediated striatal damage (McGeer and McGeer, 1978; Biziere and Coyle, 1979; Orlando et al., 2001). Interestingly, injection of group I mGluR agonists restored NMDAR-dependent excitotoxic cell death in decorticated animals, while blocking the activation of group I mGluRs was protective against QA- and NMDA-induced neuronal toxicity in animals with intact corticostriatal afferentation (Orlando et al., 2001), implicating a role for striatal mGluR activation in contributing to NMDAR-dependent excitotoxicity (see Figure 1).

NMDAR agonists are not only more selective in targeting striatal projection MSNs for neuronal death, but they are also more neurotoxic than agonists for other iGluR subclasses (reviewed in DiFiglia, 1990). In toxicity paradigms where NMDA was used as the excitotoxin, MSNs in acute striatal slices from both R6/2 and YAC72 mice demonstrated a selective enhancement of NMDAR-mediated current density and

NMDA-induced swelling, in comparison to large interneurons which are spared in HD (Cepeda et al, 2001b). In contrast, the current flux and cell swelling evoked by application of kainate were not significantly different between interneurons and projection MSNs (Cepeda et al., 2001b). These findings unmask NMDAR-specific characteristics which confer on these receptors an exquisite selectivity and efficacy in terms of their ability to elicit excitotoxic damage in striatal projection MSNs, once again confirming a likely involvement of these receptors and their altered activity in the pathogenesis of HD.

Apart from injection of animals with excitotoxins, other chemical models that recapitulate neuropathological features of HD include those that involve the use of mitochondrial toxins. In particular, striatal or systemic injection in rodents with inhibitors of mitochondrial complex II such as 3-nitropropionic acid (3-NP) or malonic acid resulted in a selective pattern of striatal neurodegeneration reminiscent of that seen in HD (Beal et al., 1993; Greene et al., 1993; Brouillet et al., 1995; Greene and Greenamyre, 1995; Bogdanov et al., 1998). Notably, cell death caused by these toxins appeared to depend on activation of NMDARs. In the rat striatum, injection of 3-NP led to increased NMDAR activation (Wüllner et al., 1994), while inhibition of NMDAR function blocked the neurotoxicity resulting from injection of malonate or 3-NP (Greene et al., 1993; Bogdanov et al., 1998). These findings suggest that NMDAR and mitochondrial functions are intimately related and implicate them, in their aberrant functional states resulting from mhtt expression, in rendering striatal projection MSNs especially susceptible to excitotoxic damage in HD.

1.3. Aberrant NMDAR Activity in HD

1.3.1. Synaptic Abnormalities in HD Models

The generation of a large array of HD models expressing part or all of the *HD* transgene in cell lines or rodents (Mangiarini et al., 1996; Hodgson et al., 1999; Reddy et al., 1998; Schilling et al., 1999; Shelbourne et al., 1999; Wheeler et al., 2000; Lin et al., 2001; Von Horsten et al., 2003) has greatly facilitated in-depth analyses of the molecular pathways involved in HD pathogenesis. As depicted in Figure 1, alterations in a variety of cellular processes have been implicated in the resulting augmentation of the sensitivity of striatal MSNs to excitotoxicity at corticostriatal synapses in HD. Among these are electrophysiological changes in the corticostriatal pathway as well as alterations in glutamate receptor sensitivity in MSNs that express mhtt. While evidence from studies in slices of 1 month-old YAC72 mice (at an age before symptom onset) demonstrated unaltered probability of evoked glutamate release from cortical afferents onto striatal MSNs relative to WT controls (Li et al., 2004), examination of other mouse models clearly revealed mhtt-dependent differences in glutamate release at corticostriatal synapses (Figure 1, point 1). In acute corticostriatal slices from R6/2 mice at the time of symptom onset, large-amplitude, spontaneous excitatory post-synaptic currents (EPSCs) were recorded at significantly higher frequencies relative to control (Cepeda et al., 2003). The implications of such bursts of enhanced cortical glutamate release remain unclear; however their occurrence early in the disease process could conceivably couple with mhtt-induced decreases in glutamate uptake by astrocytes and impairments of glutamate clearance from the synaptic cleft (Lievens et al., 2001; Behrens et al., 2002; Shin et al., 2005; Figure 1, point 2), along with increases in QA and oxidative metabolites from an

impaired kynurenine pathway as described above (Guidetti et al., 2004, 2006) to contribute to excessive activation of NMDARs leading to excitotoxic damage in striatal MSNs.

These large events appeared to be transitory, however, as the frequency of all spontaneous currents decreased with disease progression and symptomatic onset in these mice (Cepeda et al., 2003). This functional change appears to correlate structurally with diminished expression of synaptic marker proteins and a decrease in the number of spines in symptomatic R6/2 mice (Klapstein et al., 2001), consistent with a reduction in glutamatergic transmission. These observations indicating decreased glutamate release from corticostriatal synapses are in agreement with cell model studies which revealed compromised exocytic function in cells expressing polyQ-expanded htt exon 1 leading to abnormalities in neurotransmitter release (Edwardson et al., 2003). Apart from a defect in exocytosis, the properties of the vesicle release and recovery cycle that determine the amplitude and timing of neurotransmitter release also appeared to be impaired by htt polyQ expansion (reviewed in Milnerwood and Raymond, 2006). These results seem to suggest that, at later stages of disease, the initial hypersensitivity of corticostriatal signaling gives way to a reduction in glutamatergic synaptic transmission, which may effectively confer some measure of resistance against glutamate receptor-dependent insults in neurons that have already faced tremendous excitotoxic injury.

1.3.1.1. Alterations in NMDA-LTP and NMDA-LTD in HD Models

Altered cognitive function (including memory formation and information processing) as well as changes in emotions and affective behaviour are symptoms that generally precede motor dysfunction in patients in HD, although these changes could

sometimes be subtle and may not be noted until the time of clinical presentation (Lawrence et al., 1996, 1998; Jason et al., 1997; Paulsen et al., 2001). The molecular substrates which underlie memory formation as well as information acquisition and long-term storage are widely believed to involve long-term, activity-dependent changes in synaptic efficacy, many forms of which rely on NMDAR activation. Hence studies have been carried out in various transgenic and KI mouse models of HD to investigate the effects of htt polyQ expansion on NMDAR-dependent long-term potentiation (LTP) and depression (LTD).

Studies in a number of HD mouse models have revealed alterations in hippocampal LTP related to impairments of pre- and/or post-synaptic function (Hodgson et al., 1999; Usdin et al., 1999; Murphy et al., 2000; Milnerwood et al., 2006) which in some cases appeared transitory and changed over time (Hodgson et al., 1999). In YAC72 mice, high frequency stimulation (HFS) of CA1 synapses led to potentiation of NMDAR-dependent responses in 6 month-old animals, whereas the same treatment induced depression in 10 month-old animals (Hodgson et al., 1999). The CAG80 KI mouse exhibited diminished hippocampal LTP responses, likely as a result of perturbations in the pre-synaptic release of neurotransmitter (Usdin et al., 1999). Evidence for a contribution from post-synaptic changes in NMDAR signaling came from studies in R6 mice which expressed reduced LTP compared to controls; interestingly these mice also expressed a form of LTD that was absent in control animals (Murphy et al., 2000; Milnerwood et al., 2006). Such changes in hippocampal synaptic plasticity occured prior to the appearance of motor symptoms and coincided with the development of cognitive defects in the R6/2 model (Murphy et al., 2000; Cybulska-Klosowicz et al., 2004; Mazarakis et al., 2005; Milnerwood et al., 2006). Altered plasticity, in the forms of suppression of LTD expression and impairment of post-LTP synaptic depotentiation, has

also been reported at the corticostriatal synapse, both from 3-NP-treated rats (Dalbem et al., 2005; Picconi et al., 2006) and R6/2 mice (Picconi et al., 2006). Altogether, these studies to date have yielded many important findings providing invaluable insight into the possible mechanisms underlying mhtt-mediated changes in cognitive function early in HD pathogenesis.

1.3.2. Enhanced Sensitivity to NMDA in HD Mouse Models

One mechanism leading to increased excitotoxicity involves enhanced sensitivity of post-synaptic glutamate receptors, and studies in mouse models of HD have provided strong evidence in support of over-activation of NMDARs as contributing to excitotoxic damage in HD (Figure 1, point 3).

Measuring swelling of cells as a parameter to indicate the level of cellular stress, Levine and colleagues demonstrated that exposure to NMDA led to faster and more substantial swelling responses from striatal MSNs of both the CAG KI mouse expressing htt-94Q (CAG94) and the R6/2 mouse models (Levine et al., 1999). In R6/2 mice, these morphological changes were correlated with augmented peak NMDA-evoked current densities in striatal slices that appeared to be selective for NMDARs but not other iGluRs (Cepeda et al., 2001a). Similar results were obtained from striatal neurons in symptomatic and pre-symptomatic animals (Cepeda et al., 2001a) while cortical neurons, in contrast, did not display enhanced NMDAR-mediated currents (Andre et al., 2006) in agreement with the observation that these neurons do not degenerate until much later in the course of disease progression (Vonsattel and DiFiglia, 1998).

In addition to data from striatal slices, more in-depth electrophysiological analyses of NMDAR activity changes have been carried out in acutely dissociated striatal MSNs

from R6/2 mice, examining how NMDA-evoked currents and sensitivity to Mg^{2+} block are influenced by mhtt over a range of holding potentials (Starling et al., 2005). This study indicated that, while one population of neurons behaved similarly to WT controls, the other population exhibited significantly larger current flow through NMDARs with diminished sensitivity to block by extracellular Mg^{2+}. A more recent study using acutely dissociated MSNs from pre-symptomatic R6/2 mice also confirmed significantly larger NMDAR-mediated currents, even though these mice expressed lower levels of NR2A mRNA and similar amounts of NR1 and NR2B mRNA in comparison to WT littermates (Ali and Levine, 2006). Because anomalous NMDAR function is observed from striatal neurons and slices of both pre-symptomatic and symptomatic mice, aberrant NMDAR activity would therefore appear to be an early effect of mhtt expression that precedes the development of any motor deficits.

Apart from the R6/2 model, several other KI and transgenic mouse models of HD have provided additional evidence in support for sensitized NMDAR function in cells expressing mhtt. Increased response of NMDARs following exposure to NMDA was noted in immortalized striatal cells from *Hdh*^{Q111} KI mice (ST*Hdh*^{Q111} cells; Trettel et al., 2000). Whole-cell voltage-clamp recordings in a different mouse model that expresses an N-terminal fragment of human htt with 100Q (tgHD100) revealed augmented peak NMDAR current in MSNs from striatal slices of these mice (Laforet et al., 2001).

In the YAC transgenic HD mouse model expressing full-length human htt-72Q, acutely dissociated MSNs from pre-symptomatic mice and striatal MSNs cultured from neonatal mice both responded to NMDA treatment with significantly larger current densities than did WT littermates (Zeron et al., 2002, 2004), suggesting once again that the effect of mhtt on NMDAR function is an early event in HD pathogenesis, possibly occurring as early as at the time of birth. Such early alterations may lead to profound

changes in intracellular signaling, especially those pathways that involve cytosolic Ca^{2+}, thus setting the stage for increased oxidative stress and neuronal dysfunction as disease progresses.

To determine whether synaptic NMDAR-mediated currents are modulated by mhtt in a manner similar to whole-cell NMDAR currents, evoked NMDAR current was measured from striatal MSNs in acutely dissociated corticostriatal slices from ~1 month-old FVB/N WT or YAC72 mice. These studies suggested that stimulation of cortical afferents induced significantly larger synaptic NMDAR-mediated currents in YAC72 mice, in comparison to WT (Li et al., 2003, 2004). This effect was NMDAR-specific, as illustrated by a consistently larger ratio of NMDAR- to AMPAR-mediated EPSC amplitudes in YAC72 corticostriatal synapses (Li et al., 2003, 2004). Also, pre-synaptic glutamate release was not found to differ between WT and YAC72 slice preparations (Li et al., 2004), suggesting that amplitude of synaptic NMDAR currents in YAC72 striatal neurons is augmented primarily as a result of a specific mhtt-induced increase in post-synaptic NMDAR activity.

1.4. Signaling Downstream of Altered NMDAR Activity

1.4.1. Loss of Calcium Homeostasis

The high permeability of the NMDAR to Ca^{2+} makes this channel a key regulator of intracellular Ca^{2+} levels. In turn, Ca^{2+} plays an important role as a second messenger in many downtream signaling pathways. Thus changes in levels of intracellular Ca^{2+} are normally tightly regulated to ensure stringent control over Ca^{2+}-dependent signaling pathways. Under pathological conditions where levels of intracellular Ca^{2+} exceed a

certain threshold causing saturation of the Ca^{2+}-buffering machineries, degradative pathways are activated, leading to catabolic breakdown of phospholipids, nucleic acids, and proteins. Moreover, compromised mitochondrial function as a result of Ca^{2+} overload promotes free radical formation and induction of the mitochondrial permeability transition (mPT) (Dugan et al., 1995; Reynolds and Hastings, 1995; Peng and Greenamyre, 1998; reviewed in Berliocchi et al., 2005) leading to additional cellular dysfunction eventually followed by death.

Thus, Ca^{2+} homeostasis is critical to the well-being of any cell and has been shown to be compromised in cells expressing polyQ-expanded mhtt (Figure 1, point 4). Studies in transgenic mice revealed elevated levels of basal intracellular Ca^{2+} in hippocampal neurons from YAC HD mice (Hodgson et al., 1999) as well as striatal neurons from R6/2 mice (Hansson et al., 2001). Similar findings were made in a KI model, in immortalized striatal cells from mice expressing the murine htt protein with 111Q (ST*Hdh*^{Q111}; Seong et al., 2005).

Apart from basal levels, NMDAR-dependent increases in intracellular Ca^{2+} levels were also affected by expression of mhtt. For example, neurons from tgHD100 mice displayed significantly higher levels of intracellular Ca^{2+} concentrations following NMDA treatment (Laforet et al., 2001). Similarly, bath application of NMDA led to much larger increases of intracellular Ca^{2+} in striatal slices from R6/2 mice in comparison to WT controls (Cepeda et al., 2001a). Striatal MSNs from YAC46 and YAC72 mice responded to NMDA treatment with augmented cytosolic Ca^{2+} responses (Zeron et al., 2004), while cultured MSNs from a similar mouse model with an extreme polyQ repeat length of 128Q demonstrated enhanced intracellular Ca^{2+} levels following repeated application of glutamate (Tang et al., 2005). In the same YAC128 model, NMDA treatment following block of glycolytic ATP synthesis caused either delayed recovery of Ca^{2+} levels back to

baseline or complete de-regulation of Ca^{2+} immediately upon exposure to NMDA (Oliveira et al., 2006). The number of cultured striatal MSNs undergoing these NMDA-induced changes was significantly higher for YAC128 mice in comparison to WT (Oliveira et al., 2006).

Although the discussion so far has pertained mostly to NMDARs and increased Ca^{2+} levels likely due in part to altered NMDAR activity, intracellular Ca^{2+} from sources other than NMDARs was also found to be differentially regulated by WT versus mutant htt. In particular, the activation of inositol 1,4,5-trisphosphate (IP3) receptors (IP3Rs) on ER membranes gating ER Ca^{2+} stores was highly sensitized by mhtt but not WT htt (Tang et al., 2003). Mutant htt also significantly potentiated IP3R-mediated Ca^{2+} release from ER stores in mouse and rat MSNs (Tang et al., 2003, 2004).

As the findings in cultured neurons described above clearly illustrate, effects of mhtt on intracellular Ca^{2+} homeostasis occur as early as the time of birth (Zeron et al., 2004; Oliveira et al., 2006), as with mhtt-induced changes of NMDAR activity discussed in previous sections. Together these results suggest that mhtt-mediated dysregulation of Ca^{2+} signaling contributes to early cellular changes that render striatal MSNs exquisitely vulnerable in HD.

1.4.2. Mitochondrial Dysfunction in HD and Models of HD

Intact mitochondrial function is absolutely essential to the cell, not only because mitochondria are the main source of metabolic energy, but also because they play a critical role in the regulation of intracellular Ca^{2+} homeostasis. As mentioned previously in sections 1.2.6 and 1.1.4.1, inhibition of mitochondrial electron transport chain function leads to NMDAR-dependent striatal lesioning similar to that observed in HD (Beal et al.,

1993; Greene et al., 1993; Brouillet et al., 1995; Greene and Greenamyre, 1995; Bogdanov et al., 1998), and polyQ expansion in htt has been reported to contribute to mitochondrial dysfunction by blocking movement of mitochondria along neuronal processes (Trushina et al., 2004; Chang et al., 2006).

A number of changes in mitochondrial function, mostly in the direction of decreased function, have been reported in brains of HD patients. These include a reduction in mitochondrial oxygen consumption and diminished glucose metabolism (Stahl and Swanson, 1974; Leenders et al., 1986), as well as decreased cAMP levels in the cerebrospinal fluid (CSF) (Cramer et al., 1984) and post-mortem brains (Gines et al., 2003) of HD patients. Enzymes that function in oxidative phosphorylation including aconitase and mitochondrial complexes II, III, and IV, also displayed decreased activity in striatal tissue from HD patients (Brennan et al., 1985; Beal, 1995; Gu et al., 1996; Browne et al., 1997; Tabrizi et al., 1999).

In addition to changes in the CNS, aberrant mitochondrial function and anomalous energy production have also been noted in peripheral tissues of patients suffering from HD, including muscle (Koroshetz et al., 1997; Arenas et al., 1998; Saft et al., 2005) and lymphoblasts (Panov et al., 2002; Gines et al., 2003). Lymphoblasts from human HD patients, in particular, appeared to be extremely susceptible to treatment with mitochondrial toxins, displaying a remarkable increase in the extent of mitochondrial membrane depolarization and apoptotic cell death in response to cyanide or staurosporine treatment (Sawa et al., 1999).

Changes in mitochondrial functions inevitably affect cellular function, with often serious consequences in the determination of cell survival versus cell death. Under physiological conditions of neuronal activation, where moderate amounts of Ca^{2+} are taken up by mitochondria, the inner mitochondrial membrane (IMM) undergoes transient

and moderate depolarization that subsequently returns to baseline levels following removal of the Ca^{2+}-inducing stimulus. The electrochemical gradient across the IMM drives uptake of Ca^{2+} from the cytosol into the mitochondria and as such supports the major Ca^{2+}-buffering system within the cell (reviewed in Nicholls and Ward, 2000). However, application of toxic levels of stimuli such as large amounts of glutamate or NMDA generally leads to pathologically high levels of intracellular Ca^{2+}. When the concentration of intracellular Ca^{2+} exceeds 1 μM, such as occurs following NMDAR over-stimulation or release from ER stores, excessive amounts of cytosolic Ca^{2+} are loaded into mitochondria thereby causing the buffering ability of these organelles to be over-burdened. This is followed by a permanent and massive depolarization of the IMM, leading to formation and activation of the large conductance pore, mPT. Once the mPT is activated, the electrochemical gradient across the IMM that normally maintains activity of the electron transport chain to drive ATP production becomes dissipated. This renders mitochondria unable to maintain normal oxidative phosphorylation activity or to buffer Ca^{2+}, so that oxidative generation of ATP is abolished, and ATP-dependent processes such as maintenance of a hyperpolarized potential across the plasma membrane by activity of the Na^{+}/Ca^{2+} exchanger is curtailed. Production of reactive oxygen species (ROS) is increased, and Ca^{2+} is dumped back into the cytosol along with other pro-apoptotic factors leading to activation of Ca^{2+}-dependent apoptotic and excitotoxic pathways (reviewed in White and Reynolds, 1996; Duchen, 2004; Orrenius, 2004; Beal, 2005).

Because mitochondrial function is intimately linked to changes in levels of intracellular Ca^{2+}, reasoning suggests that mhtt-induced changes in Ca^{2+} homeostasis may affect mitochondria function and *vice versa*. Mitochondria isolated from striatal neurons in both rat (Brustovetsky et al., 2003) and mouse (Brustovetsky et al., 2005)

appeared to be more sensitive to changes in intracellular Ca^{2+} levels, as they were more prone to mPT formation than mitochondria isolated from cortical neurons. These results are once again in agreement with the observation in HD patients of cortical preservation until fairly late stages of disease (Vonsattel and DiFiglia, 1998).

Apart from the intrinsic susceptibility of striatal mitochondria to changes in intracellular Ca^{2+} levels, mhtt can directly modulate mitochondrial function. Like WT htt, N-terminal mhtt fragments are capable of directly binding mitochondrial membranes, an interaction which is believed to contribute to Ca^{2+} retention deficits and/or formation of the mPT (Panov et al., 2002; Choo et al., 2004). Increased tendency for Ca^{2+}-induced IMM depolarization and mPT formation was demonstrated in liver mitochondria from *Hdh*^{Q111} mice (Choo et al., 2004), and similar findings were made in lymphoblast mitochondria from HD patients (Panov et al., 2002). Mitochondrial membrane potentials in brains of YAC72 mice were also more depolarized at baseline, and underwent additional depolarization following exposure to smaller loads of Ca^{2+} as compared with WT controls (Panov et al., 2002). Other measures of mitochondrial function such as ATP and cAMP levels also indicated compromised energy production capacity, in the striatum of *Hdh*^{Q111} KI mice (Gines et al., 2003), and in immortalized striatal cells from this same mouse model (ST*Hdh*^{Q111}) (Gines et al., 2003; Seong et al., 2005). Not surprisingly, mhtt-expressing cells which exhibited impaired mitochondrial function also displayed increased sensitivity to treatment with mitochondrial toxins (Sawa et al., 1999; Gines et al., 2003; Oliveira et al., 2006; Shehadeh et al., 2006). An overall compromise in the ability of mitochondria to maintain Ca^{2+} homeostasis or to meet the metabolic demands of the cell, then, would likely act synergistically with other mhtt-induced, NMDAR-dependent pathways to produce additional oxidative damage.

With accumulating evidence indicating impairment of mitochondrial function from

studies in both HD patients and rodent models, we develop an increasing awareness of the notion that mitochondrial dysfunction greatly enhances sensitivity of striatal neurons to excitotoxic damage in HD. Together with evidence in support of a role for aberrant NMDAR activity, these results suggest that signaling events downstream of NMDAR activation are critically important in selectively targeting striatal neurons for degeneration in HD.

1.4.3. Caspase Activation

Both normal and mutant forms of htt contain consensus caspase cleavage sequences (Wellington et al., 1998, 2000), and they are indeed substrates for cleavage by these enzymes in the human brain (Wellington et al., 2002); cells within the striatum of HD patients correspondingly showed signs of apoptotic death (Dragunow et al., 1995; Sanchez et al., 1999). Mouse models of HD revealed significantly higher levels of active caspase-3 induced by stress stimuli (Sawa et al., 1999; Zeron et al., 2002), and inhibition of caspase-mediated cleavage of htt either by pharmacological blockade of the enzyme or by genetic ablation of a caspase cleavage site in mhtt successfully protected against mhtt-induced apoptotic death (Zeron et al., 2002; Graham et al., 2006). The apoptotic cascade that is in turn activated by mhtt and its cleavage products is believed to be mediated at least in part via mitochondrial dysfunction and/or activation of the intrinsic mitochondria-dependent caspase cascade (involving caspase-9), since NMDAR-dependent apoptosis was reduced upon treatment by inhibitors of the mPT or of caspase-9 (Zeron et al., 2004; Tang et al., 2005).

1.4.4. Cellular Toxicity and Involvement of NR1/NR2B-Type NMDARs

While it remains an issue of debate as to whether the excitotoxic cell death observed in HD patients and animal/cell line models of HD proceeds via apoptotic and/or necrotic pathways, a plethora of studies have investigated the role of htt polyQ expansion in mediating and modulating NMDAR-dependent excitotoxicity.

As mentioned previously, data from mouse models of HD strongly suggested sensitization of NMDARs by mhtt. One of the first demonstrations of a functional interaction between htt polyQ expansion and changes in NMDAR activity, however, came from studies using a relatively simple and well-characterized cell line model, the heterologous human embryonic kidney (HEK) 293 cells. Cells were transfected to co-express the NR1/NR2B-type NMDARs with full-length human htt containing either a normal (15Q) or expanded (138Q) polyQ tract (Chen et al., 1999b). In this model, larger NMDAR-mediated currents were observed in cells that co-expressed htt-138Q, relative to htt-15Q. A specific involvement of the NR2B subunit was suggested due to a lack of effect of mhtt expression on current mediated by the NR1/NR2A-subtype of NMDARs in this same study (Chen et al., 1999b). Similarly, use of the same transfected cell system in a subsequent study examining NMDAR-dependent cell death suggested an NR2B-selective pathway; the number of cells showing signs of apoptotic death was only increased for mhtt-expressing cells that co-expressed NR1/NR2B but not NR1/NR2A (Zeron et al., 2001).

In a different study using immortalized hippocampal HN33 cells, transient transfection of the cells with htt-48Q, but not htt-16Q, led to significantly higher levels of glutamate-induced apoptosis (Sun et al., 2001). These findings and results from the HEK293 cell line were corroborated by findings in the YAC transgenic mouse model,

where NMDA-evoked current amplitude was greatly augmented in cultured striatal MSNs from YAC72 relative to WT controls as described previously in section 1.3.2 (Zeron et al., 2002). Effects of mhtt expression on NMDA-induced cell death were also examined in cultured striatal MSNs, and MSNs from YAC transgenic mice displayed significantly augmented levels of NMDAR-mediated cell death in comparison to WT, in a polyQ length-dependent manner (Zeron et al., 2002; Shehadeh et al., 2006). Interestingly, the extent of mhtt-potentiated apoptotic death in YAC72 MSNs appeared to be tightly correlated with current flow through NMDARs, as pharmacological reduction of NMDA-induced Ca^{2+} influx in YAC72 MSNs to WT levels led to a corresponding decrease in NMDAR-dependent apoptosis, also to WT levels (Shehadeh et al., 2006).

Apoptotic death was found to be enhanced in cultured MSNs from YAC128 mice in comparison to WT controls following glutamate treatment, in a NMDAR- and mGluR-dependent manner (Tang et al., 2005; also see Figure 1, point 3). In contrast, modulation of excitotoxic cell death by mhtt appeared not to involve the AMPAR subclass of iGluRs, since AMPA treatment of cultured MSNs led to similar amounts of cell death regardless of htt polyQ length (Zeron et al., 2002).

A specific involvement of the NR2B-containing NMDARs was further confirmed, as pharmacological inhibition of the NR1/NR2B-type of NMDARs not only reduced glutamate-induced death in YAC128 MSNs (Tang et al., 2005), but also blocked more than half of the current and inhibited the majority (>80%) of NMDA-induced cell death in MSNs from both WT and YAC72 mice (Zeron et al., 2002). Cultured cerebellar granule neurons, which do not express the NR2B subunit, were examined in parallel as a control; similar levels of NMDAR-dependent cell death were observed in WT and YAC72 neurons (Zeron et al., 2002), consistent with a NR2B-selective mechanism of mhtt-elicited toxicity.

The toxicity-potentiating effect of mhtt expression, in addition to acting via

enhancement of NMDAR activity, likely also involves impairing mitochondrial function as described previously, and the two events are likely related. In fact, mounting evidence implicates dysfunctional NMDAR signaling through mitochondria in rendering MSNs more susceptible to excitotoxic damage in the presence of mhtt expression (Figure 1, point 5). A study by Stout and co-workers (1998) found mitochondrial uptake of Ca^{2+} to be critical for NMDAR-dependent excitotoxicity. Treatment with NMDA induced significantly larger depolarization of the IMM in striatal neurons from YAC46 and YAC72 mice, in comparison to WT (Zeron et al., 2004). Similarly, formation of the mPT following glutamate treatment, as determined by release of cytochrome c from the intra-mitochondrial space into the cytosol, was more readily apparent in YAC128 MSNs relative to controls (Tang et al., 2005). Conversely, treatment of MSNs from YAC transgenic mice with mitochondrial function-promoting agents dramatically decreased both the activation of caspases and the extent of NMDA-elicited apoptotic death (Zeron et al., 2004).

These findings once again clearly implicate aberrant NMDAR activity and related mitochondrial dysfunction in the enhancement of excitotoxic cell death by mhtt, even from the birth of the animal. Moreover, studies on the role of mhtt modulation of NMDAR-mediated toxicity in mouse and cell line models of HD, coupled with the observation of the disproportionate loss of striatal MSNs expressing high levels of NMDARs in HD patients (Young et al., 1988; Albin et al., 1990) as well as an enrichment of NR2B-containing NMDARs in the striatum versus other parts of the forebrain (Landwehrmeyer et al., 1995; Ghasemzadeh et al., 1996; Rigby et al., 1996; Standaert et al., 1999; Christie et al., 2000; Kuppenbender et al., 2000; Li et al., 2003), strongly suggest that the NR2B subunit plays a central role in promoting NMDAR-dependent toxicity in HD pathogenesis.

1.5. Mechanisms Underlying mHtt-Induced Alterations in NMDAR Signaling

While many studies have focused on characterizing the functional link between NMDARs and polyQ-expanded htt, the underlying physical means of association and the actual mediator(s) of mhtt action on NMDARs remain largely unknown. A number of these possibilities are illustrated in Figure 3 and summarized in the following paragraphs.

1.5.1. Interactions of NMDARs with the Actin CSK and PSD-Associated Proteins

A vast number of pathways converge on NMDARs to regulate their function. One of these pathways involves interactions with components of the CSK, which is known to play an essential role in maintaining normal neuronal function, as well as providing structural and functional regulation to receptors on the plasma membrane (Dingledine et al., 1999). Physically and structurally, this regulation takes the form of modulation of receptor targeting, anchoring, clustering, and removal, while functionally the components of the CSK such as microtubules, actin filaments, and associated proteins participate in the modulation of receptor activity and the signaling pathways downstream of receptor activation (Allison et al., 1998, 2000; reviewed in Dingledine et al., 1999).

Specifically, regulation of NMDARs by microtubules (Yuen et al., 2005) and by the actin CSK (Rosenmund and Westbrook, 1993; Allison et al., 1998; Lei et al., 2001) has been reported. The interaction between NMDARs and the actin CSK is not a direct one but rather is thought to be mediated by actin-crosslinking proteins such as α-actinins, which have been shown to directly bind NMDAR subunits NR1 and NR2B (Wyszynski et al., 1997, 1998; Allison et al., 1998; Dunah et al., 2000; reviewed in Shirao and Sekino, 2001). Proper post-synaptic localization and anchoring of the synaptic pool of NMDARs

are critically dependent on an intact actin CSK, as depolymerization of F-actin resulted in a loss of NMDARs from the PSD (Allison et al., 1998). Conversely, NMDAR activity has also been shown to regulate the actin CSK by promoting actin depolymerization (Shorte, 1997); this then affects the binding of CSK-associated proteins to NMDARS which in turn alters NMDAR function (Ehlers et al., 1996b; Wyszynski et al., 1997). Since α-actinins are crucial for linking NMDARs to actin, modulators of the α-actinin/NMDAR interaction may also regulate NMDAR function and/or subcellular localization. It is therefore interesting that one of the α-actinin isoforms, α-actinin 4, has been shown to co-immunoprecipitate with HIP-1 in HEK293 cells over-expressing these two proteins (C.D. Icton, 2001 M.Sc. thesis)

In addition to regulation by the actin CSK, members of the MAGUK family of PSD-associated scaffolding proteins have also been implicated in the regulation of NMDAR distribution as early as a decade ago (Ehlers et al., 1996a). Such scaffolding proteins include PSD-95 and SAP-102, and these PDZ-containing, CSK-associated proteins have been reported to not only regulate trafficking, surface expression and synaptic targeting of NMDARs but also modulate NMDAR function and activity (Sans et al., 2000, 2003; Roche et al., 2001; Lin et al., 2004; reviewed in Carroll and Zukin, 2002; Wenthold et al., 2003). Moreover, MAGUK family members are known to scaffold a wide array of kinases/phosphatases and other signaling molecules in close proximity to the NMDAR, and as such play a pivotal role in the regulation of cellular signaling pathways arising from NMDAR activation (reviewed in Kim and Sheng, 2004).

1.5.2. Interaction of NMDARs and mHtt via PSD-95

While numerous protein partners of htt in its normal and mutant forms have been

identified (Goehler et al., 2004; reviewed in Harjes and Wanker, 2003; Li and Li, 2004; Giorgini and Muchowski, 2005), these htt-containing protein complexes have not been reported to contain NMDARs. However, one of these htt-binding partners is the PSD-localized protein PSD-95, which as described above plays an important role in regulating the distribution and function of NMDARs. It was therefore proposed that htt and NMDARs may be physically linked via mutual interactions with PSD-95 (Sun et al., 2001; Song et al., 2003; Figure 3, point 1).

Kornau and colleagues (1995) first demonstrated a direct interaction between PSD-95 and the C-terminal tails of NR2 subunits. Subsequently PSD-95 has been shown to modulate surface NMDAR expression by stabilizing the latter in cell surface clusters (Roche et al., 2001) and also by increasing the rate of NMDAR insertion to the surface (Lin et al., 2004). Studies from both transfected 293T cells and human cortical tissue indicated an interaction of htt with PSD-95 and their association with NMDAR subunits NR1, NR2A, and NR2B (Sun et al., 2001), suggesting a physical link between htt and NMDARs via interactions with PSD-95. The htt/PSD-95 interaction is not identical for WT and mutant forms of htt but instead is weakened by expansion of the htt polyQ tract (Sun et al., 2001). Ectopic expression of mhtt led to NMDAR-dependent apoptosis which was reduced by co-expression with WT htt, and functionally, PSD-95 modulates mhtt-triggered NMDAR-mediated cell death by abolishing the rescue of mhtt toxicity by WT htt co-expression (Sun et al., 2001). Hence expansion of the htt polyQ tract, by reducing the association between mhtt and PSD-95, may effectively increase the amount of PSD-95 that is available for binding NMDARs (Sun et al., 2001). Not only would such an increase result in stabilized expression and enhanced function of NMDARs, but it could also sensitize mhtt-expressing cells to NMDAR-mediated toxicity by promoting NMDAR activity-dependent nitric oxide synthase activation and the initiation of toxic

downstream signaling events (Sattler et al., 1999).

Despite these findings, however, it remains unclear as to whether sensitization of PSD-95-over-expressing cells to mhtt-induced, NMDAR-dependent apoptosis indeed reflects an altered interaction between mhtt and PSD-95. Data from our own laboratory failed to reveal differences in the amount of PSD-95 associated with NMDARs in cortical or striatal tissue from YAC transgenic HD mice versus FVB/N WT mice (Cowan et al., 2005). Moreover, localization of PSD-95 at synapses precludes the involvement of this protein in mediating effects of mhtt on non-synaptically localized NMDARs. Instead, a putative role for actin-binding proteins in regulating NMDARs and in mediating the effects of mhtt on NMDAR function has been investigated as part of my research and will be discussed in greater detail in Chapter 4 of this thesis.

1.5.3. Phosphorylation of NMDARs

Apart from interactions with binding proteins and the CSK, NMDAR activity is also regulated in part by post-transcriptional and post-translational events. One of the most prominent post-translational modifications involves phosphorylation, and NMDAR subunits have been reported to undergo phosphorylation on both tyrosine and serine/threonine residues. Generally speaking, phosphorylation of NMDARs on tyrosine subunits by the Src family of non-receptor protein tyrosine kinases (SFKs; such as Src and Fyn) leads to increased NMDAR current and surface expression (Figure 3, point 2), while serine/threonine phosphorylation of NMDARs promotes forward trafficking of these receptors (Figure 3, point 3) (reviewed in Wang and Salter, 1994; Salter and Kalia, 2004; Wenthold et al., 2003; Prybylowski and Wenthold, 2004). Conversely, removal of phosphoryl groups from NMDAR subunits by protein tyrosine phosphatases causes an

activity-dependent reduction of surface NMDAR expression as well as decreased NMDAR current (Wang et al., 1996; Li et al., 2002; reviewed in Wang and Salter, 1994; Salter and Kalia, 2004; Prybylowski and Wenthold, 2004).

As mentioned earlier in this Introduction (see section 1.2.4), tyrosine-enriched motifs within the C-terminal tails of NR2 subunits play an important role in regulating receptor internalization and therefore the balance of NMDARs that are localized at the surface versus internally. Specifically, phosphorylation of Y837 in NR1 and the homologous residue Y842 in NR2A, as well as Y1472 in NR2B, decreases the binding of NMDARs to the clathrin adapter protein AP-2 (Roche et al., 2001; Vissel et al., 2001; reviewed in Prybylowski and Wenthold, 2004). Because AP-2 binding is necessary for clathrin-dependent endocytosis, reduced AP-2 binding results in stabilized NMDAR expression at the surface.

Interestingly, polyQ expansion in htt was shown to alter tyrosine phosphorylation on NR2B in at least one study; levels of tyrosine-phosphorylated NR2B (pY-NR2B) were significantly increased in transfected 293T or HN33 cells expressing htt-48Q, in comparison to htt-16Q-expressing cells (Song et al., 2003). Triply mutating the tyrosine residues on NR2B or treatment with a Src inhibitor had similar effects on htt-48Q-induced apoptotic death as did blocking NMDAR activity by the competitive inhibitor AP-5, suggesting NR2B phosphorylation by Src may play a role in mediating mhtt toxicity by sensitizing cells to excitotoxic stimuli (Song et al., 2003). Whether expression of mhtt in more physiologically relevant systems in fact modulates tyrosine phosphorylation status of NMDARs remains an issue of debate, however, since similar levels of tyrosine-phosphorylated NR2A and NR2B have been found in WT and R6/2 HD mice (Luthi-Carter et al., 2003).

Regulation by protein serine/threonine kinases has also been implicated in the

modulation of NMDAR trafficking and activity. Phosphorylation sites for the protein serine/threonine kinase, protein kinase C (PKC), have been identified on NMDAR subunits NR1, NR2A, and NR2B (Tingley et al., 1997; Leonard and Hell, 1997). PKC activation not only increased the amplitude of NMDAR currents, but also enhanced NMDAR channel open probability, in both *Xenopus* oocytes and neurons (Gerber et al., 1989; Chen and Huang, 1992; Xiong et al., 1998; Zheng et al., 1999; Lan et al., 2001). In addition, activation of PKC promoted delivery of new NMDARs to the cell surface via a soluble N-ethylmaleimide-sensitive fusion protein (NSF) attachment protein receptor (SNARE)-dependent exocytic pathway, although it was unclear whether direct phosphorylation of NMDARs by PKC was involved in this process (Lan et al., 2001).

Apart from the PKC phosphorylation sites at S890 and S896, the NR1 subunit is also phosphorylated on S897 by the cAMP-dependent protein serine/threonine kinase protein kinase A (PKA) (Tingley et al., 1997). Indeed, PKA activity has also been implicated in the regulation of NMDAR function (Raman et al., 1996; Westphal et al., 1999). Phosphorylation of NR1 at S896 by PKC and at S897 by PKA together suppresses the RXR ER retention signal within the C1 cassette and, in so doing, facilitates forward trafficking of NMDARs and their exit from the ER (Scott et al., 2001, 2003).

Studies attempting to find correlations between PKA activity and mhtt polyQ length have so far yielded conflicting results. While striatal MSNs from R6/2 mice displayed increased staining intensity for NR1-pS897 (Ariano et al., 2005), striatal tissue from N171-82Q HD mice expressed reduced levels of NR1-pS897 relative to WT littermates (Jarabek et al., 2004). Increased phosphorylation at either S896 or both S896 and S897 (through the use of an antibody that did not distinguish between the singly or dually phosphorylated forms) was noted in striatal tissue from YAC72 and YAC128 mice (C.

Cowan and L.A. Raymond, unpublished results), as well as in transiently transfected HEK293 cells over-expressing NMDARs along with htt-138Q (C. Sutton and L.A. Raymond, unpublished results). Hence the effects of htt polyQ expansion on NMDAR phosphorylation by PKA/PKC remain incompletely understood, with further work warranted to clarify the role that PKA/PKC may play in mediating mhtt-induced NMDAR-dependent toxicity, if any.

1.5.4. Other Possible Mechanisms of Modulation of NMDAR Activity by mHtt

While changes in single channel properties may contribute to altered NMDAR function, evidence from our laboratory suggested unaltered single channel conductance and open probability of receptors regardless of htt polyQ length (Chen et al., 1999b). Our investigation has therefore focused on other aspects of NMDAR regulation, such as changes in numbers of functional receptors.

NMDARs only become physiologically active once they are on the cell surface, either synaptically or extra-synaptically. Changes in receptor activity can therefore result not only from altered total expression of the protein, but also from perturbed surface expression and/or altered surface-to-internal ratio of distribution. To date however most studies have reported unchanged or decreased expression of NMDAR subunit proteins and mRNAs in a variety of cell line and mouse models of HD (Cha et al., 1999; Luthi-Carter et al., 2000; 2003; Li et al., 2003; Jarabek et al., 2004; Ali and Levine, 2006; the present study, see section 3.1). Therefore, a role for altered NMDAR surface expression in mediating the enhanced NMDA-induced current and toxicity remains to be explored.

1.6. Hypothesis and Rationale

The bulk of evidence amassed to date and discussed in the preceding sections suggests that, not only does expression of full-length mhtt render striatal neurons more intrinsically vulnerable to stress, it also augments NMDAR activity (especially that of the NR1/NR2B subtype) in these cells such that intracellular Ca^{2+} homeostasis is altered, degradative pathways involving catabolic enzymes are activated, and ROS are generated from dysfunctional mitochondria which undergo the mPT. To add further to neuronal damage and dysfunction, proteolytic cleavage of mhtt combines with aberrant nuclear targeting to disrupt cellular transcription as well as alter interactions of htt with other proteins, membranous organelles, and components of the UPS.

Given the amount of damage that polyQ-expanded htt can do even from the time of birth, it seems surprising that patients and animals carrying the *HD* gene do not succumb to disease any earlier than they do. In fact, neuronal loss is manifested close to the time of clinical onset, which usually occurs in middle age. On the basis of these and other findings, then, we postulate that expression of mhtt from the disease allele(s) leads to altered NMDAR function and changes in other cellular functions that deliver an excitotoxic yet sub-lethal insult to the neurons, even at birth. These changes, although insufficient on their own to cause cellular demise in young neurons, nevertheless render mhtt-expressing neurons sensitized to glutamatergic input and as such subject them to chronic excitotoxic damage.

Although cells that express mhtt will adapt to its toxic actions by triggering a program of compensatory self-defense pathways, these mechanisms will become less effective with increasing age. Likewise the UPS system, which normally performs the function of removing misfolded or otherwise toxic molecules from the cell, becomes

increasingly prone to failure as the neuron ages. Eventually the amount of damage done to the cell exceeds its capacity for repair and/or defense, and the cell becomes dysfunctional and dies.

In the face of the many therapies being tested in clinical trials which generally do not produce the same beneficial effects in human patients as they do in HD mice, a more thorough understanding of the pathways activated by mhtt underlying aberrant NMDAR signaling is absolutely required. The work in this thesis tests the following hypotheses: (1) potentiation of NMDA-induced current and toxicity as observed in the YAC HD mouse model (Zeron et al., 2002; Shehadeh et al., 2006) may be correlated with changes in surface NMDAR expression and/or altered receptor trafficking to/from the cell surface; (2) the interaction between the CSK-associated protein α-actinin 4 and HIP-1 as demonstrated in transfected HEK293 cells (C.D. Icton, 2001 M.Sc. thesis) may also be present in the striatum *in vivo* to facilitate a physical interaction between htt and NMDARs; and (3) co-expression of mhtt with NR1/NR2B-type NMDARs may lead to changes in the expression and/or distribution of several classes of proteins including protein kinases, protein phosphatases, and heat shock/stress-related proteins that impact cell function and vulnerability to apoptosis.

	Transgenic for N-terminal fragment of human mhtt			Transgenic for full-length human mhtt		Endogenous mouse htt with KI of polyQ sequence		
	R6/1, R6/2	N171	tgHD100	YAC46, YAC72, YAC128	flHD48, flHD89	CAG80	CAG94	*Hdh*Q92, *Hdh*Q111
References	1	2	3	4, 5	6	7	8	9
Promoter	Human	Prion	Rat NSE	Human	CMV	Murine	Murine	Murine
Transcript	Exon 1	cDNA for N-terminal 171aa	cDNA for N-terminal 3kb	All 67 exons	All 67 exons	CAG knock-in	CAG knock-in	CAG knock-in
# CAG repeats	120, 150	82	100	46, 72, 128	48, 89	80	94	92, 111
Striatal NMDAR protein expression	NR1 unchanged or increased, NR2A/NR2B decreased	NR2A transiently decreased	N.R.	NR1/NR2B unchanged in YAC46 or YAC72	N.R.	N.R.	N.R.	N.R.
Electrophysiological properties	Altered	N.R.	Altered	Altered	N.R.	N.R.	Altered	Altered
Hippocampal and/or striatal LTP/LTD	Altered	N.R.	N.R.	Altered	N.R.	Altered	N.R.	N.R.
Striatal NMDAR-current	Increased	N.R.	Increased	Increased	N.R.	N.R.	N.R.	N.R.
Striatal NMDAR-Ca^{++} or cell swelling response	Increased	N.R.	Increased	Increased	N.R.	N.R.	Increased	N.R.
Striatal NMDAR-mitochondrial membrane depolarization	N.R.	N.R.	N.R.	Increased	N.R.	N.R.	N.R.	N.R.
Cellular energy metabolism	N.R.	N.R.	N.R.	N.R.	Normal	N.R.	N.R.	Impaired
Striatal NMDAR toxicity	No change early, resistant late	Resistant late	Not different from WT	Increased; remains susceptible	N.R.	N.R.	N.R.	N.R.
Neuronal loss	No	No	Relatively small loss	Yes	Yes	No	N.R.	No
Aggregate formation	Widespread NIIs	NIIs and diffuse nuclear mhtt accumulation	NIIs	NIIs	Few NIIs	NIIs form late	No	NIIs

Table 1. Summary of referenced HD mouse models (adapted from Fan and Raymond, 2006). 1, Mangiarini et al., 1996; 2, Schilling et al., 1999; 3, Laforet et al., 2001; 4, Hodgson et al., 1999; 5, Slow et al., 2003; 6, Reddy et al., 1998; 7, Shelbourne et al., 1999; 8, Levine et al., 1999; 9, Wheeler et al., 2000. CMV, cytomegalovirus; NII, neuronal intranuclear inclusion; N.R., not reported; NSE, neuron-specific enolase; WT, wild-type. For other models, see www.hdfoundation.org/PDF/hdmicetable.pdf

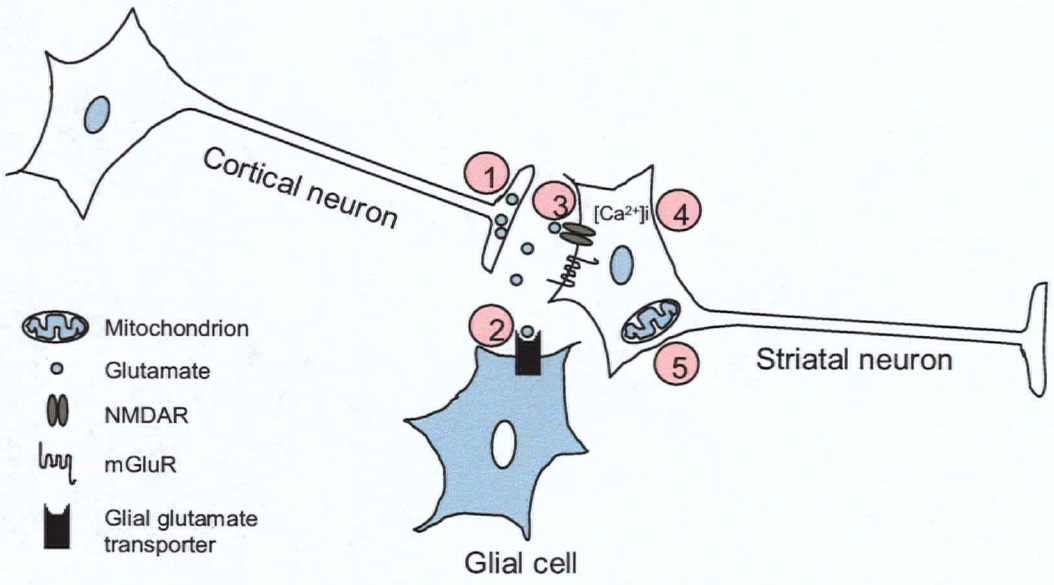

Figure 1. Cartoon of possible points along the corticostriatal pathway where dysfunction may contribute to excitotoxicity (Fan and Raymond, 2006). Excitotoxic neuronal death may result from a combination of: (1) increased glutamate release from cortical afferents; (2) reduced uptake of glutamate by glia; (3) hypersensitivity of post-synaptic NMDARs and/or augmentation of mGluR signaling; (4) altered intracellular calcium homeostasis; (5) mitochondrial dysfunction.

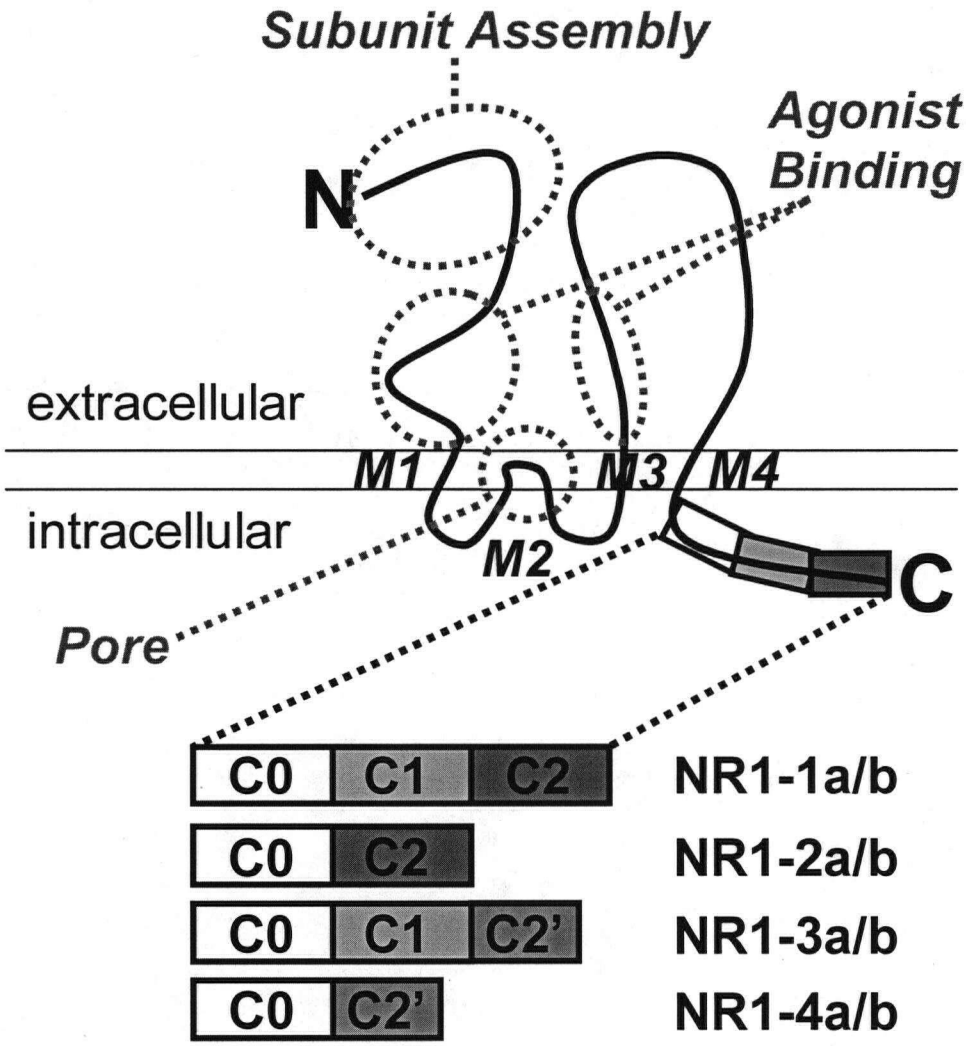

Figure 2. Cartoon of NR1 membrane topology and C-terminal splice variants. The pore-forming M2 re-entrant loop region and extracellular regions mediating subunit assembly and binding of agonist are shown for the NR1 subunit. The different combinations of alternatively spliced cassettes within the NR1 C-terminal tail are also illustrated.

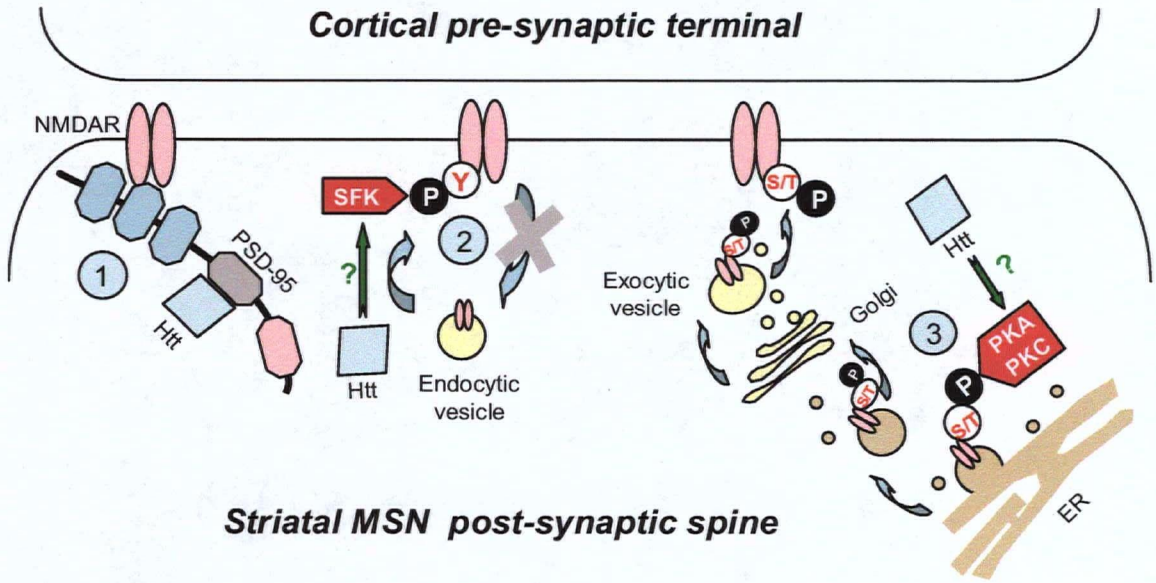

Figure 3. Cartoon of possible mechanisms underlying potentiation of NMDAR activity by mhtt (Fan and Raymond, 2006). Mutant htt may enhance NMDAR function by: (1) acting through PSD-95 to modulate NMDAR function; (2) increasing tyrosine phosphorylation of NMDARs by non-receptor tyrosine kinases, such as Src family kinases (SFKs), to stabilize surface receptor expression; (3) altering serine/threonine phosphorylation on NMDARs to modulate receptor function and/or promote forward trafficking from ER/Golgi.

CHAPTER 2. MATERIALS AND METHODS

2.1. Transgenic Mice

2.1.1. Breeding and Maintenance of Mice

Mice were bred from pairs of FVB/N WT mice or homozygous yeast artificial chromosome (YAC) transgenic mice on a pure FVB/N strain background (Hodgson et al., 1999; Slow et al., 2003; Leavitt et al., 2006). YAC46 (668 line), YAC72 (2511 line), and YAC128 (line 55) mice were used as models expressing full-length human mhtt containing 46, 72, or 128 polyQ repeats (46Q, 72Q, or 128Q). These were compared to FVB/N WT mice, or to YAC18 (212 line) that express full-length human htt with a non-pathogenic number (18Q) of polyQ repeats. All mice were bred and maintained in an enriched environment and according to Canadian Council on Animal Care (CCAC) guidelines.

2.1.2. Primary Culture of Mouse Striatal MSNs

Primary cultures of striatal MSNs were prepared as previously described (Zeron et al., 2002). Briefly, striatal tissue was dissected from postnatal day 0-1 (P0-P1) FVB/N WT, YAC18, YAC72, or YAC128 mice in ice-cold divalent-free Hanks' Balanced Salt Solution (HBSS; Invitrogen Canada Inc., Burlington, ON). Striata were manually cut into small pieces and incubated for ~10 minutes at 37 °C in HBSS containing ~40 units/ml papain before being transferred to neurobasal medium (NBM; Invitrogen Canada Inc.,

Burlington, ON) supplemented with 0.25% (w/v) bovine serum albumin (BSA), 0.25% (w/v) trypsin inhibitor, and 20 µg/ml DNAse. Cells were then dissociated by repeated passage through a graded series of Pasteur pipettes with successively smaller bore sizes, and were subsequently seeded onto 60-mm dishes or 24-well plates containing flame-sterilized 12-mm round glass coverslips (Paul Marienfeld GmbH & Co. KG, Lauda-Königshofen, Germany) that were pre-coated with 50 µg/ml lower molecular weight (MW 30,000-70,000) poly-D-lysine (PDL). Cells were seeded at a density of ~0.6 to 1 x 10^6 cells/ml and maintained in plating medium consisting of NBM supplemented with 2% (v/v) B27 (Invitrogen Canada Inc., Burlington, ON), 2 mM glutamine, and 100 units/ml penicillin-streptomycin (Invitrogen Canada Inc., Burlington, ON) in a humidified water-jacketed incubator at 37 °C 5% CO_2. Half of the existing medium was replaced with fresh medium at ~4 to 5 days *in vitro* (d.i.v.), and cells were used for experiments at 9-10 d.i.v. Under our striatal culture conditions, ~85% of cells showed features characteristic of MSNs while ~9% were astrocytes (Shehadeh et al., 2006).

2.1.2.1. Transfection of Cultured Striatal MSNs with Plasmid DNA

To introduce plasmid DNA into neurons, primary striatal MSNs cultured on PDL-coated glass coverslips were transfected using the calcium phosphate (CaP) method. To prepare for transfection, minimum essential medium (MEM) supplemented with L-glutamine (to 2 mM), sodium pyruvate (to 1 mM), penicillin-streptomycin (to 100 units/ml), fetal bovine serum (FBS; to 10%) and B27 (to 2%) (B27/MEM+ solution) was equilibrated at 37 °C 0-0.3% CO_2 for 10 minutes. Coverslips of cultured MSNs at 7 d.i.v. were then transferred to 60-mm dishes containing pre-equilibrated B27/MEM+ solution and incubated at 37 °C 0-0.3% CO_2 for 30 minutes prior to transfection. For analysis of

the effects of HIP-1 over-expression on NR1 surface expression, cells were co-transfected with plasmid DNA constructs encoding green fluorescent protein (GFP) and HIP-1, at 10 µg total DNA (comprising 5 µg each of GFP and HIP-1, or 10 µg of GFP alone as control) per 60-mm dish. Aliquots of plasmid DNA were prepared by mixing with $1/10^{th}$ volume of 3 M sodium acetate and three volumes of 100% EtOH. After brief centrifugation, plasmid DNA samples were topped up to 1400 µl final volume with 100% EtOH in a 1.5-ml microfuge tube and centrifuged for 20 minutes at 14,000 rpm at 4 °C to precipitate the DNA. The nucleic acid pellet was then resuspended in 225 µl of 0.1x Tris-EDTA buffer (0.1x TE: 2.5 mM Tris, 0.32 mM EDTA pH7.4), mixed with 25 µl of 2.5 M $CaCl_2$ and 250 µl of 2x BES solution (containing, in mM: 280 NaCl, 1.5 Na_2HPO_4, 50 BES pH6.96). The transfection mix was added to coverslips of MSNs in a 60-mm dish in 5 ml of B27/MEM+, at 500 µl per 60-mm dish of cells. Transfected cells were incubated for 2 to 3 hours at 37 °C 0-0.3% CO_2 until formation of calcium phosphate crystals became evident. At the end of transfection, neurons were washed three times with pre-warmed HBSS and replenished with conditioned medium before being transferred back to the 37 °C 5% CO_2 incubator. Transfection efficiency was assessed by fluorescence microscopy to identify GFP-expressing neurons at 24 hours following the start of transfection.

2.1.2.2. Immunofluorescent Staining and Quantification

Coverslips of striatal MSNs isolated from P0 or P1 mouse pups and cultured for 9-10 d.i.v. (with or without transfection of plasmid DNA at 7 d.i.v.) were rinsed in phosphate-buffered saline (PBS) and fixed for 15 minutes at room temperature in PBS containing 4% paraformaldehyde (PFA). For surface NR1 expression analysis, cells were then washed in PBS with gentle shaking prior to blocking in PBS containing 10%

normal goat serum (NGS) for 30 minutes, again at room temperature. In untransfected MSNs (to examine effects of htt polyQ expansion), surface NR1 was then labeled green by incubation with a mouse anti-NR1 extracellular M3-M4 loop domain primary antibody in PBS supplemented with 1% BSA for 1.5 hours followed by PBS washes and incubation with AlexaFluor 488 secondary antibody for 30 minutes at room temperature. In GFP- and GFP/HIP-1-transfected MSNs (to examine effects of HIP-1 over-expression), surface NR1 was labeled red instead by incubation with the same anti-NR1 antibody followed by a Cy3 secondary antibody. For this and all subsequent steps, cells were kept away from light. Following secondary antibody incubation, neurons were washed, permeabilized with PBS 0.5% Triton X-100 for 5 minutes at room temperature, and blocked again in PBS 10% NGS for another 30 minutes. Internal NR1 was then labeled with the same primary antibody as before, but followed by incubation with Cy3 secondary antibody in untransfected MSNs, or AlexaFluor 350 secondary antibody in GFP- and GFP/HIP-1-expressing MSNs, to label internal receptors red or blue, respectively.

In all other double immunostaining experiments, fixed neurons were washed in PBS prior to permeabilization in PBS 0.5% Triton X-100, washed again in PBS with gentle shaking, and then blocked in PBS containing 5% BSA for 30 minutes at room temperature. Subsequently, cells were incubated with primary antibodies dissolved in PBS with 2% BSA overnight at 4 °C, followed by incubation with a secondary antibody solution of 1:1000 AlexaFluor 488 anti-mouse and 1:800 AlexaFluor 594 anti-rabbit in PBS 2% BSA in the dark at room temperature for 1 to 2 hours (to label proteins of interest green and red, respectively).

All immunostained cells were washed with PBS before the coverslips were mounted onto glass slides using the Fluoromount reagent (Southern Biotechnology Associates, Inc., Birmingham, AL). Fluorescent images of cells at 630x magnification

were captured using a CCD camera mounted on a fluorescence microscope (Axiophot; Carl Zeiss, Thornburg, NY).

For surface NR1 expression analysis in untransfected MSNs to examine effects of htt polyQ expansion, the ratio of surface-to-internal NR1 signals was calculated and compared among FVB/N WT, YAC18, and YAC72 samples. Five independent experiments using different batches of cultures were performed, with samples from all 3 genotypes processed and analyzed in parallel within each experiment. In each of the 5 experiments, data was analyzed from 4 fields chosen at random in each of 5 coverslips for each genotype. Data from all 20 fields (4 fields per coverslip x 5 coverslips per genotype) were then pooled for each individual experiment.

To assess the effects of HIP-1 over-expression on the ratio of surface-to-internal NR1 expression, MSNs ectopically expressing either GFP alone or both GFP and HIP-1 were examined. In either condition, only green fluorescent cells (indicating successful transfection and expression of transgenes) were selected for analysis. Three independent transfections and experiments using different batches of cultures were performed, with samples from both conditions processed and analyzed in parallel within each experiment. In each of the 3 experiments, data was analyzed from 4 GFP- or GFP/HIP-1-transfected neurons.

To quantify NR1 expression on the surface or inside the cell, we measured intensity of NR1 staining of MSNs in both green and red channels (for untransfected MSNs), or red and blue channels (for GFP- and GFP/HIP-1-expressing MSNs), respectively. Images were exported into Northern Eclipse (Empix Imaging, Inc., Mississauga, ON), and fluorescence intensity was measured using custom-written software IDL 3.1 (T.H. Murphy, unpublished) for 12 selected sub-fields covering parts of the somata and processes of MSNs in each field. Background Intensities were

subtracted in each colour channel, and surface-to-internal ratio of NR1 expression calculated by dividing the green channel values by the red channel values in the case of untransfected MSNs, or dividing the red channel values by the blue channel values for GFP- and GFP/HIP-1-transfected MSNs. Data from all fields analyzed were then pooled for each individual experiment.

2.1.2.3. Chymotrypsin Assay

Striatal MSNs isolated from P0 or P1 mouse pups and cultured for 9-10 d.i.v. in 60-mm dishes were washed with HBSS. Sister dishes of neurons were treated with HBSS containing 1 mg/ml chymotrypsin or HBSS alone for 10 minutes at 37 °C before enzymatic activity was terminated by washing with 2 mM phenylmethylsulfonylfluoride (PMSF) in HBSS. Neurons were then harvested in 0.5 ml of ice-cold PBS and centrifuged at 14,000 rpm for 3 seconds. Cell pellets were resuspended in 100 ul PBS 1 mM EDTA/1 mM EGTA containing 1% Triton X-100 and supplemented with protease inhibitors and phosphatase inhibitors. Proteins were solubilized by sonication with a Sonicator™ Cell Disruptor model W-10 (from formerly Heat Systems Ultrasonics, now Misonix, Inc., Farmingdale, NY) for 5-10 seconds at setting 3 followed by end-over-end rotation at 4 °C for 30 minutes. The total soluble lysate was collected and quantified for protein concentration using the bicinchoninic acid (BCA) assay (Pierce Biotechnology, Inc., Rockford, IL), and equivalent amounts of proteins from each sample were resolved by sodium dodecyl sulfate-polyacrylamide gel electrophoresis (SDS-PAGE) and subjected to immunoblotting. Surface expression of NR1 or NR2B was calculated by subtracting the band density of the chymotrypsin-treated lane (representing the

chymotrypsin-resistant or internal pool of NR1 or NR2B) from that of the untreated lane (representing total NR1 or NR2B expression).

2.1.2.4. Biotinylation Assays

2.1.2.4.1. To Examine NR1/NR2B Surface Expression

Biotinylation was carried out according to a protocol modified from Ehlers, 2000 and Lin et al., 2000. Striatal MSNs cultured for 9 d.i.v. in 60-mm dishes were gradually pre-cooled to 4-10 °C to halt biological processes within the cell. Cells were washed twice with ice-cold PBS, and surface proteins were labeled with biotin by incubation in 1.5 mg/ml NHS-SS-Biotin (Pierce Biotechnology, Inc., Rockford, IL) in PBS supplemented with 0.1 mM $CaCl_2$ and 1 mM $MgCl_2$ at 2 ml/dish for 12 minutes at 4-10 °C. Excess biotin label was subsequently removed by two washes of 0.1% BSA in PBS containing 0.1 mM $CaCl_2$ and 1 mM $MgCl_2$ before cells were scraped into Harvest Buffer (HB: PBS 1 mM EDTA/1 mM EGTA supplemented with protease inhibitors) at 1 ml/dish of cells. Following centrifugation at 14,000 rpm for 3 seconds, the supernant was removed and the cell pellet resuspended in 125 µl Solubilization Buffer (SB: HB containing 1% Triton X-100). Proteins were solubilized by sonication for 8 seconds at setting 3, followed by end-over-end rotation for 30 minutes at 4 °C. During this time, NeutrAvidin biotin-binding resin (Pierce Biotechnology, Inc., Rockford, IL) was prepared as 100-µl aliquots of a 50%-slurry and equilibrated by resuspension in 20x bed volumes (1 ml) of SB with end-over-end rotation for 30 minutes at 4 °C. Following 2 minutes of centrifugation at 14,000 rpm, the SB wash was removed leaving behind ~50 µl of NeutrAvidin resin. Following solubilization of the total lysate, samples were centrifuged at 4 °C for 20

minutes at 14,000 rpm. From the total soluble lysate, 20% (25 µl) of the volume was set aside as the "lysate" sample. The remainder (80% or 100 µl) was added to 50µl of pre-equilibrated NeutrAvidin biotin-binding resin and incubated with end-over-end rotation for 2-3 hours at 4 °C. Samples were then centrifuged at 4 °C for 2 minutes at 14,000 rpm. From the supernatant, 25% (25 µl) was saved for SDS-PAGE and the rest was removed. The resin was subsequently washed four times with SB at 1 ml per sample per wash, and bound biotin-tagged proteins were eluted from the washed resin by end-over-end rotation in 60 µl of 3x protein sample buffer (3x PSB; contains 465 mM DTT added fresh at time of use, Pyronin Y red dye, 6% SDS, and 30% glycerol in 385 mM Tris-Cl pH6.8) for 30 minutes at 4 °C. Samples were then heated for 1 minute at 95-100 °C before being resolved by SDS-PAGE and subjected to immunoblotting. The biotinylation eluate fraction represents the portion of proteins present on the cell surface during the biotin labeling step which has not yet undergone proteasomal or lysosomal degradation.

2.1.2.4.2. To Examine Loss of NR1/NR2B from the Cell Surface

Figure 4 outlines the steps involved in this procedure. Striatal MSNs cultured for 9 d.i.v. in 60-mm dishes were processed and treated with biotinylation reagent as described above for examining NR1/NR2B surface expression. Following removal of excess biotin label by two washes of 0.1% BSA in PBS containing 0.1 mM $CaCl_2$ and 1 mM $MgCl_2$, cells were replaced in conditioned medium. To assess the rate of surface NR1 degradation, sister dishes of cells were treated in parallel and returned to the 37 °C 5% CO_2 incubator for 0, 12 or 24 hours before the cells were harvested by scraping into HB. Proteins were

then solubilized and biotin-tagged proteins isolated as described above. Samples were then resolved by SDS-PAGE and subjected to immunoblotting.

2.1.2.4.2.1. Blocking Degradation by Lysosomal Inhibition

The biotinylation assay was carried out as described above for the degradation assay, but with the addition of 100 µg/ml leupeptin (lysosome inhibitor; EMD Biosciences, Inc., San Diego, CA) to the culture medium one hour prior to biotin-labeling.

2.1.2.4.3. To Examine NR1/NR2B Insertion Using Chlorpromazine to Block Endocytosis and Recycling

Figure 5 outlines the steps involved in this procedure. Sister 60-mm dishes of cultured striatal MSNs at 9-10 d.i.v. were treated with the endocytosis and recycling inhibitor chlorpromazine (Wang et al., 1993; Zhu et al., 2005; Veyhl et al., 2006) for 0, 0.5, or 6 hours at 37 °C 5% CO_2. At the concentration used (10 µM), cells retained a healthy appearance up to 6 hours following treatment, while higher concentrations of drug were noted in pilot studies to cause significant morphological changes and detachment of MSNs from the culture dish over the same time period. At each time point, one dish of neurons was gradually pre-cooled to 4-10 °C to halt biological processes within the cell. Cells were washed twice with 4-10 °C PBS before surface proteins were biotin-tagged by incubation with 1.5 mg/ml NHS-SS-Biotin (Pierce Biotechnology, Inc., Rockford, IL) in PBS supplemented with 0.1 mM $CaCl_2$ and 1 mM $MgCl_2$ at 2 ml/dish for 12 minutes at 4-10 °C. Excess biotin label was removed by two washes with 0.1% BSA in PBS containing 0.1 mM $CaCl_2$ and 1 mM $MgCl_2$ and a third wash in ice-cold PBS. Cells were

then harvested and samples processed as for the surface expression and receptor loss assays as described above, followed by resolution by SDS-PAGE and immunoblotting. The biotinylation eluate fraction represents the portion of proteins present on the cell surface during the biotin labeling step.

2.1.2.5. NMDAR-Dependent Toxicity Assay

2.1.2.5.1. Induction of Toxicity

Sister coverslips of striatal MSNs from FVB/N WT, YAC72, or YAC128 mice were cultured in 24-well plates. At 9 d.i.v., neurons were exposed in parallel to vehicle dimethyl sulfoxide (DMSO) or the CK2 inhibitor 5,6-dichlorobenzimidazole riboside (DRB; final 100 μM) dissolved in DMSO and added to culture medium for 2 hours before co-treatment with either balanced salt solution (BSS; contains, in mM: 139 NaCl, 3.5 KCl, 2 $NaHCO_3$, 3 Na_2HPO_4, 10 HEPES, 11 D-glucose, 1.8 $CaCl_2$, 0.05 glycine pH ~7.35-7.40) alone (controls) or 1 mM NMDA in BSS for 10 minutes. Neurons were then washed twice with fresh culture media at 0.5 ml/well before conditioned media was added back, for incubation at 37 °C 5% CO_2 for 24 hours in the continued presence of DRB or vehicle DMSO. Subsequently, cells on coverslips were washed once in PBS, fixed for 1 hour in PBS with 4% PFA, washed three times 5 minutes each in PBS, and then stored to 4 °C in PBS containing 0.02% azide until terminal deoxynucleotidyl transferase (TdT)-mediated dUTP nick end labeling (TUNEL) was performed.

2.1.2.5.2. Analysis of Apoptotic Death

Fixed MSNs treated with NMDA in the presence or absence of CK2 inhibitors were permeabilized by treatment with PBS containing 0.25% Triton X-100 and 0.5% sodium citrate for 2 minutes on ice. Background ribonucleic acid staining was minimized by incubating with 16 µg/ml RNase for 30 minutes at room temperature. Following three washes with PBS at 0.5 ml/well per wash, nicked DNA indicative of apoptotic processes was stained by incubation of the neurons with the TUNEL reagent (Roche Diagnostics Corporation, Basel, Switzerland; 9 parts label to 1 part enzyme) at 17.5 µl per coverslip for 1 hour at 37 °C in a parafilm- and foil-wrapped 24-well plate. Following a brief rinse in PBS, neuronal nuclei were counterstained by 8 µM propidium iodide (PI) in PBS for 15 minutes at room temperature. Coverslips were then washed three more times in PBS and then mounted onto glass slides using the Fluoromount reagent. Fluorescent images of cells were captured using a CCD camera mounted on a Zeiss Axiophot microscope connected to a computer with Northern Eclipse software. Cells were scored as apoptotic only if they appeared to be positive for TUNEL staining and displayed small, condensed and blebbed nuclei, as visualized with PI. In any single experiment for each of the 3 genotypes, over 1500 neurons were counted in each treatment condition. The percentage of apoptotic nuclei after NMDA treatment was calculated by first subtracting the percentage of apoptotic cells in the corresponding control condition (i.e., DMSO or DRB in the absence of NMDA). Three independent experiments—each employing a different batch of cultured neurons—were performed for each genotype.

2.1.3. Harvesting Tissue

Tissue was harvested from FVB/N WT and transgenic YAC mice for a variety of purposes including analysis of protein expression, subcellular fractionation, and immunoprecipitation.

2.1.3.1. Immunoblot Analysis

Immunoblotting for proteins of interest was done according to standard protocols. Briefly, protein samples resolved by SDS-PAGE were transferred by wet electrophoresis onto Immobilon polyvinylidene difluoride (PVDF) membranes (Millipore, Billerica, MA). Membranes were then wetted in methanol, equilibrated in water and Tris-buffered saline (TBS), and then blocked for 2 hours in TBS containing 0.5% Tween-20 and 3% (w/v) BSA. Following a brief rinse in TBS 0.5% Tween-20 (TBS-T), membranes were incubated with primary antibody dissolved in the blocking solution typically for 1 to 2 hours with shaking at room temperature and then overnight at 4 ^{o}C. Membranes were then washed three times in TBS-T, incubated for 45 minutes at room temperature with the appropriate horseradish peroxidase-coupled secondary antibody in blocking solution, washed again, and visualized by the addition of the enhanced chemiluminescence (ECL) reagents (Amersham Biosciences, Piscataway, NJ) and exposure on film.

2.1.3.2. Examination of NR1/NR2B Expression in Mice of Different Ages

For analysis of NMDAR protein expression in the YAC mouse model, tissue from striata of 2, 6, 9, or 12 month-old FVB/N WT and YAC transgenic mice was harvested in

10x volumes of pre-chilled radioimmunoprecipitation (RIPA) buffer (50mM Tris pH7.6/150mM NaCl/1mM EDTA/1% Nonidet P-40 (NP-40)/0.5% deoxycholate/0.1% SDS), homogenized with 8 strokes at 2000 rpm using a Caframo stirrer-type R2R1-64 homogenizer (VWR International, Mississauga, ON), and quantified for protein concentration using the BCA assay. Equal amounts of protein were then resolved by SDS-PAGE and probed by immunoblotting for the relative expression of NR1 and NR2B in striatal tissue from FVB/N WT and YAC transgenic mice.

2.1.3.3. Examination of Protein Expression in Mouse Tissue to Follow Up on Kinetworks™ Results

For analysis of protein expression in mouse tissue to confirm Kinetworks™ screening results, cytosolic and particulate fractions were obtained from striatal tissues (pooled from two male animals in each N) of 2 month-old FVB/N WT, YAC72, and YAC128 mice, according to a modified protocol based on guidelines from Kinexus Bioinformatics Corp. (www.kinexus.ca). Tissues were microdissected and isolated into ice-cold detergent-free buffer supplemented with phosphatase inhibitors and protease inhibitors (DF buffer pH 7; contains in mM: 20 MOPS, 2 EGTA, 5 EDTA, 30 NaF, 40 β-glycerophosphate, 10 sodium pyrophosphate, 2 sodium orthovanadate, 1 PMSF, 0.005 pepstatin A, 0.01 leupeptin) at ~4 ml per gram of wet tissue mass (or ~400 µl for striatal tissue from 2 mice). Following homogenization for 30 seconds at 2000 rpm on ice, the lysate was centrifuged for 30 minutes at 4 °C at 100,000 x g and the resulting supernatant collected as the cytosolic fraction. The pellet was then resuspended in DF buffer supplemented with 0.5% Triton X-100 (TX buffer), also at ~4 ml per gram of initial tissue mass, before being sonicated with two 15-second pulses and centrifuged at 100,000 x g

for 30 minutes to obtain the particulate fraction (supernatant). Equivalent amounts of protein from cytosolic and particulate fractions of striatal tissues were resolved by SDS-PAGE and compared between FVB/N WT, YAC72, and YAC128 mice for the expression of the serine/threonine kinase CK2.

2.1.3.4. Subcellular Fractionation

Tissue from mouse striatum was subjected to biochemical fractionation based on a protocol modified from Dunah and Standaert (2001) and Hell and Jahn (1994). Striatal tissue was isolated and pooled from FVB/N WT or YAC72 mice (10 animals of each genotype were used for two sets of fractionations, and 30 animals each were used in a third set of fractionations), in each case from two or more litters, at 2 months of age. Tissue was homogenized with 9 strokes at 900 rpm in ice-cold homogenization buffer (HomogB; containing, in mM: 1 EGTA, 320 sucrose, 4 HEPES pH7.4) supplemented with protease inhibitors, using roughly 10 ml HomogB per gram of wet brain tissue (around 15 ml for striatal tissue from 30 mice). Homogenate was then centrifuged for 10 minutes at 1,000 x g to obtain fractions P1 and S1. S1 was further centrifuged for 15 minutes at 12,000 x g to isolate S2 and P2, the crude synaptosomal fraction. P2 was then resuspended in HomogB to two-thirds of the initial volume and centrifuged for 15 minutes at 13,000 x g to give S2' and a washed crude synaptosomal fraction P2'. The pellet was resuspended in HomogB to one-tenth of the initial volume, diluted with 9x volumes of ice-cold water, and lysed hypo-osmotically with 3 strokes at 2,000 rpm. HEPES-NaOH pH 7.4 was then added to ~8.5 mM final concentration, and the lysed P2' was then centrifuged for 20 minutes at 33,000 x g to give LP1 (heavy/synaptosomal membrane fraction) and LS1 (cytoplasm of lysed synaptosomes). LS1 and S2 were centrifuged at

165,000 x g for 2 hours to isolate LS2 (pre-synaptic cytosol)/LP2 (synaptic vesicle-enriched fraction) and S3 (cytosol)/P3 (light membrane/microsome-enriched fraction), respectively. A schematic summarizing the subcellular fractionation steps is shown in Figure 6. Fractions were then quantified for protein content, resolved by SDS-PAGE, and subjected to immunoblotting to determine the subcellular distribution of the proteins of interest.

2.1.3.5. Immunoprecipitation

2.1.3.5.1. From Mouse Forebrain Tissue

Forebrain tissue was isolated from ~2 month-old FVB/N WT or YAC72 mice and homogenized with 8 strokes at 2,000 rpm in lysis buffer containing 50 mM Tris pH9 and 1% deoxycholate with 1 mM EDTA and 1 mM EGTA, supplemented with phosphatase inhibitors and protease inhibitors, at 7 ml for ~0.4 g wet brain tissue (or ~7 ml per mouse forebrain). The homogenate was incubated for 15 minutes at 4 °C with end-over-end rotation before centrifugation at 50,000 x g for 15 minutes. The resulting supernatant ("lysate") was used for immunoprecipitation (IP) at 400 µl per sample. For each sample, 10 µg of primary antibody were added to the lysate and allowed to incubate for 1 hour at 4 °C with slow end-over-end rotation. Sixty microliters of a 50%-slurry containing a mixture of pre-equilibrated Protein A and Protein G Sepharose 4 Fast Flow resin (from formerly Amersham Pharmacia Biotech, now part of GE Healthcare Bio-Sciences Inc., Baie d'Urfe, QC) were then added and samples were incubated for an additional hour. Subsequently, samples were centrifuged briefly at 5,000 rpm and the pelleted resin washed four times in 1x Tris Wash Buffer (TWB; containing, in mM: 1 EDTA, 1 EGTA, 150 NaCl, 50 Tris pH7.4

and 1% Triton X-100) to reduce non-specific binding. The washed resin was then resuspended in 3x PSB and heated at 95-100 °C for 3-5 minutes in preparation for resolution by SDS-PAGE.

2.1.3.5.2. From Mouse Striatal Tissue

Striatal tissue was isolated from ~2 month-old FVB/N WT or YAC72 mice. Tissue was pooled from two male mice from each genotype in 2.4 ml HB supplemented with protease inhibitors and phosphatase inhibitors. Following homogenization with 8 strokes at 2,000 rpm, tissue samples were centrifuged for 5 minutes at 5,000 rpm. Supernatants were removed and the tissue pellets solubilized in lysis buffer containing either 1% NP-40/150 mM NaCl/50 mM Tris pH8 or PBS 1 mM EDTA/1 mM EGTA/0.2% SDS/0.8% Triton X-100, supplemented with phosphatase inhibitors and protease inhibitors, at 2.4 ml per sample (pooled from two pairs of striata). DNAse was added to a final concentration of 100 µg/ml, and the lysate was sonicated in two 10-second bursts at setting 3. Forty microliters from the solubilized sample was saved as "lysate", and IP was performed using 300-360 µl per sample. Each IP sample was first pre-cleared by incubation with 10 µl each of 50%-slurries of pre-equilibrated Protein A and Protein G Sepharose 4 Fast Flow resin for 1 hour at 4 °C with slow end-over-end rotation. Samples were then centrifuged briefly to sediment the resin, and pre-cleared lysates were transferred to fresh tubes containing 10 µg of primary antibody and rotated end-over-end for an additional hour. Subsequently, 15 µl each of Protein A and Protein G slurries were added to each IP sample for overnight incubation with end-over-end rotation at 4 °C. Samples were then centrifuged for 1 minute at 5,000 rpm, and the resins with bound antibody and proteins were washed five times in 1x TWB at 500 µl per sample per wash. Proteins associated

with the washed resin were then eluted by resuspending the resin in 45 µl of 3x PSB and heating at 95-100 °C for 3-5 minutes in preparation for resolution by SDS-PAGE.

2.2. HEK293 Cell Line

2.2.1. Passaging and Maintaining Cell Line

Human embryonic kidney (HEK) 293 cells were cultured as previously described (Chen et al., 1997). Briefly, cells were maintained in "MEM+", or MEM supplemented with Earle's salts, L-glutamine (to 2 mM), sodium pyruvate (to 1 mM), penicillin-streptomycin (to 100 units/ml), and fetal bovine serum (FBS; to 10%) at 37 °C 5% CO_2 in a humidified incubator. HEK cells were generally passaged every 2 to 3 days and seeded at ~1 to 2 x 10^6 cells per 10-cm culture dish.

2.2.2. Transfection of Cell Line with Plasmid DNA

For transfection of HEK293 cells by the CaP method, cells were seeded 9 to 12 hours prior to transfection at a density of ~1 to 2 x 10^6 cells per dish in 10-cm culture dishes pre-coated with 10 µg/ml higher molecular weight (MW 70,000-150,000) PDL. To prepare for transfection, aliquots containing 10-15µg of one or more plasmid DNAs were prepared by mixing with 1/10^{th} volume of 3 M sodium acetate and three volumes of 100% EtOH. For immunoprecipitation studies, each 10-cm dish of HEK cells was transfected with 5 µg each of cDNA plasmid encoding rat NR1 and NR2B subunits. For analysis of protein expression in cells over-expressing WT versus mutant htt, each 10-cm dish of HEK cells was transfected with 3 µg each of cDNA plasmid encoding rat NR1 and NR2B

along with 6 µg of plasmid DNA encoding full-length human htt with a polyQ repeat length of either 15 (htt-15Q; WT) or 138 (htt-138Q; mutant) residues. After brief centrifugation, plasmid DNA samples were topped up to 1400 µl final volume with 100% EtOH in a 1.5-ml microfuge tube and centrifuged for 20 minutes at 14,000 rpm at 4 °C to precipitate the DNA. The nucleic acid pellet was then resuspended in 450 µl of 0.1x TE, mixed with 50 µl of 2.5 M $CaCl_2$ and 500 µl of 2x BES solution, and allowed to sit at room temperature for 20 minutes. Cells to be transfected were transferred to a humidified 37°C 3% CO_2 environment and incubated for 20 minutes. Subsequently, the transfection mix was added to existing media at 1 ml per 10-cm dish of cells. Transfected cells were incubated for 8 hours at 37 °C 3% CO_2 before being washed twice with pre-warmed PBS and replenished with fresh medium. Cells were then transferred back to the 5% CO_2 incubator until they were harvested for experiments at 24 hours following the start of transfection. Transfection efficiency was determined by measuring β-galactosidase activity in a separate 10-cm dish transfected in parallel with 10 µg of β-gal plasmid cDNA, and further experiments were conducted only if transfection efficiency exceeded 50%.

2.2.2.1. β-Galactosidase Staining to Determine Transfection Efficiency

Cells transfected with plasmid DNA encoding β-galactosidase were examined for β-galactosidase activity as a measure of transfection efficiency. At 24 hours following start of transfection by the CaP method, cells were washed once with 5 ml of pre-warmed PBS before being fixed in PBS containing 0.4% glutaraldehyde and 2% formaldehyde for 5 minutes at room temperature. Following fixation, cells were washed three times with PBS and then stained with PBS containing 2 mM $MgCl_2$, 5 mM $K_3[Fe(CN)_6]$, 5 mM

$K_4Fe(CN)_6.3H_2O$, and 0.5 mg/ml X-gal (from formerly Molecular Probes, now part of Invitrogen Canada Inc., Burlington, ON) dissolved in DMSO and added fresh immediately prior to use. Stained dishes of cells were wrapped in parafilm and incubated at 37 °C for 1 hour before cell counts were performed. As cells expressing β-galactosidase react with the substrate X-gal to generate a blue colour, the number of blue cells were counted and calculated as a percentage of the total number of cells to determine transfection efficiency.

2.2.3. Immunoprecipitation

Ten-centimeter dishes of HEK293 cells transfected in duplicate with NR1/NR2B cDNA were harvested at 24 hours following start of transfection in lysis buffer containing PBS 1 mM EDTA/1 mM EGTA/0.2% SDS/0.8% Triton X-100 and supplemented with phosphatase inhibitors and protease inhibitors, at 500 µl per 10-cm dish of cells. Proteins were solubilized by sonication for 10 seconds at setting 3, and the homogenate was incubated for 30 minutes at 4 °C with end-over-end rotation before brief centrifugation at 14,000 rpm to pellet cellular debris. The resulting supernatants ("lysates") were pooled from duplicate dishes and used for IP at 300-400 µl per sample. For each sample, 5-10 µg of anti-NR2B primary antibody were added to the lysate and allowed to incubate for 1-2 hours at 4 °C with slow end-over-end rotation. Sixty microliters of a 50%-slurry containing a mixture of pre-equilibrated Protein A and Protein G Sepharose 4 Fast Flow resin were then added and samples were incubated for an additional hour. Subsequently, samples were centrifuged briefly at 5,000 rpm and the pelleted resin washed three times in 1x TWB to reduce non-specific binding. The washed resin was then resuspended in 3x PSB and heated at 95-100 °C for 3-5 minutes in preparation for resolution by SDS-PAGE.

2.2.4. NMDAR Stimulation of Transfected Cells

In certain experiments where cytosolic and particulate fractions were to be collected from NR1/NR2B/htt-15Q- or NR1/NR2B/htt-138Q-transfected HEK293 cells to examine effects of NMDAR activation, dishes of transfected cells were stimulated with NMDAR agonists prior to harvest in DF buffer. At 24 hours after transfection, culture medium was replaced with BSS or with physiological solution (PS; containing, in mM: 1.8 $CaCl_2$, 145 NaCl, 5.4 KCl, 11 D-glucose, 10 HEPES pH 7.3), with or without 1 mM NMDA/50 μM glycine for the "plus NMDAR stimulation" or "minus NMDAR stimulation" conditions, respectively. Following incubation of the cells at 37 °C 5% CO_2 for 30 minutes, cells were washed and harvested in DF buffer. Cytosolic and particulate fractions of pooled cell lysates were then harvested as described in the next section. Alternatively, in experiments where total cellular expression was measured, total soluble lysates were collected directly in TX buffer and harvested, again as described in the following section. Equivalent amounts of protein from cytosolic and particulate fractions or total soluble lysates of each condition (expressing htt-15Q or htt-138Q; with or without NMDAR stimulation) were resolved by SDS-PAGE and examined for the proteins of interest by immunoblotting.

2.2.5. Harvesting Cells for Kinetworks™ or Immunoblotting Analysis

Dishes of HEK293 cells were transfected in parallel for the WT and mutant conditions (with 3/3/6 μg of NR1/NR2B/htt-15Q or NR1/NR2B/htt-138Q plasmid DNAs, respectively) using the CaP method. In the same experiment, a control dish of cells was transfected with the β-galactosidase plasmid DNA and stained with X-gal at 24 hours

post-transfection to determine the efficiency of transfection. Experiments were continued only when more than 50% of the cells were transfected and expressing the transgenes. Harvest of cytosolic and particulate fractions from cell lysates was carried out according to a modified protocol based on guidelines from Kinexus Bioinformatics Corp. (Vancouver, BC; website at www.kinexus.ca). Briefly, cell lysates were pooled and harvested at 24 hours following the start of transfection in DF buffer at roughly 100 µl per 10^6 cells (or ~200-300 µl per 10-cm dish of cells at medium density). Samples in DF buffer were sonicated with two 15-second bursts at setting 3 with a 3-second inter-burst pause on ice. Lysates were then subjected to ultracentrifugation for 30 minutes at 4°C at 100,000 x g. The resulting supernatant was saved as the cytosolic fraction and the pellet resuspended in TX buffer at roughly half the initial volume of DF buffer used (~100-150 µl per 10-cm dish of cells). The pellet fraction was then mixed, sonicated, and centrifuged for 30 minutes at 100,000 x g as described above. The supernatant from this step was also saved and represented the particulate fraction containing detergent-soluble proteins. Total soluble fractions were harvested directly in TX buffer (instead of DF buffer) but were otherwise processed in the same way. All fractions were quantified for protein content using the BCA assay before being diluted in 4x Kinetworks™ PSB (containing 5% β-mercaptoethanol added fresh at time of use, 0.08% Bromophenol blue dye, 4% SDS, and 50% glycerol in 125 mM Tris-Cl pH6.8) and subjected to standard immunoblotting or Kinetworks™ multi-immunoblotting analyses.

Cytosolic and particulate fractions from HEK293 cells transfected with NR1/NR2B/htt-15Q or NR1/NR2B/htt-138Q (the "htt15" and "htt138" conditions, respectively) were analyzed by Kinetworks™ KPKS 1.0 Protein Kinase, KPPS 1.0 Protein Phosphatase, and KHSP 1.0 Heat Shock Protein screens. Analysis involves resolution of the lysate sample by SDS-PAGE and subsequent immunoblotting with up to three

primary antibodies per channel in a 20-channel multiblotter. Mixtures of antibodies used in a given channel were tested to rule out cross-immunoreactivity with other target proteins to be probed for in the same channel. Detailed information and protocols of the Kinetworks™ analyses have also been published previously (Pelech et al. 2003).

2.3. E. Coli Bacteria

2.3.1. Transformation with Plasmid DNA

For the purification of plasmid DNA from a pre-existing DNA stock, Subcloning Efficiency™ DH5α heat-shock competent *E. coli* bacteria (Invitrogen Canada Inc., Burlington, ON) were thawed on ice-water. 1-2 µl of plasmid stock was added to a 50-µl aliquot of competent bacteria and incubated on ice for 30 minutes before being heat shocked for 20 seconds at 37 °C. Cells were immediately placed on ice for 2 minutes following heat shock, and then diluted with 950 µl Luria broth (LB) bacterial medium (in g/L: 10 peptone/tryptone, 5 yeast extract, 10 NaCl) prior to incubation for 1 hour at 37 °C with vigorous shaking at 225 rpm. Cells were subsequently centrifuged for 5 minutes at 4,000 rpm, and the bacterial pellet resuspended in 100 µl of fresh LB medium. One, 10, and 90 µl of the bacteria were plated onto LB agar plates supplemented with the appropriate antibiotic to select for bacteria successfully transformed with the plasmid DNA.

2.3.2. Purification of Plasmid DNA

Bacteria transformed with plasmid DNA or smeared from a frozen glycerol stock were streaked onto LB agar plates containing the appropriate selective antibiotic and allowed to grow overnight at 37 °C. A single colony of bacteria was picked to inoculate a starter culture of 2 ml of antibiotic-containing fresh LB medium. Starter cultures were grown for ~8-12 hours at 37 °C with vigorous shaking at 250-300 rpm, and then diluted into 500 ml of selective LB medium. The diluted culture was further incubated at 37 °C for 12-16 hours (usually overnight) with vigorous shaking and aeration in a 2-L flask. To prepare frozen glycerol stocks of bacteria carrying plasmid DNA, 1 ml of bacterial culture is mixed with 250 µl of sterile glycerol to generate a 20% glycerol stock to be stored at -80 °C. The rest of the plasmid-containing bacterial culture grown overnight was then harvested by centrifugation at 6,000 x g for 15 minutes at 4 °C. Plasmid DNA was purified using Qiagen (Mississauga, ON) Plasmid Maxi™ or EndoFree Plasmid Maxi™ purification kits according to the manufacturer's protocol. Purified plasmids precipitated with 70% EtOH were then allowed to air-dry before being dissolved in sterile tissue-culture grade H_2O. Concentrations of the resultant plasmid DNAs were determined by optical density (OD) measurements at 260 nm (OD_{260}) in an Ultrospec 3000 UV/Visible Spectrophotometer (from formerly Pharmacia Biotech, now part of GE Healthcare Bio-Sciences Inc., Baie d'Urfe, QC), and DNA purity was assessed by calculating the ratio of OD_{260} to OD_{280} measurements.

2.3.3. Purification of GST-Fusion Proteins from Bacteria

Glutathione-S-transferase (GST) and GST-fusion proteins were expressed in DH5α or BL21 *E. coli* and purified according to the pGEX vector manufacturer's protocol (from formerly Pharmacia Biotech, now part of GE Healthcare Bio-Sciences Inc., Baie d'Urfe, QC). Briefly, overnight starter cultures of bacteria carrying inducible vectors encoding for GST, GST-HIP1 (GST fused to full-length HIP-1), or GST-HIP1-Talin (GST fused to the HIP-1 talin domain) were each used to inoculate 200 ml of 2x YT bacterial medium (in g/L: 16 tryptone/peptone, 10 yeast extract, 5 NaCl), which was then allowed to grow at 37 °C with shaking and aeration until an OD_{600} of ~0.5 was reached. Isopropyl thiogalactoside (IPTG) was then added to a final concentration of 0.2 mM to induce expression of GST and GST-fusion proteins. Bacteria were harvested at 3 hours after induction by centrifugation at 7,200 rpm for 10 minutes at 4 °C. Following removal of the supernatant, the bacterial pellet was resuspended in 10 ml of ice-cold PBS containing protease inhibitors, lysed by treatment with lysozyme at ~1 mg/ml and end-over-end rotation for 15 minutes at room temperature, sonicated with two 30-second bursts on ice, and solubilized with Triton X-100 (at 1% final concentration). The solution was then rotated end-over-end for 30 minutes at 4 °C prior to centrifugation for 10 minutes at 9,400 rpm. The soluble lysate was subsequently supplemented with 2 mM ATP and 10 mM $MgSO_4$ in a 50 mM Tris-Cl pH8 solution and incubated at 37 °C for 10 minutes with occasional mixing, in order to reduce the presence of contaminating bacterial proteins in the final eluate. GST and GST-fusion proteins were then purified by incubation for 1 hour at 4 °C or 30 minutes at room temperature with 100-200 µl of a 50% slurry of pre-equilibrated Glutathione Sepharose 4B resin (from formerly Amersham Pharmacia Biotech, now part of GE Healthcare Bio-Sciences Inc., Baie d'Urfe, QC). Resin was

washed three times with ice-cold PBS supplemented with 5 mM ATP and protease inhibitors at 1 ml/sample per wash, followed by centrifugation at 1,000 x g for 5 minutes at 4 °C and removal of the wash solution. Purified resin-bound proteins were eluted by incubating the washed resin with 50-100 µl of Glutathione Elution Buffer (GEB; 10 mM reduced glutathione, 50 mM Tris-Cl pH8) with end-over-end rotation for 10 minutes at room temperature. Resin-purified eluates were then quantified for protein content by BCA assay and used in immunoblotting or gel overlay experiments.

2.4. Plasmid DNA

β-gal, expressing *E. coli* β-galactosidase under control of the cytomegalovirus (CMV) promoter; plasmid pCMVβ acquired from Clontech (Mountain View, CA)

GFP, expressing mammalian enhanced green fluorescent protein; kind gift from Dr. El-Husseini (Canada)

GST, expressing *Schistosoma japonicum* glutathione-S-transferase under control of the inducible *tac* promoter; kind gift from Dr. Astell (Canada)

GST-HIP1, expressing GST-tagged HIP-1 protein; kind gift from Drs. Metzler and Hayden (Canada)

GST-HIP1-Talin, expressing GST-tagged HIP-1 talin domain; kind gift from Drs. Metzler and Hayden (Canada)

HIP1, expressing HIP-1 (containing the F398G point mutation to minimize toxicity from over-expression) from a pCI-derived vector; kind gift from Dr. Hayden (Canada)

Htt15, expressing full-length human htt with 15Q (WT) under control of the CMV promoter (Goldberg et al., 1996)

Htt138, expressing full-length human htt with 138Q (mutant) under control of the CMV promoter (Goldberg et al., 1996)

NR1, expressing rat NR1-1a isoform from a pRK5-derived vector under control of the CMV promoter (Raymond et al., 1996; Chen et al., 1997)

NR2B, expressing rat NR2B subunit from a pRK5-derived vector under control of the CMV promoter (Raymond et al., 1996; Chen et al., 1997)

2.5. Antibodies

Anti-α-actinin, mouse monoclonal antibody (formerly Upstate; now part of Millipore, Billerica, MA; catalogue # 05-384)

Anti-α-actinin, rabbit polyclonal antibody (Sigma-Aldrich Canada Ltd., Oakville, ON; catalogue # A-2543)

Anti-α-actinin 4, rabbit polyclonal antibody (kind gift from Dr. Yamada, Japan)

Anti-actin, goat polyclonal antibody (Santa Cruz Biotechnology, Inc., Santa Cruz, CA; catalogue # SC-1616)

Anti-calnexin, rabbit polyclonal antibody (formerly StressGen; now Nventa Biopharmaceuticals Corp., San Diego, CA; catalogue # SPA-860)

Anti-CK2, rabbit polyclonal antibody (kind gift from Dr. Pelech, Canada; Charlton et al. 1992)

Anti-GluR1, rabbit polyclonal antibody (formerly Upstate; now part of Millipore, Billerica, MA; catalogue # 06-306)

Anti-GluR1, rabbit polyclonal antibody (formerly Chemicon; now part of Millipore, Billerica, MA; catalogue # AB1504)

Anti-GroEL, rabbit polyclonal antibody (Assay Designs, Ann Arbor, MI)

Anti-GST, mouse monoclonal antibody (formerly StressGen; now Nventa; catalogue # MSA-103)

Anti-HIP-1, rabbit polyclonal antibody (kind gift from Dr. Hayden, Canada)

Anti-HIP-1 #9, mouse monoclonal antibody (kind gift from Dr. Hayden, Canada)

Anti-Hsp70, mouse monoclonal antibody (Assay Designs, Ann Arbor, MI; catalogue # SPA-810)

Anti-Hsp90, mouse monoclonal antibody (Santa Cruz Biotechnology, Inc., Santa Cruz, CA)

Anti-htt, mouse monoclonal antibody (formerly Chemicon; now part of Millipore, Billerica, MA; catalogue # MAB2166)

Anti-NR1 extracellular loop between M3 and M4, mouse monoclonal antibody (formerly Chemicon; now part of Millipore, Billerica, MA; catalogue # MAB363)

Anti-NR1A CT, rabbit polyclonal antibody (formerly Upstate; now part of Millipore, Billerica, MA; catalogue # 06-311)

Anti-NR1 C2, rabbit polyclonal antibody (PhosphoSolutions, Aurora, CO; catalogue # 1506-C2)

Anti-NR1 C2', rabbit polyclonal antibody (PhosphoSolutions, Aurora, CO; catalogue # 1507-C2')

Anti-NR2A, rabbit polyclonal antibody (formerly Upstate; now part of Millipore, Billerica, MA; catalogue # 06-313)

Anti-NR2B, mouse monoclonal antibody (BD Transduction Laboratories, San Jose, CA; catalogue # 610417)

Anti-NR2B, mouse monoclonal antibody (ABR-Affinity BioReagents, Golden, CO; catalogue # MA1-2014)

Anti-NR2B, rabbit polyclonal antibody (formerly Upstate; now part of Millipore, Billerica, MA; catalogue # 06-600)

Anti-NR2B, rabbit anti-serum (kind gift from Dr. Huganir, U.S.A.)

Anti-PSD-95, mouse monoclonal antibody (formerly Chemicon; now part of Millipore, Billerica, MA; catalogue # MAB1596)

Anti-synaptophysin, mouse monoclonal antibody (kind gift from Dr. Vincent, Canada)

Cy3 anti-mouse, secondary antibody (Jackson ImmunoResearch Laboratories, Inc., West Grove, PA)

AlexaFluor 350 anti-mouse, secondary antibody (formerly Molecular Probes; now part of Invitrogen Canada Inc., Burlington, ON)

AlexaFluor 488 anti-mouse, secondary antibody (formerly Molecular Probes; now part of Invitrogen Canada Inc., Burlington, ON)

AlexaFluor 594 anti-rabbit, secondary antibody (formerly Molecular Probes; now part of Invitrogen Canada Inc., Burlington, ON)

2.6. Gel Overlay Assay

Purified recombinant GST, GST-HIP1, and GST-HIP1-Talin were resolved by SDS-PAGE and transferred onto a PVDF membrane as for immunoblotting. The membrane was then wetted in methanol, equilibrated in H_2O and TBS, and then blocked for 2 hours at room temperature in TBS-T supplemented with 3% (w/v) BSA. Following a brief rinse in TBS-T, the membrane was incubated with 2 µg/ml recombinant α-actinin in TBS-T 3% BSA for 1.5 hours at room temperature and then washed three times with TBS-T. The membrane was subsequently probed for the binding of α-actinin to GST or

GST-fusion proteins using an anti-α-actinin primary antibody and appropriate secondary antibody as per standard immunoblotting protocols.

2.7. Materials

Chemicals and reagents were purchased from Sigma-Aldrich Canada Ltd. (Oakville, ON) unless otherwise noted.

2.8. Data Analysis

Statistically significant differences were determined using standard statistical tests. Data from experiments with two conditions or genotypes conducted in parallel were analyzed by paired t-tests. Where samples for the two conditions were processed separately, data were analyzed by unpaired t-tests. For experiments with more than two conditions, typically the 1-way ANOVA would be used followed by Bonferroni's post hoc tests for pairwise comparisons. In experiments where striatal tissue was collected from YAC72 and YAC128 mice for examination of CK2 expression, data was expressed as fold change from WT, analyzed individually by 1-sample t-tests, and compared using unpaired t-test between YAC72 and YAC128 values that were normalized to WT. In this case it was not valid or possible to use 1-way ANOVA testing because each batch of transgenic tissue (either YAC72 or YAC128) was collected in parallel with its own age-matched WT control samples, and the values for WT samples presented intrinsic variability when pooled. Data from immunostaining experiments in transfected MSNs were also expressed as surface-to-internal ratio of NR1 subunit staining intensity in GFP/HIP-1 transfected cells normalized to GFP-expressing cells, and analyzed by 1-sample t-test.

For experiments with two variables, such as the toxicity induction/TUNEL labeling studies, 2-way ANOVA was used followed by Bonferroni's post hoc tests for pairwise comparisons.

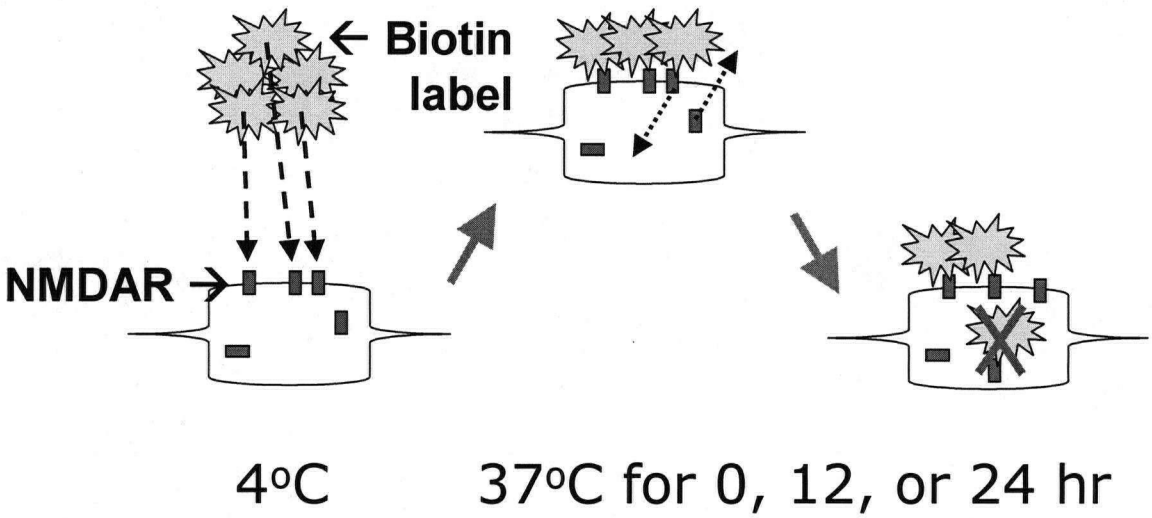

Figure 4. Schematic of biotinylation assay to examine loss of receptors from the cell surface. Sister dishes of 9-10 d.i.v. striatal MSNs in culture are incubated with NHS-SS-Biotin to label surface proteins, washed to remove excess biotin, and replaced in pre-existing culture media at 37 °C 5% CO_2. At 0, 12, or 24 hours following biotinylation, total soluble lysates are harvested from cells and incubated with NeutrAvidin resin to isolate biotin-tagged proteins. Expression of surface proteins is then examined by immunoblot analysis and compared against the internal portion represented by the pool of non biotin-tagged proteins that did not bind NeutrAvidin resin and remained in the supernatant.

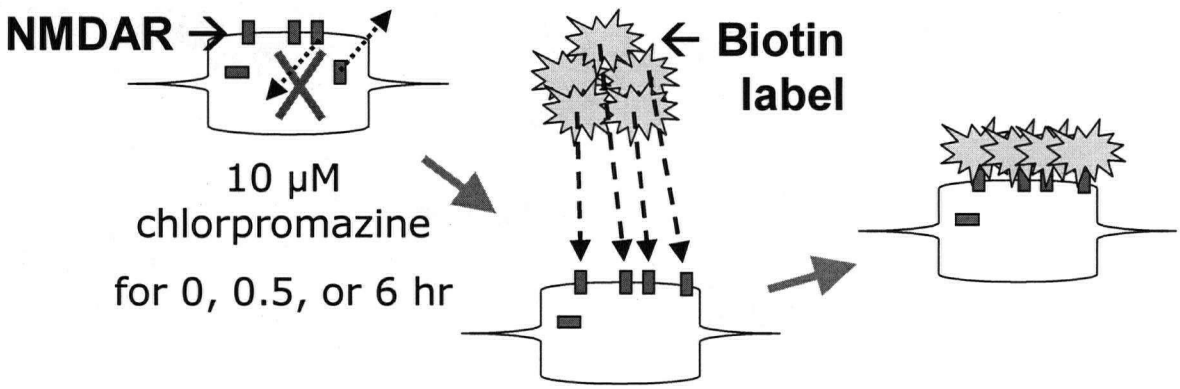

Figure 5. Schematic of biotinylation assay to examine surface protein insertion. Sister dishes of 9-10 d.i.v. striatal MSNs in culture are treated with the endocytosis and recycling inhibitor chlorpromazine for 0, 0.5, or 6 hours at 37 °C 5% CO_2. At each time point, one dish of neurons are incubated with NHS-SS-Biotin to label surface proteins, washed to remove excess biotin, and harvested for total soluble lysates. Lysates are then incubated with NeutrAvidin resin to isolate biotin-tagged proteins. Accumulation of surface proteins is examined by immunoblot analysis and compared against the internal portion represented by the pool of non biotin-tagged proteins that did not bind NeutrAvidin resin and remained in the supernatant.

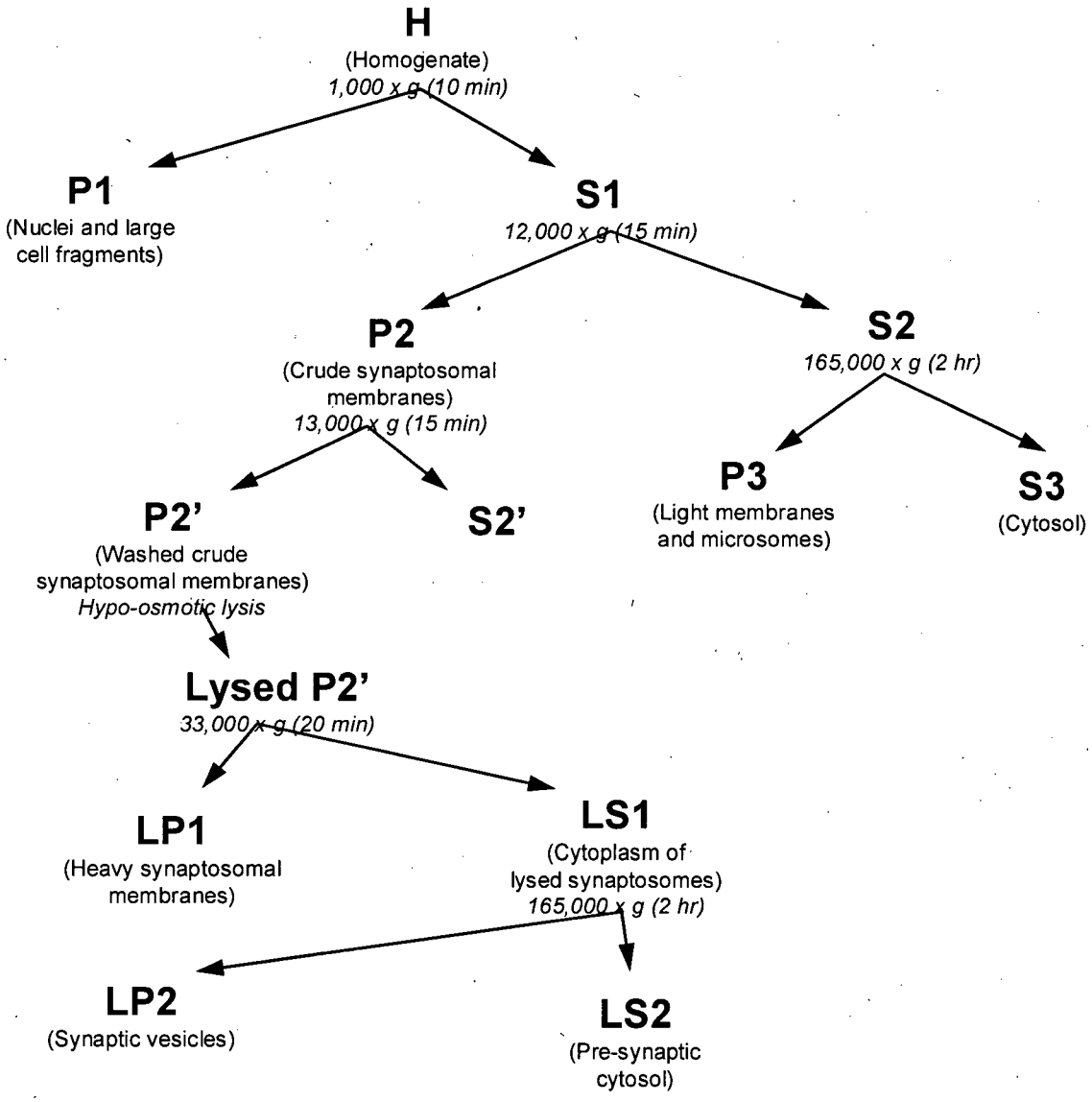

Figure 6. Schematic of subcellular fractionation protocol. Striatal tissue is pooled from 2 month-old mice, fractionated by centrifugation into various subcellular compartments, and analyzed by immunoblotting for proteins of interest. See Section 2.1.3.4 under Materials and Methods for more details on the fractionation protocol.

CHAPTER 3. ALTERED NMDAR TRAFFICKING IN YAC72 TRANSGENIC HD MOUSE MODEL

The selective vulnerability of striatal neurons to excitotoxic damage is thought to involve excessive activation of GluRs, with the NMDAR-subclass of iGluRs playing a more selective and effective role than other GluRs in this process (reviewed in DiFiglia, 1990). Given the strong evidence in support of a role for NMDARs, especially the NR1/NR2B subtype, in contributing to the excitotoxic death of neurons expressing mhtt (Zeron et al., 2002, 2004), we sought to determine whether altered NMDAR subcellular distribution to increase surface receptor numbers correlates with the potentiation of NMDA-induced current and toxicity by mhtt in the YAC mouse model of HD.

3.1. No Change in NR1/NR2B Total Expression in Striatal Tissue from YAC46 or YAC72 Mice

While the current and toxicity mediated via the NR1/NR2B subtype of NMDARs were found to be upregulated by polyQ-expanded htt (Chen et al., 1999b; Zeron et al., 2001, 2002), it remains unclear as to how mhtt exerts its effects on NMDAR activity. Immunoblotting analysis was performed to examine whether NMDAR expression may be altered by mhtt. Analysis of striatal tissue from 2 month-old FVB/N WT, YAC46, and YAC72 mice revealed that overall expression levels of NR1 and NR2B were not different and did not vary with htt polyQ length (Figure 7). This finding was extended in a time-course experiment in which we collected striatal tissue from WT and YAC72 mice at 2, 6, 9, or 12 months of age and examined NR1/NR2B expression levels. Immunoblots

showing levels of expression of NR1, NR2B, and actin (as loading control) are shown in Figure 8. We found that in striatal tissues from mice of any given age group, NR1/NR2B expression was not significantly different between WT and YAC72 mice (Figure 9) (by 2-way ANOVA: effect of genotype $F(1,16) = 0.6746$, $p = 0.4235$ for NR1; effect of genotype $F(1,16) = 0.07974$, $p = 0.7813$ for NR2B), and that NR1/NR2B expression levels did not vary with age in striatal tissue from WT mice. These results indicate that, apart from certain temporal changes in the total cellular expression of NR1/NR2B in striatal tissue from YAC72 mice of varying ages, NMDAR expression levels are unaffected by expansion of the polyQ tract in mhtt. Hence the modulation of NMDAR function by mhtt does not appear to involve changes in the overall expression levels of the NR1/NR2B receptor subtype.

3.2. Increased NMDAR Surface Expression in YAC72 MSNs

NMDAR activity is determined in large part by the complement of receptors that are expressed on the cell surface, and changes in receptor distribution or trafficking could occur without affecting total protein expression. We therefore examined NMDAR surface expression in striatal neurons from WT and YAC mice in order to assess the effects of mhtt expression on surface numbers of NMDARs.

3.2.1. By Immunofluorescent Staining

Cultured striatal MSNs grown on PDL-coated glass coverslips were used for experiments at 9-10 d.i.v. Non-permeabilized cells were first labeled with an antibody recognizing the extracellular M3-M4 loop of the NR1 subunit, followed by the AlexaFluor

488-conjugated fluorescent green secondary antibody. Cells were then permeabilized to facilitate binding of the same anti-NR1 antibody to the remainder of the receptors, representing the intracellular population of NR1, which were then labeled with the secondary Cy3-conjugated red fluorophore antibody. Although this method was not designed to provide absolute measurements of the numbers of receptors on the cell surface or inside the cell (due to the different affinities and intensities of the fluorescent secondary antibodies used), quantification of the green-to-red signals gave an estimate of the surface-to-internal NR1 expression levels. Using this method we were able to demonstrate that MSNs from YAC72 mice had ~50% higher surface NR1 expression relative to WT (Figure 10), a finding which may explain the enhanced NMDAR-mediated current/toxicity observed in this same mouse model. MSNs from YAC18 mice, which expressed htt with a non-pathogenic number of glutamine repeats (18Q), exhibited a similar proportion of surface NR1 as did WT (Figure 10B). Hence the increased proportion of surface NR1 expression appears to be caused by expression of the polyQ-expanded mhtt, instead of being a non-specific effect resulting from htt over-expression or expression of the YAC itself.

3.2.2. By Chymotrypsin Assay

Sister dishes of cultured MSNs from YAC72 or control (WT or YAC18) mice were subjected to treatment with either HBSS or with chymotrypsin-containing solution to cleave surface proteins in live cells. Immunoblot analysis then allowed comparison of the uncleaved portion with total amounts of NR1 to determine the fraction of intracellularly located NR1 (Figure 11). We found a greater reduction of NR2B as well as NR1 levels in YAC72 MSNs following chymotrypsin treatment relative to controls, implying the

presence of a larger pool of NMDARs at the surface that was accessible to the tryptic enzyme in these neurons. The smaller losses of NR1/NR2B signal from chymotrypsin treatment noted in MSNs from control mice expressing htt with a non-pathogenic polyQ length (either WT or YAC18) suggest a smaller surface portion and a correspondingly larger internal proportion of NR1 in these cells. Statistical analysis was not performed due to the small sample size (N = 2), but this finding provides an initial confirmation of our immunostaining results showing increased surface NMDAR expression in MSNs from YAC72 mice expressing polyQ-expanded mhtt, before we next moved on to further examine this phenomenon using a biotinylation-based approach as described in the next section.

3.2.3. By Biotinylation Assay

A third method with which we probed for relative levels of surface NMDARs in cells from WT or YAC72 mice is based on biotin-tagging of surface proteins. The use of Sulfo-NHS-SS-Biotin enables biotin-labeling of primary amine-containing biomolecules. Since this reagent is membrane-impermeable, intact cells could be treated to label all cell surface proteins. Subsequent lysis of cells produces two populations of proteins: one population is unlabeled representing intracellular proteins; the second, biotinylated set represents surface proteins. Biotin-labeled proteins could then be captured on resin coupled to streptavidin (with unlabeled proteins remaining in the supernatant), and then released by boiling in SDS-based protein sample buffer. Quantification of the amount of biotinylated protein compared to what remained in the supernatant of the streptavidin binding step allowed one to deduce the relative proportion of the protein that was on the cell surface initially. We found surface NR1 to comprise ~39% and ~61% of total pools

(Figure 12B), while ~53% and ~71% of total NR2B (Figure 13B) were determined to be on the cell surface of WT and YAC72 MSNs, respectively. A lower proportion of surface-localized NR1 relative to NR2B is in agreement with the presence of a substantial intracellular pool of unassembled NR1 subunits in neurons (reviewed in Wenthold et al., 2003; Prybylowski and Wenthold, 2004). Our results once again confirmed a significant increase in the amount of surface NR1 (by 56%; Figure 12) and NR2B (by 34%; Figure 13) in striatal MSNs cultured from YAC72 mice as compared with WT, in agreement with our immunostaining and chymotrypsin data. In contrast, the AMPAR subunit GluR1 did not show different surface expression levels in MSNs from WT versus YAC72 mice (Figure 14), suggesting the effect on surface expression in YAC72 MSNs expressing mhtt is selective for NMDARs but not other members of the iGluR family.

3.3. Increased Rate of NMDAR Trafficking in YAC72 MSNs

3.3.1. Increased Rate of Receptor Loss from the Cell Surface

To probe into mechanisms underlying increased steady-state surface expression levels of NR1 and NR2B in YAC72 MSNs, we investigated possible changes in the trafficking rates of NMDARs to/from the cell surface. Using a variation of the biotinylation assay mentioned above (shown in Figure 4), we tracked disappearance of biotin-labeled surface NR1 over time and compared MSNs from WT versus YAC72 mice (Figure 15A). In spite of a higher percentage of surface NR1 initially in YAC72 MSNs, by 12 and 24 hours following biotinylation the levels of NR1 remaining biotinylated had dropped to levels similar to that in WT neurons (Figure 16A, left panel). The proportion of biotinylated NR1 normalized to starting amounts at 0 hours after biotinylation indicated a more rapid

rate of degradation in the YAC72 MSNs (Figure 16B, left panel). Similarly, surface NR2B subunits labeled with biotin showed a trend towards an accelerated rate of loss in YAC72 MSNs as compared with WT (Figures 16A and 16B, right panels), in contrast to GluR1 which appeared to have similar rates of loss from the surface in MSNs from either genotype (Figure 17). To confirm that loss of biotin-tagged proteins was not the result of non-lysosome-based cleavage by enzymes such as calpains, we repeated experiments to the 12-hour time point and probed for levels of biotinylated NR1 in MSNs treated with the lysosomal inhibitor leupeptin. Treatment with leupeptin rescued the majority of NR1 signal at 12 hours following biotinylation (Figure 15B), indicating the receptor loss we observed predominantly involved degradation by the lysosome.

3.3.2. Increased Rate of Receptor Insertion to the Cell Surface

Our results showing more rapid loss of surface NMDARs in YAC72 MSNs are contrary to what one might expect, since this result cannot explain the higher basal surface expression levels of NMDARs in YAC72 MSNs. Because of this unexpected finding, we examined the rate in the other arm of trafficking – that of insertion. Together, insertion to, and removal from, the surface dictate the steady-state amounts of NMDARs that are positioned on the cell surface to carry out their prescribed physiological functions. Tracking proportions of NMDARs that are located on the cell surface via biotinylation at various times following blockade of endocytic and recycling processes allows determination of changes in cell surface expression due to insertion alone. To accomplish this, we employed the drug chlorpromazine, which is currently approved for use in the treatment of psychotic disorders. This cationic, amphiphilic compound has been shown to block clathrin-mediated receptor endocytosis and recycling by preventing

assembly of clathrin adapter protein AP-2 on clathrin-coated pits thereby causing mis-assembly of the clathrin lattice (Wang et al., 1993).

At 0, 0.5, and 6 hours following the beginning of treatment with this drug, intact cells were biotinylated to examine surface expression. In MSNs from WT mice, we found the levels of NR1 protein expressed on the cell surface to be unchanged after 6 hours of endocytic/recycling block (Figures 18, 19A and 19B left panels), indicating a lack of *de novo* insertion of NMDARs in the absence of replenishment from the recycling pool. In contrast, surface NR1 expression was up-regulated in MSNs cultured from YAC72 mice at 6 hours following chlorpromazine treatment (Figures 18, 19A and 19B left panels), with similar trends observed for the NR2B subunit (Figures 19A and 19B right panels) but not the AMPAR subunit GluR1 (Figure 20). Our results suggest that new NMDARs were being inserted into the cell surface over a 6-hour period, at least for YAC72 MSNs. At 30 minutes following chlorpromazine treatment, though, we observed a small decrease in NR1 surface expression, which is consistent with a recycling inhibition effect as noted previously (Wang et al., 1993); new receptors from the *de novo* synthesis pathway will likely not have had the chance to appear on the cell surface by this time.

Because mobilization of newly synthesized, surface-targeted proteins is not expected to be affected by treatment with chlorpromazine (Wang et al., 1993; Veyhl et al., 2006), accumulation of surface NMDARs in YAC72 MSNs at 6 hours following endocytic/recycling block by chlorpromazine likely represents insertion of new receptors from the ER/Golgi pathway. The relatively modest amounts of NMDARs that accumulated at the surface of YAC72 MSNs, along with a lack of insertion of NMDARs over the same time period in WT neurons, are surprising findings which suggest additional, non-specific effects of chlorpromazine treatment on receptor trafficking that may result in an under-estimation of the rate of NMDAR insertion. However because both

WT and YAC72 MSNs were treated and processed in parallel, the differences in forward trafficking kinetics we observed remain valid and indeed reflect a specific effect of mhtt expression.

Although it was not possible to directly compare results from surface receptor loss and insertion experiments, rough estimates of the relative rates of these processes indicated that forward trafficking of NMDARs may dominate over the reverse trafficking/degradation process to increase steady-state levels of NMDARs at the surface (see Conclusions section 6.1).

3.4. Altered Splicing of NR1 Isoform in YAC72 Striatal Tissue

Apart from subunit composition, phosphorylation, and interactions with other proteins and the CSK, NMDAR trafficking to and from the cell surface is also determined in part by alternative splicing of the NR1 subunit (see section 1.2.4 under Introduction). Specifically, different splice isoforms of NR1 mRNA regulate the rate of NMDAR export from the ER during the forward trafficking process (Okabe et al., 1999); the rate of ER export is accelerated for NR1 isoforms containing the C2' domain (Scott et al., 2001; Mu et al., 2003; see Figure 2 for NR1 splice variations). To assess the contribution of alternative splicing in promoting faster forward trafficking and insertion of NMDARs to the cell surface in striatal neurons from YAC72 mice, we analyzed the expression of C2- or C2'-containing NR1 isoforms in striatal tissue from 2 month-old WT and YAC72 mice. The antibodies we used did not distinguish between different NR1 splice variants containing the C2 cassette (including NR1-1a, NR1-1b, NR1-2a, and NR1-2b), or those containing the C2' cassette (including NR1-3a, NR1-3b, NR1-4a, and NR1-4b). Due to the differential affinities of different antibodies for their antigens, we were not able to

directly compare absolute levels of expression of C2- and C2'-containing NR1; it is however well accepted that the most abundantly expressed isoform of NR1 by far in striatal MSNs is NR1-1a (Kuppenbender et al., 1999), which contains the C2 (but not C2') cassette.

Striatal tissues from WT and YAC72 mice appeared to express comparable levels of the C2-containing NR1 isoforms, and expression of C2'-containing NR1 was also similar in tissues from either genotype (Figure 21). However, changes at the subcellular level could occur without affecting overall expression of different NR1 splice variants. We therefore prepared subcellular fractions from striatal tissue of 2 month-old WT or YAC72 mice and analyzed the relative expression of the C2'- and C2-containing NR1 isoforms. A schematic detailing the protocol for subcellular fraction is shown in Figure 6. Subcellular fractions were first characterized to ensure proper separation of the different intracellular compartments: immunoblotting for synaptophysin affirmed LP2 as the pre-synaptic membrane fraction, concentration of calnexin in P3 confirmed this as the ER/microsome-containing fraction, and enrichment of PSD-95 in LP1 was consistent with this being the fraction comprised of heavy synaptosomal membranes from the post-synaptic compartment (Figure 22A).

Importantly, in YAC72 striatum we found a significant enrichment of the C2'-containing isoforms of NR1 (as compared with C2-containing NR1) in a subcellular fraction composed primarily of light microsomal compartments such as ER membranes and other vesicular membranes (Figures 22B and 22C), thought to be a mobile fraction involved in trafficking of NMDARs. The syaptosomal compartment, in contrast, did not show an increase in the amount of C2'-containing NR1 isoforms relative to NR1 C2 in YAC72 versus WT striatal tissue (Figures 22B and 22C). An increase in synaptic NMDAR content would require a corresponding increase in PDZ domain-containing proteins to

anchor the receptors at the synapse (Barria and Malinow, 2002; Prybylowski et al., 2005), although we have found no evidence thus far to suggest that PDZ proteins may be increased in either total lysates or LP1 fractions from YAC72 striatum, relative to WT (M.M.Y. Fan and C.M. Cowan, unpublished observations). It is therefore possible that the enhanced surface delivery of NMDARs in YAC72 striatal MSNs adds to the pool of non-synaptically localized NMDARs and in so doing promote cell death signaling by glutamate activation of extra-synaptic NMDARs (Hardingham and Bading, 2003).

3.5. Differential Interaction of NR1 C2' Splice Isoform with NR2 Subunits in YAC72 Striatal Tissue

Previous studies have shown that C2'-containing NR1 isoforms can traffic to the cell surface membrane without complexing with NR2 (reviewed in Wenthold et al., 2003). Given our observation of a relative increase in NR1 C2'-containing isoforms in the mobile vesicular fraction, next we determined whether the proportion of NR1 C2' isoforms was increased in NR2-containing NMDAR complexes in YAC72 striatum. To this end, we assessed the amounts of C2'-containing NR1 isoforms relative to total NR1 that were co-immunoprecipitated by antibodies directed against NR2A or NR2B.

As is expected for subunits known to assemble into receptor complexes, NR1 (including the C2'-containing isoforms) was found to co-precipitate with both NR2A (Figure 23A) and NR2B (Figure 23B) subunits in immunoprecipitation experiments from WT or YAC72 striatal tissue. Antibody-free control samples were processed in parallel and confirmed lack of non-specific binding of proteins to the resin (Figure 23C). Pooled results (Figure 24A) indicated that the ratio of co-immunoprecipitated NR1 C2' isoforms to NR1 levels (representing all isoforms) was higher in YAC72 striatal tissue than WT for

both anti-NR2A and anti-NR2B samples; importantly, the fold-increase was significantly larger in anti-NR2B precipitates than in anti-NR2A precipitates (1.77 ± 0.13 compared with 1.32 ± 0.08; Figure 24B). These findings indicate an increase in the numbers of NMDARs assembled from NR1 isoforms containing the C2' cassette, preferentially with NR2B, in YAC72 striatal tissue. Our data are also consistent with previous studies indicating that the NR1/NR2B subtype of NMDARs is selectively involved in mediating enhanced current/toxicity by mhtt (Chen et al., 1999b; Zeron et al., 2001, 2002; also see Introduction, section 1.4.4). The increase in NR1 C2'-containing NMDARs may contribute to faster forward trafficking of receptors to account for higher basal expression levels of NMDARs at the surface as described earlier in this thesis.

3.6. Summary

Earlier results from our laboratory indicating enhanced NMDAR-mediated current and toxicity in cultured or acutely dissociated striatal MSNs expressing polyQ-expanded mhtt may now be explained, at least in part, by an up-regulation of steady-state NMDAR numbers on the cell surface. This thesis reports work showing increased surface-to-internal ratio of NR1 and NR2B subunits using a variety of methods, including immunostaining, chymotrypsin-cleavage of surface proteins, and biotinylation-based assays. Furthermore, modified biotinylation experiments showed generally more rapid trafficking of the NMDAR proteins, including faster loss of surface proteins as well as an accelerated rate of *de novo* insertion into the cell surface membrane in the absence of endocytosis/recycling activities. The higher rate of insertion in striatal neurons from YAC72 mice expressing mhtt correlated with a relative enhancement of the C2'-containing NR1 isoforms in the subcellular fraction containing vesicular components

involved in transit of proteins including NMDARs to/from the cell surface. Moreover, the association of C2'-containing NR1 isoforms with NR2B, more than with NR2A, was enriched in YAC72 compared with WT striatal tissue. Together, our findings suggest that enhanced surface expression of NR2B-containing NMDARs in YAC72 MSNs results from a mhtt-mediated change in the balance of NMDAR forward trafficking and loss from the surface.

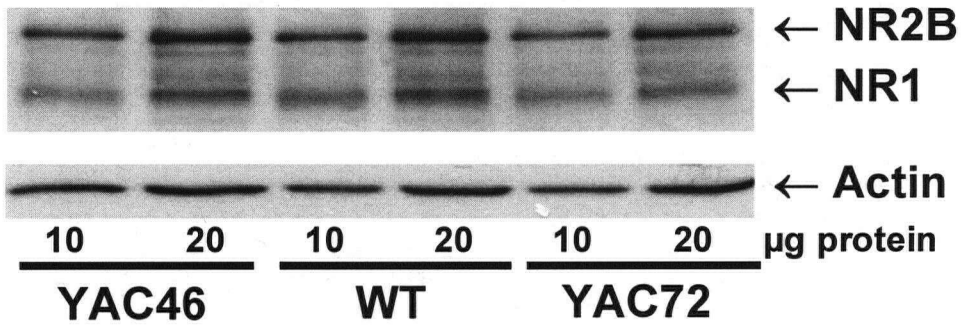

Figure 7. NR1/NR2B total expression is not different in striatal tissue from 2 month-old FVB/N WT, YAC46, or YAC72 mice (Li et al., 2003). Striatal lysates are loaded at 10-ug and 20-µg per lane, and subsequently immunoblotted for NR1 and NR2B expression. Actin expression is used as loading control. Immunoblot shown is representative of three independent experiments using two different tissue batches.

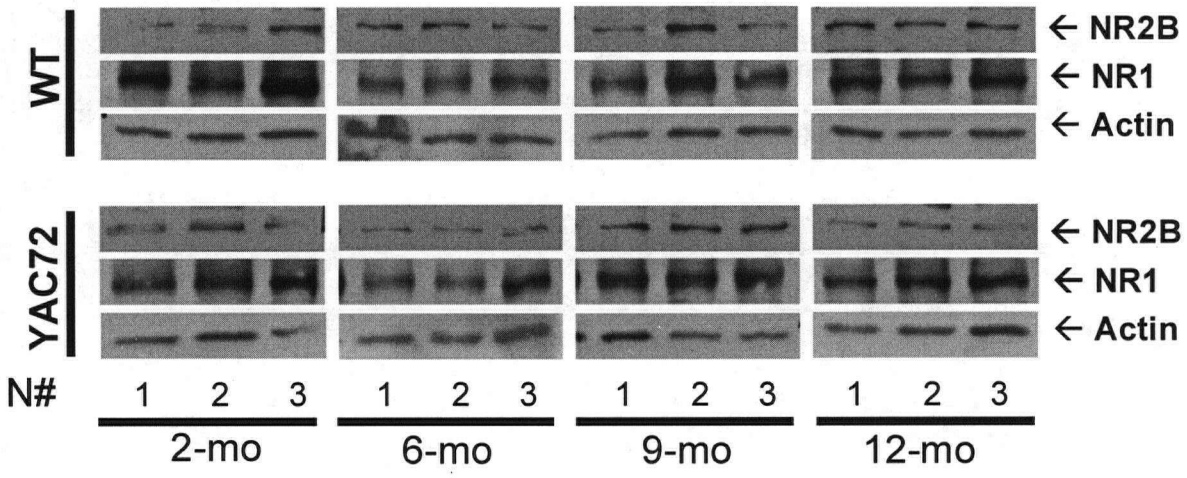

Figure 8. NR1/NR2B total expression is not different in striatal tissue from FVB/N WT or YAC72 mice at 2, 6, 9, or 12 months of age. Striatal lysates are collected in triplicate from mice at each age and analyzed in parallel for NR1/NR2B expression. Actin expression is used as loading control.

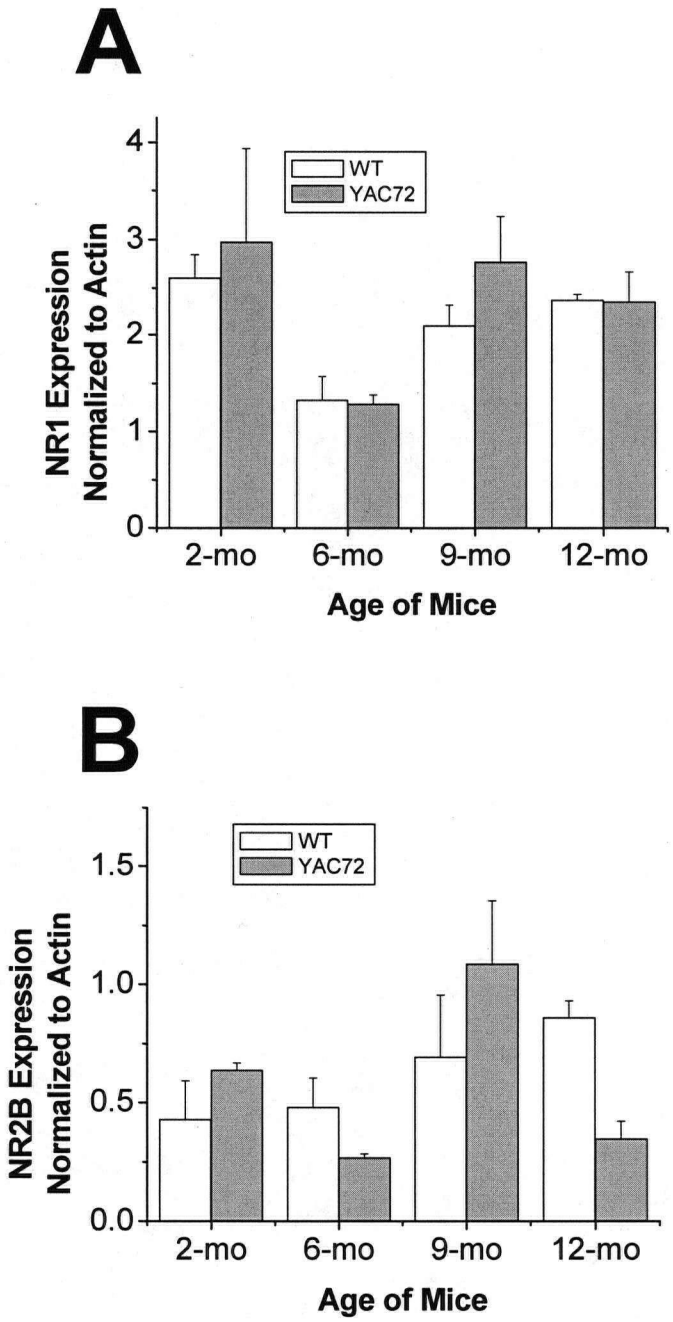

Figure 9. Plots comparing NR1 and NR2B expression levels in striatal tissue from WT and YAC72 mice, grouped by age. Bars represent mean of (A) NR1 or (B) NR2B expression normalized to actin, ± SEM from N = 3 independent samples at each age for every genotype, with striatal tissue pooled from 2 mice per sample. No significant effect of genotype is observed for overall NR1 or NR2B expression levels in striatal tissue from mhtt-expressing YAC72 mice versus WT mice at any age examined (2, 6, 9, or 12 months), by 2-way ANOVA.

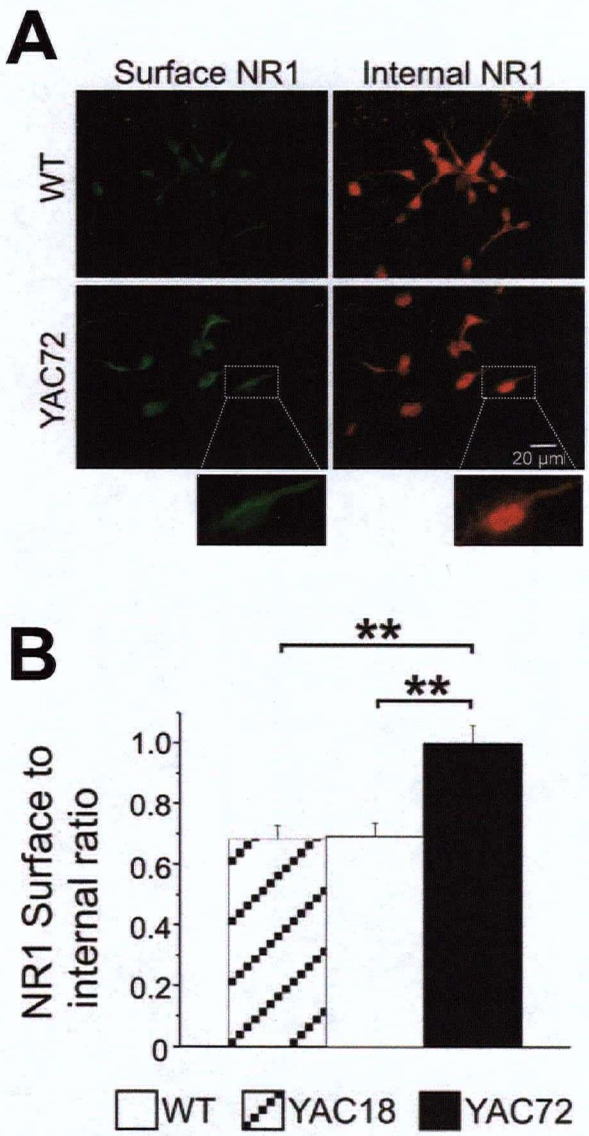

Figure 10. Immunofluorescent staining demonstrates increased proportion of surface NR1 in MSNs from YAC72 mice (contributed by L. Zhang; Fan et al., 2007). (A) Representative pictographs of cultured MSNs fixed at 9-10 d.i.v. and immunostained for surface and internal populations of NR1 are shown for WT and YAC72 mice, with insets depicting an enlarged sample neuron; following initial fixation of the neurons in 4% PFA, all subsequent steps of the immunostaining protocol, fluorescence imaging and image capturing are performed in parallel for both genotypes. (B) Intensity of fluorescent staining is quantified for both surface (green) and internal (red) NR1 in MSNs from WT, YAC18, and YAC72 mice. Proportion of NR1 expressed at the cell surface is determined by taking a ratio of surface-to-internal NR1 staining. Bars represent mean ratio ± SEM from N = 5 independent experiments. Every experiment uses an individual batch of cultured MSNs for each genotype and is performed in parallel for all three genotypes. Subsequent data analysis is also performed in parallel, using 5 coverslips of each genotype per experiment and 4 fields chosen at random from each coverslip (giving a total of 20 measurements). ** Significantly different compared to WT or YAC18, $p < 0.01$ by 1-way ANOVA, Bonferroni post-test.

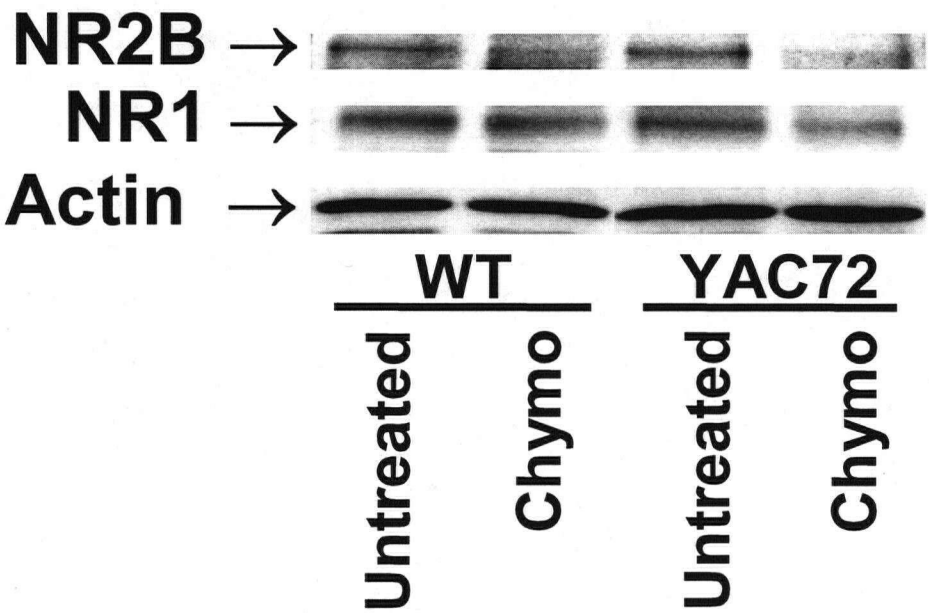

Figure 11. Representative immunoblot of NR1/NR2B levels in 9-10 d.i.v. MSNs from YAC72 versus WT mice with or without chymotrypsin treatment. Sister dishes of cultured MSNs are treated with HBSS alone or HBSS containing 1 mg/ml chymotrypsin to cleave cell surface proteins. Protein levels remaining following treatment are examined by immunoblotting to determine the relative proportions of surface versus internal NMDARs. Actin is also shown as loading control. Immunoblot shown is representative of 2 independent experiments where YAC72 samples were processed in parallel with either paired WT or YAC18 cultures.

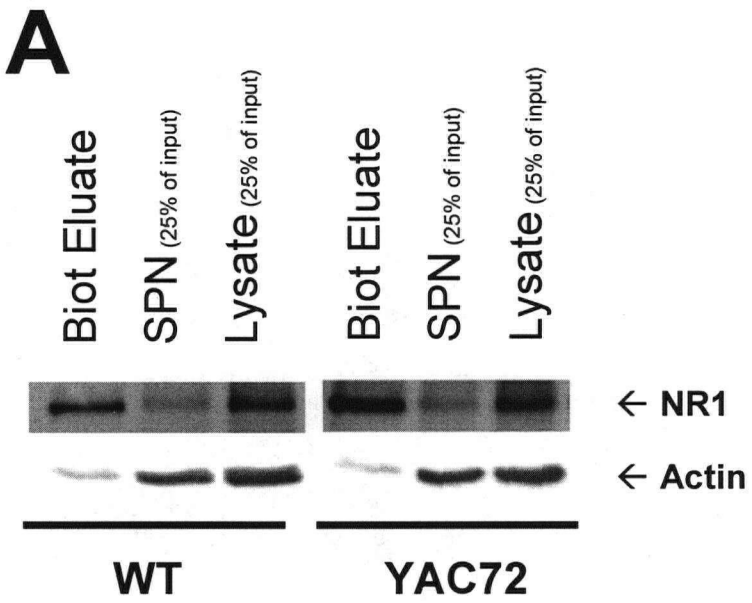

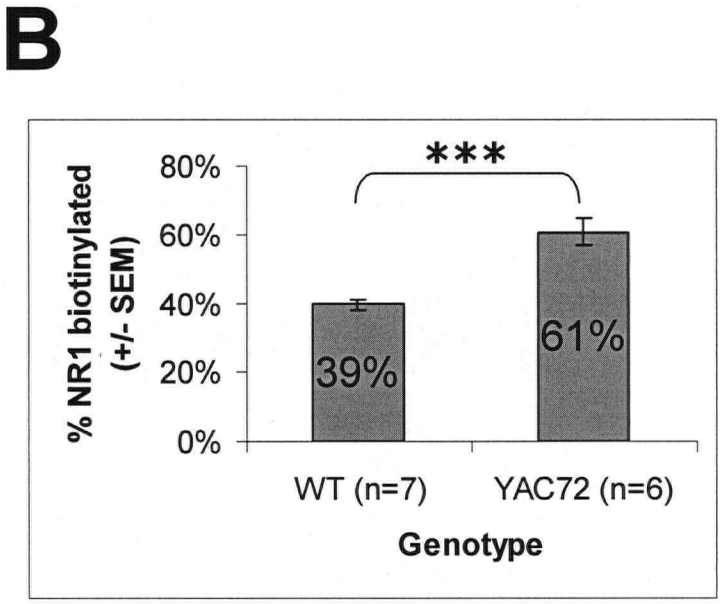

Figure 12. Biotinylation assay demonstrates increased proportion of surface NR1 in MSNs from YAC72 mice. (A) Representative immunoblot depicts NR1 levels present in the "Biot Eluate" fraction representing surface NR1, and the "SPN" fraction representing internal, non biotin-tagged NR1, in MSNs from FVB/N WT or YAC72 mice. Actin is shown as a control to confirm selective labeling of surface but not internal proteins by biotin. (B) Band densities are measured for each of "Biot Eluate" and "SPN" and the percent surface NR1 expression calculated as ("Biot Eluate" ÷ "Total" * 100%) where "Total" is the sum of "Biot Eluate" and four times the signal from the "SPN" lane. Bars represent mean percent surface expression ± SEM from N = 7 (WT) or 6 (YAC72) independent experiments performed with different batches of cultured neurons. *** Significantly different compared to WT, $p < 0.001$ by unpaired t-test.

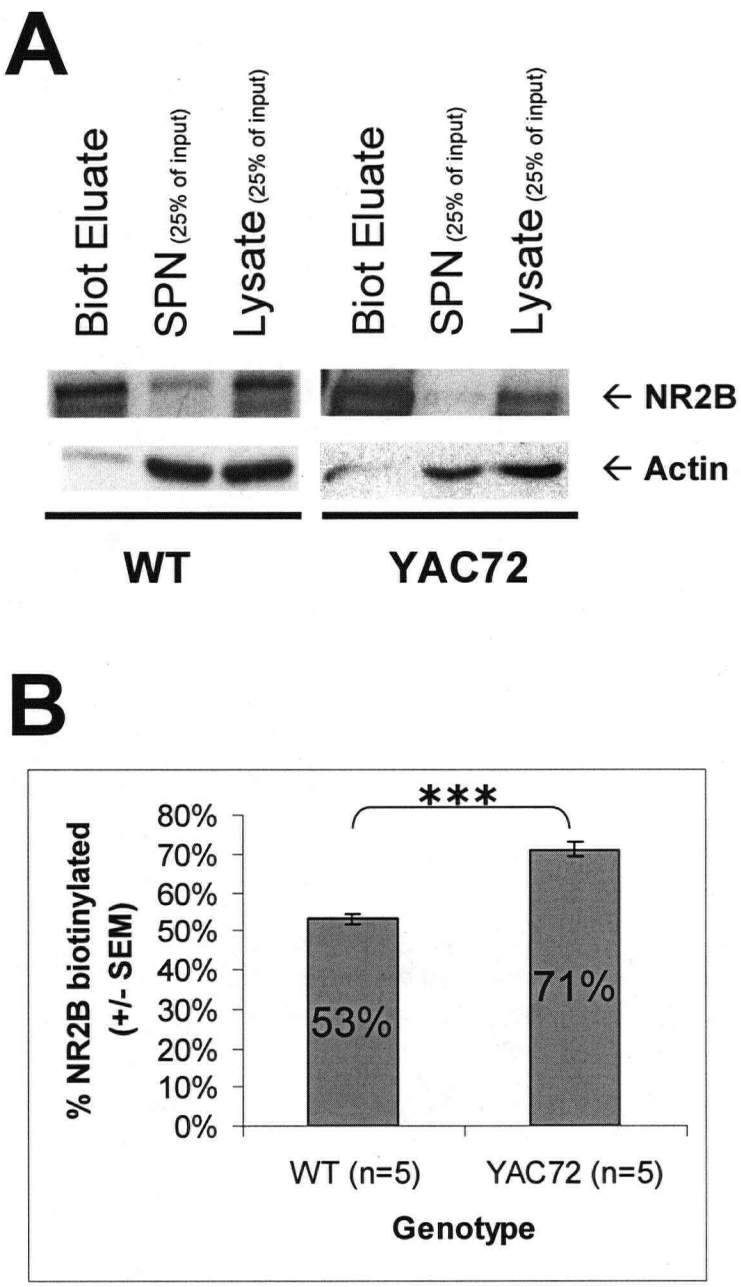

Figure 13. Biotinylation assay demonstrates increased proportion of surface NR2B in MSNs from YAC72 mice. (A) Representative immunoblot depicts NR2B levels present in the "Biot Eluate" fraction representing surface NR2B, and the "SPN" fraction representing internal, non biotin-tagged NR2B, in MSNs from FVB/N WT or YAC72 mice. Actin is shown as a control to confirm selective labeling of surface but not internal proteins by biotin. (B) Band densities are measured for each of "Biot Eluate" and "SPN" and the percent surface NR2B expression calculated as ("Biot Eluate" ÷ "Total" * 100%) where "Total" is the sum of "Biot Eluate" and four times the signal from the "SPN" lane. Bars represent mean percent surface expression ± SEM from N = 5 independent experiments performed with different batches of cultured neurons for each genotype. *** Significantly different compared to WT, $p < 0.001$ by unpaired t-test.

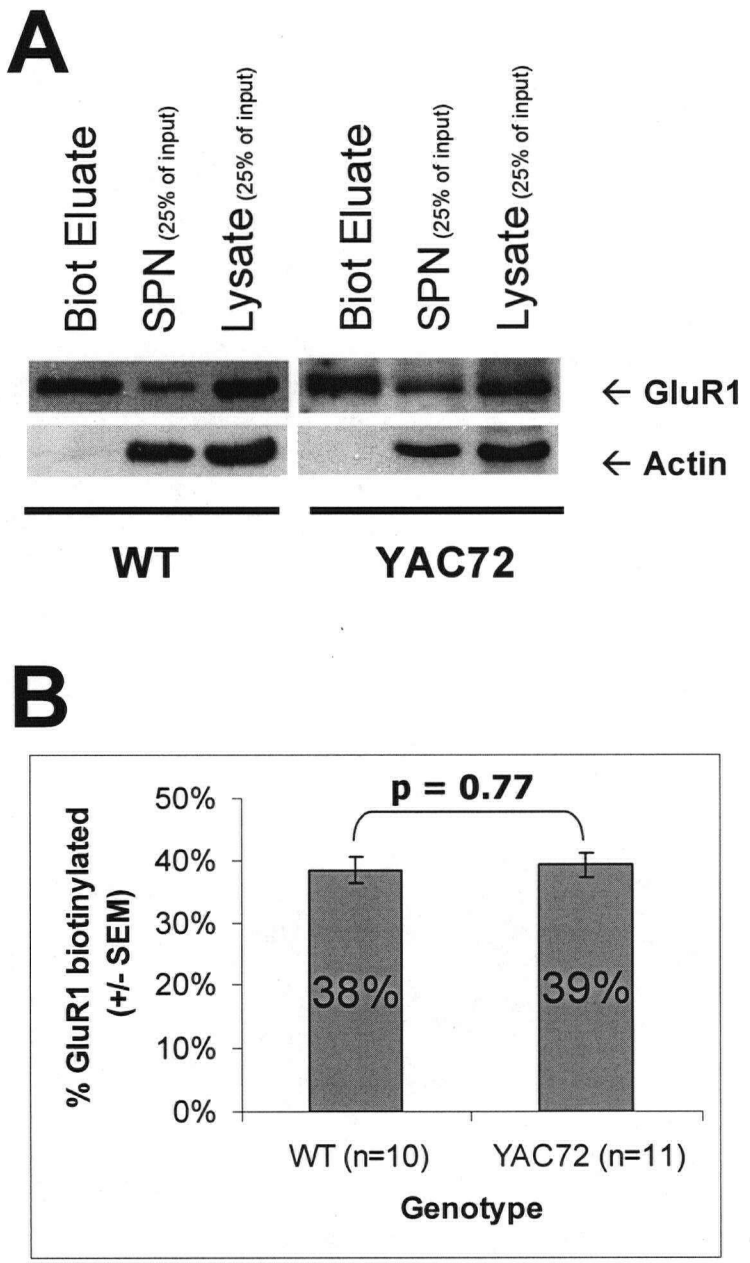

Figure 14. Biotinylation assay demonstrates unchanged proportion of surface GluR1 in MSNs from YAC72 mice. (A) Representative immunoblot depicts GluR1 levels present in the "Biot Eluate" fraction representing surface GluR1, and the "SPN" fraction representing internal, non biotin-tagged GluR1, in MSNs from FVB/N WT or YAC72 mice. Actin is shown as a control to confirm selective labeling of surface but not internal proteins by biotin. (B) Band densities are measured for each of "Biot Eluate" and "SPN" and the percent surface GluR1 expression calculated as ("Biot Eluate" ÷ "Total" * 100%) where "Total" is the sum of "Biot Eluate" and four times the signal from the "SPN" lane. Bars represent mean percent surface expression ± SEM from N = 10 (WT) or 11 (YAC72) independent experiments performed with different batches of cultured neurons. Values are not significantly different to each other by unpaired t-test.

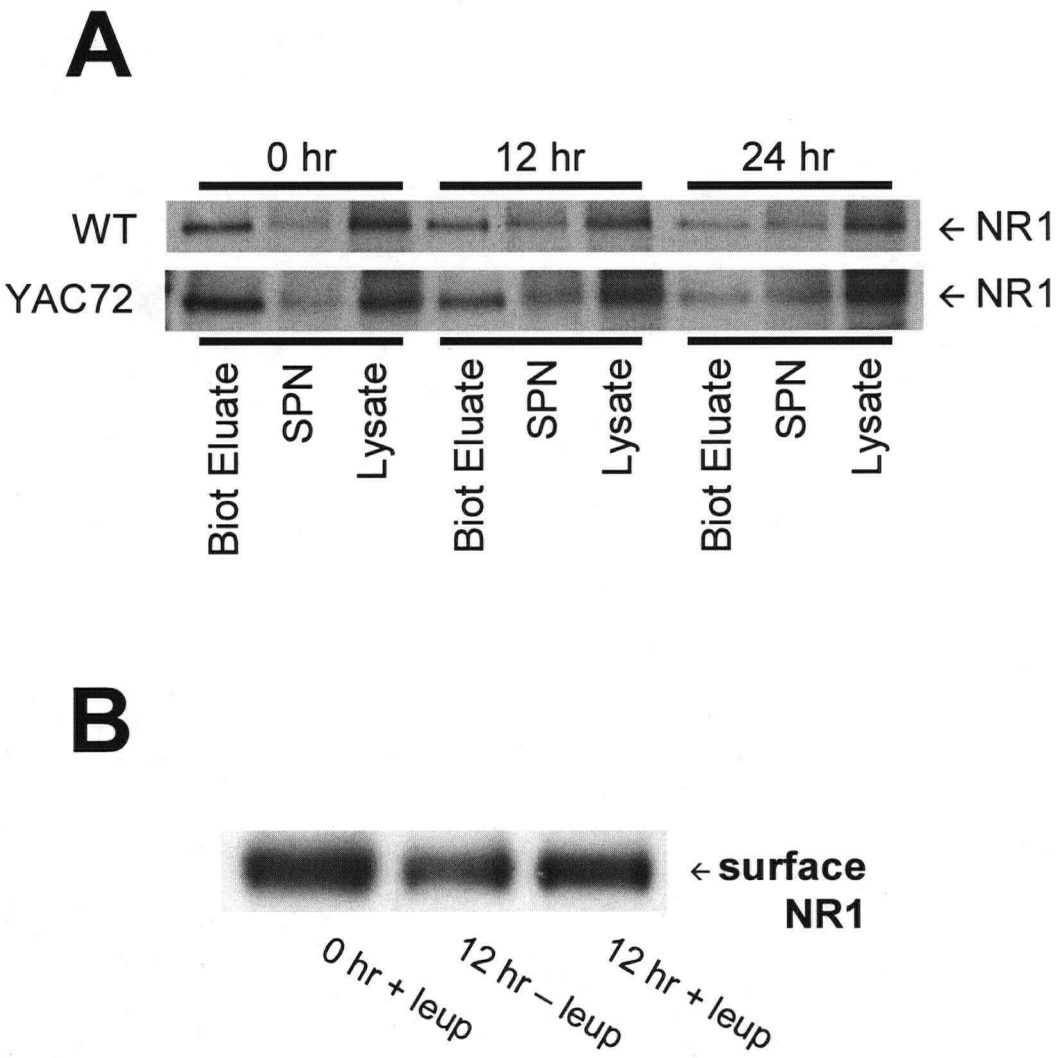

Figure 15. Representative immunoblots illustrating loss of biotin-tagged NR1 over time in MSNs from WT and YAC72 mice. (A) Sister dishes of 9-10 d.i.v. striatal MSNs in culture are subjected to biotinylation as described in the legend to Figure 4. At 0, 12, or 24 hours following biotinylation, total soluble lysates are harvested from cells and incubated with NeutrAvidin resin to isolate biotin-tagged proteins. "Biot Eluate", biotinylation eluate; "SPN", supernatant. (B) Reduction of biotinylated NR1 signal over time reflects loss of surface proteins through lysosomal degradation. Cultured striatal MSNs at 9-10 d.i.v. are pre-treated for 1 hour with the lysosomal inhibitor leupeptin prior to biotinylation as described above. Levels of biotinylated NR1 are then assessed at 0 or 12 hours following biotinylation. Immunoblot shown is representative of 3 independent experiments from different batches of neurons. "-leup", without leupeptin pre-treatment; "+leup", with leupeptin pre-treatment.

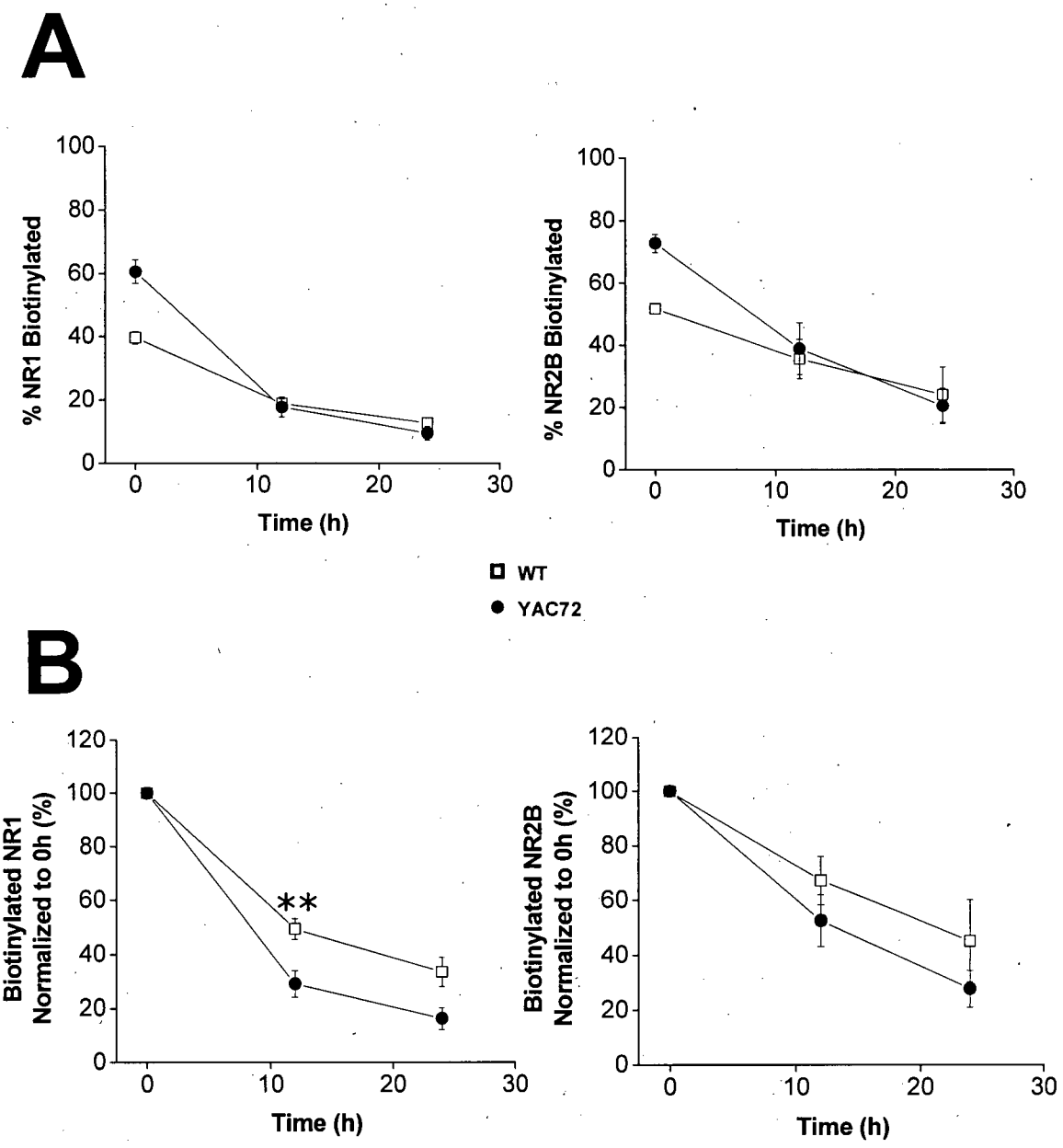

Figure 16. Enhanced rate of loss of surface-labeled NR1/NR2B in MSNs from YAC72 mice. (A) Plot compares loss of biotin-tagged NR1 (left panel) and NR2B (right panel) over time in MSNs from WT versus YAC72 mice. Values represent mean percent surface expression ± SEM from N = 5-12 (NR1) or 2-3 (NR2B) independent experiments from different batches of cultured neurons. (B) Values at 12- and 24-hour time points are normalized to the 0-hour time point set to 100% and are plotted as mean percent ± SEM from N = 5-12 (NR1; left panel) or 2-3 (NR2B; right panel) independent experiments from different batches of cultured neurons. ** Significantly different compared to WT, $p < 0.01$ by unpaired t-test.

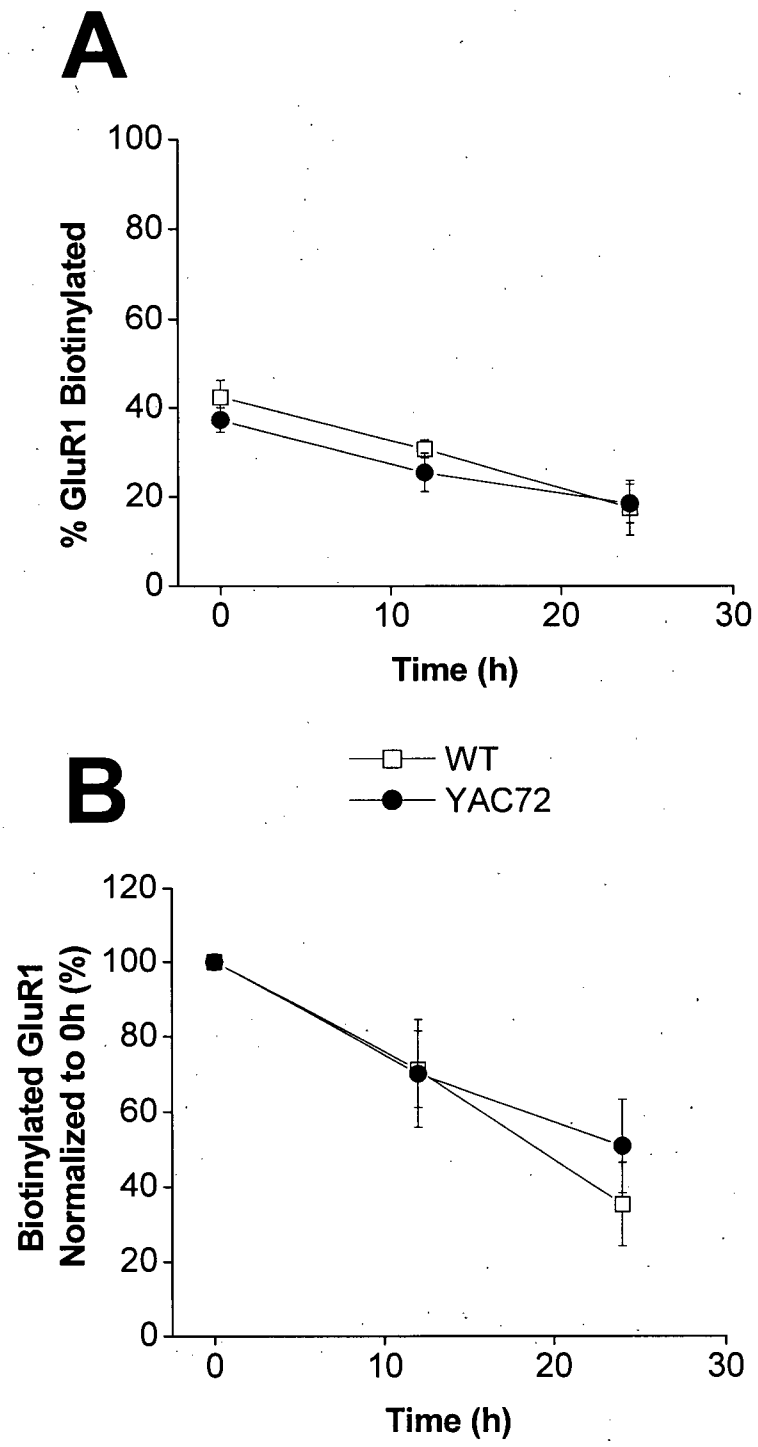

Figure 17. Plots comparing loss of surface-labeled GluR1 in MSNs from WT and YAC72 mice. (A) Loss of biotin-tagged GluR1 over time in MSNs from WT versus YAC72 mice is shown. Values represent mean percent surface expression ± SEM from N = 2-6 independent experiments from different batches of cultured neurons. (B) Values at 12- and 24-hour time points are normalized to the 0-hour time point set to 100% and are plotted as mean percent ± SEM from N = 2-6 independent experiments from different batches of cultured neurons.

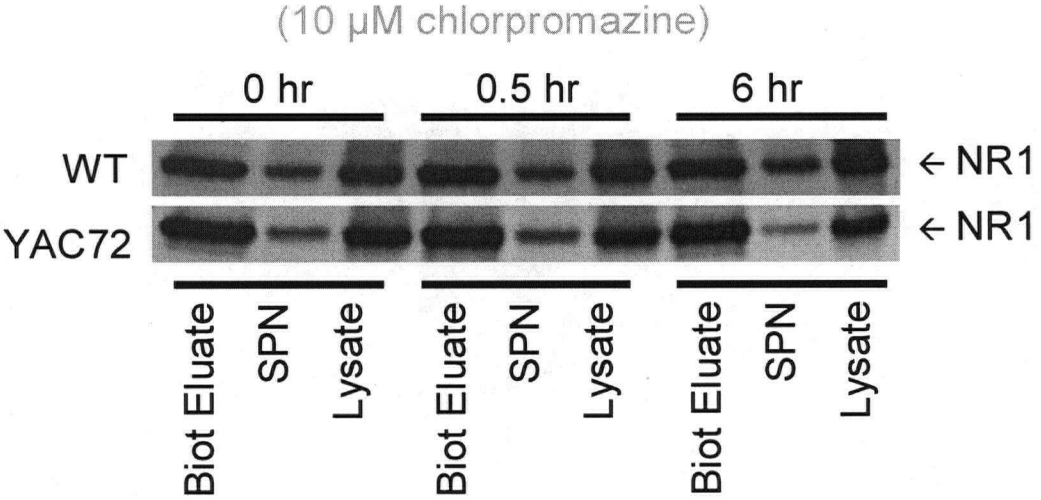

Figure 18. Representative immunoblots illustrating insertion of NR1 to the cell surface over time in MSNs from WT and YAC72 mice. Sister dishes of 9-10 d.i.v. striatal MSNs in culture are subjected to biotinylation as described for the insertion assay in the legend to Figure 5. At 0, 0.5, or 6 hours following chlorpromazine treatment, neurons are biotinylated and harvested for total soluble lysates. Lysates are then incubated with NeutrAvidin resin to isolate biotin-tagged proteins. "Biot Eluate", biotinylation eluate; "SPN", supernatant.

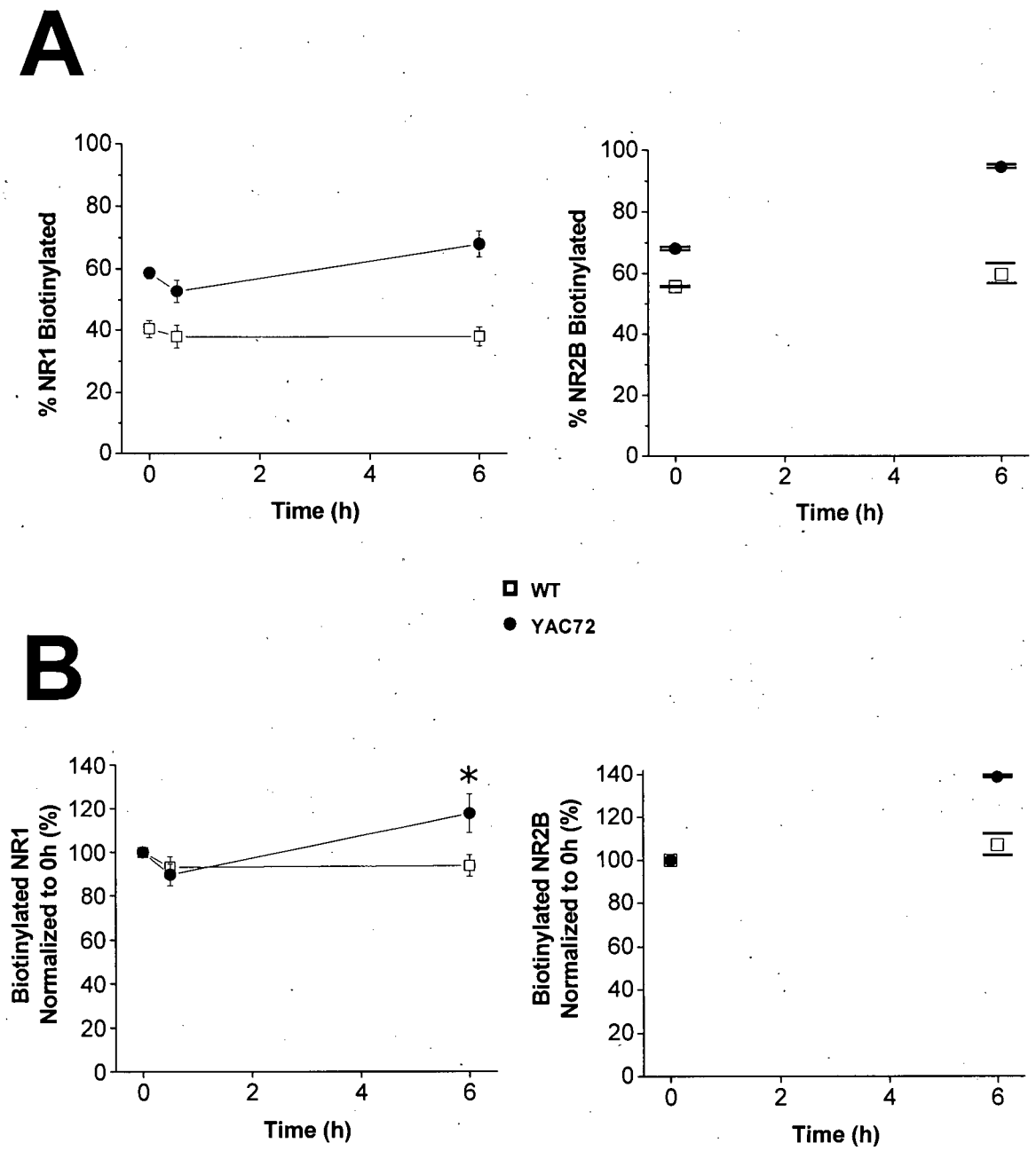

Figure 19. Insertion of NR1/NR2B to the cell surface proceeds more rapidly in MSNs from YAC72 mice. (A) Plot compares insertion of NR1 (left panel) and NR2B (right panel) to the cell surface over time in MSNs from WT versus YAC72 mice, following chlorpromazine treatment. Values represent mean percent surface expression ± SEM from N = 6-8 (NR1), or mean from N = 2 (NR2B), independent experiments from different batches of cultured neurons. Data values used to calculate the mean for NR2B are indicated with horizontal lines. (B) Values at 0.5- and 6-hour time points (for NR1) or 6-hour time point only (for NR2B) are normalized to the 0-hour time point set to 100% and are plotted as mean percent ± SEM from N = 6-8 (NR1; left panel), or mean from N = 2 (NR2B; right panel), independent experiments from different batches of cultured neurons. Data values used to calculate the mean for NR2B are indicated with horizontal lines. * Significantly different compared to WT, $p < 0.05$ by unpaired t-test.

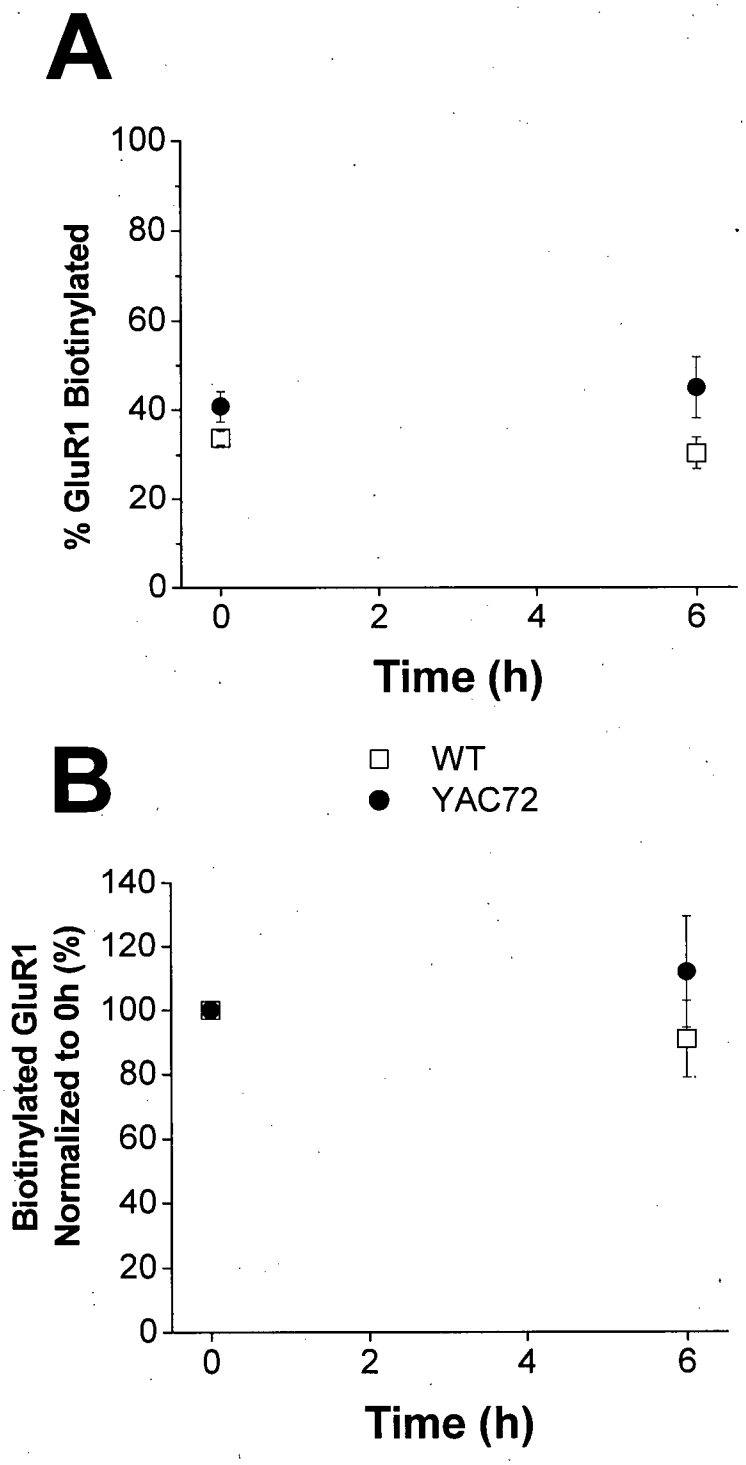

Figure 20. Plots comparing insertion of GluR1 in MSNs from WT and YAC72 mice. (A) Insertion of GluR1 over time following chlorpromazine treatment in MSNs from WT versus YAC72 mice is shown. Values represent mean percent surface expression ± SEM from N = 4 independent experiments from different batches of cultured neurons. (B) Values at the 6-hour time point are normalized to the 0-hour time point set to 100% and are plotted as mean percent ± SEM from N = 4 independent experiments from different batches of cultured neurons.

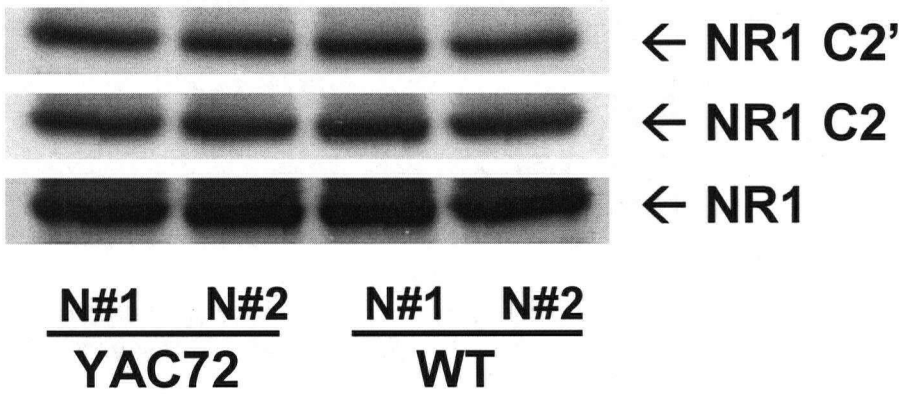

Figure 21. NR1 C2 and NR1 C2' expression is not different in striatal tissue from 2 month-old FVB/N WT or YAC72 mice. Striatal lysates are collected in duplicate from mice at 2 months of age and analyzed in parallel for expression of NR1 isoforms containing either the C2 or C2' cassette. NR1 expression is shown as loading control.

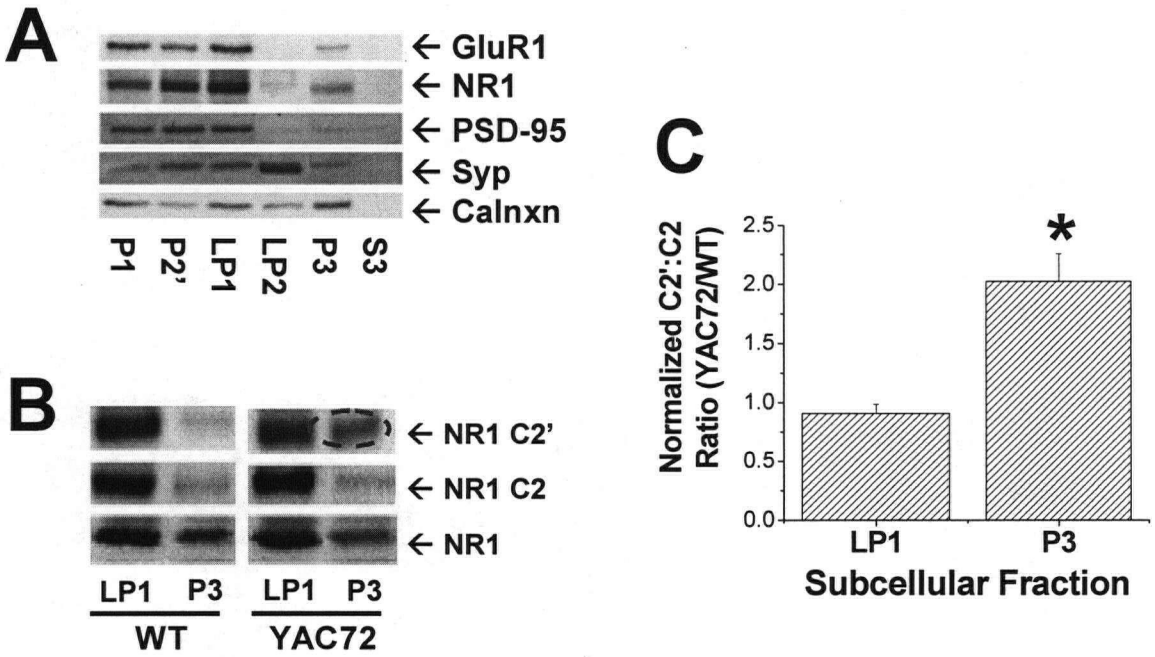

Figure 22. Increased YAC72/WT ratio of NR1 C2'-to-C2 expression in microsome-enriched fraction. (A) Characterization of subcellular fractions. Fractionated subcellular compartments of striatal tissue from FVB/N WT mice are resolved by SDS-PAGE, where equivalent amounts of protein are loaded for each fraction. GluR1 and NR1 are present in both LP1 and P3 fractions, while the post-synaptic marker protein PSD-95 is enriched in LP1. Synaptophysin (Syp) is most highly concentrated in the LP2 fraction, as expected for a pre-synaptic protein. Calnexin (Calnxn) on the other hand is abundantly expressed in the P3 fraction confirming this to be the ER/microsome-enriched fraction. Immunoblot shown is representative of three independent fractionation experiments using different batches of tissue. P1, large cell fragments/nuclei; P2', washed crude synaptosomal fraction; LP1, heavy/synaptosomal membranes; LP2, synaptic vesicle-enriched fraction; P3, light membranes/microsome-enriched fraction; S3, cytosolic fraction. (B) Representative immunoblot depicts expression of NR1, NR1 C2, and NR1 C2' in LP1 and P3 fractions of striatal tissue from 2 month-old YAC72 and WT mice. (C) C2'-to-C2 ratios are quantified from LP1 and P3 fractions of striatal tissue from 2 month-old YAC72 versus WT mice. Ratios are individually calculated for each genotype, and the YAC72 ratio is then normalized to the WT one in each paired experiment. Bars represent mean normalized C2'-to-C2 ratio ± SEM from N = 3 independent fractionation experiments each of striatal tissue pooled from 10 to 30 mice per genotype. * Significantly different compared to LP1, $p < 0.05$ by paired t-test.

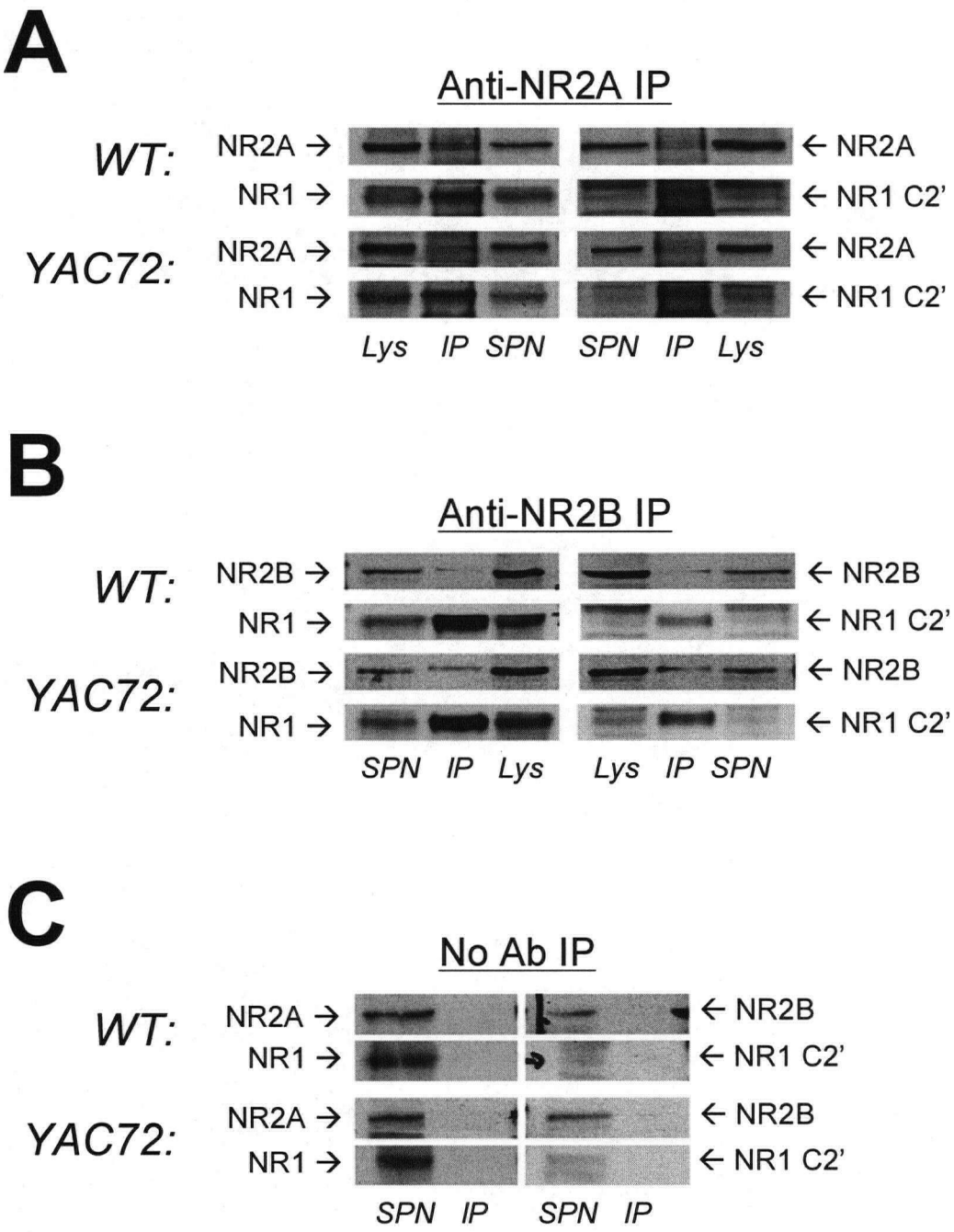

Figure 23. Representative immunoblots illustrating co-immunoprecipitation of NR1 or NR1 C2' with NR2 subunits in striatal tissue from 2 month-old WT or YAC72 mice. Immunoprecipitation is carried out using (A) anti-NR2A or (B) anti-NR2B antibodies, and antibody-free controls are shown in (C). Interacting NR1 subunits (total population or only the C2'-containing population) are detected by immunoblotting. "Lys", lysate; "IP", immunoprecipitate; "SPN", supernatant.

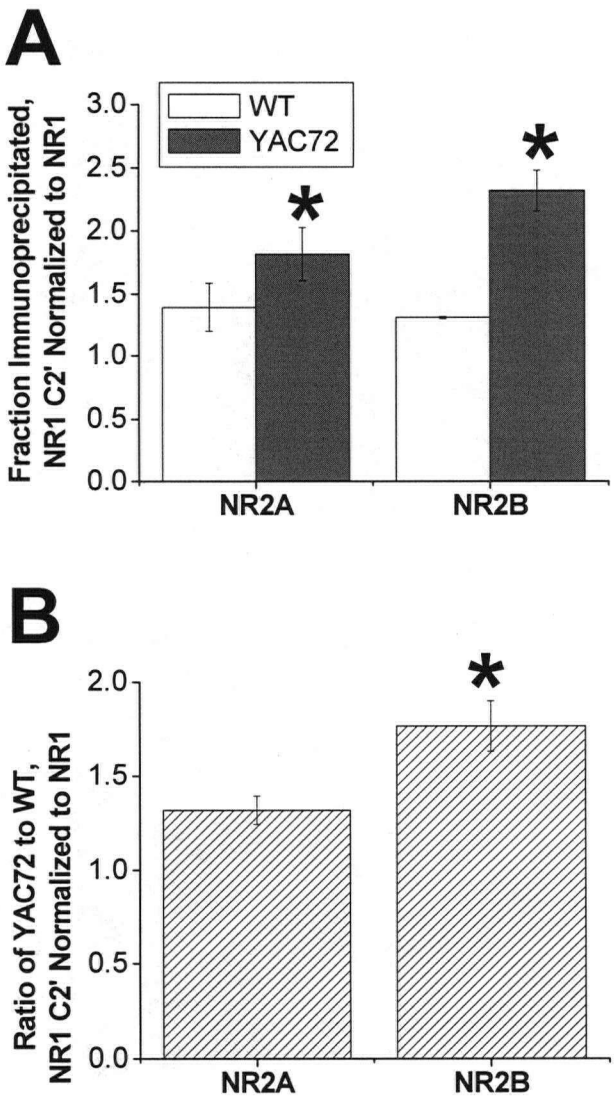

Figure 24. Plots comparing fraction of immunoprecipitated NR1 C2' normalized to NR1 in anti-NR2 precipitates from striatal tissue of 2 month-old WT or YAC72 mice. (A) Band densities are measured for each of "IP" and "SPN", and relative amounts of immunoprecipitated protein are calculated as ("IP" ÷ "Total") where "Total" is the sum of "IP" and ("SPN" * Dilution Factor). Fractions of immunoprecipitated NR1 C2' are then normalized to fractions of immunoprecipitated NR1, and this ratio is calculated for both anti-NR2A and anti-NR2B precipitates from WT and YAC72 striatal tissue to allow comparison of the amount of C2'-containing NR1 that co-precipitates with NR2A versus NR2B subunits in either genotype, normalized to total precipitated NR1. Bars represent mean normalized immunoprecipitated NR1 C2'-to-NR1 ratio ± SEM from N = 3 experiments each for WT and YAC72 performed in parallel. * Significantly different compared to WT, $p < 0.05$ by paired t-test. (B) Plot illustrates the fold change in normalized NR1 C2'-to-NR1 ratios from (A) above in YAC72 versus WT samples, for each of anti-NR2A and anti-NR2B precipitates. Bars represent mean fold change ± SEM from N = 3 experiments each for WT and YAC72 performed in parallel. * Significantly different compared to NR2A, $p < 0.05$ by paired t-test.

CHAPTER 4. HIP-1 AND α-ACTININS LINK HUNTINGTIN WITH NMDARS

4.1. Role for HIP-1 in Receptor Trafficking

Htt interacts with numerous protein partners including htt-interacting protein-1 (HIP-1), a protein which shares considerable sequence homology with the yeast cytoskeletal protein Sla2p (Kalchman et al., 1997; Wanker et al., 1997). HIP-1 associates specifically with the N-terminus of human htt, and both proteins appear to be enriched in membrane compartments after subcellular fractionation (Wanker et al., 1997). The htt/HIP-1 interaction, as demonstrated by yeast two-hybrid screening, appears to weaken with increasing polyQ length in htt (Kalchman et al., 1997).

Thus far the function of HIP-1 has not been clearly delineated, but sequence analysis revealed the presence of a death effector domain (DED), a coiled-coil region, as well as a C-terminal domain with significant sequence identity to talin (Kalchman et al., 1997; Wanker et al., 1997). The DED region was responsible for HIP-1 toxicity leading to caspase 3-dependent apoptotic death in cells over-expressing HIP-1 (Hackam et al., 2000). Co-expression of a fragment of WT htt that bound HIP-1 protected against HIP-1-mediated cell death (Hackam et al., 2000), further implicating HIP-1 as a pro-apoptotic mediator. As the strength of the htt/HIP-1 interaction is decreased with increasing htt polyQ length, cells expressing mhtt have less htt-associated HIP-1. Gervais and co-workers (2002) found that non-htt-associated HIP-1 bound to the HIP-1 protein interactor HIPPI to recruit procaspase-8 and activate the apoptotic cascade, thereby implicating a possible role for HIP-1 in HD pathogenesis.

Apart from its apoptosis-inducing functions, HIP-1 was found to be associated with clathrin-coated vesicles and to bind components of the clathrin-mediated endocytic machinery including clathrin and its adaptor protein AP-2 (Metzler et al., 2001). Intact full-length HIP-1 was required for proper clathrin-mediated endocytosis, as over-expression of various HIP-1 fragments acted in a dominant negative manner to potently inhibit this process (Metzler et al., 2001). Further evidence in support of a role for HIP-1 in clathrin-dependent endocytosis came from studies in liposomal membranes from HIP-1 knock-out (KO) mice which demonstrated reduced endocytic protein complex assembly (Metzler et al., 2003). Additionally, clathrin-dependent internalization of AMPARs following receptor stimulation was impaired in cultured hippocampal neurons from HIP-1 KO mice, indicating an involvement of HIP-1 in the regulation of AMPAR trafficking in the CNS (Metzler et al., 2003).

4.2. Role for Actin-Binding Proteins in Regulating NMDARs

NMDAR activity is well known to be regulated by components of the cellular CSK (Rosenmund and Westbrook, 1993; Allison et al., 1998; Lei et al., 2001; Yuen et al., 2005; also see Introduction section 1.5.1). In particular, depolymerization of F-actin resulted in a loss of post-synaptic glutamate receptors including the NMDARs (Allison et al., 1998), suggesting a role for the actin CSK in anchoring these receptors at the synapse. Scaffolding proteins of the MAGUK family such as PSD-95 and SAP-102 (Sans et al., 2000; Lin et al., 2004; reviewed in Carroll and Zukin, 2002; Wenthold et al., 2003; Kim and Sheng, 2004), along with actin-binding proteins such as the α-actinins (Wyszynski et al., 1997, 1998; Allison et al., 1998; Dunah et al., 2000; reviewed in Shirao and Sekino, 2001), act in conjunction with the actin CSK to maintain and anchor NMDARs at the PSD.

A direct interaction between α-actinins and NMDAR subunits NR1 and NR2B suggested the former may be responsible for mediating the attachment of NMDA glutamate receptors to the actin CSK. Of the four isoforms of α-actinins that have been identified (α-actinins 1 to 4), two (α-actinins 2 and 3) are isoforms found in skeletal muscle (Beggs et al., 1992) while the remaining two (α-actinins 1 and 4) are not. While it remains unresolved as to which isoform(s) is (are) expressed in brain, studies from our laboratory indicated that α-actinin 4, but not α-actinin 2, is the predominant isoform expressed in the mouse forebrain (C.D. Icton, 2001 M.Sc. thesis).

α-Actinins are ubiquitous actin-binding proteins that share sequence and structural homology with spectrin and dystrophin (Byers et al., 1989; Dubreuil et al., 1989; Chan et al., 1998; Viel, 1999). Given the presence of a talin-like domain within the HIP-1 protein, a potential interaction between spectrin-like α-actinins and talin-containing HIP-1 was investigated due to previous reports of interactions between these two modular domains in other proteins (Cohen and Foley, 1984; Ohanian et al., 1984; Podgorski and Elbaum, 1985; Podgorski et al., 1988; Takeuchi et al., 1994; Diakowski et al., 2006). A cartoon of selected modular domains in HIP-1 and α-actinin proteins is shown in Figure 25.

4.3. Interaction of HIP-1 and α-Actinin with NMDARs

4.3.1. Co-Localization of HIP-1 with α-Actinin 4 in Mouse Striatal MSNs

Previous studies in our laboratory demonstrated an interaction between HIP-1 and α-actinin 4 by co-immunoprecipitation when these proteins are over-expressed in a heterologous cell line, the HEK293 cells (C.D. Icton, 2001 M.Sc. thesis). To examine if

these endogenous proteins also associate with each other in mouse striatal neurons, immunofluorescent staining was done to assess their cellular distribution. Cultured striatal MSNs from FVB/N WT mice were double-labeled for HIP-1 (coupled to fluorescent green secondary antibody) and α-actinin 4 (coupled to fluorescent red secondary antibody). The cellular and dendritic expression patterns were found to be similar and overlapping between HIP-1 and α-actinin 4 (Figure 26; also investigated more extensively in L. Sornarajah, 2004 B.Sc. thesis), suggesting these proteins may be present in the same locations within the cell to interact with each other.

4.3.2. HIP-1 and α-Actinin 4 Interact with NMDARs by Co-Immunoprecipitation

To determine whether the interaction between HIP-1 and α-actinin 4 may serve to bring HIP-1 (and by extension, htt) into close physical proximity to NMDARs to facilitate modulation of NMDAR activity by htt, we asked if these proteins could interact with NMDARs, again using HEK293 cells as our model for these studies. HEK293 cells transfected with NMDAR subunits NR1/NR2B were subjected to immunoprecipitation experiments using an antibody directed against the NR2B subunit. HIP-1 and α-actinin 4 (both of which are endogenously expressed in HEK293 cells) were found to co-precipitate with NR2B (Figure 27), suggesting the possible interaction of HIP-1/α-actinin 4 with NMDARs in a complex. However, because NMDARs are not endogenously expressed in HEK293 cells, we sought to examine the HIP-1/α-actinin interaction in a more physiologically relevant system where the interaction may have a functional role in mediating the effects of WT or mutant htt on NMDAR activity. As with the HEK293 cells, immunoprecipitation of HIP-1 from striatal or forebrain tissue of 2 month-old FVB/N mice successfully brought down α-actinin 4 (Figure 28A). Moreover, anti-HIP-1 antibodies also

co-precipitated NMDAR subunit NR2B (Figure 28B), indicating the presence of NMDARs as part of a larger macromolecular complex containing HIP-1 and α-actinins. Conversely, immunoprecipitation using antibodies directed against the NR2B subunit also pulled down HIP-1 (Figure 28C). Although we had limited success in using anti-α-actinin antibodies in immunoprecipitation experiments to bring down HIP-1, the difficulty was likely due to the multi-functional role of the actin-crosslinking proteins within the cell and their involvement in a large number of protein interactions apart from binding HIP-1.

4.3.3. HIP-1, α-Actinin 4, and NMDARs Co-Fractionate

To assess whether the components of this putative macromolecular complex are present in the same subcellular locations to facilitate interactions among these proteins and bring htt into close proximity to NMDARs, we performed subcellular fractionation of striatal tissue from 2 month-old FVB/N mice as decribed previously (Figure 6) and probed for proteins of interest in the different fractions obtained.

Post-synaptic glutamate receptors such as NR1 and GluR1 were found to be enriched in both the LP1 and P3 fractions (Figure 22A), representing pools at the synapse and in transit to or from the surface, respectively. Importantly, α-actinin and actin were also present – while HIP-1 and htt were concentrated – in the P3 fraction (Figure 29), which is the mobile fraction consisting of light membranes including ER and vesicular components responsible for carrying membrane proteins such as NMDARs to and from the surface. These data, along with co-immunoprecipitation results showing that HIP-1, α-actinin, and NR2B are found in a complex in mouse forebrain tissue (Figure 28), suggest that interaction of these proteins may function to regulate the movement of newly

assembled NMDARs exiting from the ER, or else modulate the endocytosis/recycling of NMDARs from or to the cell surface.

4.3.4. Direct Interaction between HIP-1 and α-Actinin

While HIP-1 and α-actinins have been shown to co-exist as part of the same complex by co-immunoprecipitation studies and to have overlapping distribution intracellularly by subcellular fractionation and immunostaining, these methods could not determine whether the interaction between the two proteins was direct or not. To address the question of whether HIP-1 can directly bind α-actinin, we expressed a GST-fused HIP-1 protein (GST-HIP1) and assessed its ability to bind recombinant α-actinin protein *in vitro* in a gel overlay assay. The time course of the induction and expression of the recombinant proteins was examined, and our observations suggested that induction of protein expression yielded maximal amounts of recombinant proteins for harvest by three hours following induction of the bacterial culture by IPTG (Figure 30A). Interaction between the recombinant GST-HIP1 and α-actinin proteins was observed, as immunoblotting for α-actinin revealed binding of the protein to immobilized GST-HIP1 (but not GST or GST-HIP1-Talin) on the Immobilon membrane (Figure 30B). These results provide evidence that HIP-1 can directly interact with α-actinins, although it remains uncertain as to which domain(s) within each protein may be responsible for mediating this interaction. The GST-fusion protein expressing only the talin domain of HIP-1 (GST-HIP1-Talin) failed to bind α-actinins, in contrast to our predictions based on previously documented spectrin-talin domain interactions. This may indicate a lack of involvement of this region in mediating HIP-1/α-actinin binding, or else the expression of

the talin domain alone may not be sufficient for the protein to assume the proper conformation essential for mediating appropriate interactions with protein partners of HIP-1. A model of how we believe htt to interact with NMDARs though HIP-1/α-actinin interactions based on our findings is shown in Figure 31.

4.4. HIP-1 Over-Expression Increases NR1 Surface Expression in Striatal MSNs

Having determined that HIP-1 and α-actinins can directly interact and co-exist in a multi-protein complex with NMDARs, we asked whether HIP-1 modulated NMDAR expression and/or trafficking since HIP-1 has been shown to be involved in the regulation of trafficking of AMPARs (Metzler et al., 2003, 2007). We co-transfected plasmids expressing HIP-1 and GFP into MSNs in culture and measured surface and internal NR1 expression by immunofluorescent staining. The method used was similar to that described previously for green/red labeling of surface/internal NR1 (see sections 2.1.2.2 and 3.2.1), except different fluorophore-coupled secondary antibodies were used due to overlap of emission wavelengths from AlexaFluor 488 and GFP. In this case, labeled surface NR1 was visualized by the Cy3-conjugated fluorescent red secondary antibody, while intracellular NR1 was visualized by AlexaFluor 350-conjuated fluorescent blue secondary antibody. Red-to-blue signals were quantified in GFP-expressing cells that morphologically resembled MSNs to provide an estimate of the surface-to-internal NR1 expression levels, and MSNs co-expressing HIP-1 and GFP were compared to those transfected with GFP alone (control). We found that, on average, MSNs over-expressing HIP-1 had ~30% higher surface NR1 expression relative to controls (Figure 32), suggesting that HIP-1 over-expression enhances NR1 surface expression, possibly by recruiting/stabilizing receptors at the surface, modulating receptor internalization, or

regulating NMDAR forward trafficking from the Golgi. Since the strength of HIP-1/htt interaction is weakened with increasing htt polyQ length (Kalchman et al., 1997), the effects of htt polyQ expansion on HIP-1 could be similar to HIP-1 over-expression in terms of up-regulating the number of non-htt-associated HIP-1 molecules. Because both htt polyQ expansion and HIP-1 over-expression led to enhanced surface expression of NR1 in cultured MSNs, mhtt may be mediating its effects on NMDAR function/trafficking in part by reducing the proportion of htt-bound HIP-1. The presence or absence of htt or mhtt within an NMDAR-associated complex containing HIP-1 may differentially affect how HIP-1 modulates NMDAR function and/or trafficking.

4.5. Summary

Despite a lack of evidence to date implicating a direct role of HIP-1 in the pathogenesis of HD, our data indicate that HIP-1 is able to form a multi-protein complex with NMDARs that includes actin-crosslinking proteins such as the α-actinins, and to modulate NMDAR expression at the cell surface. Specifically, we found that HIP-1 associated with α-actinin 4 and NMDAR subunits by co-immunoprecipitation, and that these proteins have overlapping subcellular distributions. Moreover, *in vitro* experiments demonstrated a direct interaction between recombinant α-actinin and HIP-1, although the regions mediating this interaction have not been identified. The association of HIP-1 with NMDAR complexes likely plays a role in the regulation of NMDAR activity/expression, as NMDAR distribution within neurons over-expressing HIP-1 was shifted towards increased surface expression. A preliminary model could be assembled based on these findings: expression of mhtt leads to decreased interaction of mhtt with its endogenous protein

partner, HIP-1. Non-htt-associated HIP-1 then acts to promote surface NMDAR expression (which may be selective for NR1 C2'- and NR2B-containing receptors; see sections 3.4 and 3.5), which in turn causes increased NMDAR-mediated current and excitotoxic cell death when the receptors are activated. In this way, the htt/HIP-1/α-actinin/NMDAR link provides a mechanism through which mhtt may modulate NMDAR expression and function as observed in various cellular and mouse models of HD.

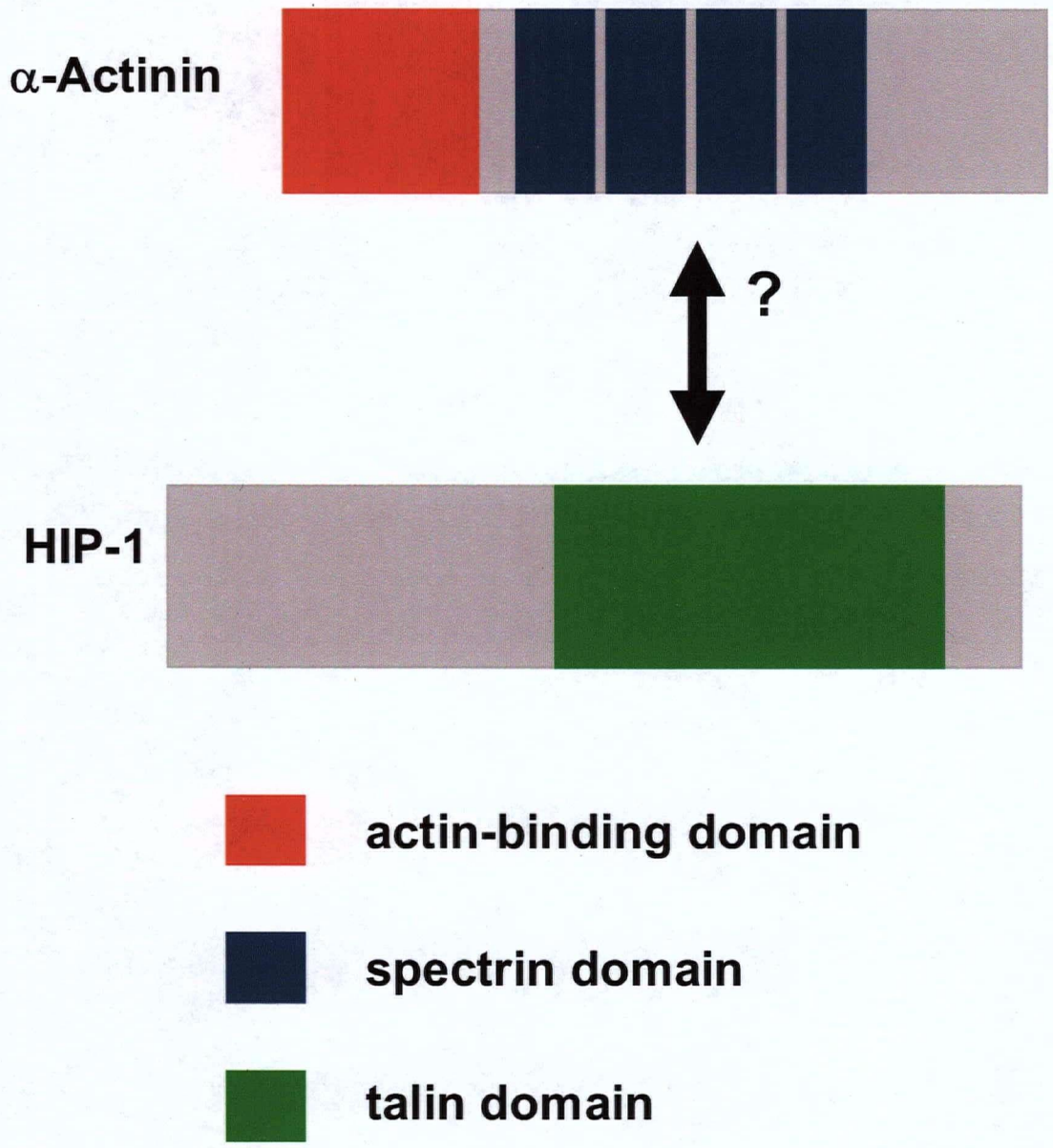

Figure 25. Schematic of selected modular domains in HIP-1 and α-actinin proteins. Spectrin domains within α-actinins are hypothesized to be able to bind talin domains such as the one present in the HIP-1 protein. Interaction between HIP-1 and α-actinins may serve to bring HIP-1 and htt into close proximity to NMDARs.

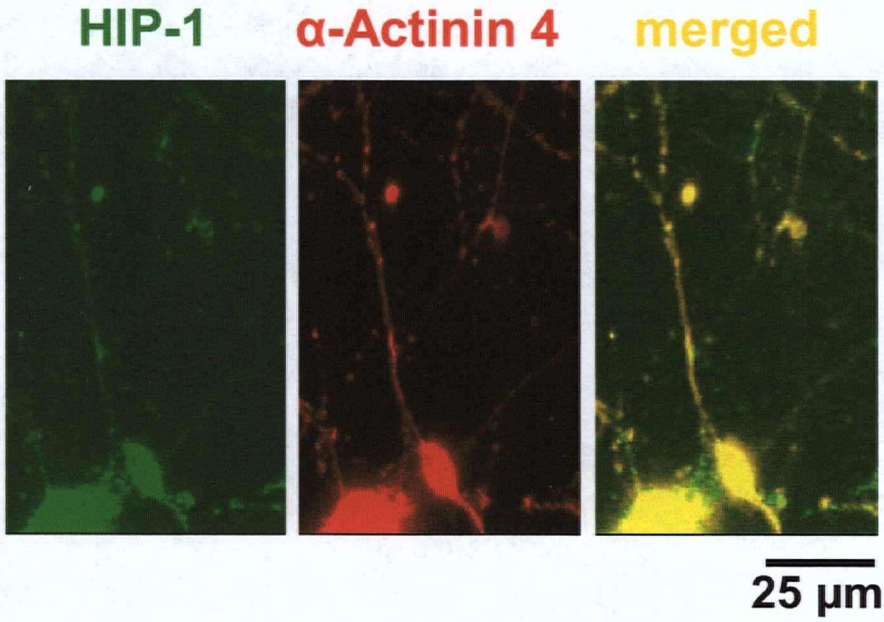

Figure 26. HIP-1 and α-actinin 4 co-localize by immunostaining in mouse striatal MSNs. Striatal MSNs cultured from P0-P1 FVB/N mouse pups are fixed at 9-10 d.i.v. and immunostained for HIP-1 (green) and α-actinin 4 (red). Signals are merged in the right-hand panel to view co-localization, where yellow represents overlapping areas. Pictograph shown is representative of at least three independent experiments using different batches of cultured neurons.

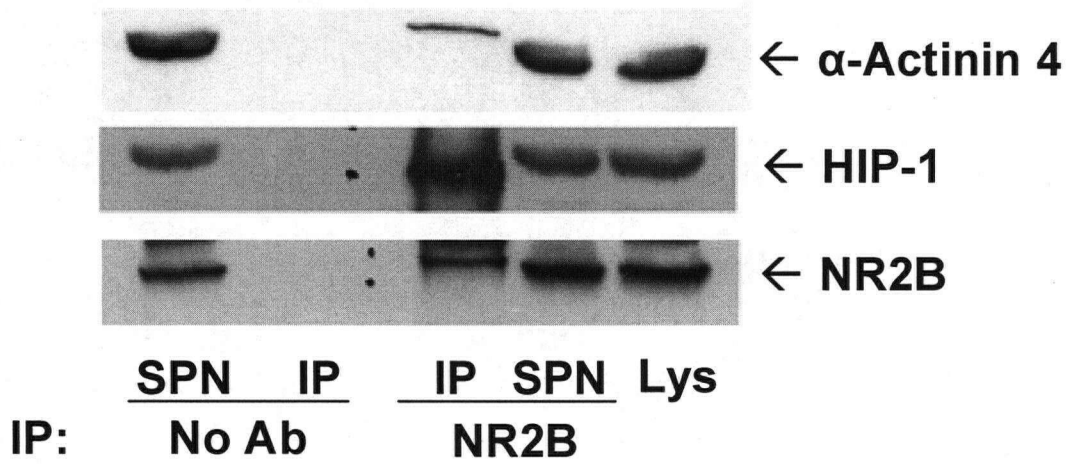

Figure 27. HIP-1 and α-actinin 4 interact with NMDARs in transfected HEK293 cells by co-immunoprecipitation. Immunoprecipitation is carried out using anti-NR2B antibodies, and examined for co-precipitation of HIP-1 and α-actinin 4. Immunoblot shown is representative of at least three experiments using independent batches of cells transfected individually. "Lys", lysate; "IP", immunoprecipitate; "SPN", supernatant; "No Ab", antibody-free control.

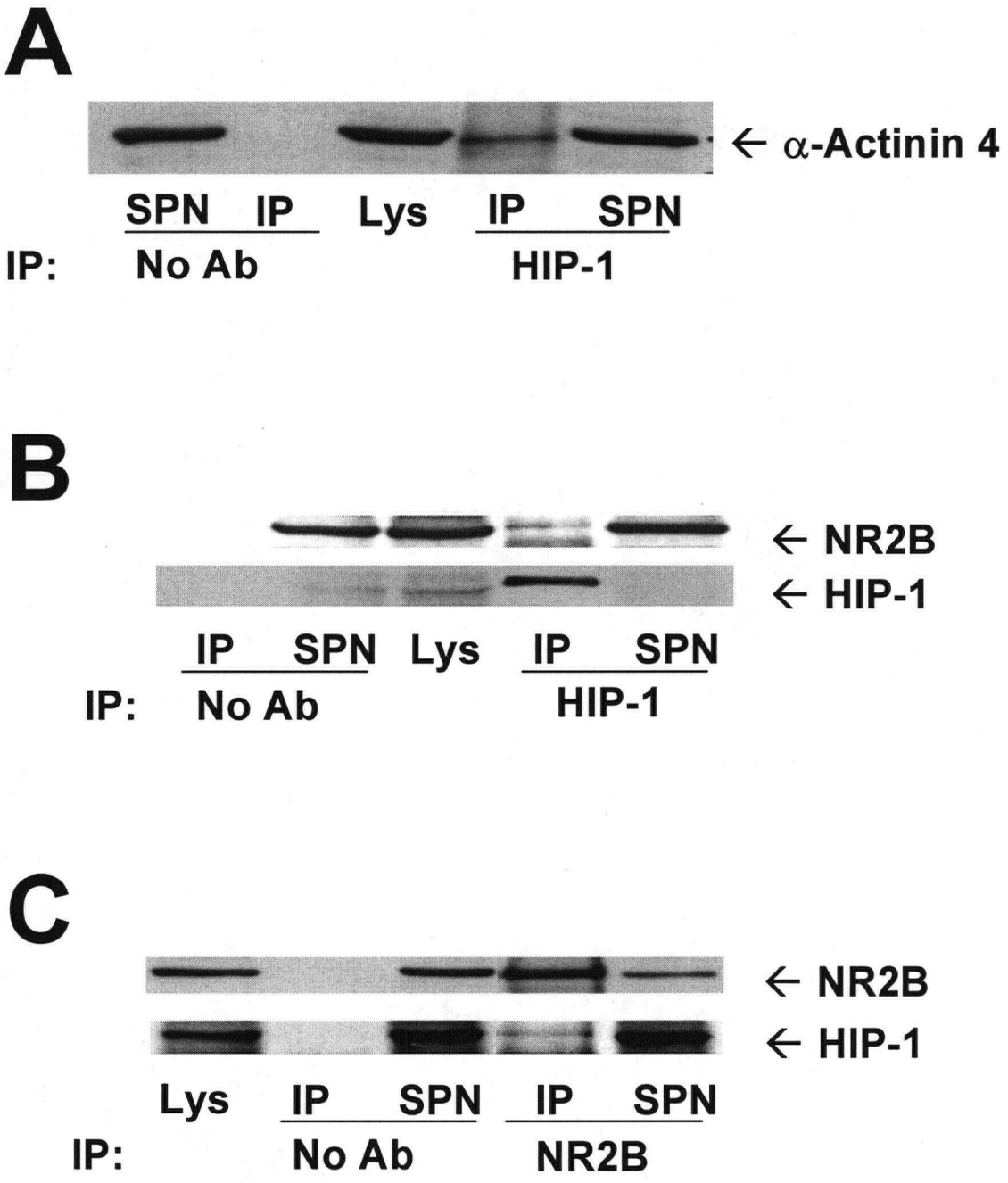

Figure 28. HIP-1 and α-actinin 4 interact with NMDARs in mouse forebrain tissue by co-immunoprecipitation. Immunoprecipitation is carried out using (A, B) anti-HIP-1 or (C) anti-NR2B antibodies, and examined for co-precipitation of (A) α-actinin 4, (B) NR2B, or (C) HIP-1 proteins. Immunoblot shown in each sub-panel is representative of at least three independent experiments using different tissue batches. "Lys", lysate; "IP", immunoprecipitate; "SPN", supernatant; "No Ab", antibody-free control.

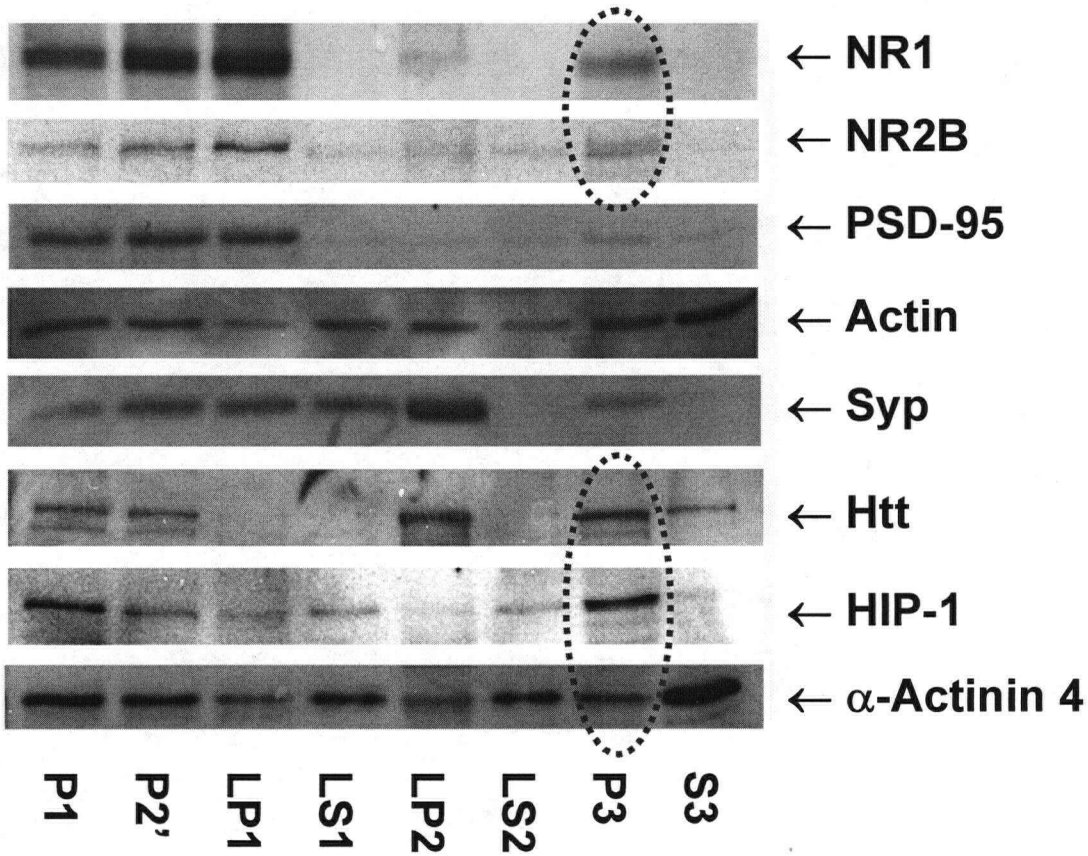

Figure 29. HIP-1, α-actinin 4, and NMDARs co-fractionate in mouse striatal tissue. Equivalent amounts of protein from various fractions obtained in subcellular fractionation experiments are resolved by SDS-PAGE and probed for proteins of interest. Htt, HIP-1, α-actinin 4 and NMDAR subunits NR1 and NR2B all have overlapping subcellular distribution in the P3 fraction. Syp, synaptophysin. P1, large cell fragments/nuclei; P2', washed crude synaptosomal fraction; LP1, heavy/synaptosomal membranes; LS1, cytoplasm of lysed synaptosomes; LP2, synaptic vesicle-enriched fraction; LS2, pre-synaptic cytosol; P3, light membranes/microsome-enriched fraction; S3, cytosolic fraction.

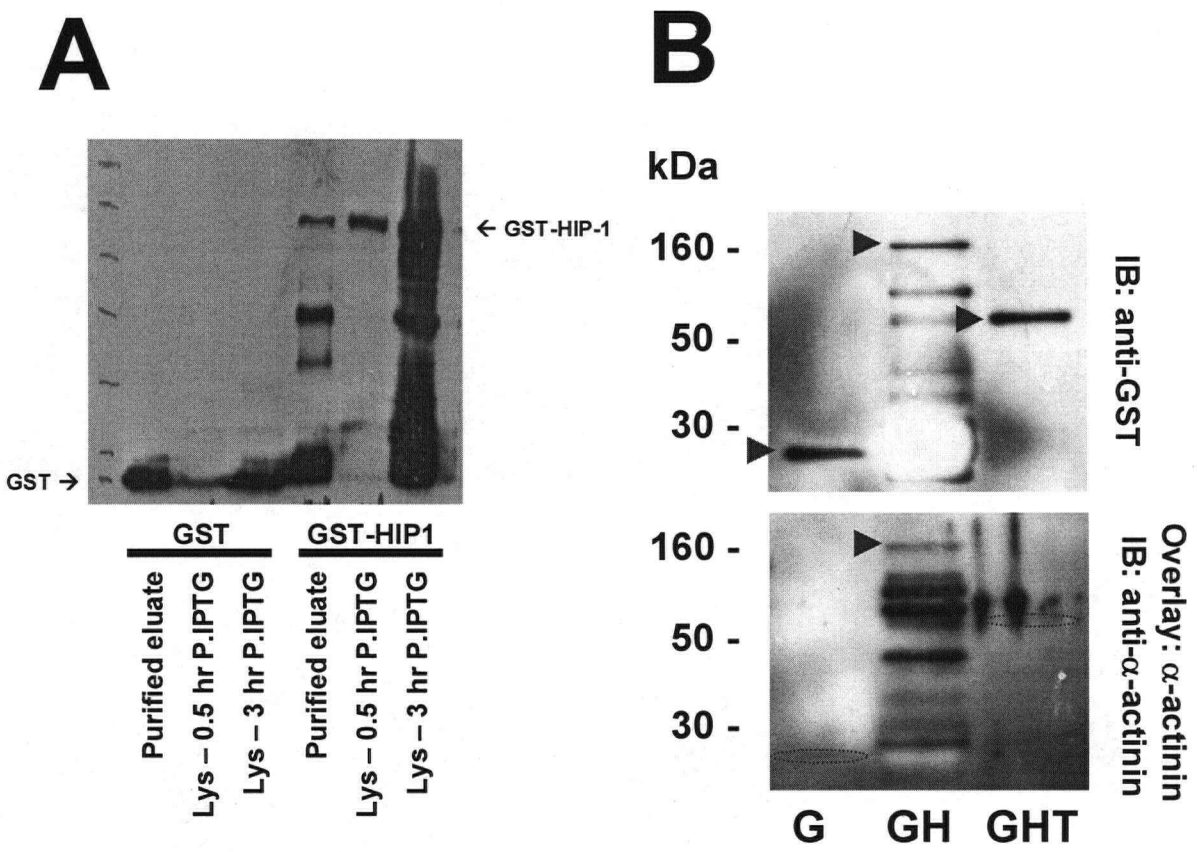

Figure 30. HIP-1 binds directly to α-actinin by gel overlay assay. (A) Induction of GST protein expression from *E. coli* bacteria. Cultures of bacteria carrying vectors encoding for GST or GST-fusion proteins are grown until the log phase is reached before being induced for GST protein expression by addition of IPTG. Expression of GST and GST-fusion proteins is confirmed by immunoblotting with an anti-GST antibody on eluates purified with glutathione sepharose resin at 5 µg per lane, or bacterial lysates (Lys) obtained at 0.5 or 3 hours post-induction (P.IPTG) at 10 µl per lane. (B) Equivalent amounts of bacterially purified GST, GST-HIP-1, and GST-HIP1-Talin proteins are resolved by SDS-PAGE and overlaid with solution containing recombinant α-actinin protein purified from chicken gizzard (~80% purity). Binding of α-actinin to the purified GST and GST-fusion proteins is subsequently determined by immunoblotting for α-actinin (lower panel), and expression of the GST-fusion proteins confirmed by immunoblotting with an anti-GST antibody (upper panel). Immunoblots shown are representative of at least three independent experiments. Arrowheads indicate species at MW corresponding to full-length GST or GST-fusion proteins. G, GST; GH, GST-HIP-1; GHT, GST-HIP1-Talin.

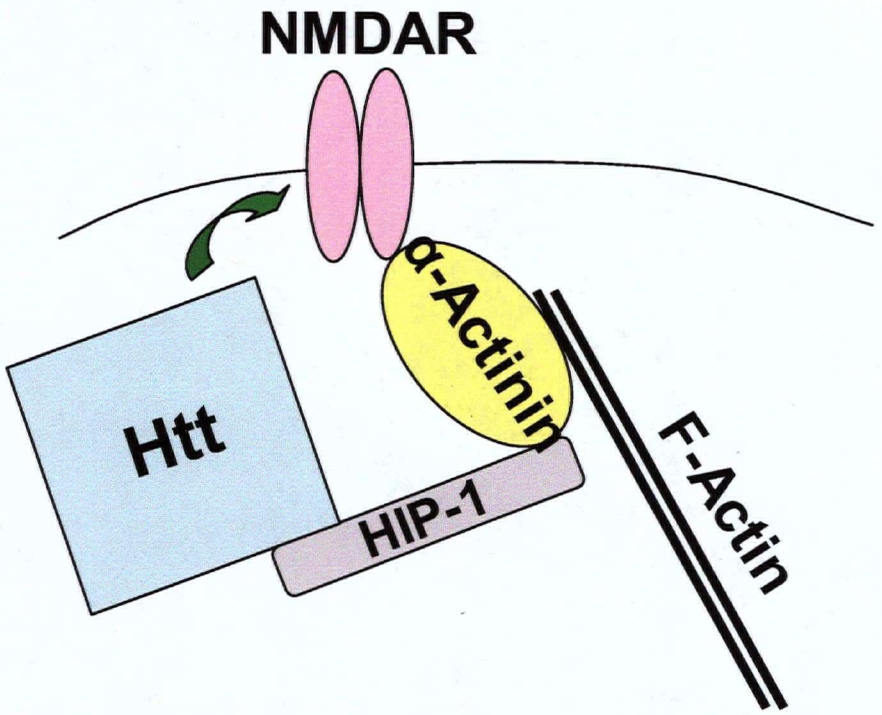

Figure 31. Cartoon of hypothesized HIP-1/α-actinin interactions in linking htt to NMDARs. Based on results described in this thesis, we propose that HIP-1 may interact with α-actinin to bring htt into close proximity with NMDARs.

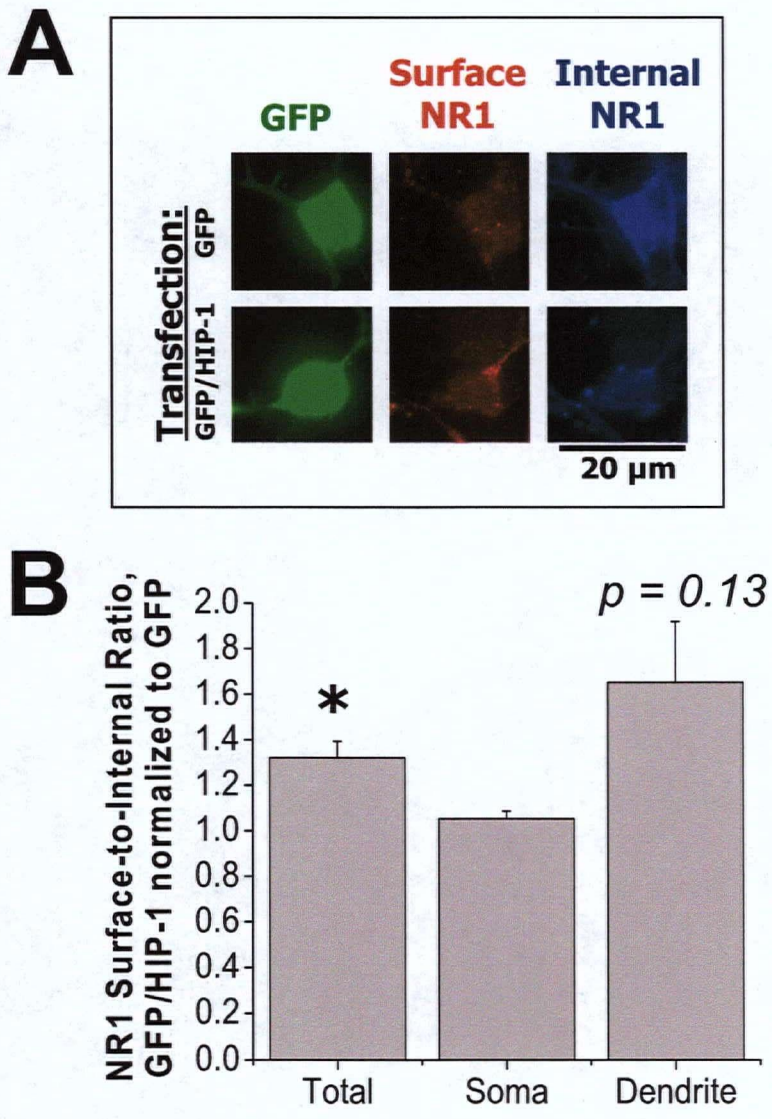

Figure 32. Immunofluorescent staining demonstrates increased proportion of surface NR1 in MSNs over-expressing HIP-1. (A) Representative pictographs show cultured MSNs transfected with GFP and HIP-1 plasmids or GFP alone at 7 d.i.v., fixed at 9-10 d.i.v., and immunostained for surface (red) and internal (blue) populations of the NR1 subunit. All steps of culturing, transfection, fixation, immunostaining, fluorescence imaging and image capturing are performed in parallel for both conditions within each experiment. Only cells that fluoresce green are included for analysis. (B) Intensity of fluorescent staining is quantified for both surface and internal NR1 in MSNs transfected with either GFP alone or GFP and HIP-1. Proportion of NR1 expressed at the cell surface is determined by taking a ratio of surface-to-internal NR1 staining, and compared between GFP-expressing cells and GFP/HIP-1-expressing cells. Bars represent mean ratio of GFP/HIP-1-expressing cells normalized to GFP-expressing cells, ± SEM from N = 3 experiments. Each experiment involves an independent transfection of GFP/HIP-1 and GFP in parallel, and subsequent data analysis is also performed in parallel from 4 transfected neurons per condition in every experiment. * Significantly different than one, $p < 0.05$ by 1-sample t-test of data values normalized to the GFP condition.

CHAPTER 5. KINETWORKS™ PROFILING OF PROTEIN EXPRESSION CHANGES IN CELLS EXPRESSING mHTT

5.1. Introduction to Kinetworks™ Screening Technique

Findings from our laboratory indicate that current and toxicity resulting from NMDAR activation are enhanced in striatal neuronal cultures from YAC transgenic mice expressing mhtt, in a NR1/NR2B subtype-selective and htt polyQ length-dependent manner (Zeron et al., 2002; Shehadeh et al., 2006). Studies in a heterologous cell line, the HEK293 cells, also corroborated these results. Not only did over-expression of NR1/NR2B (but not NR1/NR2A) receptors lead to increased peak current density through NMDARs in cells co-expressing htt containing 138Q (htt-138Q; mutant) relative to htt-15Q (containing 15Q; WT) (Chen et al., 1999b); co-expression of NR1/NR2B with htt-138Q also led to significantly higher levels of NMDAR-dependent apoptotic cell death (relative to NR1/NR2A, or htt-15Q) (Zeron et al., 2001). Comparable effects of mhtt expression on the function of NR2B-containing NMDARs in these two model systems suggest that heterologous expression systems such as the HEK293 cell line may be a valid model in which to investigate further the mechanisms underlying the effects of mhtt expression.

Results from high-throughput analyses of gene expression changes (at the level of mRNA expression) have been documented in a variety of cellular and rodent models of HD (Luthi-Carter et al., 2000, 2002a, 2002b, 2003; Sipione et al., 2002). Studies to address global protein expression changes resulting from mhtt polyQ expansion have yet to be done, and they are of special importance as the sum of all regulatory influences on

gene transcription, translation, and post-translational modifications are ultimately reflected in the profile of protein expression.

To obtain the first clues into what changes at the protein level may be induced by or mediate the effects of mhtt expression, we employed a multi-immunoblotting proteomics screening technique, referred to as the Kinetworks™ screens (Hu et al., 2003a, 2003b; Pelech et al., 2003), to examine expression changes for a panel of 78 protein kinases, 18 protein phosphatases, and 25 heat shock/stress-related proteins in HEK293 cells over-expressing NR1/NR2B subtype of NMDARs as well as either WT htt (htt-15Q) or mhtt (htt-138Q). In all experiments involving use of NR1/NR2B/htt-15Q or htt-138Q-transfected cells, transfection efficiency of >50% (as determined by β-galactosidase staining of a dish of cells transfected in parallel with β-gal cDNA) was requisite for continuation of the experiment. Furthermore, comparable transgene expression in each case was verified by immunoblotting (data not shown).

For Kinetworks™ screens, lysates (collected for total protein or fractionated into cytosolic versus particulate fractions) were resolved by SDS-PAGE and immunoblotted in a 20-channel multiblotter with up to three antibodies per channel. Antibodies used were pre-validated and tested to rule out cross-reactivity with other immunogen targets within a given channel. Kinetworks™ analyses facilitate high-throughput and rapid detection of expression changes of proteins and have been reported for their usefulness in identifying target proteins with expression changes under different conditions (Hu et al., 2003a, 2003b). Reproducibility of protein band densities obtained in these screens has been determined to be within 15-20% when identical samples and experimental conditions were used; hence changes of greater than ~25% in band density would be deemed significant.

In these studies, transfected HEK293 cells were used not only because they mimic the effects observed in the YAC HD mouse model with respect to the effects of mhtt expression on NMDAR activity, but also because this cell line is a uniform and well-characterized model system with homogeneous cellular metabolic and gene expression profiles. We chose not to use striatal tissue in these screens so as to avoid possible confounding factors associated with the intrinsic heterogeneity of tissue samples. Cultured striatal neurons were likely more uniform in their gene expression profile, but these were prepared from litters of newborn mouse pups and could not be obtained in large enough quantities to yield sufficient protein content for analysis as individual samples in such screens.

5.2. Results from KPKS Protein Kinase Screens

Protein expression in Kinetworks™ screens is quantified on the basis of signal intensity from ECL detection. Values of less than ~500 (expression level in arbitrary units) in theory (or ~3000 in actual practice) are considered background. Changes of less than ~25% from initial values are considered insignificant. Because the number of proteins with signal intensities larger than 500 and exhibiting 25% or greater change in expression exceeds our capacity to perform follow-up experiments, we imposed additional selection criteria for our screens and have chosen to report only those proteins with expression signal intensities of greater than 5000 and that changed by 50% or more from the "htt15" to the "htt138" condition.

Most of the 78 protein kinases examined in the KPKS screen were readily identifiable by the pre-validated antibodies in cytosolic and particulate fractions from transfected HEK293 cells, with the exception of the following protein kinases which

appeared not to be expressed in readily detectable quantities in our system: BTK, CaMK1, CaMK4, CDK2, CK1ε, GCK, IKKα, JAK2, Lck, MKK7, Mnk2, Nek2, PAK1, PAK3, PDK1, Pim1, PKCα, PKCε, PKCγ, PKCθ, PKR, PYK2, and RSK2. Example blots from the actual screen are shown in Figure 33 with the list of protein kinases tabulated in Table 2. Raw values from quantification of band densities are plotted in Figure 34.

In this initial screen, we investigated whether proteins of interest shifted their distribution between cytosolic and particulate pools. Protein kinases that met our selection criteria include the following: protein serine/threonine kinases casein kinase 2 (CK2) α" subunit and Jun N-terminal kinase (JNK; also known as stress-activated protein kinase SAPK), which displayed increased expression in the particulate sample from cells expressing mhtt ("htt138" condition) at 68% and 67%, respectively. Expression of cyclin-dependent kinase 5 (CDK5) was also altered by htt polyQ expansion, showing a 125% increase in the cytosolic fraction from htt138-expressing cells. Decreases in either cytosolic or particulate fractions in mhtt-expressing cells were also observed, most notably for hematopoietic progenitor kinase 1 (HPK1) which was virtually undetectable in the particulate fraction from cells expressing mhtt. Expression levels and changes for these kinases and proteins in other categories which met our selection criteria are summarized in Tables 5 and 6.

5.3. Results from KPPS Protein Phosphatase Screens

Analysis of the protein phosphatase screen (KPPS; Hu et al., 2003a, 2003b) revealed numerous changes as well, out of a total of 18 protein phosphatases which were examined. A sample blot from the screen is shown in Figure 35, and the list of protein phosphatases tabulated in Table 3. Raw values from quantification of band densities are

plotted in Figure 36. Protein tyrosine phosphatase 1B (PTP-1B) and protein phosphatase 5 (PP5) both showed increased expression in the particulate fraction from cells expressing htt138 (at 178% and 202%, respectively), whereas increased expression was noted in the cytosolic fraction of mhtt-expressing cells for protein phosphatase 2A – A regulatory subunits (α/β isoforms) (PP2A/Aα/β) (at 82%) (Tables 5 and 6).

5.4. Results from KHSP Heat Shock Protein Screens

Twenty-five proteins involved in heat shock and/or stress response pathways were also examined by Kinetworks™ analysis in the KHSP screen, a sample blot of which is shown in Figure 37. The list of stress/heat shock proteins examined is tabulated in Table 4, and protein expression is quantified and plotted in Figure 38. Again, most proteins were readily detectable in the screen, with the exception of Cox-2, ERp57, Grp94, HSF4, and HspBP1. Of the heat shock/stress-related proteins examined, those that met our selection criteria of greater than 5000 units with a ≥50% change from the WT condition (expressing htt-15Q) to the mutant one (expressing htt-138Q) included the following (as summarized in Tables 5 and 6): the 72 kDa ER protein (ERp72) and heat shock protein 90 (Hsp90) both displayed significantly up-regulated expression in the particulate fraction of htt138-expressing cells, at 503% and 7387% increase, respectively. In cytosolic samples, 70 kDa heat shock protein 1A (Hsp70) expression was increased by 52% in cells expressing mhtt. Expression of the chaperonin heat shock 60 kDa protein 1 (GroEL) was increased in both the cytosolic and particulate fractions from htt138-expressing cells, with a robust 122% increase in the cytosolic fraction and an increase of similar magnitude (at 128%) in the particulate fraction.

5.5. NMDAR Expression- and Activity-Dependent Increase in Cytosolic Hsp70

While different trinucleotide repeat disorders are known to be caused by mutations in different, unrelated genes, many systems modeling these diseases have indicated that this diverse group of disorders may share certain cellular response pathways or mechanisms, including misfolding and accumulation of the mutated proteins in insoluble aggregates or inclusion bodies leading to cellular dysfunction and death. In cells over-expressing fragments of mhtt containing the polyQ tract, for example, insoluble inclusion bodies appeared to be formed by these aggregation-prone proteins due to a reduction in the capacity of the UPS to degrade misfolded proteins (Waelter et al., 2001). Manipulating expression of molecular chaperones and heat shock proteins has been shown in many cases to modulate the deleterious effects of mutant protein expression on protein aggregation and/or cellular toxicity (Cummings et al., 1998, 2001; Chai et al., 1999; Warrick et al., 1999; Carmichael et al., 2000; Jana et al., 2000; Kazemi-Esfarjani and Benzer, 2000; Kobayashi et al., 2000; Muchowski et al., 2000; Zhou et al., 2001; Bonini, 2002; Wyttenbach et al., 2002; Adachi et al., 2003; Ishihara et al., 2003; Katsuno et al., 2005).

In the context of HD, the molecular chaperone Hsp70 has been shown to be co-localized with a mhtt fragment in inclusion bodies in transfected cells as a result of the polyQ expansion (Wyttenbach et al., 2000). Other studies have suggested that over-expression of Hsp70 could reverse the toxic effects of mhtt expression (Carmichael et al., 2000; Jana et al., 2000; Wyttenbach et al., 2002). Because our laboratory has previously demonstrated that NMDAR-dependent toxicity varied with htt polyQ length (Zeron et al., 2001, 2002; Shehadeh et al., 2006) and, more importantly, that pharmacological reduction of current flux through NMDARs successfully reduced

mhtt-induced apoptotic cell death (Shehadeh et al., 2006), we were interested in examining possible alterations in the expression of this molecular chaperone in the presence of mhtt and/or NMDARs.

To this end, we transfected heterologous HEK293 cells with constructs expressing various combinations of htt-15Q, htt-138Q, and/or NR1/NR2B to determine the effects of expression of WT or mutant htt alone or in the presence of NMDAR co-expression. Our initial KHSP screen which compared samples from cells expressing NR1/NR2B/htt-15Q versus NR1/NR2B/htt-138Q suggested up-regulated levels of Hsp70 in the cytosolic fraction in htt-138Q-expressing cells (Figure 38, Table 6). With this set of experiments we confirmed our earlier findings; cells expressing htt-138Q with NR1/NR2B displayed enhanced cytosolic Hsp70 expression levels as compared with cells expressing NR1/NR2B/htt-15Q (Figure 39A). Moreover, our results indicated that the mhtt-dependent increase in cytosolic Hsp70 required co-expression of NMDARs, since cytosolic expression of Hsp70 was similar in cells that expressed either htt-15Q alone or htt-138Q alone, and levels were also lower than in cells co-expressing NR1/NR2B/htt-138Q.

Apart from changes in Hsp70 expression arising from htt polyQ expansion in the presence of NMDAR expression, results from our initial KPKS and KHSP screens also indicated up-regulation in certain cytosolic or particulate fractions of several other proteins involved in the heat shock and/or stress-response pathway, including CK2, GroEL, and Hsp90 in the particulate fraction from cells over-expressing NR1/NR2B/htt-138Q (Figures 34 and 38, Table 6). Effects of agonist-dependent activation of NMDARs on expression of these proteins were investigated. We found expression of these stress-activated proteins in the particulate fraction to be consistently enhanced by NMDAR stimulation (using 1 mM NMDA in conjunction with 50 μM glycine)

in cells expressing htt-138Q versus htt-15Q, to much larger extents than in the absence of stimulation (Figure 39B, Table 7). Mutant htt-induced increases in cytosolic or particulate expression of these heat shock/stress-related proteins therefore appear not only to depend on NMDAR expression, but also to be potentiated by agonist stimulation of the receptor.

5.6. Analyzing Total Expression of Selected Protein Targets

Total cellular levels of expression were also measured for selected protein targets, to provide some indication as to whether mhtt expression and NMDAR activation affected not only protein expression and/or distribution in cytosolic or particulate fractions individually, but also total protein expression. HEK293 cells over-expressing NR1/NR2B and htt-15Q or htt-138Q were treated with NMDAR agonists and harvested for total soluble lysate. Samples resolved by SDS-PAGE were immunoblotted for the following protein targets: CDK5, CK2, eIF2a, ERK1/2, ERp72, GroEL, HO2, Hsp60, Hsp70, Hsp90, Hsp105, PKCz, PP2A/Aα/β, PP5, PPV/C, and PTP-1B (Figure 40). No significant difference was found for any of the proteins examined regardless of htt polyQ length (15Q versus 138Q) or NMDAR activity (with stimulation versus without) (Figure 41) (by 2-way ANOVA: effect of condition $F(3,240) = 0.2524$, $p = 0.8596$). Hence it does not appear as though co-expression of NR1/NR2B and mhtt affects total protein expression levels of a variety of signaling proteins, nor is total expression affected by NMDAR activity.

5.7. Role of Increased CK2 Expression in Membrane Compartments

5.7.1. Increased CK2 Expression in Particulate Fraction from YAC Mouse Striatum

Casein kinase 2 (CK2) is ubiquitously expressed in many tissues and is involved in such important biological processes as cell survival, tumour formation, viral infection, and a number of neural functions (Blanquet, 2000; Faust and Montenarh, 2000; Sayed et al., 2000; Ahmed et al., 2002; Korolchuk and Banting, 2002; Litchfield, 2003; Meggio and Pinna, 2003). Specifically, because CK2 has been shown to be implicated in the modulation of NMDAR function (Lieberman and Mody, 1999; Chung et al., 2004; Soto et al., 2004), we decided to investigate the role of CK2 expression changes in the particulate fraction of cells co-expressing NMDARs and mhtt based on results from our initial screens (Figure 34B, Table 6) and from the agonist stimulation experiments (Figure 39B, Table 7) described above.

To first confirm htt polyQ length-dependent changes in CK2 expression in a more physiologically relevant system, we analyzed CK2 expression in cytosolic and particulate fractions of striatal tissue from 2 month-old FVB/N WT, YAC72, or YAC128 mice (Figure 42A). As in transfected HEK293 cells, a trend towards an increase in CK2 expression was noted in the particulate fraction from striatal tissue expressing polyQ-expanded htt containing 72Q (YAC72 mice). A longer polyQ stretch of 128Q (in YAC128 mice) potentiated this increase further and led to significantly higher levels of CK2 expression in the particulate fraction as compared with WT (Figure 42B). Because this protein is induced under conditions associated with cellular stress, mhtt-mediated increases in expression of CK2 in the membrane fraction, along with the altered expression pattern of

other stress response proteins mentioned in preceding sections, likely represent the stressed cell's response to combat the deleterious effects of mhtt expression.

5.7.2. CK2 Activity Protects Against NMDAR-Mediated Apoptotic Death in mHtt-Expressing Cells

To ask whether up-regulation of membrane-bound CK2 expression ameliorates mhtt-induced, NMDAR-dependent toxicity, striatal neuronal cultures were pre-treated with a CK2 inhibitor to block its kinase activity before being subjected to brief NMDAR-dependent excitotoxic challenge consisting of treatment with 1 mM NMDA and 50 μM glycine for 10 minutes. Extent of cell death by apoptosis in NMDA/glycine-treated cultures was later assessed by PI/TUNEL staining. Only those cells that were positive for TUNEL labeling and displayed blebbed, condensed nuclei were considered to be apoptotic. Using this method, we were able to recapitulate results previously reported from our laboratory demonstrating a htt polyQ length-dependence in the amount of apoptosis that ensues from NMDAR over-activation in otherwise naïve cultures (without pre-treatment with other agents or drugs) (Figures 43 and 44A). Interestingly, treatment with the CK2 inhibitor DRB significantly enhanced NMDAR-mediated apoptosis in striatal neurons from YAC72 and YAC128 mice, relative to treatment with vehicle DMSO (Figures 43 and 44A), but did not significantly affect NMDA-induced apoptosis in WT MSNs. These results indicate that CK2 activity may play a role in protecting against NMDAR-dependent excitotoxic cell death, and that loss of CK2 activity leads to more pronounced apoptotic cell death in cells expressing mhtt. Up-regulation of membrane-bound CK2 expression in transgenic HD mice may therefore be part of a defense program launched by the cell to counter the toxic effects of mhtt expression.

5.8. Summary

We used various Kinetworks™ multi-immunoblotting screens to examine expression of 78 protein kinases, 18 protein phosphatases, and 25 heat shock/stress proteins in HEK293 cells over-expressing the NR1/NR2B subtype of NMDARs and htt-15Q or htt-138Q to determine the effects of mhtt polyQ expansion on global protein expression in cells co-expressing NR1/NR2B receptors. The distribution between cytosolic and membrane fractions of multiple proteins involved in the heat shock response pathway were altered in cells expressing mhtt. Specifically, a mhtt-induced increase in Hsp70 expression in the cytosolic fraction appeared to depend on NR1/NR2B co-expression and was potentiated further by NMDAR stimulation. However, NMDAR activity and expression of mhtt appeared not to affect the total cellular expression of any of the proteins investigated.

The protein serine/threonine kinase CK2 was found to be increased in the particulate fraction of cells expressing mhtt, a result that was confirmed in striatal tissue of YAC transgenic mice expressing full-length mhtt. Since NMDARs are integral membrane proteins, a shift in localization of CK2 to the membrane fraction from the cytosol could impact NMDAR phosphorylation and function. Indeed, we found that inhibiting CK2 activity in striatal neurons from YAC72 and YAC128 (but not WT) mice significantly intensified apoptosis resulting from NMDA insult. Results from our studies indicate an up-regulation of some components of the stress response pathway in either the cytosolic or particulate cellular fractions, in the presence of polyQ-expanded mhtt and NR1/NR2B, which may reflect an attempt by the cell to combat the detrimental effects stemming from mhtt expression.

1	BMX	27	Fyn	53	PKA
2	BTK	28	GCK	54	PKBa
3	CaMK1	29	Grk2(BARK2)	55	PKCa
4	CaMK4	30	Gsk3a	56	PKCb
5	CaMKK	31	Gsk3b	57	PKCg
6	CDK1	32	Hpk1	58	PKCd
7	CDK2	33	IKKa	59	PKCe
8	CDK4	34	JAK1	60	PKCl
9	CDK5	35	JAK2	61	PKCm
10	CDK6	36	Ksr1	62	PKCq
11	CDK7	37	Lck	63	PKCz
12	CDK9	38	Lyn	64	PKG1
13	CK1d	39	MEK1	65	PKR
14	CK1e	40	MEK2	66	PYK2
15	CK2a	41	MKK4	67	Raf1
16	CK2a'	42	MKK6	68	RafB
17	CK2a"	43	MKK7	69	ROKa
18	Cot	44	Mnk2	70	RSK1
19	Csk	45	Mos1	71	RSK2
20	DAPK	46	Mst1	72	S6K p70
21	DNAPK	47	Nek2	73	SAPK
22	ERK1	48	p38 MAPK	74	Src
23	ERK2	49	PAK1	75	Syk
24	ERK3	50	PAK3	76	Yes1
25	ERK6	51	PDK1	77	ZAP70
26	FAK	52	Pim1	78	ZIP

Table 2. List of protein kinases examined in Kinetworks™ KPKS screen.

1	KAP	10	PP2B/Aα
2	LAR	11	PP2C/Cδ
3	MKP-1	12	PP2X/C
4	MKP-2	13	PP5 (PPT)
5	PP1/Cα	14	PPV/C
6	PP1/Cβ	15	PPX/A'2
7	PP1/Cγ	16	PTP-1B
8	PP2A/Aα/β	17	PTP-1C
9	PP2A/Cα/β	18	PTP-1D

Table 3. List of protein phosphatases examined in Kinetworks™ KPPS screen.

1	APG1	14	HO2
2	APG2	15	Hsc70
3	Cox-2	16	HSF4
4	eIF2a	17	Hsp105
5	ERp57	18	Hsp25
6	ERp72	19	Hsp40
7	GroEL	20	Hsp47
8	Grp75	21	Hsp60
9	Grp78	22	Hsp70
10	Grp94	23	Hsp90
11	hHR23B	24	HspBP1
12	Hip	25	ST1/Hop-p60
13	HO1		

Table 4. List of stress/heat shock proteins examined in Kinetworks™ KHSP screen.

(a) Protein Kinases

	htt15 cyto	htt138 cyto	htt15 partic	htt138 partic
CK2	26246	31206	15501	26077
CDK4	3954	5945	1995	2437
CDK5	5371	12105	4107	2852
ERK1	12343	13982	7350	3384
HPK1	4089	3894	5159	
PKCl			5614	2095
PKCz	4021	6782		2005
RSK1	16938	19936	7691	3292
SAPKb	7050	7223	3553	5943

(b) Protein Phosphatases

	htt15 cyto	htt138 cyto	htt15 partic	htt138 partic
PP2A/A-alpha/beta	14304	26003	34023	16569
PTP1B	2311	891	7261	20156
PP5 (PPT)	10020	4786	1806	5450

(c) Heat Shock/Stress Proteins

	htt15 cyto	htt138 cyto	htt15 partic	htt138 partic
ERp72	19302	12404	3119	18800
eIF2a	13721	8719	9128	13809
Hsp60	2328	1401	3638	6591
GroEL	3851	8555	6824	15537
Hsp70	11017	16736	19658	21908
Hsp90	6735	4451	114	8527

Table 5. Expression levels of selected proteins from KPKS, KPPS, and KHSP screens. Expression levels (in arbitrary units) of selected (a) protein kinases, (b) protein phosphatases, and (c) stress/heat shock protein pathway-related proteins in the cytosolic and particulate fractions from HEK293 cells in the "htt15" and "htt138" conditions are tabulated. Only those protein targets with measurement value(s) of greater than 5000 counts by ECL emission and displaying a 50% or greater change in expression have been included in this list. Values for each condition (htt15 versus htt138) are the averaged results from three individual transfections of six 10-cm dishes of HEK293 cells per transfection. Htt15, transfected with htt-15Q/NR1/NR2B; htt138, transfected with htt-138Q/NR1/NR2B. Cyto, cytosolic; partic, particulate.

% Change in Expression of Selected Proteins ("htt138" compared with "htt15")

(a) Protein Kinases

	Cyto	Partic
CK2 (35)	19% ↑	68% ↑
CDK4 (35)	50% ↑	22% ↑
CDK5 (28)	125% ↑	31% ↓
ERK1 (40)	13% ↑	54% ↓
HPK1 (87)	5% ↓	100% ↓
PKCl (62)	-	63% ↓
PKCz (88)	69% ↑	Increase
RSK1 (73)	18% ↑	57% ↓
SAPKb (38)	2% ↑	67% ↑

(b) Protein Phosphatases

	Cyto	Partic
PP2A/A-alpha/beta	82% ↑	51% ↓
PTP1B	61% ↓	178% ↑
PP5 (PPT)	52% ↓	202% ↑

(c) Heat Shock/Stress Proteins

	Cyto	Partic
ERp72	36% ↓	503% ↑
eIF2a	36% ↓	51% ↑
Hsp60	40% ↓	81% ↑
GroEL	122% ↑	128% ↑
Hsp70	52% ↑	11% ↑
Hsp90	34% ↓	7387% ↑

Table 6. Summary of changes in expression levels of selected proteins from KPKS, KPPS, and KHSP screens. Changes in expression profiles of (a) protein kinases, (b) protein phosphatases, and (c) stress/heat shock protein pathway-related proteins in the cytosolic and particulate fractions from HEK293 cells are tabulated as percent change (up- or down-regulation) in the "htt138" condition as compared with the control "htt15" condition. Only those protein targets with measurement value(s) of greater than 5000 counts by ECL emission and displaying a 50% or greater change in expression have been included in this list. Cyto, cytosolic; partic, particulate.

(a) Normalized to actin levels

	15	15N	138	138N
CK2 (Partic)	146.9	121.0	143.4	178.5
GroEL (Partic)	60.9	76.2	128.6	168.6
Hsp90 (Partic)	88.0	80.3	115.5	179.9
Hsp70 (Cyto)	49.0	54.2	87.3	138.2

(b) Normalized to 15N levels

	15	15N	138	138N
CK2 (Partic)	100	82	98	122
GroEL (Partic)	100	125	211	277
Hsp90 (Partic)	100	91	131	204
Hsp70 (Cyto)	100	111	178	282

Table 7. **Quantification of results from immunoblot analysis of selected protein targets as shown in Figure 39B.** Values reported have been normalized to actin levels and are representative of two independent experiments using different batches of transfected HEK cells. 15, transfected with htt-15Q/NR1/NR2B and non-stimulated; 15N, transfected with htt-15Q/NR1/NR2B and stimulated with 1 mM NMDA/ 50 μM glycine; 138, transfected with htt-138Q/NR1/NR2B and non-stimulated; 138N, transfected with htt-138Q/NR1/NR2B and stimulated with 1 mM NMDA/ 50 μM glycine. Cyto, cytosolic; partic, particulate.

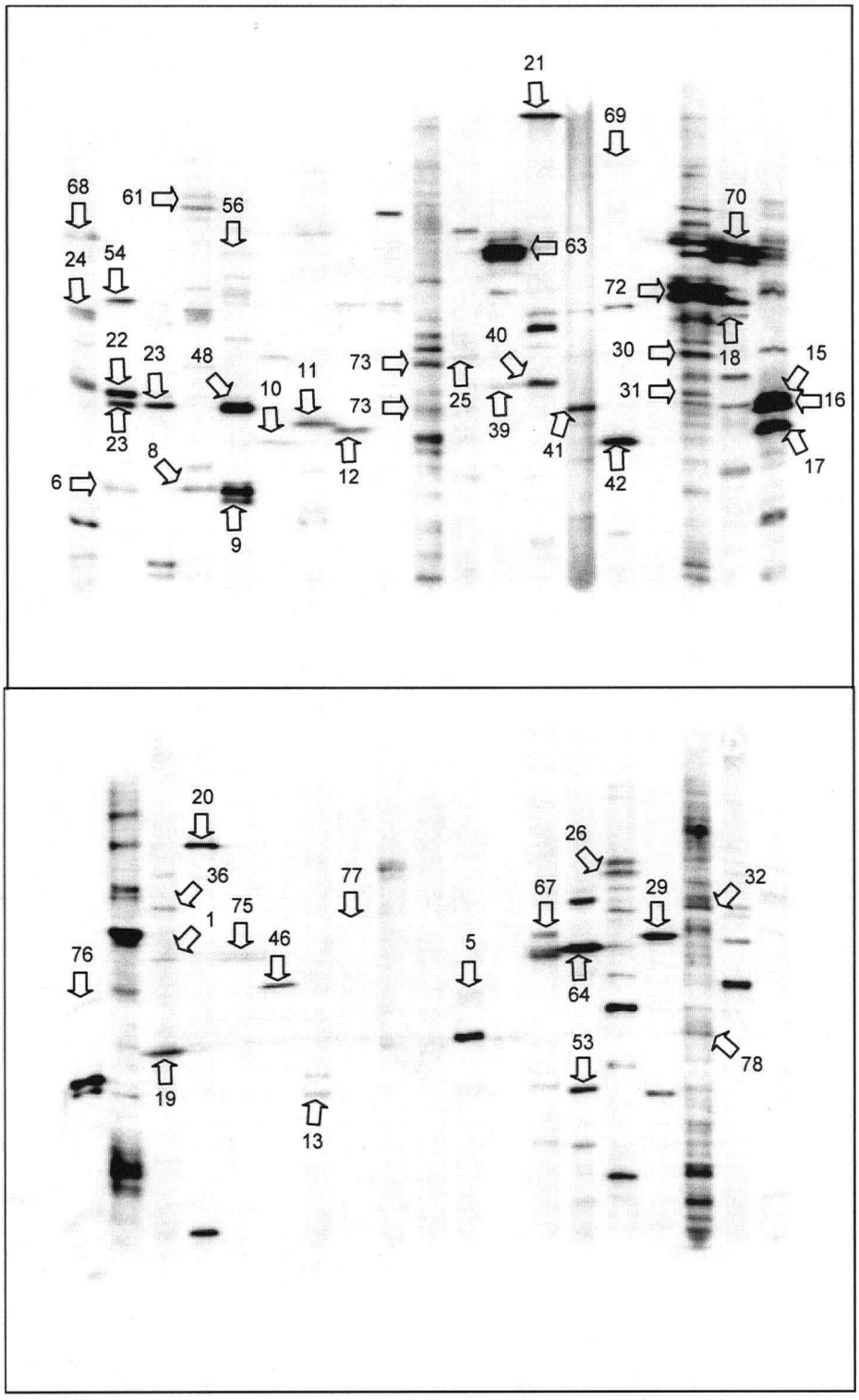

Figure 33. Sample Kinetworks™ KPKS screen results. Actual immunoblot results are shown for cytosolic fractions from HEK293 cells transfected with htt-15Q/NR1/NR2B. Bands which correspond to known protein targets are indicated by arrows and numbers, and identities of these protein kinases are tabulated in Table 2.

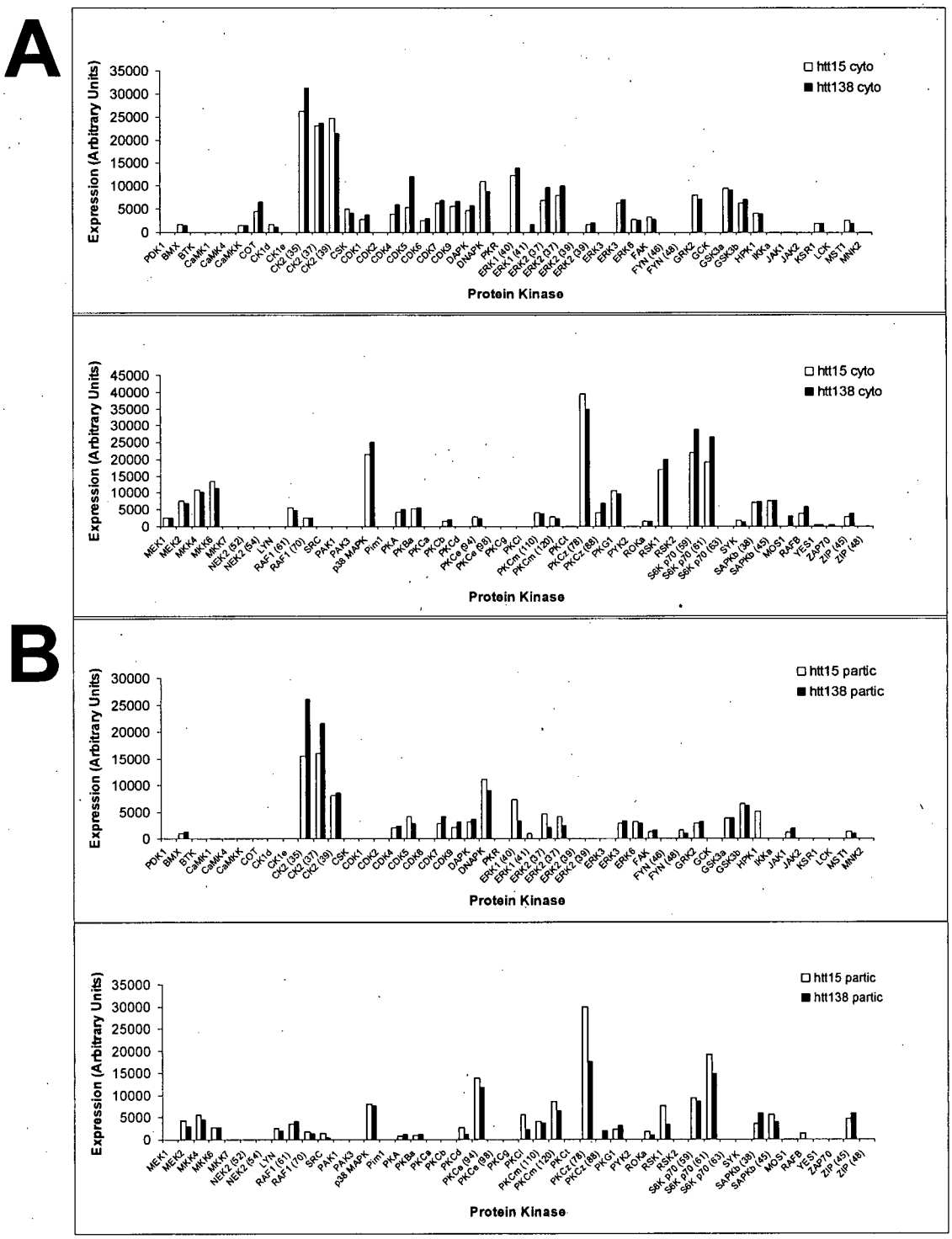

Figure 34. Plots of quantified Kinetworks™ KPKS screen results. Expression levels of protein kinases shown in Figure 33 are quantified for both (A) cytosolic and (B) particulate fractions from HEK293 cells transfected with htt-15Q/NR1/NR2B ("htt15" condition) or htt-138Q/NR1/NR2B ("htt138" condition). Values for each condition are the averaged results from three individual transfections of six 10-cm dishes of HEK293 cells per transfection. Cells are harvested for analysis only when transfection efficiency exceeds 50%. Cyto, cytosolic; partic, particulate.

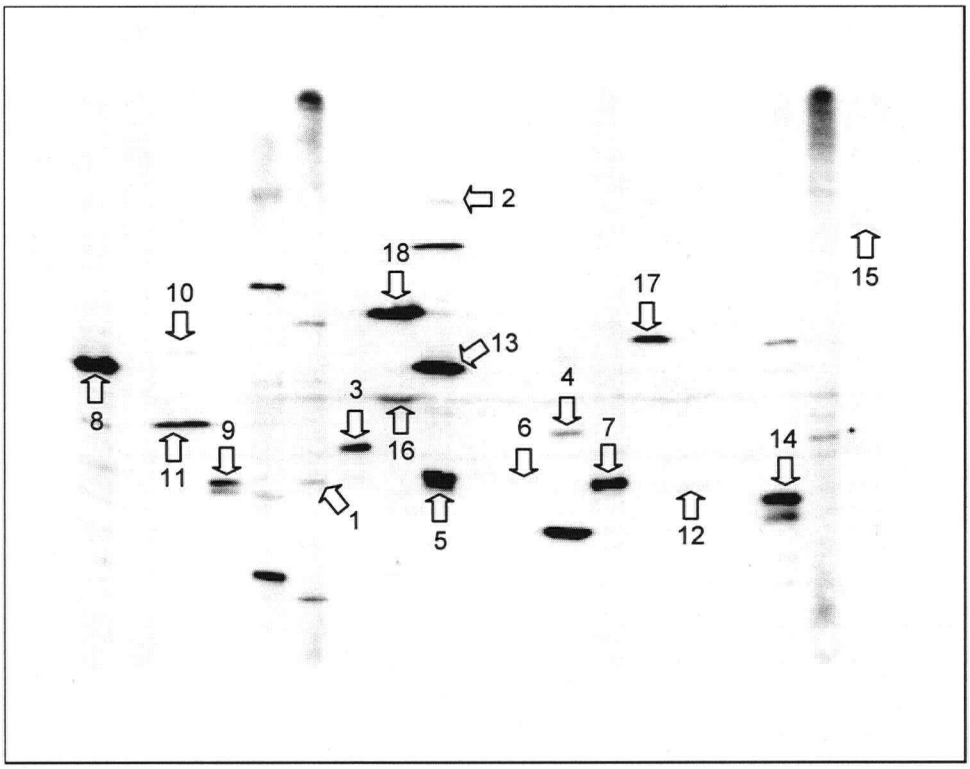

Figure 35. Sample Kinetworks™ KPPS screen results. Actual immunoblot results are shown for cytosolic fractions from HEK293 cells transfected with htt-15Q/NR1/NR2B. Bands which correspond to known protein targets are indicated by arrows and numbers, and identities of these protein phosphatases are tabulated in Table 3.

A

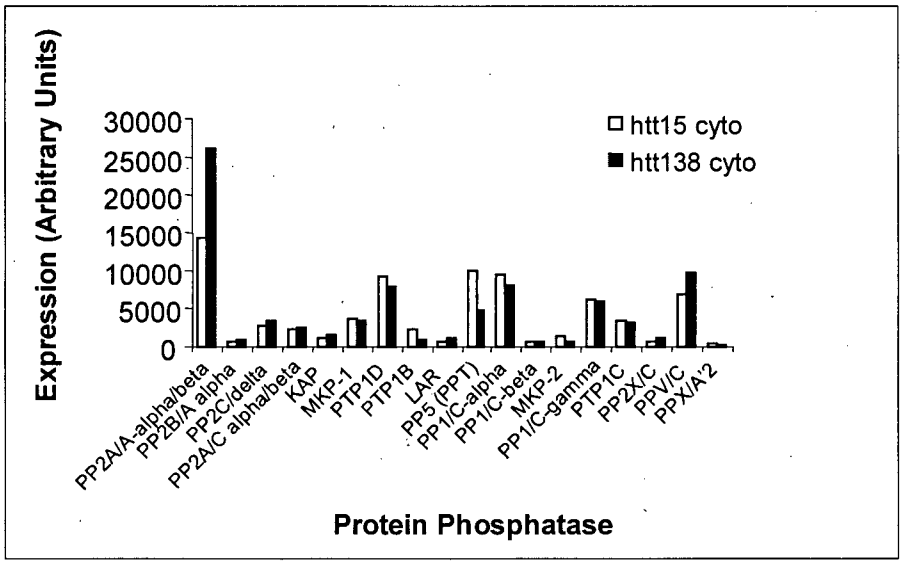

B

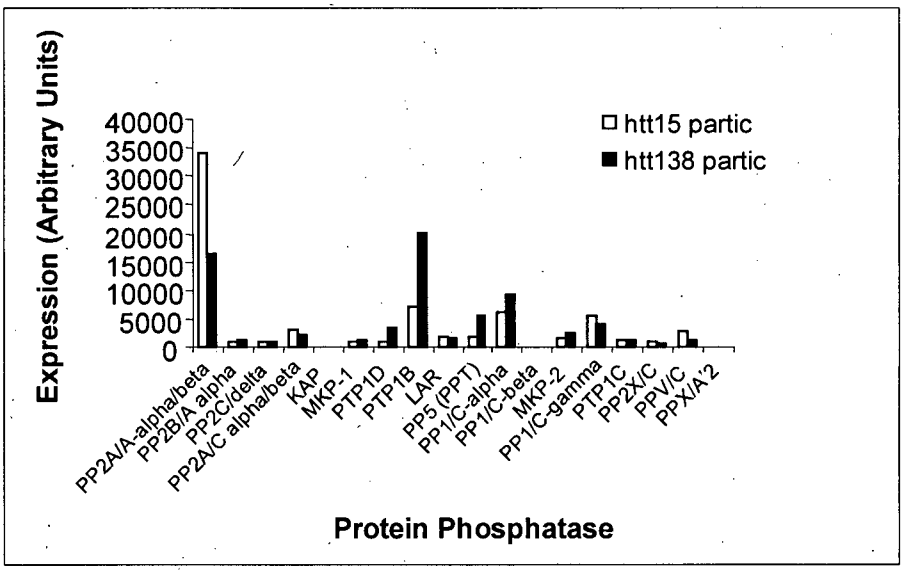

Figure 36. Plots of quantified Kinetworks™ KPPS screen results. Expression levels of protein phosphatases shown in Figure 35 are quantified for both (A) cytosolic and (B) particulate fractions from HEK293 cells transfected with htt-15Q/NR1/NR2B ("htt15" condition) or htt-138Q/NR1/NR2B ("htt138" condition). Values for each condition are the averaged results from three individual transfections of six 10-cm dishes of HEK293 cells per transfection. Cells are harvested for analysis only when transfection efficiency exceeds 50%. Cyto, cytosolic; partic, particulate.

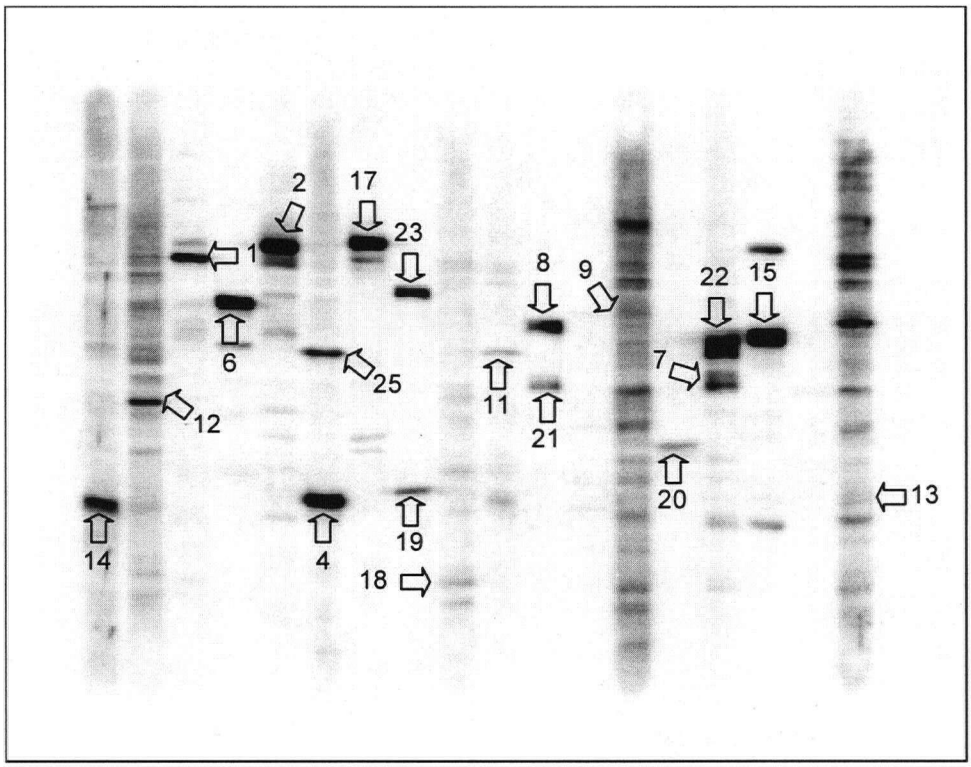

Figure 37. Sample Kinetworks™ KHSP screen results. Actual immunoblot results are shown for cytosolic fractions from HEK293 cells transfected with htt-15Q/NR1/NR2B. Bands which correspond to known protein targets are indicated by arrows and numbers, and identities of these stress/heat shock proteins are tabulated in Table 4.

A

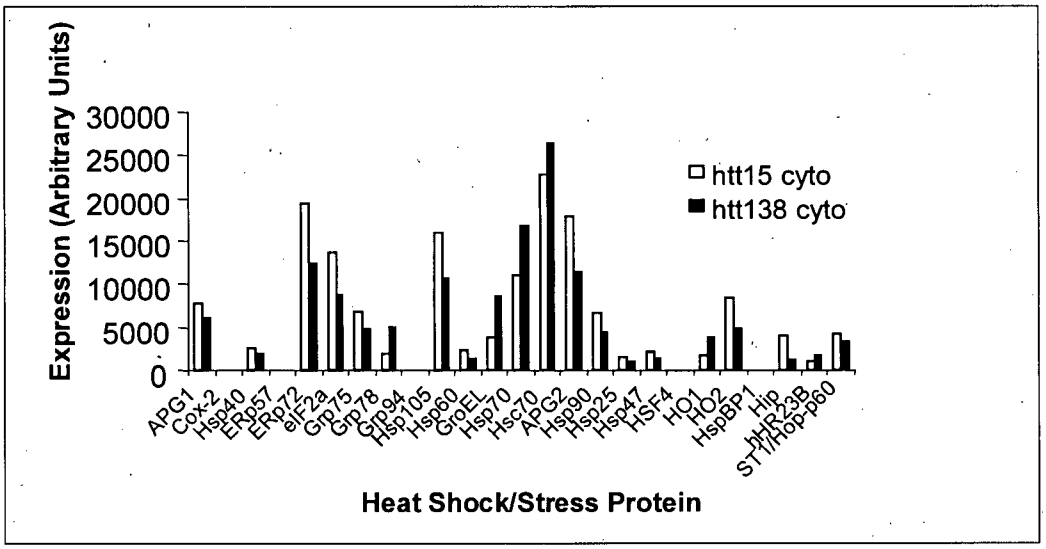

B

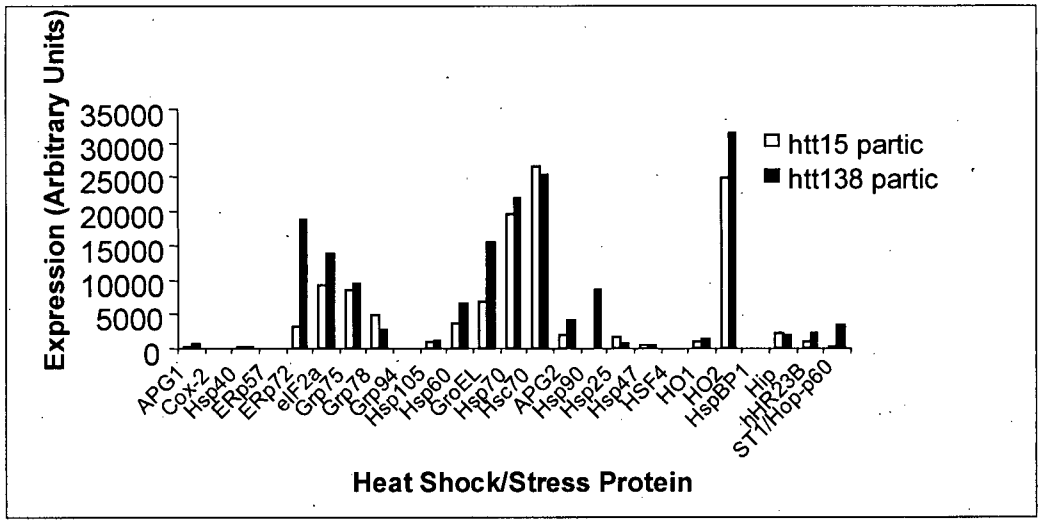

Figure 38. Plots of quantified Kinetworks™ KHSP screen results. Expression levels of stress/heat shock proteins shown in Figure 37 are quantified for both (A) cytosolic and (B) particulate fractions from HEK293 cells transfected with htt-15Q/NR1/NR2B ("htt15" condition) or htt-138Q/NR1/NR2B ("htt138" condition). Values for each condition are the averaged results from three individual transfections of six 10-cm dishes of HEK293 cells per transfection. Cells are harvested for analysis only when transfection efficiency exceeds 50%. Cyto, cytosolic; partic, particulate.

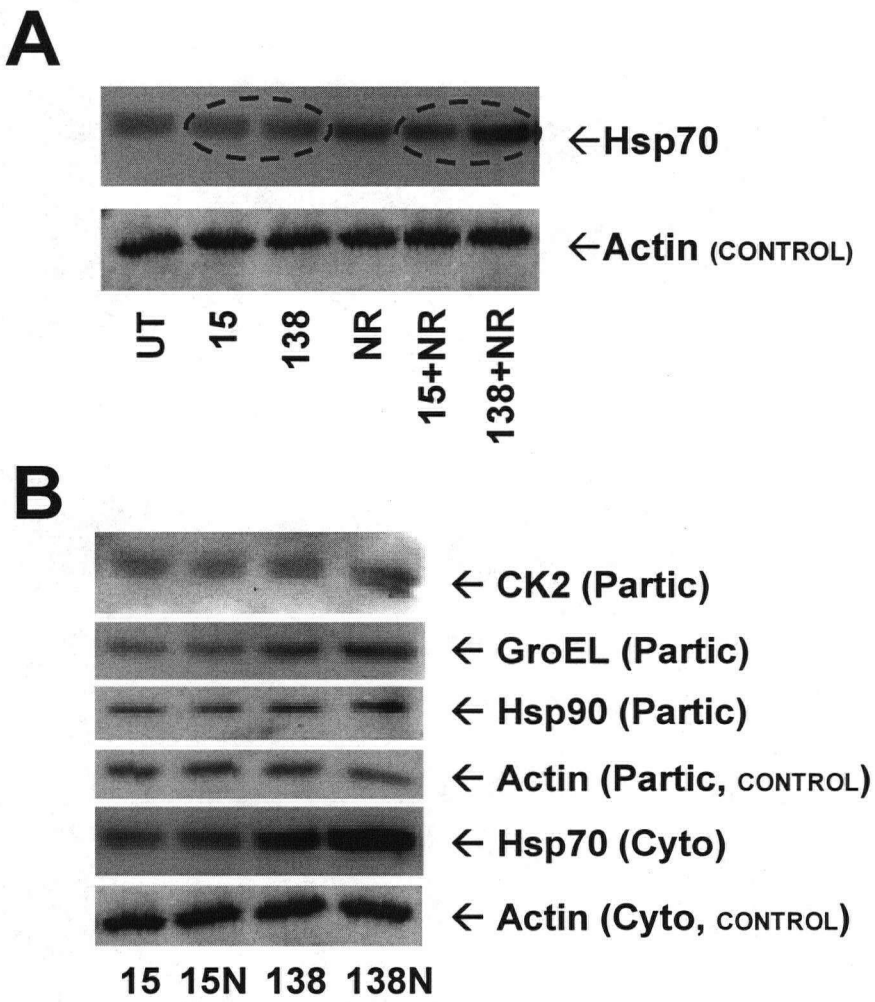

Figure 39. Up-regulation of cytosolic Hsp70 expression by mhtt depends on co-expression of NMDARs and is enhanced by NMDAR activity. (A) Expression levels of Hsp70 in cytosolic fractions from HEK293 cells transfected with various constructs are examined. Equivalent amounts of protein from all conditions are resolved by SDS-PAGE, and cytosolic actin expression is shown to control for loading variability. Immunoblot shown is representative of data from at least four experiments using two different batches of transfected cells. UT, untransfected; 15, transfected with htt-15Q; 138, transfected with htt-138Q; NR, transfected with NR1/NR2B; 15+NR, transfected with htt-15Q/NR1/NR2B; 138+NR, transfected with htt-138Q/NR1/NR2B. (B) Representative immunoblots show expression levels of Hsp70 in cytosolic fractions and CK2, GroEL, and Hsp90 in particulate fractions from transfected HEK293 cells, with or without NMDAR stimulation. Equivalent amounts of protein from all conditions are resolved by SDS-PAGE, and actin expression is shown to control for loading variability. Immunoblots shown are representative of data from at least two experiments using different batches of transfected cells. 15, transfected with htt-15Q/NR1/NR2B and non-stimulated; 15N, transfected with htt-15Q/NR1/NR2B and stimulated with 1 mM NMDA/ 50 μM glycine; 138, transfected with htt-138Q/NR1/NR2B and non-stimulated; 138N, transfected with htt-138Q/NR1/NR2B and stimulated with 1 mM NMDA/ 50 μM glycine. Cyto, cytosolic; partic, particulate.

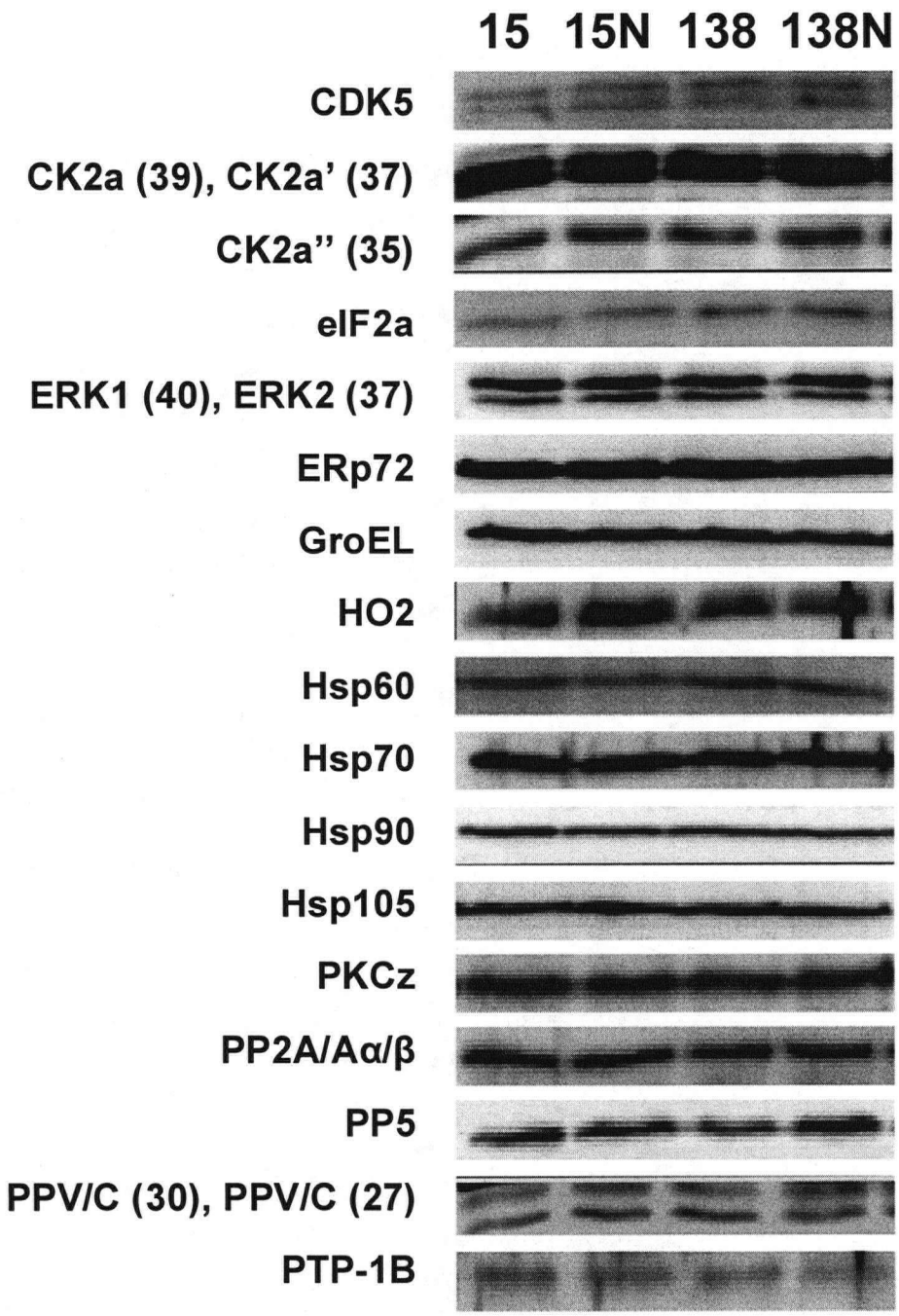

Figure 40. Immunoblots for total cellular expression of selected proteins from transfected HEK293 cells with or without NMDAR stimulation. Equivalent amounts of protein from total cell lysates harvested in parallel from HEK293 cells in the "htt15" and "htt138" conditions, with or without NMDAR activation, are resolved by SDS-PAGE. Immunoblots shown are representative of four experiments using different batches of transfected cells. 15, transfected with htt-15Q/NR1/NR2B and non-stimulated; 15N, transfected with htt-15Q/NR1/NR2B and stimulated with 1 mM NMDA/ 50 μM glycine; 138, transfected with htt-138Q/NR1/NR2B and non-stimulated; 138N, transfected with htt-138Q/NR1/NR2B and stimulated with 1 mM NMDA/ 50 μM glycine.

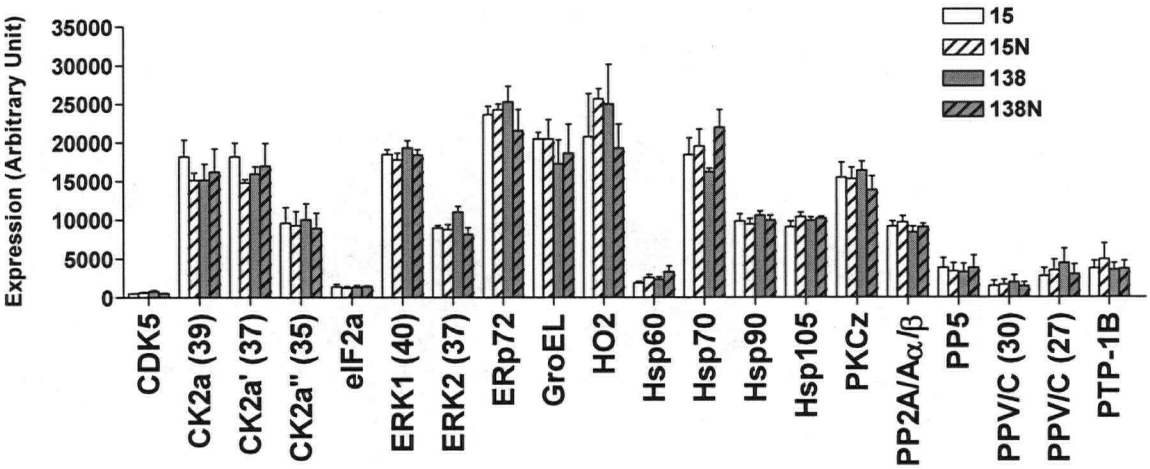

Figure 41. Quantification of total cellular expression of selected proteins from transfected HEK293 cells with or without NMDAR stimulation. Proteins shown in Figure 40 are quantified for total expression levels. Bars represent mean ± SEM from N = 4 experiments using different batches of transfected cells. Cells are harvested for analysis only when transfection efficiency exceeds 50%. No significant effect of condition (genotype or stimulation) is observed for overall expression levels of each protein examined, by 2-way ANOVA. 15, transfected with htt-15Q/NR1/NR2B and non-stimulated; 15N, transfected with htt-15Q/NR1/NR2B and stimulated with 1 mM NMDA/ 50 µM glycine; 138, transfected with htt-138Q/NR1/NR2B and non-stimulated; 138N, transfected with htt-138Q/NR1/NR2B and stimulated with 1 mM NMDA/ 50 µM glycine.

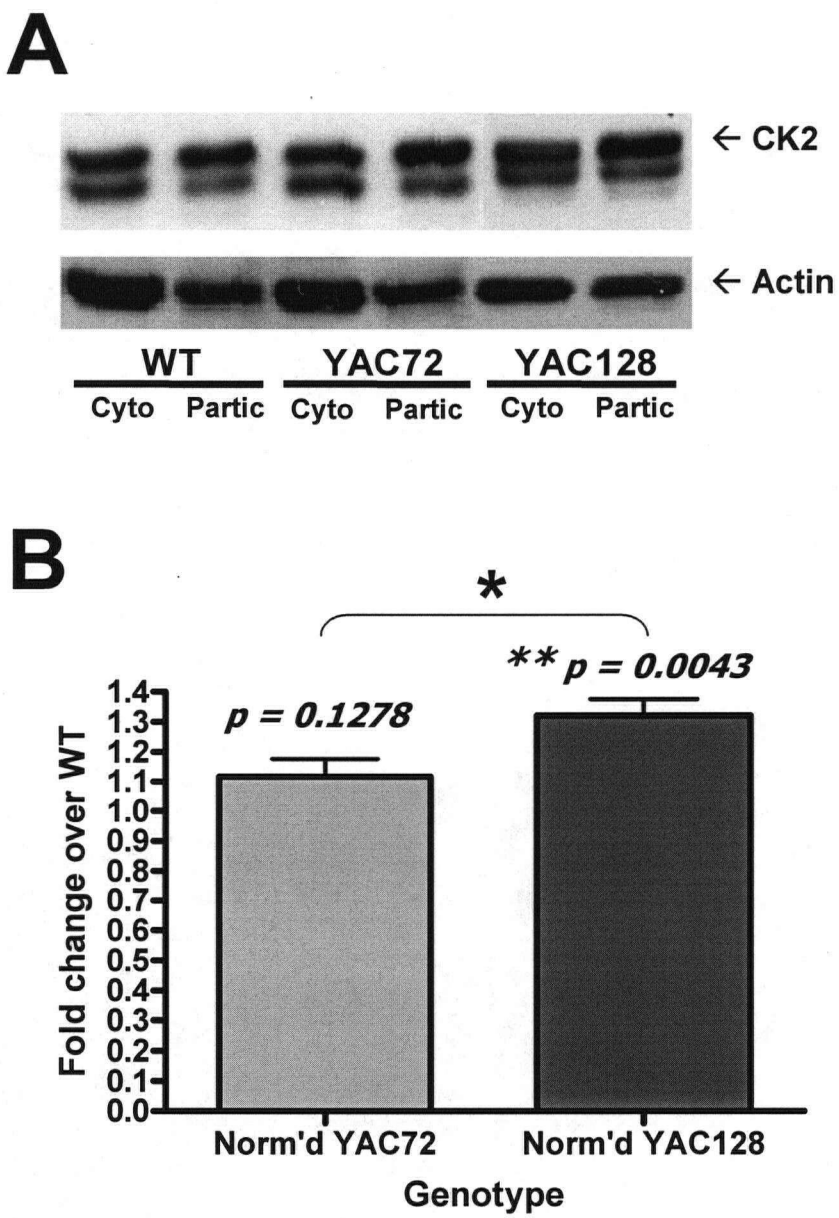

Figure 42. Particulate CK2 expression is up-regulated in striatal tissue from mice expressing mhtt. (A) Striatal tissue from FVB/N WT, YAC72, or YAC128 mice is fractionated into cytosolic and particulate compartments and analyzed for CK2 expression. Ten micrograms of protein are loaded for each sample, and actin expression is shown to control for loading variability. Immunoblot shown is representative of five experiments for each genotype, using striatal tissue pooled from two mice in every experiment. Cyto, cytosolic; partic, particulate. (B) Changes in particulate expression of CK2 (normalized to actin) in striatal tissue from YAC72 and YAC128 mice are compared against WT. Plot compares the relative fold change in normalized particulate CK2 expression in YAC transgenic mice over WT values. Bars represent mean fold change ± SEM from N = 5 independent experiments for each genotype. * Significantly different compared to normalized YAC72 values, $p < 0.05$ by unpaired t-test. ** Significantly different than one, $p < 0.01$ by 1-sample t-test of data values normalized to WT.

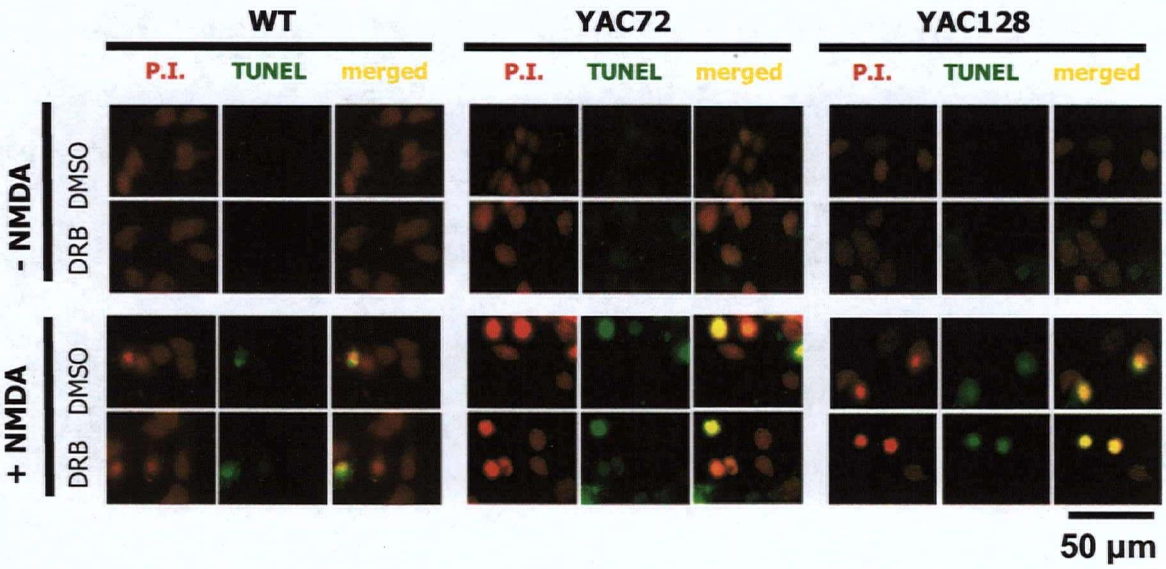

Figure 43. NMDA-induced apoptosis in MSNs from FVB/N WT, YAC72, or YAC128 mice in the presence or absence of CK2 inhibition. Neurons are pre-treated with vehicle DMSO or CK2 inhibitor DRB prior to NMDA insult. Representative pictographs of MSNs treated at 9 d.i.v., fixed at 10 d.i.v., and stained with TUNEL and propidium iodide (PI) are shown for WT, YAC72, and YAC128 mice. Following initial fixation of the neurons in 4% PFA, all subsequent steps of the TUNEL labeling protocol, fluorescence imaging and image capturing are performed in parallel for both treatment groups within each genotype in each experiment.

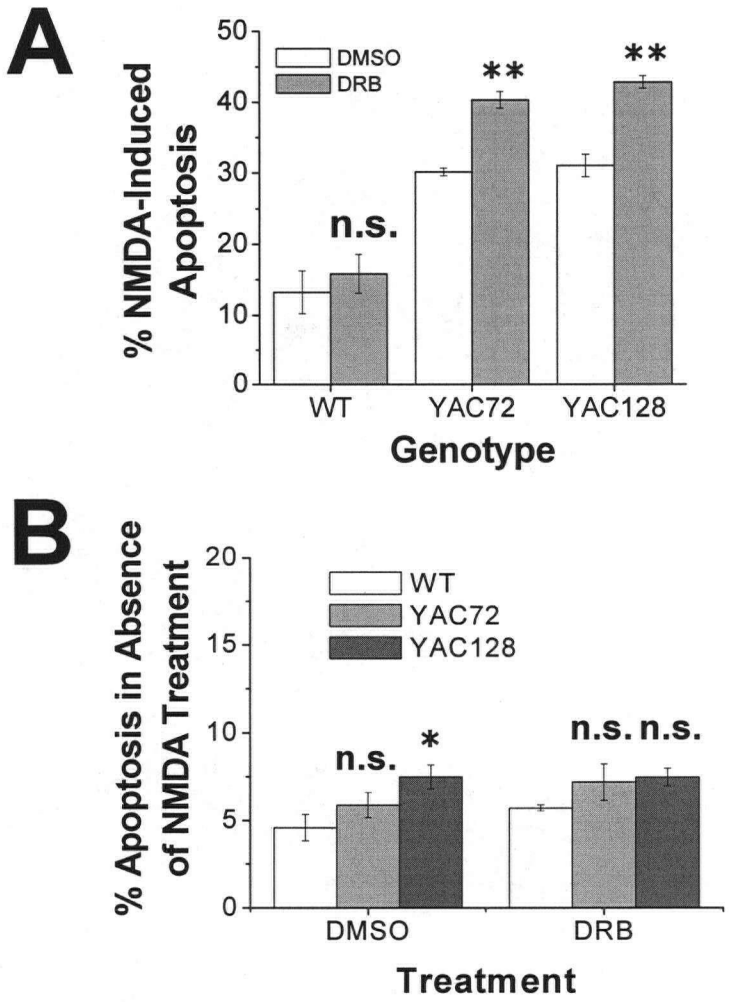

Figure 44. Blockade of CK2 activity in mouse striatal MSNs exacerbates NMDAR-mediated mhtt-induced apoptosis. Apoptotic death in cultured striatal MSNs from WT, YAC72, or YAC128 mice is assessed by TUNEL assay 24 hours after exposure to 1 mM NMDA/50 μM glycine. Neurons are pre-treated with vehicle DMSO or CK2 inhibitor DRB prior to NMDA insult. (A) Extent of apoptotic death 24 hours following NMDA insult in the presence or absence of CK2 inhibition as visualized by TUNEL labeling is quantified. Bars represent mean percent apoptosis ± SEM, after subtraction of values obtained in the absence of NMDA exposure for each experiment, from N = 3 different batches of cultured neurons for each treatment condition. Statistical significance is determined by 2-way ANOVA followed by Bonferroni post-test (main effect of genotype $F(2,6) = 54.04$, $p = 0.0001$; main effect of drug $F(1,6) = 71.77$, $p = 0.0001$; significant interaction of genotype and drug $F(2,6) = 8.602$, $p = 0.0173$). n.s., not significantly different; ** $p < 0.01$, significantly different compared to DMSO. (B) Verification of control levels of apoptotic death, in the absence of NMDA treatment, in cultured MSNs from WT, YAC72, or YAC128 mice 26 hours after treatment with vehicle DMSO or CK2 inhibitor DRB. Bars represent mean percent apoptosis ± SEM from N = 3 different batches of cultured neurons for each treatment condition. Statistical significance is determined by 2-way ANOVA followed by Bonferroni post-test. n.s., not significantly different; * $p < 0.05$, significantly different compared to WT.

CHAPTER 6. CONCLUSIONS

6.1. Mechanisms of Modulation of NMDAR Activity/Trafficking by mHtt

We investigated the expression of NR1 and NR2B NMDAR subunits in mouse striatal tissue to determine whether overall expression changes could account for the NR1/NR2B-specific changes in current and toxicity associated with mhtt expression (Chen et al., 1999b; Zeron et al., 2001, 2002). We report here that total NR1/NR2B expression did not appear to vary with htt polyQ length in animals ranging from 2 months (early symptomatic) to 12 months (late symptomatic) of age, confirming previous results indicating a lack of change in overall NR1/NR2B expression in striatal tissue from 2 month-old WT, YAC46, and YAC72 mice (Li et al., 2003; see Figure 7). Over a range of animal ages, striatal NR1/NR2B expression also did not vary in WT animals. Interestingly, we found some rather unexpected temporal changes in NMDAR subunit expression in YAC72 striatal tissue: NR1 was down-regulated at 6 months while NR2B was increased at 9 months of age. However, the sample size (N = 3) is small, and the relatively large variation in the data may preclude any truly meaningful statistical analysis. Further experiments are required to confirm the apparent temporal changes in overall NR2B expression in YAC72 striatum.

Despite a lack of change in overall NMDAR expression in mice expressing mhtt with varying polyQ lengths, we are nevertheless able to uncover additional details about the mechanisms through which mhtt mediates its neurotoxic effects, including the role that htt plays in the modulation of NMDAR activity, based on the results from studies described in the current thesis. While it has previously been reported from mouse and

cellular models of HD that the amplitude of NMDAR-dependent current and extent of NMDA-induced cell death vary with mhtt polyQ length (Chen et al., 1999b; Zeron et al., 2001, 2002; Shehadeh et al., 2006), we demonstrate for the first time the underlying cellular mechanisms which may account for this effect. We found in YAC72 MSNs a significant up-regulation of the proportion of NR1 and NR2B subunits expressed on the cell surface, as compared with other members of the iGluR family such as the AMPAR subunit GluR1. The lack of mhtt effect on GluR1 surface expression is consistent with a selective interaction between NMDARs and mhtt, as illustrated by a larger NMDAR- to AMPAR-EPSC ratio in the absence of pre-synaptic changes in YAC transgenic mice expressing mhtt (Li et al., 2003, 2004).

The underlying cause of this increase in surface NMDAR expression was also investigated in this thesis. Because rates of receptor movement to and from the surface must both contribute to the achievement and maintenance of any given steady-state of surface NMDAR expression, we reasoned that increased surface-to-internal ratio of NMDAR expression in YAC72 MSNs may be due to changes in the kinetics of receptor trafficking. In contrast to our initial hypothesis that higher surface levels may result from slower turnover rates, we actually observed a more rapid rate of loss of NMDAR subunit NR1 from the surface reflecting predominantly the degradation of NR1 via lysosomes. This finding, however, is in agreement with a previous study demonstrating mhtt-mediated enhancement of expression of lysosomal proteases and activation of the lysosomal degradation pathway (Kegel et al., 2000). Importantly, analysis of insertion kinetics revealed a significantly faster rate of insertion of new NMDARs to the cell surface in MSNs from YAC72 mice, an effect which once again seemed to be selective for NMDARs as GluR1 insertion rates were not found to be significantly different between WT and YAC72 MSNs.

Because of differences in the experimental protocols used to investigate surface receptor loss versus insertion, it is not possible to directly compare findings from the two assays. Interpolation from our data in assays tracking receptor loss from the surface suggests that roughly 25% of the initial surface receptor pool at any given time are lost (and presumably degraded) over a 6-hour duration in MSNs from WT mice, while in the same time period ~30% of NR1 are lost from the surface in YAC72 MSNs. Therefore, the relative amount of receptor loss in MSNs from YAC72 mice exceeded that of WT by ~5% over a 6-hour period. In the same length of time, insertion of new NMDARs (apart from replenishment from recycling pools) led to ~15% more NMDARs on the cell surface, as compared to WT which did not appear to have any incorporation of new receptors at all.

6.1.1. Limitations of Methods Available for Measuring Forward Trafficking

The apparent paucity of NR1 insertion to the cell surface in WT MSNs is in contrast to electrophysiological studies in our laboratory demonstrating a small but measurable recovery of NMDAR current (and hence surface receptor number) in cells within 15 minutes following irreversible blockade of NMDAR function by MK-801 treatment (Fan et al., 2007). We attribute this recovery to replenishment by a plasma membrane-proximal pool of recycling receptors, which was not expected to happen in our biotinylation assays because the drug that we used is known to block both endocytic and recycling processes within the cell. Our inability to observe *de novo* NMDAR insertion in WT MSNs nevertheless remains a concern, as proteins should normally undergo a continuous cycle of degradation and new synthesis/insertion apart from the recycling arm. It is therefore possible that treatment with chlorpromazine may have additional, unexpected effects on receptor forward trafficking. Alternatively, chlorpromazine-induced disruption of the

endocytic arm of trafficking may lead to a corresponding compensatory inhibition of constitutive receptor exocytosis and insertion, as these two processes have been suggested to be tightly coupled in the maintenance of constitutive AMPAR cycling over a period of minutes (Lledo et al., 1998; Man et al., 2000; Wang and Linden, 2000; reviewed in Groc and Choquet, 2006). However, it is unclear whether this homeostatic mechanism applies also to NMDARs or persists over the 6-hour period examined in our experiments.

While the use of chlorpromazine may indirectly inhibit constitutive exocytic processes and therefore not permit an absolute measurement of receptor insertion, parallel treatment of WT and YAC72 MSNs with this drug nevertheless revealed differences in receptor delivery rates that suggest this inhibitory effect is at least partially overcome in YAC72 MSNs because of accelerated forward trafficking in these neurons.

Aside from the use of chlorpromazine, we made attempts at measuring receptor delivery using other published techniques, which met with limited success. To directly examine forward trafficking of newly synthesized NMDARs, we metabolically labeled MSNs in culture and performed sequential biotinylation to tag surface proteins, immunoprecipitation to concentrate NMDAR complexes, and subsequent NeutrAvidin pull-down to isolate the surface pool of NMDARs as per Mu and colleagues (2003). Exposure to film would then, in theory, allow detection specifically of newly synthesized NMDARs within this surface pool, as new receptors would be labeled with ^{35}S due to the incorporation of radioactive methionine residues during *de novo* synthesis. We found to our dismay that at the end of this rather lengthy procedure, the resulting radioactive signal was far too weak for either qualitative or quantitative measurement purposes despite the use of fresh radioisotope at the beginning of the experiment and metabolic labeling for an adequate length of time according to previously published procedures. As such we were

not able to determine whether forward delivery of newly synthesized NMDARs was different in WT versus YAC72 MSNs.

We also did pilot experiments to measure surface accumulation of NMDARs using other conventional methods to block endocytosis. Cultured MSNs were exposed to hypertonic sucrose, a treatment known to inhibit clathrin-mediated endocytosis (Carroll et al., 1999; Man et al., 2000; Nong et al., 2003; Wang et al., 2004), before being biotinylated at either 0 or 6 hours following treatment. While others have shown that changes in AMPAR trafficking could be detected generally within 30 minutes of hypertonic sucrose treatment, we chose to examine NMDAR insertion at the 6-hour time point on the basis of previous reports indicating purportedly slower turnover/trafficking rates of NMDARs in comparison to AMPARs (Lissin et al., 1998; Carroll et al., 1999; Man et al., 2000; Nong et al., 2003). At 2-3 hours following sucrose exposure, however, cells had assumed a rounded morphology, which became more pronounced by 6 hours. Although the neurons remained largely attached to the culture dish for the duration of the experiment, we had concerns about the validity of data obtained from these cells as they had clearly become unhealthy by the time of biotinylation. The morphological changes we observed were very likely accompanied by changes in cell signaling pathways, which would affect the ability of the cell to maintain normal biological processes such as endocytosis and exocytosis of membrane proteins. Hence any measurement of protein delivery to the cell surface under such circumstances would not accurately reflect the physiological rate of receptor trafficking, and as such these studies were abandoned.

Another method previously reported to block clathrin-mediated endocytosis involves the use of the membrane-permeant, dynamin-derived myristoylated peptide myr-Dyn. This peptide acts in a dominant negative fashion to block recruitment of full-length dynamin to amphiphysin at clathrin-coated pits (Carroll et al., 1999; Nong et al.,

2003; Wang et al., 2004). In our hands, treatment of cultured MSNs with the myr-Dyn peptide for either 0.5 or 6 hours did not appreciably alter the proportion of surface-expressed NR1 in either YAC72 or WT MSNs in comparison to sister dishes of cultured neurons exposed to the control, scrambled version of the peptide, in spite of proper peptide storage and handling procedures. The concentration that we used (10 μM) was based on published procedures, although higher concentrations of use (at 50 μM; Nong et al., 2003) have also been reported. Due to the preliminary nature of these pilot experiments and the limited quantity of peptide available to us at the time, we decided to follow up instead with the use of chlorpromazine to block endocytosis, which we found to give promising results based on initial dose-response studies.

6.1.2. Enhanced Trafficking of NMDARs Composed of NR1 C2' and NR2B

Our data from biotinylation experiments of chlorpromazine-treated neurons clearly indicate that, while mhtt expression in YAC72 MSNs somehow leads to faster loss of NMDARs from the surface, forward NMDAR trafficking rates are enhanced to even greater extents and dominate to generate higher steady-state levels of surface NMDAR expression in these cells. Forward trafficking is regulated in multiple ways, including through changes in phosphorylation of NMDARs, differential expression of NMDAR subunits and/or isoforms, and association with other proteins or the CSK. Based on earlier findings suggesting enhancement of NR1/NR2B forward trafficking by replacement of the NR1 C2 cassette with C2' (Mu et al., 2003), we investigated the possibility that alternative splicing may contribute to the faster forward trafficking we observed for NMDARs in YAC72 MSNs.

Comparison of the relative expression of C2'- versus C2-containing NR1 isoforms in subcellular fractions revealed a significant shift towards the C2'-containing isoform of NR1 in the mobile, ER-containing and microsome-enriched fraction (P3) of YAC72 mouse striatum, compared to the synaptosomal region (LP1). A lack of change in the ratio of NR1 isoforms containing C2' versus C2 in the LP1 fraction indicates that NR1 C2'-containing NMDAR complexes are not preferentially trafficked to the synapses. These data suggest that NMDARs enriched in NR1 isoforms containing the C2' cassette may be predominantly targeted for expression at non-synaptic plasma membranes, which are included in the light membrane P3 fraction. Moreover, we found increased association of NR1 C2' with NR2B subunits in striatal tissue from YAC72 mice, consistent with a NR2B-selective mechanism of mhtt-mediated neurotoxicity and greater numbers of NR2B-containing NMDARs being mobilized more quickly through the forward trafficking pathway onto the membrane at extra-synaptic locations. Differential expression of NR2A- and NR2B-containing NMDARs at synaptic and extra-synaptic sites may have important consequences for cellular signaling networks, as differences in pro-survival transcriptional activation pathways and in the determination of the direction of synaptic plasticity have been reported depending on the localization and/or subunit composition of NMDARs (Hardingham and Bading, 2003; Liu et al., 2004).

6.1.3. Implications for YAC128 HD Mice

In the studies described in the current thesis, we have not looked at YAC128 mice in detail apart from an examination of the CK2 protein expression pattern in striatal cytosolic and particulate fractions and the demonstration that inhibition of CK2 activity in striatal MSNs from these mice exacerbated NMDAR-dependent cell death to similar

levels as in YAC72 mice, relative to WT MSNs (section 5.7). The YAC128 mice express mhtt with a more extreme polyQ expansion length of 128Q (Slow et al., 2003) consistent with juvenile-onset HD and exhibit relatively early degeneration of striatal neurons (Slow et al., 2003; Van Raamsdonk et al., 2005). Because disease progresses more quickly in these mice than in similar YAC models expressing mhtt with more moderate polyQ lengths, the YAC128 mice have measurable endpoints for pre-clinical testing and have become the model of choice among the full-length mouse HD models. Because of the increasingly widespread use of these mice in pre-clinical testing, it is crucial to be able to correlate results from therapeutic studies in the YAC128 mouse model with corresponding changes at the molecular and cellular level. A thorough understanding of the effects of htt-128Q expression in these mice is therefore necessary.

As noted in the Introduction (section 1.2.6), YAC128 mice exhibit similar defects in the kynurenine pathway of tryptophan degradation as do human HD patients and the R6/2 mouse model leading to increased formation of oxidative species and the NMDAR agonist QA (Guidetti et al., 2004, 2006). From birth, these mice also displayed disrupted Ca^{2+} homeostasis and compromised mitochondrial function. Not only did repeated application of glutamate result in elevated intracellular Ca^{2+} levels in cultured MSNs from P0-P1 animals of this genotype (Tang et al., 2005), but coincident block of glycolysis further exacerbated NMDA-induced Ca^{2+} de-regulation in these neurons (Oliveira et al., 2006), in comparison to controls (see section 1.4.1). The extent of cytochrome c release from the intra-mitochondrial space into the cytosol also revealed an increased tendency of cultured MSNs from YAC128 mice to undergo the mPT following glutamate insult, and significantly higher levels of glutamate-induced, NMDAR-dependent apoptotic death were found in these neurons in comparison to WT (Tang et al., 2005; see section 1.4.4). Exposure to sub-saturating concentrations of NMDA (which induced non-maximal levels

of death in MSNs from YAC72 mice) further illustrated a clear correlation between htt polyQ length and extent of NMDAR-dependent apoptotic cell death in MSNs from YAC transgenic mice, with YAC128 > YAC72 > YAC18 (Shehadeh et al., 2006).

Although these changes in NMDAR-dependent toxicity, Ca^{2+}-handling, and mitochondrial function are similar to findings in YAC72 mice which express mhtt with a more moderate polyQ length, these mice did not appear to share a common mechanistic pathway in ultimately causing NMDAR-mediated apoptotic death. Unlike the YAC72 mice, MSNs from YAC128 mice had peak NMDA-induced current densities and NMDAR-mediated Ca^{2+} loads that were not significantly different than WT (Fernandes et al., submitted for publication). Unchanged NMDAR-mediated current was in agreement with a lack of effect of htt-128Q on the relative distribution of NMDARs; immunostaining studies failed to identify changes in the proportion of NR1 subunits located at the surface versus intracellularly (L. Zhang and L.A. Raymond, unpublished results). In contrast to results from other YAC transgenic mice which we have examined, YAC128 mice displayed reduced striatal NR2B expression at 12 months of age (J. Shehadeh and L.A. Raymond, unpublished results; see section 1.2.5). These data collectively indicate that mhtt-elicited toxicity in YAC128 MSNs does not involve changes at the level of NMDAR current and/or expression (surface and total).

While changes in surface NMDAR expression in YAC72 striatal neurons may be explained in part by altered splicing of NR1 and accelerated forward trafficking of receptors, it is not clear what other factors may contribute to enhanced NMDAR activity. As discussed in section 1.5.3 of the Introduction, phosphorylation of NMDARs is extremely important in the regulation of NMDAR function, with serine phosphorylation at amino acid positions 896 and 897 on the NR1 subunit acting to promote forward trafficking of NMDARs (Scott et al., 2001, 2003). Our laboratory has investigated the

phosphorylation status of these sites in striatal tissue from WT and YAC transgenic mice and concluded that YAC128 mice expressed similar levels of S896- and S896/S897-phosphorylated NR1 in the striatum as did YAC72 mice, and both of these were higher than in WT or YAC18 mice (C. Cowan and L.A. Raymond, unpublished results). Whereas increased pS896/pS897 would be consistent with faster forward movement of receptors through the ER/Golgi networks in YAC72, it is not known what role increased phosphorylation of these sites plays in YAC128 mice where surface NMDAR expression does not appear to be altered.

Serine phosphorylation of the NR2B subunit also contributes to modulation of NMDAR trafficking and function. Specifically, phosphorylation at S1480 of NR2B by CK2 decreases surface levels of NR2B-containing NMDARs by interfering with their interaction with PDZ proteins at the PSD (Chung et al., 2004). Interesting, we found increased CK2 expression in the membrane fraction of heterologous cells co-expressing NR1/NR2B with htt-138Q, and in the particulate fractions from YAC72 and YAC128 striatal tissue, compared to cells and neurons that expressed WT htt (see Results sections 5.2 and 5.7.1). Sensitivity to NMDA-induced toxicity was also similarly augmented by inhibition of CK2 activity in cultured striatal MSNs from both YAC128 and YAC72 mice (section 5.7.2), suggesting that CK2 played a protective role against NMDAR-dependent excitotoxic cell death, especially for cells that expressed mhtt. In the YAC128 mouse striatum, CK2 activity could conceivably contribute to increased pS1480 levels to maintain relatively low levels of surface NMDAR expression. However, the same cannot be said for YAC72 mice, which express a higher proportion of surface NMDARs than do YAC128 mice. Moreover, transfected HEK293 cells expressing NR1/NR2B did not show increased pS1480 levels when co-trasfected with htt-138Q (as compared with htt-15Q) (C. Sutton and L.A. Raymond, unpublished results), although in these same

transfected cells total surface NR1 expression was not found to be different between htt-15Q- and htt-138Q-expressing cells (Chen et al., 1999b). It remains unclear as to whether heterologous cells transfected with htt-138Q more closely resembles the YAC128 model, or YAC mice which express less extreme polyQ lengths of 72Q or 46Q.

6.2. Physical Link between NMDARs and Htt

To determine what actually mediates the physical link between NMDARs and htt to facilitate the actions of mhtt on NMDAR function, we probed for interactions between the htt-interacting protein HIP-1 and NMDAR-binding α-actinins. Confirming earlier findings from our laboratory using a transfected heterologous cell line, we demonstrated interaction of HIP-1 and α-actinin 4 by co-immunoprecipitation in mouse forebrain tissue. These proteins also co-localized and co-fractionated with each other, and HIP-1 and α-actinin 4 also bound NMDARs. We were not able to co-precipitate HIP-1 using antibodies directed against α-actinin 4 or α-actinin proteins in general, likely due to the widespread involvement of these actin-crosslinking proteins in numerous processes within the cell and therefore a relatively small fraction involved in binding to HIP-1 and NMDARs at any given time. However, we would argue that lack of HIP-1 detection in anti-α-actinin immunoprecipitates does not imply a lack of interaction between these proteins, since use of HIP-1 antibodies evidently brought down significant amounts of α-actinin 4.

We further confirmed a direct interaction between these two proteins using a gel overlay assay where recombinant α-actinin protein was tested for binding to immobilized HIP-1. We initially hypothesized that interaction between HIP-1 and α-actinin may be mediated via their talin-like and spectrin-like domains, respectively, but a HIP-1 fragment

consisting only of the talin domain failed to bind α-actinin in these same studies. In an attempt to further examine whether the HIP-1 talin region may be able to bind α-actinin, we performed similar gel overlay assays on autospot membranes (prepared with help from Dr. W. Campbell and J. Guo; also see Guo et al., 2004) with 20-mer peptides spaced 2 amino acids apart and spanning the sequence of the C-terminal 561 amino acids of human HIP-1 protein which corresponds to the talin domain. The signals we obtained from α-actinin binding to the membrane were unfortunately not consistent across repeated experiments, and were often not significantly above background (data not shown). We therefore conclude that either the talin domain is not involved in mediating the HIP-1/α-actinin interaction, or else expression of the talin domain alone or 20-mer peptides thereof is not sufficient to enable proper protein folding to take place such that the appropriate tertiary structure is not present to permit binding to normal binding partners of HIP-1. Perhaps mutational analyses in conjunction with yeast two-hybrid or other interaction studies will facilitate the identification of the regions within HIP-1 which are involved in binding to α-actinin.

6.2.1. Modulation of NMDARs by HIP-1

If HIP-1 is involved in mediating the effects of mhtt or normal WT htt on NMDAR activity, manipulating HIP-1 levels would be expected to have an effect on NMDAR function and/or expression. We indeed found this to be the case from MSNs over-expressing HIP-1, where surface expression of the NR1 subunit was up-regulated akin to the difference observed between YAC72 and WT MSNs. While striatal MSNs from YAC72 mice had ~50% higher ratio of surface-to-internal expression of NR1 than did WT

MSNs, the increase in NR1 surface expression in MSNs over-expressing HIP-1 was not as dramatic, at only ~30% compared with controls. Since expansion of the polyQ tract in htt weakens its interaction with HIP-1, expression of mhtt would enlarge the pool of free, non-htt-bound HIP-1 which is believed to contribute to mhtt-mediated neurotoxicity and HD pathogenesis by recruiting and activating caspase-8 (Gervais et al., 2002). Apart from this role, HIP-1 was also shown to regulate trafficking of AMPARs, as it appeared to be required for clathrin-dependent internalization of AMPARs following agonist stimulation in a cultured neuronal model (Metzler et al., 2003). On the other hand, taking into consideration our data from Chapter 3 indicating that the rate of NMDAR insertion to the neuronal surface membrane is increased while loss from the surface is not slowed, it would seem that HIP-1 plays more of a role in promoting surface expression of NMDARs rather than altering internalization rate. A recent study has shown that another huntingtin-interacting protein, HAP-1, plays a role in promoting recycling of γ-aminobutyric acid (GABA) type A receptors back to the cell surface (Kittler et al., 2004). HIP-1 may act in a similar way to enhance the rate of NMDAR recycling back to the surface, or else facilitate forward mobilization of receptors from the Golgi, thus shifting the balance of receptor distribution towards increased steady-state levels of expression at the surface. In this way, expression of mhtt may act in part through HIP-1 to alter distribution of NMDARs to facilitate increased Ca^{2+} influx and excitotoxicity mediated by these receptors.

6.3. Effect of Htt PolyQ Expansion on Expression and/or Distribution of Signaling Proteins

On a more global scale, a series of high-throughput screens were performed in an attempt to reveal additional clues as to what other proteins relevant to NMDAR function may be affected (in terms of expression levels and/or distribution) by htt polyQ expansion. HEK293 cells were transfected with plasmids encoding NR1/NR2B along with either htt-15Q (WT) or htt-138Q (mutant), and harvested for both cytosolic and particulate fractions. Although signaling pathways in transfected HEK293 cells (which are of non-neuronal origin) cannot possibly fully recapitulate those activated in neurons, we have reason to believe that cells co-transfected with htt and NMDARs could be used to model certain aspects of NMDAR activation in neurons (Chen et al., 1999b; Zeron et al., 2001, 2002). Our data from transfected HEK cells indicate that, of the proteins which were examined, the vast majority were not differentially expressed in either fraction. This is not unexpected considering that for HD and other late-onset diseases, most cellular signaling must remain intact in order to maintain close-to-normal cell function at least until symptom onset. Being able to replicate the values for most proteins from one condition to another in fact reassures us as to the reproducibility of the screens and confirms this as a valid approach to identify possible targets with expression changes for further investigation.

Where substantial change was observed, it was generally in the form of a shift in distribution either from the cytosolic to the particulate fraction or *vice versa*, in cells expressing mhtt relative to WT htt. Most of these changes involved kinases and proteins of the stress response pathway such as CK2, ERp72, GroEL, Hsp70, and Hsp90. To better define whether these changes occurred solely as a result of htt polyQ expansion, or

whether they depended on co-expression of NMDARs, we transfected HEK293 cells with various constructs to express only htt-15Q, htt-138Q, NR1/NR2B NMDARs, or NMDARs along with either htt-15Q or htt-138Q. Our results suggested that polyQ expansion alone was not sufficient to enhance cytosolic Hsp70 levels but instead relied on simultaneous co-expression of NR1/NR2B NMDARs.

The effect of NMDAR activation was also tested, and we found mhtt-induced changes to be potentiated by agonist-stimulation of NMDARs, likely as part of a defensive response launched by the cell to combat excitotoxic pathways stemming from NMDAR activation in conjunction with mhtt expression. It is unclear as to whether potentiation of these stress-related proteins would play a protective role, although molecular chaperones such as Hsp70 have been previously documented to suppress toxicity associated with expanded polyQ tracts (Chai et al., 1999; Warrick et al., 1999; Carmichael et al., 2000; Jana et al., 2000; Kazemi-Esfarjani and Benzer, 2000; Kobayashi et al., 2000; Muchowski et al., 2000; Cummings et al., 2001; Bonini, 2002; Wyttenbach et al., 2002; Adachi et al., 2003; Ishihara et al., 2003). In a mouse neuronal cell line stably expressing N-terminally truncated polyQ-expanded htt, a number of chaperones were shown to co-localize with htt-containing aggregates (Jana et al., 2000). In these cells, expression of Hsp70 was also dramatically induced upon expression of polyQ-expanded mhtt, and over-expression of chaperones successfully inhibited both aggregate formation and mhtt-induced cell death (Jana et al., 2000). These findings are in agreement with a recent study demonstrating a positive correlation between Hsp70 expression levels and neuronal survival; the more vulnerable striatal and cortical neurons in culture were found to have significantly lower levels of CBP-mediated Hsp70 expression than neurons cultured from the cerebellum, a region less severely affected in HD (Tagawa et al., 2007). A different study, however, reported an enhancement of inclusion formation by heat shock protein

over-expression in heterologous cells that were co-transfected with a htt exon 1 fragment containing an expanded polyQ (Wyttenbach et al., 2000), thus highlighting once again our need for an improved understanding of the roles that these molecular chaperones play in protein folding under conditions of stress.

Total cellular expression for selected proteins identified from the initial screens as having altered expression in cytosolic and/or particulate fractions was also examined, to determine whether mhtt expression and NMDAR activation affected not only cytosolic or particulate levels and/or distribution, but led to changes in overall protein expression levels as well. From four sets of samples that were transfected, treated, and collected independently, we found no significant difference in overall expression levels of the proteins examined regardless of htt polyQ length or NMDAR activity, suggesting mhtt expression in the presence of agonist-stimulated NMDARs did not affect overall transcription and translation of these proteins.

6.3.1. Modulation of NMDAR Activity by CK2 in the Context of HD

CK2 was one of the protein kinases studied in these screens, and this serine/threonine protein kinase exhibited a robust increase in particulate expression in our initial KPKS screen. CK2 is known to be activated under conditions of stress and is involved in a wide array of biological processes including cell survival, tumorigenesis, and response to viral infection (Faust and Montenarh 2000; Sayed et al., 2000; Ahmed et al., 2002; Litchfield 2003; Meggio and Pinna 2003). One well known neuronal substrate of CK2 is the PKC and Casein Kinase Substrate in Neurons-1 (PACSIN-1), a htt-interacting protein which – like HIP-1 – has been implicated in clathrin-mediated endocytosis (Modregger et al., 2002). Of special importance to us, however, is the possibility that CK2

may be implicated in the regulation of NMDAR function directly or indirectly through PSD-95, since both PSD-95 and NMDAR subunit NR2B have been identified as phosphorylation substrates of CK2, and modulation of NMDAR function by CK2 has been reported (Lieberman and Mody, 1999; Chung et al., 2004; Soto et al., 2004). It was therefore conceivable that the effect of htt polyQ expansion on NMDAR expression and/or function may be mediated in part through signaling pathways involving this kinase. We confirmed the expression of this protein kinase in striatal tissue from FVB/N WT and YAC mice expressing htt with expanded polyQ tracts (YAC72 and YAC128), and noted that particulate expression of CK2 was increased in the YAC mice relative to WT, similar to findings from HEK cells that over-expressed mhtt compared to WT as shown in the KPKS screen.

To better understand the role of CK2 up-regulation in particulate fractions from striatal tissue expressing mhtt, we used pharmacological inhibition to test the effect of CK2 activity blockade. We employed a previously described TUNEL-based toxicity paradigm to ask whether CK2 inhibition mitigates or exacerbates apoptotic death in cultured striatal neurons exposed to NMDA, and whether the effects of CK2 inhibition differed with varying htt polyQ length. Our results from this study confirmed earlier findings indicating a polyQ length-dependent potentiation of NMDAR-mediated apoptotic death by mhtt (Zeron et al., 2002; Shehadeh et al., 2006). When CK2 activity was abolished, we observed significantly elevated levels of cell death resulting from NMDAR over-activation in MSNs from both YAC72 and YAC128 transgenic mice.

Our results therefore indicate that, in cells expressing polyQ-expanded htt, CK2 plays a protective role against NMDA-associated toxicity. Because CK2-mediated phosphorylation of NR2B disrupts the latter's interaction with PSD-95 leading to decreased NR2B surface expression levels (Chung et al., 2004), a reduction in CK2

activity would be expected to stabilize or increase NR2B surface expression and thereby facilitate NMDAR-dependent excitotoxic death. Hence it would be of interest to determine whether the potentiation of NMDA-induced apoptotic death by CK2 inhibition in our studies resulted from changes to the phosphorylation state and/or surface expression of the NR2B subunit, and whether such changes would be modulated by expression of mhtt. Moreover, since receptor surface expression is regulated by endocytosis and our studies indicate a role for HIP-1 in the modulation of NMDAR surface expression, the CK2 substrate and htt-interactor PACSIN-1 deserves greater attention as an additional regulator of the clathrin-dependent endocytic process and therefore a likely mediator of the effects of mhtt on NMDAR expression and/or function. Likewise, the role of p53 as a possible mediator of mhtt-induced, CK2-dependent toxicity warrants further examination in light of the known interaction between p53 with htt (Steffan et al., 2000), along with previous findings demonstrating the regulation of p53 activity by CK2 (Schuster et al., 1999; Pospisilova et al., 2004) and *vice versa* (Schuster et al., 2001).

6.4. Selective Vulnerability of Striatal MSNs in HD

As much progress has been made in recent years on the elucidation of the functions of WT and mutant forms of htt, as well as the identification of protein interactors of htt, the mechanisms underlying the late onset of striatal degeneration in HD are becoming increasingly well understood. In HD mouse models, early effects of mhtt expression on corticostriatal signaling, NMDAR function, Ca^{2+} homeostasis, and mitochondrial activity create sub-toxic levels of neuronal stress, which may then trigger activation of a variety of signaling pathways to alter gene transcription, degrade cellular components, generate oxidative damage, and impair neuronal function (summarized in

Figure 45). Persistent over-activation of NMDARs leads to chronic exposure to these toxic stimuli and events, which continue to accumulate over time until, with age, the neurons become unable to handle the stress any longer and therefore degenerate.

While the early molecular triggers leading to late-onset neurodegeneration are becoming better defined, few studies have specifically addressed the underlying causes and mechanisms of the selective degeneration observed in HD. Expression of htt is widespread and not particularly enriched in the striatum, nor are proteins that bind htt differentially expressed in striatal MSNs. It is therefore likely that properties intrinsic to striatal MSNs and/or alterations in selected protein-protein interactions involving htt and regulated by mhtt polyQ length may play a role in rendering these neurons particularly susceptible to excitotoxic damage in HD.

Specifically, the relative enrichment of NR2B subunit expression (versus NR2A) in striatum as compared to other parts of the forebrain (Landwehrmeyer et al., 1995; Ghasemzadeh et al., 1996; Rigby et al., 1996; Standaert et al., 1999; Christie et al., 2000; Kuppenbender et al., 2000; Li et al., 2003) implicates this subunit as one possible candidate in conferring a selective vulnerability of striatal neurons to mhtt-mediated toxicity. Evidence to support this idea came from studies in both transfected HEK293 cells and striatal MSNs from YAC transgenic mice demonstrating mhtt-induced potentiation of current and apoptotic death mediated by the NR1/NR2B, but not NR1/NR2A, subtype of NMDARs (Chen et al., 1999b; Zeron et al., 2001, 2002). The results from studies described in this thesis provide additional insight into the mechanisms underlying this potentiation.

Our findings of enhanced surface expression of NR1 and NR2B subunits due to accelerated forward mobilization of NMDARs through the ER/Golgi network may be a result of altered post-transcriptional and/or post-translational modifications of these

receptors, along with perturbed interactions with the actin CSK or other proteins that are responsible for NMDAR trafficking, targeting, and anchoring to the cell surface. The increased ratio of C2'-to-C2 NR1 splice variants that we observed in the ER/microsome fraction in YAC72 striatum would favor a faster exit rate of NMDARs from the ER (Figure 46, point 1). It is therefore notable that we also found increased NR1 C2' incorporation into NR2B- (and to a lesser extent, NR2A-) containing NMDAR complexes in YAC72 striatal tissue compared with WT.

The fact that we demonstrated the co-association of HIP-1, α-actinin, htt and NR2B in complexes co-immunoprecipitated from striatal tissue suggests an additional mechanism for selectively enhancing surface expression of NR2B-containing NMDARs. We showed that HIP-1 and α-actinin interact, and a previous report indicated that α-actinin associates with NR1 and NR2B but not NR2A (Wyszynski et al., 1997). Moreover, HIP-1 is part of the clathrin complex involved in receptor forward trafficking through the Golgi network, as well as in receptor endocytosis and recycling, and data shown in this thesis indicate that increased levels of HIP-1 result in enhanced NMDAR surface expression in striatal MSNs (Figure 46, point 2). Thus, the enrichment of NR2B expression in striatal neurons coupled with mhtt-induced alterations in the trafficking of predominantly NR2B-containing receptors together may confer a selective vulnerability of striatal neurons to NMDAR-mediated excitotoxic damage and contribute to the selective pattern of neurodegeneration observed in HD.

6.5. Future Directions

We now have in our hands a greater number of puzzle pieces which together fit into a larger overall picture called Huntington's disease. One of the future challenges will

be the task of trying to position these puzzle pieces relative to one another, although many questions remain unresolved. While we have now determined that mhtt may increase surface NMDAR expression by modulating the incorporation of different NR1 splice variants into mobile receptor pools as well as by acting via its protein partners to modulate NMDAR distribution, we have not exhausted the possibilities of how else mhtt could act to modulate NMDAR activity, or non-NMDAR-dependent routes of toxicity in HD. As described in section 1.5.3 of the Introduction, and also section 6.1.3 of this Chapter in the context of the YAC128 model, phosphorylation clearly plays a pivotal role in determining NMDAR function, expression, and trafficking, but so far the link between NMDAR phosphorylation and polyQ expansion in mhtt has not been thoroughly examined.

Our data indicated a shift in the distribution of C2'- versus C2-containing NR1 isoforms to compartments in transit to/from the cell surface, although the mechanistic details underlying this change are as yet undefined. Further work also needs to be done to characterize the mobile vesicular pool of NMDARs to determine whether it actually comprises pools of receptors travelling in opposing directions to and from the surface and, if so, whether C2'- and C2-containing NR1 isoforms are differentially expressed in different pools.

We observed that over-expression of HIP-1 led to a similar increase in surface NR1 expression as did mhtt expression in YAC72 mice; in the absence of additional information we can only speculate a role for HIP-1 in promoting recycling and/or forward trafficking of NMDARs to the cell surface. Further testing will be necessary to confirm or disprove this idea, and to examine whether the HIP-1-induced enhancement of surface proportion of NMDARs shares a common mechanistic pathway with the increase

resulting from mhtt polyQ expansion, for instance through a change in alternative splicing of NR1 and/or differential association of the NR2B subunit with different NR1 isoforms.

With respect to the physical interaction between α-actinin and HIP-1 linking htt to NMDARs, it has not been determined whether this interaction varies according to htt polyQ length, or whether mhtt alters other aspects of NMDAR functional modulation by actin-binding proteins or the actin CSK. It is also not known as to which regions of the two proteins mediate the HIP-1/α-actinin interaction. Identification of these regions (from mutational or other studies) will certainly prove useful in facilitating the development of molecular tools such as dominant negative peptides, to allow determination of the functional consequences of blocking this interaction and to test whether this interaction is required for the effects of HIP-1 on NMDAR surface expression.

These and numerous other questions abound, and substantial amounts of work still need to be done to further characterize the many mechanisms, pathways, and proteins that have been uncovered to date. Nevertheless, we hope the findings we report in the present thesis add to previous work by others and allow us to begin to unravel the complex changes in cellular signaling resulting from htt polyQ expansion that underlie disease pathogenesis in HD.

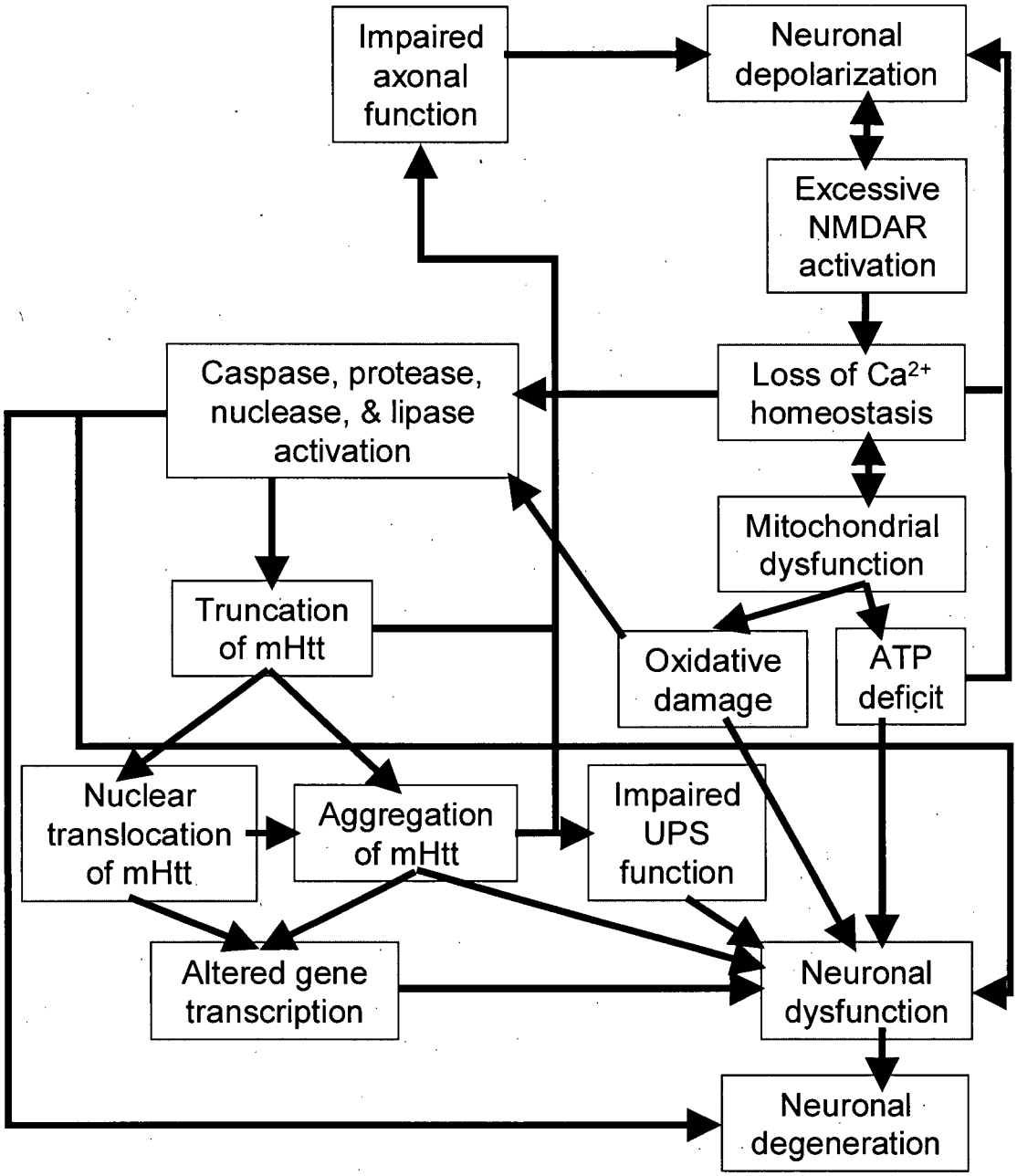

Figure 45. Flowchart illustrating cellular processes affected by expression of mhtt. These processes can each contribute to neuronal dysfunction and/or degeneration individually or in conjunction with other processes; they are directly or indirectly modulated by mhtt expression and are interconnected in numerous ways to form feed-forward signaling loops.

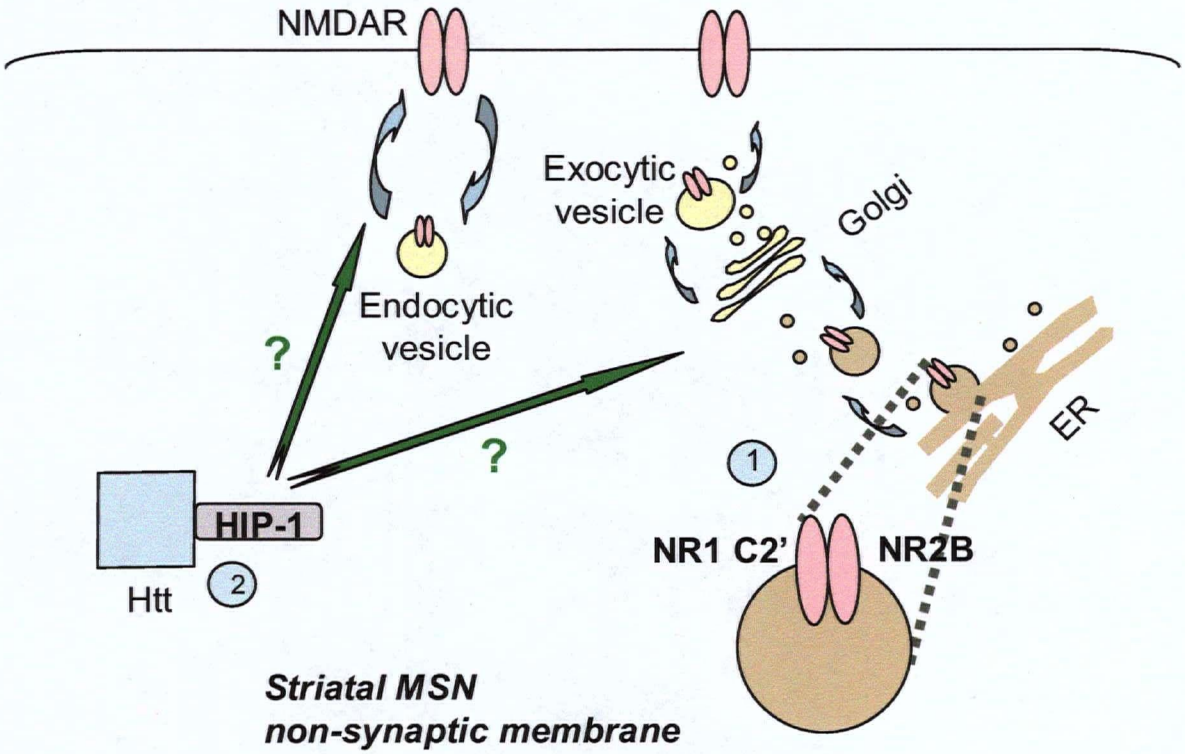

Figure 46. Cartoon of possible mechanisms underlying potentiation of NMDAR activity by mhtt at non-synaptic sites. At non-synaptic membranes, mhtt may enhance NMDAR surface expression by: (1) promoting NMDAR delivery to the cell surface by modulating splicing of NR1 subunit to increase proportion of C2'-containing isoforms being complexed with NR2B subunits and trafficked through the ER/Golgi network; (2) interacting with protein partners such as HIP-1 to (putatively) promote increased delivery and/or recycling of NMDARs back to the surface.

BIBLIOGRAPHY

Adachi, H., Katsuno, M., Minamiyama, M., Sang, C., Pagoulatos, G., Angelidis, C., Kusakabe, M., Yoshiki, A., Kobayashi, Y., Doyu, M., Sobue, G., 2003. Heat shock protein 70 chaperone overexpression ameliorates phenotypes of the spinal and bulbar muscular atrophy transgenic mouse model by reducing nuclear-localized mutant androgen receptor protein. J. Neurosci. 23, 2203-2211.

Ahmed, K., Gerber, D.A., Cochet, C., 2002. Joining the cell survival squad: an emerging role for protein kinase CK2. Trends Cell. Biol. 12, 226-230.

Akazawa, C., Shigemoto, R., Bessho, Y., Nakanishi, S., Mizuno, N., 1994. Differential expression of five N-methyl-D-aspartate receptor subunit mRNAs in the cerebellum of developing and adult rats. J. Comp. Neurol. 347, 150-160.

Albin, R.L., Young, A.B., Penney, J.B., Handelin, B., Balfour, R., Anderson, K.D., Markel, D.S., Tourtellotte, W.W., Reiner, A., 1990. Abnormalities of striatal projection neurons and N-methyl-D-aspartate receptors in presymptomatic Huntington's disease. N. Engl. J. Med. 322, 1293–1298.

Albin, R.L., Reiner, A., Anderson, K.D., Dure, L.S.4th, Handelin, B., Balfour, R., Whetsell, W.O.Jr., Penney J.B., Young, A.B., 1992. Preferential loss of striato-external pallidal projection neurons in presymptomatic Huntington's disease. Ann. Neurol. 31, 425-430.

Ali, N.J., Levine, M.S., 2006. Changes in expression of N-methyl-D-aspartate receptor subunits occur early in the R6/2 mouse model of Huntington's disease. Dev. Neurosci. 28, 230-238.

Allison, D.W., Gelfand, V.I., Spector, I., Craig, A.M., 1998. Role of actin in anchoring postsynaptic receptors in cultured hippocampal neurons: differential attachment of NMDA versus AMPA receptors. J. Neurosci. 18, 2423-2436.

Allison, D.W., Chervin, A.S., Gelfand, V.I., Craig, A.M., 2000. Postsynaptic scaffolds of excitatory and inhibitory synapses in hippocampal neurons: maintenance of core components independent of actin filaments and microtubules. J. Neurosci. 20, 4545-4554.

Andrade, M.A., Bork, P., 1995. HEAT repeats in Huntington's disease protein. Nat. Genet. 11, 115-116.

Andrade, M.A., Perez-Iratxeta, C., Ponting, C.P., 2001. Protein repeats: structures, functions, and evolution. J. Struct. Biol. 134, 117-131.

Andre, V.M., Cepeda, C., Venegas, A., Gomez, Y., Levine, M.S., 2006. Altered cortical glutamate receptor function in the R6/2 model of Huntington's disease. J. Neurophysiol. 95, 2108-2119.

Arenas, J., Campos, Y., Ribacoba, R., Martin, M.A., Rubio, J.C., Ablanedo, P., Cabello, A., 1998. Complex I defect in muscle from patients with Huntington's disease. Ann. Neurol. 43, 397-400.

Ariano, M.A., Wagle, N., Grissell, A.E., 2005. Neuronal vulnerability in mouse models of Huntington's disease: membrane channel protein changes. J. Neurosci. Res. 80, 634-645.

Aronin, N., Chase, K., Young, C., Sapp, E., Schwarz, C., Matta, N., Kornreich, R., Landwehrmeyer, B., Bird, E., Beal, M.F., Vonsattel, J.P., Smith, T., Carraway, R., Boyce, F.M., Young, A.B., Penney, J.B., DiFiglia, M., 1995. CAG expansion affects the expression of mutant huntingtin in the Huntington's disease brain. Neuron 15, 1193-1201.

Arrasate, M., Mitra, S., Schweitzer, E.S., Segal, M.R., Finkbeiner, S., 2004. Inclusion body formation reduces levels of mutant huntingtin and the risk of neuronal death. Nature 431, 805-810.

Asztely, F., Gustafsson, B., 1996. Ionotropic glutamate receptors: their role in the expression of hippocampal synaptic plasticity. Mol. Neurobiol. 12, 1–11.

Barria, A., Malinow, R., 2002. Subunit-specific NMDA receptor trafficking to synapses. Neuron 35, 345-353.

Bartlett, T.E., Bannister, N.J., Collett, V.J., Dargan, S.L., Massey, P.V., Bortolotto, Z.A., Fitzjohn, S.M., Bashir, Z.I., Collingridge, G.L., Lodge, D., 2006. Differential roles of NR2A and NR2B-containing NMDA receptors in LTP and LTD in the CA1 region of two-week old rat hippocampus. Neuropharmacology [Epub ahead of print].

Beal, M.F., 1995. Aging, energy, and oxidative stress in neurodegenerative diseases. Ann. Neurol. 38, 357-366.

Beal, M.F., 2005. Mitochondria take center stage in aging and neurodegeneration. Ann. Neurol. 58, 495-505.

Beal, M.F., Kowall, N.W., Ellison, D.W., Mazurek, M.F., Swartz, K.J., Martin, J.B., 1986. Replication of neurochemical characteristics of Huntington's disease by quinolinic acid. Nature 321, 168-171.

Beal, M.F., Ferrante, R.J., Swartz, K.J., Kowall, N.W., 1991. Chronic quinolinic acid lesions in rats closely resemble Huntington's disease. J. Neurosci. 11, 1649-1659.

Beal, M.F., Brouillet, E., Jenkins, B.G., Ferrante, R.J., Kowall, N.W., Miller, J.M., Storey, E., Srivastava, R., Rosen, B.R., Hyman, B.T., 1993. Neurochemical and histologic characterization of striatal excitotoxic lesions produced by the mitochondrial toxin 3-nitopropionic acid. J. Neurosci. 13, 4181-4192.

Becher, M.W., Kotzuk, J.A., Sharp, A.H., Davies, S.W., Bates, G.P., Price, D.L., Ross, C.A., 1998. Intranuclear neuronal inclusions in Huntington's disease and

dentatorubral and pallidoluysian atrophy: correlation between the density of inclusions and IT15 CAG triplet repeat length. Neurobiol. Dis. 4, 387-397.

Beggs, A.H., Byers, T.J., Knoll, J.H., Boyce, F.M., Bruns, G.A., Kunkel, L.M., 1992. Cloning and characterization of two human skeletal muscle alpha-actinin genes located on chromosomes 1 and 11. J. Biol. Chem. 267, 9281-9288.

Behrens, P.F., Franz, P., Woodman, B., Lindenberg, K.S., Landwehrmeyer, G.B., 2002. Impaired glutamate transport and glutamate-glutamine cycling: downstream effects of the Huntington mutation. Brain 125, 1908-1922.

Berberich, S., Punnakkal, P., Jensen, V., Pawlak, V., Seeburg, P.H., Hvalby, O., Kohr, G., 2005. Lack of NMDA receptor subtype selectivity for hippocampal long-term potentiation. J. Neurosci. 25, 6907-6910.

Berberich, S., Jensen, V., Hvalby, O., Seeburg, P.H., Kohr, G., 2006. The role of NMDAR subtypes and charge transfer during hippocampal LTP induction. Neuropharmacology [Epub ahead of print].

Berliocchi, L., Bano, D., Nicotera, P., 2005. Ca^{2+} signals and death programmes in neurons. Phil. Trans. R. Soc. Lond. B Biol. Sci. 360, 2255-2258.

Bittenbender, J.B., Quadfasel, F.A., 1962. Rigid and akinetics forms of Huntington's chorea. Arch. Neurol. 7, 275-288.

Biziere, K., Coyle, J.T., 1979. Effects of cortical ablation on the neurotoxicity and receptor binding of kainic acid in the striatum. J. Neurosci. Res. 4, 383-398.

Blanquet, P.R., 2000. Casein kinase 2 as a potentially important enzyme in the nervous system. Prog. Neurobiol. 60, 211-246.

Bliss, T.V., Collingridge, G.L., 1993. A synaptic model of memory: long-term potentiation in the hippocampus. Nature 361, 31-39.

Bogdanov, M.B., Ferrante, R.J., Kuemmerle, S., Klivenyi, P., Beal, M.F., 1998. Increased vulnerability to 3-nitropropionic acid in an animal model of Huntington's disease. J. Neurochem. 71, 2642-2644.

Bonini, N.M., 2002. Chaperoning brain degeneration. Proc. Natl. Acad. Sci. U.S.A., 99 Suppl. 4, 16407-16411.

Boutell, J.M., Thomas, P., Neal, J.W., Weston, V.J., Duce, J., Harper, P.S., Jones, A.L., 1999. Aberrant interactions of transcriptional repressor proteins with the Huntington's disease gene product, huntingtin. Hum. Mol. Genet. 8, 1647-1655.

Brennan, W.A.Jr., Bird, E.D., Aprille, J.R., 1985. Regional mitochondrial respiratory activity in Huntington's disease brain. J. Neurochem. 44, 1948-1950.

Brinkman, R. R., Mezei, M. M., Theilmann, J., Almqvist, E., Hayden, M. R., 1997. The likelihood of being affected with Huntington disease by a particular age, for a specific CAG size. Am. J. Hum. Genet. 60, 1202–1210.

Brouillet, E., Hantraye, P., Ferrante, R.J., Dolan, R., Leroy-Willig, A., Kowall, N.W., Beal, M.F., 1995. Chronic mitochondrial energy impairment produces selective striatal degeneration and abnormal choreiform movements in primates. Proc. Natl. Acad. Sci. U.S.A. 92, 7105-7109.

Browne, S.E., Bowling, A.C., MacGarvey, U., Baik, M.J., Berger, S.C., Muqit, M.M., Bird, E.D., Beal, M.F., 1997. Oxidative damage and metabolic dysfunction in Huntington's disease: selective vulnerability of the basal ganglia. Ann. Neurol. 41, 646-653.

Brustovetsky, N., Brustovetsky, T., Purl, K.J., Capano, M., Crompton, M., Dubinsky, J.M., 2003. Increased susceptibility of striatal mitochondria to calcium-induced permeability transition. J. Neurosci. 23, 4858-4867.

Brustovetsky, N., LaFrance, R., Purl, K.J., Brustovetsky, T., Keene, C.D., Low, W.C., Dubinsky, J.M., 2005. Age-dependent changes in the calcium sensitivity of striatal mitochondria in mouse models of Huntington's disease. J. Neurochem. 93, 1361-1370.

Burke, J.R., Enghild, J.J., Martin, M.E., Jou, Y.S., Myers, R.M., Roses, A.D., Vance, J.M., Strittmatter, W.J., 1996. Huntingtin and DRPLA proteins selectively interact with the enzyme GAPDH. Nat. Med. 2, 347-350.

Byers, T.J., Husain-Chishti, A., Dubreuil, R.R., Branton, D., Goldstein, L.S., 1989. Sequence similarity of the amino-terminal domain of Drosophila beta spectrin to alpha actinin and dystrophin. J. Cell Biol. 109, 1633-1641.

Carmichael, J., Chatellier, J., Woolfson, A., Milstein, C., Fersht, A.R., Rubinsztein, D.C., 2000. Bacterial and yeast chaperones reduce both aggregate formation and cell death in mammalian cell models of Huntington's disease. Proc. Natl. Acad. Sci. U.S.A. 97, 9701-9705.

Carroll, R.C., Beattie, E.C., Xia, H., Luscher, C., Altschuler, Y., Nicoll, R.A., Malenka, R.C., von Zastrow, M., 1999. Dynamin-dependent endocytosis of ionotropic glutamate receptors. Proc. Natl. Acad. Sci. U.S.A. 96, 14112-14117.

Carroll, R.C., Zukin, R.S., 2002. NMDA-receptor trafficking and targeting: implications for synaptic transmission and plasticity. Trends Neurosci. 25, 571-577.

Cattaneo, E., 2003. Dysfunction of wild-type huntingtin in Huntington disease. News Physiol. Sci. 18, 34-37.

Cattaneo, E., Rigamonti, D., Goffredo, D., Zuccato, C., Squitieri, F., Sipione, S., 2001. Loss of normal Huntingtin function: new developments in Huntington's disease research. Trends Neurosci. 24, 182-188.

Cepeda, C., Ariano, M.A., Calvert, C.R., Flores-Hernandez, J., Chandler, S.H., Leavitt, B.R., Hayden, M.R., Levine, M.S., 2001a. NMDA receptor function in mouse models of Huntington disease. J. Neurosci. Res. 66, 525-539.

Cepeda, C., Itri, J.N., Flores-Hernandez, J., Hurst, R.S., Calvert, C.R., Levine, M.S., 2001b. Differential sensitivity of medium- and large-sized striatal neurons to NMDA but not kainate receptor activation in the rat. Eur. J. Neurosci. 14, 1577-1589.

Cepeda, C., Hurst, R.S., Calvert, C.R., Hernandez-Echeagaray, E., Nguyen, O.K., Jocoy, E., Christian, L.J., Ariano, M.A., Levine, M.S., 2003. Transient and progressive electrophysiological alterations in the corticostriatal pathway in a mouse model of Huntington's disease. J. Neurosci. 23, 961-969.

Cha, J.-H.J., 2000. Transcriptional dysregulation in Huntington's disease. Trends Neurosci. 23, 387-392.

Cha, J.H., Kosinski, C.M., Kerner, J.A., Alsdorf, S.A., Mangiarini, L., Davies, S.W., Penney, J.B., Bates, G.P., Young, A.B., 1998. Altered brain neurotransmitter receptors in transgenic mice expressing a portion of an abnormal human Huntington disease gene. Proc. Natl. Acad. Sci. U.S.A. 95, 6480-6485.

Cha, J.-H.J., Frey, A.S., Alsdorf, S.A., Kerner, J.A., Kosinski, C.M., Mangiarini, L., Penney, J.B.Jr., Davies, S.W., Bates, G.P., Young, A.B., 1999. Altered neurotransmitter receptor expression in transgenic mouse models of Huntington's disease. Phil. Trans. R. Soc. Lond. B. 354, 981-989.

Chai, Y., Koppenhafer, S.L., Bonini, N.M., Paulson, H.L., 1999. Analysis of the role of heat shock protein (Hsp) molecular chaperones in polyglutamine disease. J. Neurosci. 19, 10338-10347.

Chan, Y., Tong, H.Q., Beggs, A.H., Kunkel, L.M., 1998. Human skeletal muscle-specific alpha-actinin-2 and -3 isoforms form homodimers and heterodimers in vitro and in vivo. Biochem. Biophys. Res. Commun. 248, 134-139.

Chang, D.T.W., Rintoul, G.L., Pandipati, S., Reynolds, I.J., 2006. Mutant huntingtin aggregates impair mitochondrial movement and trafficking in cortical neurons. Neurobiol. Dis. 22, 388-400.

Chatterton, J.E., Awobuluyi, M., Premkumar, L.S., Takahashi, H., Talantova, M., Shin, Y., Cui, J., Tu, S., Sevarino, K.A., Nakanishi, N., Tong, G., Lipton, S.A., Zhang, D., 2002. Excitatory glycine receptors containing the NR3 family of NMDA receptor subunits. Nature 415, 793-798.

Chen, L., Huang, L.Y., 1992. Protein kinase C reduces Mg2+ block of NMDA-receptor channels as a mechanism of modulation. Nature 356, 521-523.

Chen, N., Moshaver, A., Raymond, L.A., 1997. Differential sensitivity of recombinant N-methyl-D-aspartate receptor subtypes to zinc inhibition. Mol. Pharmacol. 51, 1015-1023.

Chen, N., Luo, T., Raymond, L.A., 1999a. Subtype-dependence of NMDA receptor channel open probability. J. Neurosci. 19, 6844-6854.

Chen, N., Luo, T., Wellington, C., Metzler, M., McCutcheon, K., Hayden, M.R., Raymond, L.A., 1999b. Subtype-specific enhancement of NMDA receptor currents by mutant huntingtin. J. Neurochem. 72, 1890-1898.

Chen, S., Berthelier, V., Yang, W., Wetzel, R., 2001. Polyglutamine aggregation behavior in vitro supports a recruitment mechanism of cytotoxicity. J. Mol. Biol. 311, 173-182.

Choo, Y.S., Johnson, G.V., MacDonald, M., Detloff, P.J., Lesort, M., 2004. Mutant huntingtin directly increases susceptibility of mitochondria to the calcium-induced permeability transition and cytochrome *c* release. Hum. Mol. Genet. 13, 1407-1420.

Christie, J.M., Jane, D.E., Monaghan, D.T., 2000. Native N-methyl-D-aspartate receptors containing NR2A and NR2B subunits have pharmacologically distinct competitive antagonist binding sites. J. Pharmacol. Exp. Ther. 292, 1169-1174.

Chung, H.J., Huang, Y.H., Lau, L.-F., Huganir, R.L., 2004. Regulation of the NMDA receptor complex and trafficking by activity-dependent phosphorylation of the NR2B subunit PDZ ligand. J. Neurosci. 24, 10248-10259.

Ciechanover, A., 1994. The ubiquitiin-proteasome proteolytic pathway. Cell 79, 13-21.

Cingolani, G., Petosa, C., Weis, K., Muller, C.W., 1999. Structure of importin-β bound to the IBB domain of importin-α. Nature 399, 221-229.

Cohen, C.M., Foley, S.F., 1984. Biochemical characterization of complex formation by human erythrocyte spectrin, protein 4.1, and actin. Biochemistry 23, 6091-6098.

Conn, P.J., Pin, J.P., 1997. Pharmacology and functions of metabotropic glutamate receptors. Annu. Rev. Pharmacol. Toxicol. 37, 205-237.

Cooper, J.K., Schilling, G., Peters, M.F., Herring, W.J., Sharp, A.H., Kaminsky, Z., Masone, J., Khan, F.A., Delanoy, M., Borchelt, D.R., Dawson, V.S., Dawson, T.M., Ross, C.A., 1998. Truncated N-terminal fragments of huntingtin with expanded glutamine repeats form nuclear and cytoplasmic aggregates in cell culture. Hum. Mol. Genet. 7, 783-790.

Cornett, J., Cao, F., Wang, C.E., Ross, C.A., Bates, G.P., Li, S.H., Li, X.J., 2005. Polyglutamine expansion of huntingtin impairs its nuclear export. Nat. Genet. 37, 198-204.

Courey, A.J., Holtzman, D.A., Jackson, S.P., Tjian, R., 1989. Synergistic activation by the glutamine-rich domains of human transcription factor Sp1. Cell 59, 827-836.

Cowan, C.M., Hayden, M.R., Raymond, L.A., 2005. Effect of mutant huntingtin on NMDA receptor phosphorylation. Society for Neuroscience 35th Annual Meeting. Program # 90.8.

Coyle, J.T., Schwarcz, R., 1976. Lesion of striatal neurons with kainic acid provides a model for Huntington's chorea. Nature 263, 244-246.

Cramer, H., Warter, J.M., Renaud, B., 1984. Analysis of neurotransmitter metabolites and adenosine 3',5'-monophosphate in the CSF of patients with extrapyramidal motor disorders. Adv. Neurol. 40, 431-435.

Cull-Candy, S., Brickley, S., Farrant, M., 2001. NMDA receptor subunits: diversity, development and disease. Curr. Opin. Neurobiol. 11, 327-335.

Cull-Candy, S.G., Leszkiewicz, D.N., 2004. Role of distinct NMDA receptor subtypes at central synapses. Sci. S.T.K.E. 2004, re16.

Cummings, C.J., Mancini, M.A., Antalffy, B., DeFranco, D.B., Orr, H.T., Zoghbi, H.Y., 1998. Chaperone suppression of aggregation and altered subcellular proteasome localization imply protein misfolding in SCA1. Nat. Genet. 19, 148-154.

Cummings, C.J., Sun, Y., Opal, P., Antalffy, B., Mestril, R., Orr, H.T., Dillmann, W.H., Zoghbi, H.Y., 2001. Over-expression of inducible HSP70 chaperone suppresses neuropathology and improves motor function in SCA1 mice. Hum. Mol. Genet. 10, 1511-1518.

Cummings, C.J., Zoghbi, H.Y., 2000. Fourteen and counting: unraveling trinucleotide repeat diseases. Hum. Mol. Genet. 9, 909-916.

Cybulska-Klosowicz, A., Mazarakis, N.K., Van Dellen, A., Blakemore, C., Hannan, A.J., Kossut, M., 2004. Impaired learning-dependent cortical plasticity in Huntington's disease transgenic mice. Neurobiol. Dis. 17, 427-434.

Dalbem, A., Silveira, C.V., Pedroso, M.F., Breda, R.V., Werne Baes, C.V., Bartmann, A.P., da Costa, J.C., 2005. Altered distribution of striatal activity-dependent synaptic plasticity in the 3-nitropropionic acid model of Huntington's disease. Brain Res. 1047, 148-158.

Davies, S.W., Turmaine, M., Cozens, B.A., DiFiglia, M., Sharp, A.H., Ross, C.A., Scherzinger, E., Wanker, E.E., Mangiarini, L., Bates, G.P., 1997. Formation of neuronal intranuclear inclusions underlies the neurological dysfunction in mice transgenic for the HD mutation. Cell 90, 537-548.

Davies, S., Ramsden, D.B., 2001. Huntington's disease. J. Clin. Pathol.: Mol. Pathol. 54, 409-413.

Del Toro, D., Canals, J.M., Gines, S., Kojima, M., Egea, G., Alberch, J., 2006. Mutant huntingtin impairs the post-Golgi trafficking of brain-derived neurotrophic factor but not its Val66Met polymorphism. J. Neurosci. 26, 12748-12757.

Diakowski, W., Grzybek, M., Sikorski, A.F., 2006. Protein 4.1, a component of the erythrocyte membrane skeleton and its related homologue proteins forming the protein 4.1/FERM superfamily. Folia Histochem. Cytobiol. 44, 231-248.

DiFiglia, M., 1990. Excitotoxic injury of the neostriatum: a model for Huntington's disease. Trends Neurosci. 13, 286–289.

DiFiglia, M., Sapp, E., Chase, K., Schwarcz, C., Meloni, A., Young, C., Martin, E., Vonsattel, J.P., Carraway, R., Reeves, S.A., Boyce, F.M., Aronin, N., 1995. Huntingtin is a cytoplasmic protein associated with vesicles in human and rat brain neurons. Neuron 14, 1075-1081.

DiFiglia, M., Sapp, E., Chase, K.O., Davies, S.W., Bates, G.P., Vonsattel, J.P., Aronin, N., 1997. Aggregation of huntingtin in neuronal intranuclear inclusions and dystrophic neurites in brain. Science 277, 1990-1993.

Dingledine, R., Borges, K., Bowie, D., Traynelis S.F., 1999. The glutamate receptor ion channels. Pharmacol. Rev. 51, 7-61.

Dragunow, M., Faull, R.L., Lawlor, P., Beiharz, E.J., Singleton, K., Walker, E.B., Mee, E., 1995. In situ evidence for DNA fragmentation in Huntington's disease striatum and Alzheimer's disease temporal lobes. Neuroreport 6, 1053-1057.

Dubreuil, R.R., Byers, T.J., Sillman, A.L., Bar-Zvi, D., Goldstein, L.S., Branton, D., 1989. The complete sequence of Drosophila alpha-spectrin: conservation of structural domains between alpha-spectrins and alpha-actinin. J. Cell Biol. 109, 2197-2205.

Duchen, M.R., 2004. Roles of mitochondria in health and disease. Diabetes 53, S96-S102.

Dugan, L.L., Sensi, S.L., Canzoniero, L.M., Handran, S.D., Rothman, S.M., Lin, T.S., Goldberg, M.P., Choi, D.W., 1995. Mitochondrial production of reactive oxygen species in cortical neurons following exposure to N-methyl-D-aspartate. J. Neurosci. 15, 63777–63788.

Dunah, A.W., Standaert, D.G., 2001. Dopamine D1 receptor-dependent trafficking of striatal NMDA glutamate receptors to the postsynaptic membrane. J. Neurosci. 21, 5546-5558.

Dunah, A.W., Wyszynski, M., Martin, D.M., Sheng, M., Standaert, D.G., 2000. Alpha-actinin-2 in rat striatum: localization and interaction with NMDA glutamate receptor subunits. Brain Res. Mol. Brain Res. 79, 77-87.

Duyao, M.P., Auerbach, A.B., Ryan, A., Persichetti, F., Barnes, G.T., McNeil, S.M., Ge, P., Vonsattel, J.P., Gusella, J.F., Joyner, A.L., et al., 1995. Inactivation of the mouse Huntington's disease gene homolog Hdh. Science 269, 407-410.

Dyer, R.B., McMurray, C.T., 2001. Mutant protein in Huntington disease is resistant to proteolysis in affected brain. Nat. Genet. 29, 270-278.

Edwardson, J.M., Wang, C.T., Gong, B., Wyttenbach, A., Bai, J., Jackson, M.B., Chapman, E.R., Morton, A.J., 2003. Expression of mutant huntingtin blocks exocytosis in PC12 cells by depletion of complexin II. J. Biol. Chem. 278, 30849-30853.

Ehlers, M.D., 2000. Reinsertion or degradation of AMPA receptors determined by activity-dependent endocytic sorting. Neuron 28, 511-525.

Ehlers, M.D., Mammen, A.L., Lau, L.F., Huganir, R.L., 1996a. Synaptic targeting of glutamate receptors. Curr. Opin. Cell Biol. 8, 484-489.

Ehlers, M.D., Zhang, S., Bernhadt, J.P., Huganir, R.L., 1996b. Inactivation of NMDA receptors by direct interaction of calmodulin with the NR1 subunit. Cell 84, 745-755.

Engelsen, B., 1986. Neurotransmitter glutamate: its clinical importance. Acta Neurol. Scand. 74, 337-355.

Fan, M.M.Y., Fernandes, H.B., Zhang, L.Y.J., Hayden, M.R., Raymond, L.A., 2007. Altered NMDA receptor trafficking in a yeast artificial chromosome transgenic mouse model of Huntington's disesase. J. Neurosci. 27, 3768-3779.

Fan, M.M.Y., Raymond, L.A., 2006. N-methyl-D-aspartate (NMDA) receptor function and excitotoxicity in Huntington's disease. Prog. Neurobiol. doi:10.1016/j.pneurobio.2006.11.003 (Article in Press).

Faust, M., Montenarh, M., 2000. Subcellular localization of protein kinase CK2. A key to its function? Cell Tissue Res. 301, 329-340.

Fernandes, H.B., Baimbridge, K.G., Church, J., Hayden, M.R., Raymond, L.A., Mitochondrial sensitivity and altered calcium handling underlie enhanced NMDA-induced apoptosis in YAC128 model of Huntington's disease. Manuscript submitted for publication.

Ferrante, R.J., Kowall, N.W., Beal, M.F., Richardson, E.P.Jr., Bird, E.D., Martin, J.B., 1985. Selective sparing of a class of striatal neurons in Huntington's disease. Science 230, 561-563.

Ferrante, R.J., Kowall, N.W., Beal, M.F., Martin, J.B., Bird, E.D., Richardson, E.P.Jr., 1987. Morphologic and histochemical characteristics of a spared subset of striatal neurons in Huntington's disease. J. Neuropathol. Exp. Neurol. 46, 12-27.

Ferrante, R.J., Kowall, N.W., Cipolloni, P.B., Storey, E., Beal, M.F., 1993. Excitotoxin lesions in primates as a model for Huntington's disease: histopathologic and neurochemical characterization. Exp. Neurol. 119, 46-71.

Ferrer, I., Goutan, E., Marin, C., Rey, M.J., Ribalta, T., 2000. Brain-derived neurotrophic factor in Huntington disease. Brain Res. 866, 257-261.

Fusco, F.R., Chen, Q., Lamoreaux, W.J., Figueredo-Cardenas, G., Jiao, Y., Coffman, J.A., Surmeier, D.J., Honig, M.G., Carlock, L.R., Reiner, A., 1999. Cellular localization of huntingtin in striatal and cortical neurons in rats: lack of correlation with neuronal vulnerability in Huntington's disease. J. Neurosci. 19, 1189-1202.

Gauthier, L.R., Charrin, B.C., Borrell-Pages, M., Dompierre, J.P., Rangone, H., Cordelieres, F.P., De Mey, J., MacDonald, M.E., Lessmann, V., Humbert, S., Saudou, F., 2004. Huntingtin controls neurotrophic support and survival of neurons by enhancing BDNF vesicular transport along microtubules. Cell 118, 127-138.

Gerber, G., Kangrga, I., Ryu, P.D., Larew, J.S., Randic, M., 1989. Multiple effects of phorbol esters in the rat spinal dorsal horn. J. Neurosci. 9, 3606-3617.

Gerber, H.P., Seipel, K., Georgiev, O., Hofferer, M., Hug, M., Rusconi, S., Schaffner, W., 1994. Transcriptional activation modulated by homopolymeric glutamine and proline stretches. Science 263, 808-811.

Gervais, F.G., Singaraja, R., Xanthoudakis, S., Gutekunst, C.A., Leavitt, B.R., Metzler, M., Hackam, A.S., Tam, J., Vaillancourt, J.P., Houtzager, V., Rasper, D.M., Roy, S., Hayden, M.R., Nicholson, D.W., 2002. Recruitment and activation of caspase-8 by the Huntingtin-interacting protein Hip-1 and a novel partner Hippi. Nat. Cell Biol. 4, 95-105.

Ghasemzadeh, M.B., Sharma, S., Surmeier, D.J., Eberwine, J.H., Chesselet, M.F., 1996. Multiplicitiy of glutamate receptor subunits in single striatal neurons: an RNA amplification study. Mol. Pharmacol. 49, 852-859.

Gines, S., Seong, I.S., Fossale, E., Ivanova, E., Trettel, F., Gusella, J.F., Wheeler, V.C., Persichetti, F., MacDonald, M.E., 2003. Specific progressive cAMP reduction implicates energy deficit in presymptomatic Huntington's disease knock-in mice. Hum. Mol. Genet. 12, 497-508.

Gines, S., Bosch, M., Marco, S., Gavalda, N., Diaz-Hernandez, M., Lucas, J.J., Canals, J.M., Alberch, J., 2006. Reduced expression of the TrkB receptor in Huntington's disease mouse models and in human brain. Eur. J. Neurosci. 23, 649-658.

Giorgini, F., Muchowski, P.J., 2005. Connecting the dots in Huntington's disease with protein interaction networks. Genome Biol. 6, 210.

Goehler, H., Lalowski, M., Stelzl, U., Waelter, S., Stroedicke, M., Worm, U., Droege, A., Lindenberg, K.S., Knoblich, M., Haenig, C., Herbst, M., Suopanki, J., Scherzinger, E., Abraham, C., Bauer, B., Hasenbank, R., Fritzsche, A., Ludewig, A.H., Bussow, K., Coleman, S.H., Gutekunst, C.A., Landwehrmeyer, B.G., Lehrach, H., Wanker, E.E., 2004. A protein interaction network links GIT1, an enhancer of huntingtin aggregation, to Huntington's disease. Mol. Cell. 15, 853-865.

Goldberg, Y.P., Nicholson, D.W., Rasper, D.M., Kalchman, M.A., Koide, H.B., Graham, R.K., Bromm, M., Kazemi-Esfarjani, P., Thornberry, N.A., Vaillancourt, J.P., Hayden, M.R., 1996. Cleavage of huntingtin by apopain, a proapoptotic cysteine protease, is modulated by the polyglutamine tract. Nat. Genet. 13, 442-449.

Graham, R.K., Deng, Y., Slow, E.J., Haigh, B., Bissada, N., Lu, G., Pearson, J., Shehadeh, J., Bertram, L., Murphy, Z., Warby, S.C., Doty, C.N., Roy, S., Wellington, C.L., Leavitt, B.R., Raymond, L.A., Nicholson, D.W., Hayden, M.R., 2006. Cleavage at the caspase-6 site is required for neuronal dysfunction and degeneration due to mutant huntingtin. Cell 125, 1179-1191.

Graveland, G.A., Williams, R.S., DiFiglia, M., 1985. Evidence for degenerative and regenerative changes in neostriatal spiny neurons in Huntington's disease. Science 227, 770-773.

Green, H., 1993. Human genetic diseases due to codon reiteration: relationship to evolutionary mechanism. Cell 74, 955-956.

Greene, J.G., Greenamyre, J.T., 1995. Characterization of the excitotoxic potential of the reversible succinate dehydrogenase inhibitor malonate. J. Neurochem. 64, 430-436.

Greene, J.G., Porter, R.H., Eller, R.V., Greenamyre, J.T., 1993. Inhibition of succinate dehydrogenase by malonic acid produces and "excitotoxic" lesion in rat striatum. J. Neurochem. 61, 1151-1154.

Groc, L., Choquet, D., 2006. AMPA and NMDA glutamate receptor trafficking: multiple roads for reaching and leaving the synapse. Cell Tissue Res. 326, 423-438.

Gu, M., Gash, M.T., Mann, V.M., Javoy-Agid, F., Cooper, J.M., Schapira, A.H., 1996. Mitochondrial defect in Huntington's disease caudate nucleus. Ann. Neurol. 39, 385-389.

Guidetti, P., Luthi-Carter, R.E., Augood, S.J., Schwarcz, R., 2004. Neostriatal and cortical quinolinate levels are increased in early grade Huntington's disease. Neurobiol. Dis. 17, 455-461.

Guidetti, P., Bates, G.P., Graham, R.K., Hayden, M.R., Leavitt, B.R., MacDonald, M.E., Slow, E.J., Wheeler, V.C., Woodman, B., Schwarcz, R., 2006. Elevated brain 3-hydroxykynurenine and quinolinate levels in Huntington disease mice. Neurobiol. Dis. 23, 190-197.

Gunawardena, S., Her, L.S., Brusch, R.G., Laymon, R.A., Niesman, I.R., Gordesky-Gold, B., Sintasath, L., Bonini, N.M., Goldstein, L.S.B., 2003. Disruption of axonal transport by loss of huntingtin or expression of pathogenic polyQ proteins in Drosophila. Neuron 40, 25-40.

Guo, J.P., Petric, M., Campbell, W., McGeer, P.L., 2004. SARS corona virus peptides recognized by antibodies in the sera of convalescent cases. Virology 324, 251-256.

Gusella, J.F., MacDonald, M.E., 2000. Molecular genetics: unmasking polyglutamine triggers in neurodegenerative disease. Nature Rev. 1, 109-115.

Gutekunst, C.A., Li, S.H., Yi, H., Ferrante, R.J., Li, X.J., Hersch, S.M., 1998. The cellular and subcellular localization of huntingtin-associated protein 1 (HAP1): comparison with huntingtin in rat and human. J. Neurosci. 18, 7674-7686.

Gutekunst, C.A., Li, S.H., Yi, H., Mulroy, J.S., Kuemmerle, S., Jones, R., Rye, D., Ferrante, R.J., Hersch, S.M., Li, X.J., 1999. Nuclear and neuropil aggregates in Huntington's disease: relationship to neuropathology. J. Neurosci. 19, 2522, 2534.

Hackam, A.S., Hodgson, J.G., Singaraja, R., Zhang, T., Gan, L., Gutekunst, C.A., Hersch, S.M., Hayden, M.R., 1999a. Evidence for both the nucleus and cytoplasm as subcellular sites of pathogenesis in Huntignton's disease in cell culture and in transgenic mice expressing mutant huntingtin. Philos. Trans. R. Soc. Lond. B Biol. Sci. 354, 1047-1055.

Hackam, A.S., Singaraja, R., Zhang, T., Gan, L., Hayden, M.R., 1999b. In vitro evidence for both the nucleus and cytoplasm as subcellular sites of pathogenesis in Huntington's disease. Hum. Mol. Genet. 8, 25-33.

Hackam, A.S., Yassa, A.S., Singaraja, R., Metzler, M., Gutekunst, C.A., Gan, L., Warby, S., Wellington, C.L., Vaillancourt, J., Chen, N., Gervais, F.G., Raymond, L., Nicholson, D.W, Hayden, M.R., 2000. Huntingtin interacting protein 1 induces apoptosis via a novel caspase-dependent death effector domain. J. Biol. Chem. 275, 41299-41308.

Hantraye, P., Riche, D., Maziere, M., Isacson, O., 1990. A primate model of Huntington's disease: behavioral and anatomical studies of unilateral excitotoxic lesions of the caudate-putamen in the baboon. Exp. Neurol. 108, 91-104.

Hansson, O., Guatteo, E., Mercuri, N.B., Bernardi, G., Li, X.-J., Castilho, R.F., Brundin, P., 2001. Resistance to NMDA toxicity correlates with appearance of nuclear inclusions, behavioural deficits and changes in calcium homeostasis in mice transgenic for exon 1 of the huntingtin gene. Eur. J. Neurosci. 14, 1492-1504.

Hardingham, G.E., Bading, H., 2003. The Yin and Yang of NMDA receptor signaling. Trends Neurosci. 26, 81-89.

Hardingham, G.E., Fukunaga, Y., Bading, H., 2002. Extrasynaptic NMDARs oppose synaptic NMDARs by triggering CREB shut-off and cell death pathways. Nat. Neurosci. 5, 405-414.

Harjes, P., Wanker, E.E., 2003. The hunt for huntingtin function: interaction partners tell many different stories. Trends Biochem. Sci. 28, 425-433.

Harper, P.S., 1991. Huntington's disease. Harper, P.S. (Ed.) WB Saunders Co. Ltd., London.

Hayden, M.R., Berkowicz, A.L., Beighton, P.H., Yiptong, C., 1981. Huntington's chorea on the island of Mauritius. S. Afr. Med. J. 60, 1001-1002.

Hebb, C., 1970. CNS at the cellular level: identity of transmitter agents. Annu. Rev. Physiol. 32, 165-192.

Hell, J.W., Jahn, R., 1994. Preparation of synaptic vesicles from mammalian brain. In: Cell biology: a laboratory handbook Vol. I (J.E. Celis, ed.), pp567-574. San Diego: Academic Press, Inc.

Ho, L.W., Brown, R., Maxwell, M., Wyttenbach, A., Rubinsztein, D.C., 2001. Wild type huntingtin reduces the cellular toxicity of mutant huntingtin in mammalian cell models of Huntington's disease. J. Med. Genet. 38, 450-452.

Hodgson, J.G., Agopyan, N., Gutekunst, C.A., Leavitt, B.R., LePiane, F., Singaraja, R., Smith, D.J., Bissada, N., McCutcheon, K., Nasir, J., Jamot, L., Li, X.J., Stevens, M.E., Rosemond, E., Roder, J.C., Phillips, A.G., Rubin, E.M., Hersch, S.M., Hayden, M.R., 1999. A YAC mouse model for Huntington's disease with full-length mutant huntingtin, cytoplasmic toxicity, and selective striatal neurodegeneration. Neuron 23, 181-192.

Hollmann, M., Boulter, J., Maron, C., Beasley, L., Sullivan, J., Pecht, G., Heinemann, S., 1993. Zinc potentiates agonist-induced currents at certain splice variants of the NMDA receptor. Neuron 10, 943-954.

Hu, J.H., Chernoff, K., Pelech, S., Krieger, C., 2003a. Protein kinase and protein phosphatase expression in the central nervous system of G93A mSOD over-expressing mice. J. Neurochem. 85, 422-431.

Hu, J.H., Zhang, H., Wagey, R., Krieger, C., Pelech, S.L., 2003b. Protein kinase and protein phosphatase expression in amyotrophic lateral sclerosis spinal cord. J. Neurochem. 85, 432-442.

Huang, C.C., Faber, P.W., Persichetti, F., Mittal, V., Vonsattel, J.P., MacDonald, M.E., Gusella, J.F., 1998. Amyloid formation by mutant huntingtin: threshold, progressivity and recruitment of normal polyglutamine proteins. Somat. Cell Mol. Genet. 24, 217-233.

Humbert, S., Bryson, E.A., Cordelieres, F.P., Connors, N.C., Datta, S.R., Finkbeiner, S., Greenberg, M.E., Saudou, F., 2002. The IGF-1/Akt pathway is neuroprotective in Huntington's disease and involves huntingtin phosphorylation by Akt. Dev. Cell 2, 831-837.

Huntington's Disease Collaborative Research Group, 1993. A novel gene containing a trinucleotide repeat that is expanded and unstable on Huntington's disease chromosomes. Cell 72, 971-983.

Icton, C.D., 2001. Probing the interaction between huntingtin and NMDA receptors. M.Sc. thesis.

Ishihara, K., Yamagishi, N., Saito, Y., Adachi, H., Kobayashi, Y., Sobue, G., Ohtsuka, K., Hatayama, T., 2003. Hsp105alpha suppresses the aggregation of truncated androgen receptor with expanded CAG repeats and cell toxicity. J. Biol. Chem. 278, 25143-25150.

Ishii, T., Moriyoshi, K., Sugihara, H., Sakurada, K., Kadotani, H., Yokoi, M., Akazawa, C., Shigemoto, R., Mizuno, N., Masu, M., Nakanishi, S., 1993. Molecular characterization of the family of the N-methyl-D-aspartate receptor subunits. J. Biol. Chem. 268, 2836-2843.

Jana, N.R., Tanaka, M., Wang, G., Nukina, N., 2000. Polyglutamine length-dependent interaction of Hsp40 and Hsp70 family chaperones with truncated N-terminal huntingtin: their role in suppression of aggregation and cellular toxicity. Hum. Mol. Genet. 9, 2009-2018.

Jana, N.R., Zemskov, E.A., Wang, G., Nukina, N., 2001. Altered proteasomal function due to the expression of polyglutamine-expanded truncated N-terminal huntingtin induces apoptosis by caspase activation through mitochondrial cytochrome c release. Hum. Mol. Genet. 10, 1049-1059.

Jarabek, B.R., Yasuda, R.P., Wolfe, B.B., 2004. Regulation of proteins affecting NMDA receptor-induced excitotoxicity in a Huntington's mouse model. Brain 127, 505-516.

Jason, G.W., Suchowersky, O., Pajurkova, E.M., Graham, L., Klimek, M.L., Garber, A.T., Poirier-Heine, D., 1997. Cognitive manifestations of Huntington disease in relation to genetic structure and clinical onset. Arch. Neurol. 54, 1081-1088.

Kalchman, M.A., Koide, H.B., McCutcheon, K., Graham, R.K., Nichol, K, Nishiyama, K., Kazemi-Esfarjani, P., Lynn, F.C., Wellington, C., Metzler, M., Goldberg, Y.P., Kanazawa, I., Gietz, R.D., Hayden, M.R., 1997. HIP1, a human homologue of S. cerevisiae Sla2p, interacts with membrane-associated huntingtin in the brain. Nat. Genet. 16, 44-53.

Katsuno, M., Sang, C., Adachi, H., Minamiyama, M., Waza, M., Tanaka, F., Doyu, M., Sobue, G., 2005. Pharmacological induction of heat-shock proteins alleviates polyglutamine-mediated motor neuron disease. Proc. Natl. Acad. Sci. U.S.A. 102, 16801-16806.

Kazemi-Esfarjani, P., Benzer, S., 2000. Genetic suppression of polyglutamine toxicity in Drosophila. Science 287, 1837-1840.

Kegel, K.B., Kim, M., Sapp, E., McIntyre, C., Castano, J.G., Aronin, N., DiFiglia, M., 2000. Huntingtin expression stimulates endosomal-lysosomal activity, endosome tabulation, and autophagy. J. Neurosci. 20, 7268-7278.

Kegel, K.B., Sapp, E., Yoder, J., Cuiffo, B., Sobin, L., Kim, Y.J., Qin, Z.H., Hayden, M.R., Aronin, N., Scott, D.L., Isenberg, G., Goldmann, W.H., DiFiglia, M., 2005. Huntingtin associates with acidic phospholipids ad the plasma membrane. J. Biol. Chem. 280, 36464-36473.

Kew, J.N., Kemp, J.A., 2005. Ionotropic and metabotropic glutamate receptor structure and pharmacology. Psychopharmacology (Berl). 179, 4-29.

Kim, E., Sheng, M., 2004. PDZ domain proteins of synapses. Nat. Rev. Neurosci. 5, 771-781.

Kittler, J.T., Thomas, P., Tretter, V., Bogdanov, Y.D., Haucke, V., Smart, T.G., Moss, S.J., 2004. Huntingtin-associated protein 1 regulates inhibitory synaptic transmission by modulating gamma-aminobutyric acid type A receptor membrane trafficking. Proc. Natl. Acad. Sci. U.S.A., 101, 12736-12741.

Klapstein, G.J., Fisher, R.S., Zanjani, H., Cepeda, C., Jokel, E.S., Chesselet, M.F., Levine, M.S., 2001. Electrophysiological and morphological changes in striatal spiny neurons in R6/2 Huntington's disease transgenic mice. J. Neurophysiol. 86, 2667-2677.

Kobayashi, Y., Kume, A., Li, M., Doyu, M., Hata, M., Ohtsuka, K., Sobue, G., 2000. Chaperones Hsp70 and Hsp40 suppress aggregate formation and apoptosis in cultured neuronal cells expressing truncated androgen receptor protein with expanded polyglutamine tract. J. Biol. Chem. 275, 8772-8778.

Kornau, H.C., Schenker, L.T., Kennedy, M.B., Seeburg, P.H., 1995. Domain interaction between NMDA receptor subunits and the postsynaptic density protein PSD-95. Science 269, 1737-1740.

Korolchuk, V.I., Banting, G., 2002. CK2 and GAK/auxillin2 are major protein kinases in clathrin-coated vesicles. Traffic. 3, 428-439.

Koroshetz, W.J., Jenkins, B.G., Rosen, B.R., Beal, M.F., 1997. Energy metabolism defects in Huntington's disease and effects of coenzyme Q10. Ann. Neurol. 41, 160-165.

Kuemmerle, S., Gutekunst, C.A., Klein, A.M., Li, X.J., Li, S.H., Beal, M.F., Hersch, S.M., Ferrante, R.J., 1999. Huntingtin aggregates may not predict neuronal death in Huntington's disease. Ann. Neurol. 46, 842-849.

Kuppenbender, K.D., Albers, D.S., Iadarola, M.J., Landwehrmeyer, G.B., Standaert, D.G., 1999. Localization of alternatively spliced NMDAR1 glutamate receptor isoforms in rat striatal neurons. J. Comp. Neurol. 415, 204-217.

Kuppenbender, K.D., Standaert, D.G., Feuerstein, T.J., Penney, J.B.Jr., Young, A.B., Landwehrmeyer, G.B., 2000. Expression of NMDA receptor subunit mRNAs in neurochemically identified projection and interneurons in the human striataum. J. Comp. Neurol. 419, 407-421.

Laforet, G.A., Sapp, E., Chase, K., McIntyre, C., Boyce, F.M., Campbell, M., Cadigan, B.A., Warzecki, L., Tagle, D.A., Reddy, P.H., Cepeda, C., Calvert, C.R., Jokel, E.S., Klapstein, G.J., Ariano, M.A., Levine, M.S., DiFiglia, M., Aronin, N., 2001. Changes in cortical and striatal neurons predict behavioral and electrophysiological abnormalities in a transgenic murine model of Huntington's disease. J. Neurosci. 21, 9112-9123.

Lan, J.Y., Skeberdis, V.A., Jover, T., Grooms, S.Y., Lin, Y., Araneda, R.C., Zheng, X., Bennett, M.V., Zukin, R.S., 2001. Protein kinase C modulates NMDA receptor trafficking and gating. Nat. Neurosci. 4, 382-390.

Landwehrmeyer, G.B., Standaert, D.G., Testa, C.M., Penney, J.B.Jr., Young, A.B., 1995. NMDA receptor subunit mRNA expression by projection neurons and interneurons in rat striatum. J. Neurosci. 15, 5297-5307.

Laube, B., Kuhse, J., Betz, H., 1998. Evidence for a tetrameric structure of recombinant NMDA receptors. J. Neurosci. 18, 2954-2961.

Laurie, D.J., Bartke, I., Schoepfer, R., Naujoks, K., Seeburg, P.H., 1997. Regional, developmental and interspecies expression of the four NMDAR2 subunits, examined using monoclonal antibodies. Brain Res. Mol. Brain Res. 51, 23-32.

Lawrence, A.D., Sahakian, B.J., Hodges, J.R., Rosser, A.E., Lange, K.W., Robbins, T.W., 1996. Executive and mnemonic functions in early Huntington's disease. Brain 119, 1633-1645.

Lawrence, A.D., Hodges, J.R., Rosser, A.E., Kershaw, A., French-Constant, C., Rubinsztein, D.C., Robbins, T.W., Sahakian, B.J., 1998. Evidence for specific cognitive deficits in preclinical Huntington's disease. Brain 121, 1329-1341.

Leavitt, B.R., Van Raamsdonk, J.M., Shehadeh, J., Fernandes, H., Murphy, Z., Graham, R.K., Wellington, C.L., Raymond, L.A., Hayden, M.R., 2006. Wild-type huntingtin protects neurons from excitotoxicity. J. Neurochem. 96, 1121-1129.

Leenders, K.L., Frackowiak, R.S., Quinn, N., Marsden, C.D., 1986. Brain energy metabolism and dopaminergic function in Huntington's disease measured *in vivo* using positron emission tomography. Mov. Disord. 1, 69-77.

Lei, S., Czerwinska, E., Czerwinski, W., Walsh, M.P., MacDonald, J.F., 2001. Regulation of NMDA receptor activity by F-actin and myosin light chain kinase. J. Neurosci. 21, 8464-8472.

Leonard, A.S., Hell, J.W., 1997. Cyclic AMP-dependent protein kinase and protein kinase C phosphorylate N-methyl-D-aspartate receptors at different sites. J. Biol. Chem. 272, 12107-12115.

Levine, M.S., Klapstein, G.J., Koppel, A., Gruen, E., Cepeda, C., Vargas, M.E., Jokel, E.S., Carpenter, E.M., Zanjani, H., Hurst, R.S., Efstratiadis, A., Zeitlin, S., Chesselet,

M.-F., 1999. Enhanced sensitivity to N-methyl-D-aspartate receptor activation in transgenic and knockin mouse models of Huntington's disease. J. Neurosci. Res. 58, 515-532.

Li, B., Chen, N., Luo, T., Otsu, Y., Murphy, T.H., Raymond, L.A., 2002. Differential regulation of synaptic and extra-synaptic NMDA receptors. Nat. Neurosci. 5, 833-834.

Li, H., Li, S.H., Yu, Z.X., Shelbourne, P., Li, X.J., 2001. Huntingtin aggregate-associated axonal degeneration is an early pathological event in Huntington's disease mice. J. Neurosci. 21, 8473-8481.

Li, J.H., Wang, Y.H., Wolfe, B.B., Krueger, K.E., Corsi, L, Stocca, G., Vicini, S., 1998. Developmental changes in localization of NMDA receptor subunits in primary cultures of cortical neurons. Eur. J. Neurosci. 10, 1704-1715.

Li, L., Fan, M., Icton, C.D., Chen, N., Leavitt, B.R., Hayden, M.R., Murphy, T.H., Raymond, L.A., 2003. Role of NR2B-type NMDA receptors in selective neurodegeneration in Huntington disease. Neurobiol. Aging 24, 1113-1121.

Li, L., Murphy, T.H., Hayden, M.R., Raymond, L.A., 2004. Enhanced striatal NR2B-containing N-methyl-D-aspartate receptor-mediated synaptic currents in a mouse model of Huntington disease. J. Neurophysiol. 92, 2738-2746.

Li, S.-H., Cheng, A.L., Li, X.-J., 1999. Cellular defects and altered gene expression in PC12 cells stably expressing mutant huntingtin. J. Neurosci. 19, 5159-5172.

Li, S.-H., Li, X.-J., 2004. Huntingtin-protein interactions and the pathogenesis of Huntington's disease. Trends Genet. 20, 146-154.

Lieberman, D.N., Mody, I., 1999. Casein kinase-II regulates NMDA channel function in hippocampal neurons. Nat. Neurosci. 2, 125-132.

Lievens, J.C., Woodman, B., Mahal, A., Spasic-Boscovic, O., Samuel, D., Kerkerian-Le Goff, L., Bates, G.P., 2001. Impaired glutamate uptake in the R6 Huntington's disease transgenic mice. Neurobiol. Dis. 8, 807-821.

Lin, C.H., Tallaksen-Greene, S., Chien, W.M., Cearley, J.A., Jackson, W.S., Crouse, A.B., Ren, S., Li, X.J., Albin, R.L., 2001. Neurological abnormalities in a knock-in mouse model of Huntington's disease. Hum. Mol. Genet. 10, 137-144.

Lin, J.W., Ju, W., Foster, K., Lee, S.H., Ahmadian, G., Wyszynski, M., Wang, Y.T., Sheng, M., 2000. Distinct molecular mechanisms and divergent endocytotic pathways of AMPA receptor internalization. Nat. Neurosci. 3, 1282-1290.

Lin, Y., Skeberdis, V.A., Francesconi, A., Bennett, M.V., Zukin, R.S., 2004. Postsynaptic density protein-95 regulates NMDA channel gating and surface expression. J. Neurosci. 24, 10138-10148.

Lissin, D.V., Gomperts, S.N., Carroll, R.C., Christine, C.W., Kalman, D., Kitamura, M., Hardy, S., Nicoll, R.A., Malenka, R.C., von Zastrow, M., 1998. Activity differentially regulates the surface expression of synaptic AMPA and NMDA glutamate receptors. Proc. Natl. Acad. Sci. U.S.A., 95, 7097-7102.

Litchfield, D.W., 2003. Protein kinase CK2: structure, regulation and role in cellular decisions of life and death. Biochem. J. 369(Pt 1), 1-15.

Liu, L., Wong, T.P., Pozza, M.F., Lingenhoehl, K., Wang, Y., Sheng, M., Auberson, Y.P., Wang, Y.T., 2004. Role of NMDA receptor subtypes in governing the direction of hippocampal synaptic plasticity. Science 304, 1021-1024.

Lledo, P.-M., Zhang, X., Sudhof, T.C., Malenka, R.C., Nicoll, R.A., 1998. Postsynaptic membrane fusion and long-term potentiation. Science 279, 399-403.

Lucas, D.R., Newhouse, J.P., 1957. The toxic effect of sodium L-glutamate on the inner layers of the retina. A.M.A. Arch. Ophthalmol. 58, 193-201.

Luthi-Carter, R., Strand, A., Peters, N.L., Solano, S.M., Hollingsworth, Z.R., Menon, A.S., Frey, A.S., Spektor, B.S., Penney, E.B., Schilling, G., Ross, C.A., Borchelt, D.R., Tapscott, S.J., Young, A.B., Cha, J.-H.J., Olson, J.M., 2000. Decreased expression of striatal signaling genes in a mouse model of Huntington's disease. Hum. Mol. Genet. 9, 1259-1271.

Luthi-Carter, R., Hanson, S.A., Strand, A.D., Bergstrom, D.A., Chun, W., Peters, N.L., Woods, A.M., Chan, E.Y., Kooperberg, C., Krainc, D., Young, A.B., Tapscott, S.J., Olson, J.M., 2002a. Dysregulation of gene expression in the R6/2 model of polyglutamine disease: parallel changes in muscle and brain. Hum. Mol. Genet. 11, 1911-1926.

Luthi-Carter, R., Strand, A.D., Hanson, S.A., Kooperberg, C., Schilling, G., La Spada, A.R., Merry, D.E., Young, A.B., Ross, C.A., Borchelt, D.R., Olson, J.M., 2002b. Polyglutamine and transcription: gene expression changes shared by DRPLA and Huntington's disease mouse models reveal context-independent effects. Hum. Mol. Genet. 11, 1927-1937.

Luthi-Carter, R., Apostol, B.L., Dunah, A.W., DeJohn, M.M., Farrell, L.A., Bates, G.P., Young, A.B., Standaert, D.G., Thompson, L.M., Cha, J.-H.J., 2003. Complex alteration of NMDA receptors in transgenic Huntington's disease mouse brain: analysis of mRNA and protein expression, plasma membrane association, interacting proteins, and phosphorylation. Neurobiol. Dis.14, 624-636.

Man, H.Y., Lin, J.W., Ju, W.H., Ahmadian, G., Liu, L., Becker, L.E., Sheng, M., Wang, Y.T., 2000. Regulation of AMPA receptor-mediated synaptic transmission by clathrin-dependent receptor internalization. Neuron 25, 649-662.

Mangiarini, L., Sathasivam, K., Seller, M., Cozens, B., Harper, A., Hetherington, C., Lawton, M., Trottier, Y., Lehrach, H., Davies, S.W., Bates, G.P., 1996. Exon 1 of the

HD gene with an expanded CAG repeat is sufficient to cause a progressive neurological phenotype in transgenic mice. Cell 87, 493-506.

Maren, S., Baudry, M., 1995. Properties and mechanisms of long-term synaptic plasticity in the mammalian brain: relationships to learning and memory. Neurobiol. Learn. Mem. 63, 1–18.

Massey, P.V., Johnson, B.E., Moult, P.R., Auberson, Y.P., Brown, M.W., Molnar, E., Collingridge, G.L., Bashir, Z.I., 2004. Differential roles of NR2A and NR2B-containing NMDA receptors in cortical long-term potentiation and long-term depression. J. Neurosci. 24, 7821-7828.

Mauceri, D., Gardoni, F., Marcello, E., Di Luca, M., 2007. Dual role of CaMKII-dependent SAP97 phosphorylation in mediating trafficking and insertion of NMDA receptor subunit NR2A. J. Neurochem. 100, 1032-1046.

Mayer, M.L., Westbrook, G.L., Guthrie, P.B., 1984. Voltage-dependent block by Mg2+ of NMDA responses in spinal cord neurones. Nature 309, 261-263.

Mazarakis, N.K., Cybulska-Klosowicz, A., Grote, H., Pang, T., Van Dellen, A., Kossut, M., Blakemore, C., Hannan, A.J., 2005. Deficits in experience-dependent cortical plasticity and sensory-discrimination learning in presymptomatic Huntington's disease mice. 25, 3059-3066.

McBain, C.J., Mayer, M.L., 1994. N-methyl-D-aspartic acid receptor structure and function. Physiol. Rev. 74, 723-760.

McCampbell, A., Taylor, J.P., Taye, A.A., Robitschek, J., Li, M., Walcott, J., Merry, D., Chai, Y., Paulson, H., Sobue, G., Fischbeck, K.H., 2000. CREB-binding protein sequestration by expanded polyglutamine. Hum. Mol. Genet. 9, 2197-2202.

McGeer, E.G., McGeer, P.L., 1976. Duplication of biochemical changes of Huntington's chorea by intrastriatal injections of glutamic and kainic acids. Nature 263, 517-519.

McGeer, E.G., McGeer, P.L., 1978. Some factors influencing the neurotoxicity of intrastriatal injections of kainic acid. Neurochem. Res. 3, 501-517.

McIlhinney, R.A., Molnar, E., Atack, J.R., Whiting, P.J., 1996. Cell surface expression of the human N-methyl-D-aspartate receptor subunit 1a requires the co-expression of the NR2A subunit in transfected cells. Neuroscience 70, 989-997.

McIlhinney, R.A., Le Bourdelles, B., Molnar, E., Tricaud, N., Streit, P., Whiting, P.J., 1998. Assembly intracellular targeting and cell surface expression of the human N-methyl-D-aspartate receptor subunits NR1a and NR2A in transfected cells. Neuropharmacology 37, 1355-1367.

Meddows, E., Le Bourdelles, B., Grimwood, S., Wafford, K., Sandhu, S., Whiting, P., McIlhinney, R.A., 2001. Identification of molecular determinants that are important

in the assembly of N-methyl-D-aspartate recetors. J. Biol. Chem. 276, 18795-18803.

Meggio, F., Pinna, L.A., 2003. One-thousand-and-one substrates of protein kinase CK2? FASEB J. 17, 349-368.

Menalled, L.B., Chesselet, M.F., 2002. Mouse models of Huntington's disease. Trends Pharmacol. Sci. 23, 32-39.

Metzler, M., Legendre-Guillemin, V., Gan, L., Chopra, V., Kwok, A., McPherson, P.S., Hayden, M.R., 2001. HIP1 functions in clathrin-mediated endocytosis through binding to clathrin and adaptor protein 2. J. Biol. Chem. 276, 39271-39276.

Metzler, M., Li, B., Gan, L., Georgiou, J., Gutekunst, C.A., Wang, Y., Torre, E., Devon, R.S., Oh, R., Legendre-Guillemin, V., Rich, M., Alvarez, C., Gertsenstein, M., McPherson, P.S., Nagy, A., Wang, Y.T., Roder, J.C., Raymond, L.A., Hayden, M.R., 2003. Disruption of the endocytic protein HIP1 results in neurological deficits and decreased AMPA receptor trafficking. EMBO J. 22, 3254-3266.

Metzler, M., Gan, L., Wong, T.P., Liu, L., Helm, J., Liu, L., Georgiou, J., Wang, Y., Bissada, N., Cheng, K., Roder, J.C., Wang, Y.T., Hayden, M.R., 2007. NMDA receptor function and NMDA receptor-dependent phosphorylation of huntingtin is altered by the endocytic protein HIP1. J. Neurosci. 27, 2298-2308.

Michaelis, E.K., 1998. Molecular biology of glutamate receptors in the central nervous system and their role in excitotoxicity, oxidative stress and aging. Prog. Neurobiol. 54, 369-415.

Milnerwood, A.J., Cummings, D.M., Dallerac, G.M., Brown, J.Y., Vatsavayai, S.C., Hirst, M.C., Rezaie, P., Murphy, K.P., 2006. Early development of aberrant synaptic plasticity in a mouse model of Huntington's disease. Hum. Mol. Genet. 15, 1690-1703.

Milnerwood, A.J., Raymond, L.A., 2006. Synaptic abnormalities associated with Huntington's disease. In: Dityatev, A., El-Husseini, A. (Eds.), Molecular Mechanisms of Synaptogenesis. Springer U.S.A., New York, pp. 457-472.

Modregger, J., DiProspero, N.A., Charles, V., Tagle, D.A., Plomann, M., 2002. PACSIN 1 interacts with huntingtin and is absent from synaptic varicosities in presymptomatic Huntington's disease brains. Hum. Mol. Genet. 11, 2547-2558.

Monyer, H., Sprengel, R., Schoepfer, R., Herb, A., Higuchi, M., Lomeli, H., Burnashev, N., Sakmann, B., Seeburg, P.H., 1992. Heteromeric NMDA receptors: molecular and functional distinction of subtypes. Science 256, 1217-1221.

Monyer, H., Burnashev, N., Laurie, D.J., Sakmann, B., Seeburg, P.H., 1994. Developmental and regional expression in the rat brain and functional properties of four NMDA receptors. Neuron 12, 529-540.

Morishita, W., Lu, W., Smith, G.B., Nicoll, R.A., Bear, M.F., Malenka, R.C., 2006. Activation of NR2B-containing NMDA receptors is not required for NMDA receptor-dependent long-term depression. Neuropharmacology [Epub ahead of print].

Mu, Y., Otsuka, T., Horton, A.C., Scott, D.B., Ehlers, M.D., 2003. Activity-dependent mRNA splicing controls ER export and synaptic delivery of NMDA receptors. Neuron 40, 581-594.

Muchowski, P.J., Schaffar, G., Sittler, A., Wanker, E.E., Hayer-Hartl, M.K., Hartl, F.U., 2000. Hsp70 and hsp40 chaperones can inhibit self-assembly of polyglutamine proteins into amyloid-like fibrils. Proc. Natl. Acad. Sci. U.S.A. 97, 7841-7846.

Murphy, K.P., Carter, R.J., Lione, L.A., Mangiarini, L., Mahal, A., Bates, G.P., Dunnett, S.B., Morton, A.J., 2000. Abnormal synaptic plasticity and impaired spatial cognition in mice transgenic for exon 1 of the human Huntington's disease mutation. J. Neurosci. 20, 5115-5123.

Nasir, J., Floresco, S.B., O'Kusky, J.R., Diewert, V.M., Richman, J.M., Zeisler, J., Borowski, A., Marth, J.D., Phillips, A.G., Hayden, M.R., 1995. Targeted disruption of the Huntington's disease gene results in embryonic lethality and behavioral and morphological changes in heterozygotes. Cell 81, 811-823.

Neuwald, A.F., Hirano, T., 2000. HEAT repeats associated with condensins, cohesins, and other complexes involved in chromosome-related functions. Genome Res. 10, 1445-1452.

Nicholls, D.G., Ward, M.W., 2000. Mitochondrial membrane potential and neuronal glutamate excitotoxicity: mortality and millivolts. Trends Neurosci. 23, 166-174.

Nong, Y., Huang, Y.Q., Ju, W., Kalia, L.V., Ahmadian, G., Wang, Y.T., Salter, M.W., 2003. Glycine binding primes NMDA receptor internalization. Nature 422, 302-307.

Nowak, L., Bregestovski, P., Ascher, P., Herbet, A., Prochiantz, A., 1984. Magnesium gates glutamate-activated channels in mouse central neurones. Nature 307, 462-465.

Ohanian, V., Wolfe, L.C., John, K.M., Pinder, J.C., Lux, S.E., Gratzer, W.B., 1984. Analysis of the ternary interaction of the red cell membrane skeletal proteins spectrin, actin, and 4.1. Biochemistry 23, 4416-4420.

Okabe, S., Miwa, A., Okado, H., 1999. Alternative splicing of the C-terminal domain regulates cell surface expression of the NMDA receptor NR1 subunit. J. Neurosci. 19, 7781-7792.

Oliveira, J.M.A., Chen, S., Almeida, S., Riley, R., Gonçalves, J., Oliveira, C.R., Hayden, M.R., Nicholls, D.G., Ellerby, L.M., Rego, A.C., 2006. Mitochondrial-depdent Ca^{2+} handling in Huntington's disease striatal cells: effect of histone deacetylase inhibitors. Neurobiol. Dis. 26, 11174-11186.

Ordway, J.M., Tallaksen-Greene, S., Gutekunst, C.A., Bernstein, E.M., Cearley, J.A., Wiener, H.W., Dure, L.S.4th, Lindsey, R., Hersch, S.M., Jope, R.S., Albin, R.L., Detloff, P.J., 1997. Ectopically expressed CAG repeats cause intranuclear inclusions and a progressive late onset neurological phenotype in the mouse. Cell 91, 753-763.

Orlando, L.R., Alsdorf, S.A., Penney, J.B.Jr., Young, A.B., 2001. The role of group I and group II metabotropic glutamate receptors in modulation of striatal NMDA and quinolinic acid toxicity. Exp. Neurol. 167, 196-204.

Orrenius, S., 2004. Mitochondrial regulation of apoptotic cell death. Toxicol. Lett. 149, 19-23.

Ozawa, S., Kamiya, H., Tsuzuki, K., 1998. Glutamate receptors in the mammalian central nervous system. Prog. Neurobiol. 54, 581-618.

Pahl, H.L., Baeuerle, P.A., 1996. Control of gene expression by proteolysis. Curr. Opin. Cell Biol. 8, 340-347.

Panov, A.V., Gutekunst, C.A., Leavitt, B.R., Hayden, M.R., Burke, J.R., Strittmatter, W.J., Greenamyre, J.T., 2002. Early mitochondrial calcium defects in Huntington's disease are a direct effect of polyglutamines. Nat. Neurosci. 5, 731-736.

Paoletti, P., Neyton, J., 2006. NMDA receptor subunits: function and pharmacology. Curr. Opin. Pharmacol. 6, 1-9.

Pardo, R., Colin, E., Regulier, E., Aebischer, P., Deglon, N., Humbert, S., Saudou, F., 2006. Inhibition of calcineurin by FK506 protects against polyglutamine-huntingtin toxicity through an increase of huntingtin phosphorylation at S421. J. Neurosci. 26, 1635-1645.

Paulsen, J.S., Ready, R.E., Hamilton, J.M., Mega, M.S., Cummings, J.L., 2001. Neuropsychiatric aspects of Huntington's disease. J. Neurol. Neurosurg. Psychiatry 71, 310-314.

Pelech, S., Sutter, C., Zhang, H., 2003. Kinetworks™ protein kinase multiblot analysis. Methods Mol. Biol. 218, 99-111.

Peng, T., Greenamyre, J.T., 1998. Privileged access to mitochondria of calcium influx through N-methyl-D-aspartate receptors. Mol. Pharmacol. 53, 974–980.

Perez-Otano, I., Schulteis, C.T., Contractor, A., Lipton, S.A., Trimmer, J.S., Sucher, N.J., Heinemann, S.F., 2001. Assembly with the NR1 subunit is required for surface expression of NR3A-containing NMDA receptors. J. Neurosci, 21, 1228-1237.

Perutz, M.F., 1996. Glutamine repeats and inherited neurodegenerative diseases: molecular aspects. Curr. Opin. Struct. Biol. 6, 848-858.

Perutz, M.F., Johnston, T., Suzuki, M., Finch, J.T., 1994. Glutamine as polar zippers: their possible role in neurodegenerative diseases. Proc. Natl. Acad. Sci. U.S.A. 91, 5355-5358.

Peters, M.F., Nucifora, F.C.Jr., Kushi, J., Seaman, H.C., Cooper, J.K., Herring, W.J., Dawson, V.L., Dawson, T.M., Ross, C.A., 1999. Nuclear targeting of mutant huntingtin increases toxicity. Mol. Cell. Neurosci. 14, 121-128.

Philpot, B.D., Sekhar, A.K., Shouval, H.Z., Bear, M.F., 2001. Visual experience and deprivation bidirectionally modify the composition and function of NMDA receptors in visual cortex. Neuron 29, 157-169.

Picconi, B., Passino, E., Sgobio, C., Bonsi, P., Barone, I., Ghiglieri, V., Pisani, A., Bernardi, G., Ammassari-Teule, M., Calabresi, P., 2006. Plastic and behavioral abnormalities in experimental Huntington's disease: a crucial role for cholinergic interneurons. Neurobiol. Dis. 22, 143-152.

Podgorski, A., Alster, P., Elbaum, D., 1988. Interactions among red cell membrane proteins. Biochemistry 27, 609-614.

Podgorski, A., Elbaum, D., 1985. Properties of red cell membrane proteins: mechanism of spectrin and band 4.1 interaction. Biochemistry 24, 7871-7876.

Pospisilova, S., Brazda, V., Kucharikova, K., Luciani, M.G., Hupp, T.R., Skladal, P., Palecek, E., Vojtesek, B., 2004. Activation of the DNA-binding ability of latent p53 protein by protein kinase C is abolished by protein kinase CK2. Biochem. J. 378, 939-947.

Prybylowski, K., Chang, K., Sans, N., Kan, L., Vicini, S., Wenthold, R.J., 2005. The synaptic localization of NR2B-containing NMDA receptors is controlled by interactions with PDZ proteins and AP-2. Neuron 47, 845-857.

Prybylowski, K., Wenthold, R.J., 2004. N-methyl-D-aspartate receptors: subunit assembly and trafficking to the synapse. J. Biol. Chem. 279, 9673-9676.

Raman, I.M., Tong, G., Jahr, C.E., 1996. Beta-adrenergic regulation of synaptic NMDA receptors by cAMP-dependent protein kinase. Neuron 16, 415-421.

Rangone, H., Poizat, G., Troncoso, J., Ross, C.A., MacDonald, M.E., Saudou, F., Humbert, S., 2004. The serum- and glucocorticoid-induced kinase SGK inhibits mutant huntingtin-induced toxicity by phosphorylating serine 421 of huntingtin. Eur. J. Neurosci. 19, 273-279.

Raymond, L.A., Moshaver, A., Tingley, W.G., Huganir, R.L., 1996. Glutamate receptor ion channel properties predict vulnerability to cytotoxicity in a transfected nonneuronal cell line. Mol. Cell. Neurosci. 7, 102-115.

Reddy, P.H., Williams, M., Charles, V., Garrett, L., Pike-Buchanan, L., Whetsell, W.O.Jr., Miller, G., Tagle, D.A., 1998. Behavioural abnormalities and selective neuronal loss

in HD transgenic mice expressing mutated full-length HD cDNA. Nat. Genet. 20, 198-202.

Reddy, P.H., Charles, V., Williams, M., Miller, G., Whetsell Jr., W.O., Tagle, D.A., 1999. Transgenic mice expressing mutated full-length HD cDNA: a paradigm for locomotor changes and selective neuronal loss in Huntington's disease. Phil. Trans. R. Soc. Lond. B 354, 1035-1045.

Reiner, A., Albin, R.L., Anderson, K.D., D'Amato, C.J., Penney, J.B., Young, A.B., 1988. Differential loss of striatal projection neurons in Huntington disease. Proc. Natl. Acad. Sci. U.S.A. 85, 5733-5737.

Reynolds, I.J., Hastings, T.G., 1995. Glutamate induces the production of reactive oxygen species in cultured forebrain neurons following NMDA receptor activation. J. Neurosci. 15, 3318–3327.

Richfield, E.K., Maguire-Zeiss, K.A., Vonkeman, H.E., Voorn, P., 1995. Preferential loss of preproenkephalin versus preprotachykinin neurons from the striatum of Huntington's disease patients. Ann. Neurol. 38, 852-861.

Rigamonti, D., Bauer, J.H., De-Fraja, C., Conti, L., Sipione, S., Sciorati, C., Clementi, E., Hackam, A., Hayden, M.R., Li, Y., Cooper, J.K., Ross, C.A., Govoni, S., Vincenz, C., Cattaneo, E., 2000. Wild-type huntingtin protects from apoptosis upstream of caspase-3. J. Neurosci. 20, 3705-3713.

Rigby, M., Le Bourdelles, B., Heavens, R.P., Kelly, S., Smith, D., Butler, A., Hammans, R., Hills, R., Xuereb, J.H., Hill, R.G., Whiting, P.J., Sirinathsinghji, D.J., 1996. The messenger RNAs for the N-methyl-D-aspartate receptor subunits show region-specific expression of different subunit composition in the human brain. Neuroscience 73, 429-447.

Rintoul, G.L., Filiano, A.J., Brocard, J.B., Kress, G.J., Reynolds, I.J., 2003. Glutamate decreases mitochondrial size and movement in primary forebrain neurons. J. Neurosci. 23, 7881-7888.

Roche, K.W., Standley, S., McCallum, J., Dune Ly, C., Ehlers, M.D., Wenthold, R.J., 2001. Molecular determinants of NMDA receptor internalization. Nat. Neurosci. 4, 794-802.

Rosenmund, C., Westbrook, G.L., 1993. Calcium-induced actin depolymerization reduces NMDA channel activity. Neuron 10, 805-814.

Ross, C.A., 2002. Polyglutamine pathogenesis: emergence of unifying mechanisms for Huntington's disease and related disorders. Neuron 35, 819-822.

Rothman, S.M., Olney, J.W., 1995. Excitotoxicity and the NMDA receptor – still lethal after eight years. Trends Neurosci. 18, 57-58.

Rubinsztein, D.C., 2002. Lessons from animal models of Huntington's disease. Trends Genet. 18, 202-209.

Rumbaugh, G., Vicini, S., 1999. Distinct synaptic and extrasynaptic NMDA receptors in developing cerebellar granule neurons. J. Neurosci. 19, 10603-10610.

Saft, C., Zange, J., Andrich, J., Muller, K., Lindenberg, K., Landwehrmeyer, B., Vorgerd, M., Kraus, P.H., Przuntek, H., Schols, L., 2005. Mitochondrial impairment in patients and asymptomatic mutation carriers of Huntington's disease. Mov. Disord. 20, 674-679.

Salter, M.W., Kalia, L.V., 2004. Src kinases: a hub for NMDA receptor regulation. Nat. Rev. Neurosci. 5, 317-328.

Sanberg, P.R., Calderon, S.F., Giordano, M., Tew, J.M., Norman, A.B., 1989. The quinolinic acid model of Huntington's disease: locomotor abnormalities. Exp. Neurol. 105, 45-53.

Sanchez, I., Xu, C.J., Juo, P., Kakizaka, A., Blenis, J., Yuan, J., 1999. Caspase-8 is required for cell death induced by expanded polyglutamine repeats. Neuron 22, 623-633.

Sans, N., Petralia, R.S., Wang, Y.X., Blahos, J.2nd, Hell, J.W., Wenthold, R.J., 2000. A developmental change in NMDA receptor-associated proteins at hippocampal synapses. J. Neurosci. 20, 1260-1271.

Sans, N., Prybylowski, K., Petralia, R.S., Chang, K., Wang, Y.X., Racca, C., Vicini, S., Wenthold, R.J., 2003. NMDA receptor trafficking through an interaction between PDZ proteins and the exocyst complex. Nat. Cell Biol. 5, 520-530.

Sapp, E., Ge, P., Aizawa, H., Bird, E., Penney, J., Young, A.B., Vonsattel, J.P., DiFiglia, M., 1995. Evidence for a preferential loss of enkephalin immunoreactivity in the external globus pallidus in low grade Huntington's disease using high resolution image analysis. Neuroscience 64, 397-404.

Sapp, E., Penney, J., Young, A., Aronin, N., Vonsattel, J.P., DiFiglia, M., 1999. Axonal transport of N-terminal huntingtin suggests early pathology of corticostriatal projections in Huntington's disease. J. Neuropathol. Exp. Neurol. 58, 165-173.

Sattler, R., Xiong, Z., Lu, W.Y., Hafner, M., MacDonald, J.F., Tymianski, M., 1999. Specific coupling of NMDA receptor activation to nitric oxide neurotoxicity by PSD-95 protein. Science 284, 1845-1848.

Saudou, F., Finkbeiner, S., Devys, D., Greenberg, M.E., 1998. Huntingtin acts in the nucleus to induce apoptosis but death does not correlate with the formation of intranuclear inclusions. Cell 95, 55-66.

Sawa, A., Wiegand, G.W., Cooper, J., Margolis, R.L., Sharp, A.H., Lawler, J.F.Jr., Greenamyre, J.T., Snyder, S.H., Ross, C.A., 1999. Increased apoptosis of

Huntington disease lymphoblasts associated with repeat length-dependent mitochondrial depolarization. Nat. Med. 5, 1194-1198.

Sayed, M., Kim, S.O., Salh, B.S, Issinger, O.G., Pelech, S.L., 2000. Stress-induced activation of protein kinase CK2 by direct interaction with p38 mitogen-activated protein kinase. J. Biol. Chem. 275, 16569-16573.

Schaffar, G., Breuer, P., Boteva, R., Behrends, C., Tzvetkov, N., Strippel, N., Sakahira, H., Siegers, K., Hayer-Hartl, M., Hartl, F.U., 2004. Cellular toxicity of polyglutamine expansion proteins: mechanism of transcription factor deactivation. Mol. Cell 15, 95-105.

Schilling, G., Becher, M.W., Sharp, A.H., Jinnah, H.A., Duan, K., Kotzuk, J.A., Slunt, H.H., Ratovitski, T., Cooper, J.K., Jenkins, N.A., Copeland, N.G., Price, D.L., Ross, C.A., Borchelt, D.R., 1999. Intranuclear inclusions and neuritic aggregates in transgenic mice expressing a mutant N-terminal fragment of huntingtin. Hum. Mol. Genet. 8, 397-407.

Schuster, N., Prowald, A., Schneider, E., Scheidtmann, K.H., Montenarh, M., 1999. Regulation of p53 mediated transactivation by the beta-subunit of protein kinase CK2. FEBS Lett. 447, 160-166.

Schuster, N., Gotz, C., Faust, M., Schneider, E., Prowald, A., Jungbluth, A., Montenarh, M., 2001. Wild-type p53 inhibits protein kinase CK2 activity. J. Cell. Biochem. 81, 172-183.

Schwarcz, R., Bennett, J.P.Jr., Coyle, J.T.Jr., 1977. Loss of striatal serotonin synaptic receptor binding induced by kainic acid lesions: correlations with Huntington's disease. J. Neurochem. 4, 867-869.

Schwarcz, R., Foster, A.C., French, E.D., Whetsell, W.O. Jr., Kohler, C., 1984. Excitotoxic models for neurodegenerative disorders. Life Sci. 35, 19-32.

Scott, D.B., Blanpied, T.A., Swanson, G.T., Zhang, C., Ehlers, M.D., 2001. An NMDA receptor ER retention signal regulated by phosphorylation and alternative splicing. J. Neurosci. 21, 3063-3072.

Scott, D.B., Blanpied, T.A., Ehlers, M.D., 2003. Coordinated PKA and PKC phosphorylation suppresses RXR-mediated ER retention and regulates the surface delivery of NMDA receptors. Neuropharmacology 45, 755-767.

Seong, I.S., Ivanova, E., Lee, J.-M., Choo, Y.S., Fossale, E., Anderson, M., Gusella, J.F., Laramie, J.M., Myers, R.H., Lesort, M., MacDonald, M.E., 2005. HD CAG repeat implicates a dominant property of huntingtin in mitochondrial energy metabolism. Hum. Mol. Genet. 14, 2871-2880.

Sharp, A.H., Loev, S.J., Schilling, G., Li, S.-H., Li, X.-J., Bao, J., Wagster, M.V., Kotzuk, J.A., Steiner, J.P., Lo, A., Hedreen, J., Sisodia, S., Snyder, S.H., Dawson, T.M.,

Ryugo, D.K., Ross, C.A., 1995. Widespread expression of Huntington's disease gene (IT15) protein product. Neuron 14, 1065-1074.

Shehadeh, J., Fernandes, H.B., Zeron Mullins M.M., Graham, R.K., Leavitt, B.R., Hayden, M.R., Raymond, L.A., 2006. Striatal neuronal apoptosis is preferentially enhanced by NMDA receptor activation in YAC transgenic mouse model of Huntington disease. Neurobiol. Dis. 21, 392-403.

Shelbourne, P.F., Killeen, N., Hevner, R.F., Johnston, H.M., Tecott, L., Lewandoski, M., Ennis, M., Ramirez, L., Li, Z., Iannicola, C., Littman, D.R., Myers, R.M., 1999. A Huntington's disease CAG expansion at the murine Hdh locus is unstable and associated with behavioural abnormalities in mice. Hum. Mol. Genet. 8, 763-774.

Shin, J.Y., Fang, Z.H., Yu, Z.X., Wang, C.E., Li, S.H., Li, X.J., 2005. Expression of mutant huntingtin in glial cells contributes to neuronal excitotoxicity. J. Cell Biol. 171, 1001-1012.

Shirao, T., Sekino, Y., 2001. Clustering and anchoring mechanisms of molecular constituents of postsynaptic scaffolds in dendritic spines. Neurosci. Res. 40, 1-7.

Shorte, S.L., 1997. N-methyl-D-aspartate evokes rapid net depolymerization of filamentous actin in cultured rat cerebellar granule cells. J. Neurophysiol. 78, 1135-1143.

Sieradzan, K.A., Mann, D.M., 2001. The selective vulnerability of nerve cells in Huntington's disease. Neuropathol. Appl. Neurobiol. 27, 1-21.

Sieradzan, K.A., Mechan, A.O., Jones, L., Wanker, E.E., Nukina, N., Mann, D.M., 1999. Huntington's disease intranuclear inclusions contain truncated, ubiquitinated huntingtin protein. Exp. Neurol. 156, 92-99.

Sipione, S., Rigamonti, D., Valenza, M., Zuccato, C., Conti, L., Pritchard, J., Kooperberg, C., Olson, J.M., Cattaneo, E., 2002. Early transcriptional profiles in huntingtin-inducible striatal cells by microarray analyses. Hum. Mol. Genet. 11, 1953-1965.

Sisodia, S.S., 1998. Nuclear inclusions in glutamine repeat disorders: are they pernicious, coincidental, or beneficial? Cell 95, 1-4.

Sittler, A., Walter, S., Wedemeyer, N., Hasenbank, R., Scherzinger, E., Eickhoff, H., Bates, G.P., Lehrach, H., Wanker, E.E., 1998. SH3GL3 associates with the Huntingtin exon 1 protein and promotes the formation of polygln-containing protein aggregates. Mol. Cell 2, 427-436.

Slow, E.J., van Raamsdonk, J., Rogers, D., Coleman, S.H., Graham, R.K., Deng, Y., Oh, R., Bissada, N., Hossain, S.M., Yang, Y.Z., Li, X.J., Simpson, E.M., Gutekunst, C.A., Leavitt, B.R., Hayden, M.R., 2003. Selective striatal neuronal loss in a YAC128 mouse model of Huntington disease. Hum. Mol. Genet. 12, 1555-1567.

Slow, E.J., Graham, R.K., Osmand, A.P., Devon, R.S., Lu, G., Deng, Y., Pearson, J., Vaid, K., Bissada, N., Wetzel, R., Leavitt, B.R., Hayden, M.R., 2005. Absence of behavioral abnormalities and neurodegeneration in vivo despite widespread neuronal huntingtin inclusions. Proc. Natl. Acad. Sci. U.S.A. 102, 11402-11407.

Song, C., Zhang, Y, Parsons, C.G., Liu, Y.F., 2003. Expression of polyglutamine-expanded huntingtin induces tyrosine phosphorylation of N-methyl-D-aspartate receptors. J. Biol. Chem. 278, 33364-33369.

Soriano, F.X., Papadia, S., Hofmann, F., Hardingham, N.R., Bading, H., Hardingham, G.E., 2006. Preconditioning doses of NMDA promote neuroprotection by enhancing neuronal excitability. J. Neurosci. 26, 4509-4518.

Sornarajah, L., 2004. Understanding protein-protein interactions in the pathology of Huntington's disease. B.Sc. thesis.

Soto, D., Pancetti, F., Marengo, J.J., Sandoval, M., Sandoval, R., Orrego, F., Wyneken, U., 2004. Protein kinase CK2 in postsynaptic densities: phosphorylation of PSD-95/SAP90 and NMDA receptor regulation. Biochem. Biophys. Res. Commun. 322, 542-550.

Stahl, W.L., Swanson, P.D., 1974. Biochemical abnormalities in Huntington's chorea brains. Neurology 24, 813-819.

Standaert, D.G., Friberg, I.K., Landwehrmeyer, G.B., Young, A.B., Penney, J.B.Jr., 1999. Expression of NMDA glutamate receptor subunit mRNAs in neurochemically identified projection and interneurons in the striatum of the rat. Brain Res. Mol. Brain Res. 64, 11-23.

Standley, S., Roche, K.W., McCallum, J., Sans, N., Wenthold, R.J., 2000. PDZ domain suppression of an ER retention signal in NMDA receptor NR1 splice variants. Neuron 28, 887-898.

Starling, A.J., Andre, V.M., Cepeda, C., de Lima, M., Chandler, S.H., Levine, M.S., 2005. Alterations in N-methyl-D-aspartate receptor sensitivity and magnesium blockade occur early in development in the R6/2 mouse model of Huntington's disease. J. Neurosci. Res. 82, 377-386.

Steffan, J.S., Kazantsev, A., Spasic-Boskovic, O., Greenwald, M., Zhu, Y.Z., Gohler, H., Wanker, E.E., Bates, G.P., Housman, D.E., Thompson, L.M., 2000. The Huntington's disease protein interacts with p53 and CREB-binding protein and represses transcription. Proc. Natl. Acad. Sci. U.S.A. 97, 6763-6768.

Steffan, J.S., Agrawal, N., Pallos, J., Rockabrand, E., Trotman, L.C., Slepko, N., Illes, K., Lukacsovich, T., Zhu, Y.Z., Cattaneo, E., Pandolfi, P.P., Thompson, L.M., Marsh, J.L., 2004. SUMO modification of Huntingtin and Huntington's disease pathology. Science 304, 100-104.

Stocca, G., Vicini, S., 1998. Increased contribution of NR2A subunit to synaptic NMDA receptors in developing rat cortical neurons. J. Physiol. 507, 13-24.

Stout, A.K., Raphael, H.M., Kanterewicz, B.I., Klann, E., Reynolds, I.J., 1998. Glutamate-induced neuron death requires mitochondrial calcium uptake. Nat. Neurosci. 1, 366-373.

Strehlow, A.N., Li, J.Z., Myers, R.M., 2006. Wild-type huntingtin participates in protein trafficking between the Golgi and the extracellular space. Hum. Mol. Genet. [Dec 22; epub ahead of print.]

Sugars, K.L., Rubinsztein, D.C., 2003. Transcriptional abnormalities in Huntington disease. Trends Genet. 19, 233-238.

Sun, Y., Savanenin, A., Reddy, P.H., Liu, Y.F., 2001. Polyglutamine-expanded huntingtin promotes sensitization of N-methyl-D-aspartate receptors via post-synaptic density 95. J. Biol. Chem. 276, 24713-24718.

Suopanki, J., Gotz, C., Lutsch, G., Schiller, J., Harjes, P., Hermann, A., Wanker, E.E., 2006. Interaction of huntingtin fragments with brain membranes – clues to early dysfunction in Huntington's disease. J. Neurochem. 96, 870-884.

Szebenyi, G., Morfini, G.A., Babcock, A., Gould, M., Selkoe, K., Stenoien, D.L., Young, M., Faber, P.W., MacDonald, M.E., McPhaul, M.J., Brady, S.T., 2003. Neuropathogenic forms of huntingtin and androgen receptor inhibit fast axonal transport. Neuron 40, 41-52.

Tabrizi, S.J., Cleeter, M.W., Xuereb, J., Taanman, J.W., Cooper, J.M., Schapira, A.H., 1999. Biochemical abnormalities and excitotoxicity in Huntington's disease brain. Ann. Neurol. 45, 25-32.

Tagawa, K., Marubuchi, S., Qi, M.-L., Enokido, Y., Tamura, T., Inagaki, R., Murata, M., Kanazawa, I., Wanker, E.E., Okazawa, H., 2007. The induction levels of heat shock protein 70 differentiate the vulnerabilities to mutant huntingtin among neuronal subtypes. J. Neurosci. 27, 868-880.

Takeuchi, K., Kawashima, A., Nagafuchi, A., Tsukita, S., 1994. Structural diversity of band 4.1 superfamily members. J. Cell Sci. 107, 1921-1928.

Tang, T.-S., Tu, H., Chan, E.Y.W., Maximov, A., Wang, Z., Wellington, C.L., Hayden, M.R., Bezprozvanny, I., 2003. Huntingtin and huntingtin-associated protein 1 influence neuronal calcium signaling mediated by inositol-(1,4,5) triphosphate receptor type 1. Neuron 39, 227-239.

Tang, T.-S., Tu, H., Orban, P.C., Chan, E.Y.W., Hayden, M.R., Bezprozvanny, I., 2004. HAP1 facilitates effects of mutant huntingtin on inositol 1,4,5-trisphosphate-induced Ca^{2+} release in primary culture of striatal medium spiny neurons. Eur. J. Neurosci. 20, 1779-1787.

Tang, T.-S., Slow, E., Lupu, V., Stavrovskaya, I.G., Sugimori, M., Llinas, R., Kristal, B.S., Hayden, M.R., Bezprozvanny, I., 2005. Disturbed Ca^{2+} signaling and apoptosis of medium spiny neurons in Huntington's disease. Proc. Natl. Acad. Sci. U.S.A. 102, 2602-2607.

Thomas, C.G., Miller, A.J., Westbrook, G.L., 2006. Synaptic and extrasynaptic NMDA receptor NR2 subunits in cultured hippocampal neurons. J. Neurophysiol. 95, 1727-1734.

Tingley, W.G., Ehlers, M.D., Kameyama, K., Doherty, C., Ptak, J.B., Riley, C.T., Huganir, R.L., 1997. Characterization of protein kinase A and protein kinase C phosphorylatioin of the N-methyl-D-aspartate receptor NR1 subunit using phosphorylation site-specific antibodies. J. Biol. Chem. 272, 5157-5166.

Tobin, A.J., Signer, E.R., 2000. Huntington's disease: the challenge for cell biologists. Trends Cell Biol. 10, 531-536.

Tovar, K.R., Westbrook, G.L., 1999. The incorporation of NMDA receptors with a distinct subunit composition at nascent hippocampal synapses in vitro. J. Neurosci. 19, 4180-4188.

Trettel, F., Rigamonti, D., Hilditch-Maguire, P., Wheeler, V.C., Sharp, A.H., Persichetti, F., Cattaneo, E., MacDonald, M.E., 2000. Dominant phenotypes produced by the HD mutation in STHdh(Q111) striatal cells. Hum. Mol. Genet. 9, 2799-2809

Trottier, Y., Devys, D., Imbert, G., Saudou, F., An, I., Lutz, Y., Weber, C., Agid, Y., Hirsch, E.C., Mandel, J.-L., 1995. Cellular localization of the Huntington's disease protein and discrimination of the normal and mutated form. Nature Genet. 10, 104-110.

Truant, R., Atwal, R., Burtnik, A., 2006. Hypothesis: huntingtin may function in membrane association and vesicular trafficking. Biochem. Cell Biol. 84, 912-917.

Truant, R., Atwal, R.S., Burtnik, A., 2007. Nucleocytoplasmic trafficking and transcription effects of huntingtin in Huntington's disease. Prog. Neurobiol. doi:10.1016/j.pneurobio.2006.11.004 (Article in Press).

Trushina, E., Dyer, R.B., Badger, J.D.II, Ure, D., Eide, L., Tran, D.D., Vrieze, B.T., Legendre-Guillemin, V., McPherson, P.S., Mandavilli, B.S., Van Houten, B., Zeitlin, S., McNiven, M., Aebersold, R., Hayden, M., Parisi, J.E., Seeberg, E., Dragatsis, I., Doyle, K., Bender, A., Chacko, C., McMurray, C.T., 2004. Mutant huntingtin impairs axonal trafficking in mammalian neurons in vivo and in vitro. Mol. Cell. Biol. 24, 8195-8209.

Usdin, M.T., Shelbourne, P.F., Myers, R.M., Madison, D.V., 1999. Impaired synaptic plasticity in mice carrying the Huntington's disease mutation. Hum. Mol. Genet. 8, 839-846.

Van Dijk, J.G., Van der Velde, E.A., Roos, R.A., Bruyn, G.W., 1986. Juvenile Huntington disease. Hum. Genet. 73, 235-239.

Van Raamsdonk, J.M., Pearson, J., Rogers, D.A., Bissada, N., Vogl, A.W., Hayden, M.R., Leavitt, B.R., 2005. Loss of wild-type huntingtin influences motor dysfunction and survival in the YAC128 mouse model of Huntington disease. Hum. Mol. Genet. 14, 1379-1392.

Veyhl, M., Keller, T., Gorboulev, V., Vernaleken, A., Koepsell, H., 2006. RS1 (RSC1A1) regulates the exocytotic pathway of Na^+-D-glucose cotransporter SGLT1. Am. J. Physiol. Renal Physiol. 291, F1213-F1223.

Vicini, S., Wang, J.F., Li, J.H., Zhu, W.J., Wang, Y.H., Luo, J.H., Wolfe, B.B., Grayson, D.R., 1998. Functional and pharmacological differences between recombinant N-methyl-D-aspartate receptors. J. Neurophysiol. 79, 555-566.

Viel, A., 1999. Alpha-actinin and spectrin structures: an unfolding family story. FEBS Lett. 460, 391-394.

Vissel, B., Krupp, J.J., Heinemann, S.F., Westbrook, G.L., 2001. A use-dependent tyrosine dephosphorylation of NMDA receptors is independent of ion flux. Nat. Neurosci. 4, 587-596.

Von Horsten, S., Schmitt, I., Nguyen, H.P., Holzmann, C., Schmidt, T., Walther, T., Bader, M., Pabst, R., Kobbe, P., Krotova, J., Stiller, D., Kask, A., Vaarmann, A., Rathke-Hartlieb, S., Schulz, J.B., Grasshoff, U., Bauer, I., Vieira-Saecker, A.M., Paul, M., Jones, L., Lindenberg, K.S., Landwehrmeyer, B., Bauer, A., Li, X.J., Riess, O., 2003. Transgenic rat model of Huntington's disease. Hum. Mol. Genet. 12, 617-624.

Vonsattel, J.P., DiFiglia, M., 1998. Huntington disease. J. Neuropathol. Exp. Neurol. 57, 369-384.

Vonsattel, J.P., Myers, R.H., Stevens, T.J., Ferrante, R.J., Bird, E.D., Richardson, E.P.Jr., 1985. Neuropathological classification of Huntington's disease. J. Neuropathol. Exp. Neurol. 44, 559-577.

Waelter, S., Boeddrich, A., Lurz, R., Scherzinger, E., Lueder, G., Lehrach, H., Wanker, E.E., 2001. Accumulation of mutant huntingtin fragments in aggresome-like inclusion bodies as a result of insufficient protein degradation. Mol. Biol. Cell 12, 1393-1407.

Wang, L.H., Rothberg, K.G., Anderson, R.G., 1993. Mis-assembly of clathrin lattices on endosomes reveals a regulatory switch for coated pit formation. J. Cell Biol. 123, 1107-1117.

Wang, Y., Ju, W., Liu, L., Fam, S., D'Souza, S., Taghibiglou, C., Salter, M., Wang, Y.T., 2004. Alpha-amino-3-hydroxy-5-methylisoxazole-4-propionic acid subtype glutamate receptor (AMPAR) endocytosis is essential for N-methyl-D-aspartate-induced neuronal apoptosis. J. Biol. Chem. 279, 41267-41270.

Wang, Y.T., Linden, D.J., 2000. Expression of cerebellar long-term depression requires postsynaptic clathrin-mediated endocytosis. Neuron 25, 635-647.

Wang, Y.T., Salter, M.W., 1994. Regulation of NMDA receptors by tyrosine kinases and phosphatases. Nature 369, 233-235.

Wang, Y.T., Yu, X.M., Salter, M.W., 1996. Ca(2+)-independent reduction of N-methyl-D-aspartate channel activity by protein tyrosine phosphatase. Proc. Natl. Acad. Sci. U.S.A. 93, 1721-1725.

Wanker, E.E., Rovira, C., Scherzinger, E., Hasenbank, R., Walter, S., Tait, D., Colicelli, J., Lehrach, H., 1997. HIP-1: a huntingtin interacting protein isolated by the yeast two-hybrid system. Hum. Mol. Genet. 6, 487-495.

Warby, S.C., Chan, E.Y., Metzler, M., Gan, L., Singaraja, R.R., Crocker, S.F., Robertson, H.A., Hayden, M.R., 2005. Huntingtin phosphorylation on serine 421 is significantly reduced in the striatum and by polyglutamine expansion *in vivo*. Hum. Mol. Genet. 14, 1569-1577.

Warrick, J.M., Chan, H.Y., Gray-Board, G.L., Chai, Y., Paulson, H.L., Bonini, N.M., 1999. Suppression of polyglutamine-mediated neurodegeneration in Drosophila by the molecular chaperone HSP70. Nat. Genet. 23, 425-428.

Waxman, E.A., Lynch, D.R., 2005. N-methyl-D-aspartate receptor subtypes: multiple roles in excitotoxicity and neurological disease. Neuroscientist 11, 37-49.

Wellington, C.L., Ellerby, L.M., Hackam, A.S., Margolis, R.L., Trifiro, M.A., Singaraja, R., McCutcheon, K., Salvesen, G.S., Propp, S.S., Bromm, M., Rowland, K.J., Zhang, T., Rasper, D., Roy, S., Thornberry, N., Pinsky, L., Kakizuka, A., Ross, C.A., Nicholson, D.W., Bredesen, D.E., Hayden, M.R., 1998. Caspase cleavage of gene products associated with triplet expansion disorders generates truncated fragments containing the polyglutamine tract. J. Biol. Chem. 273, 9158-9167.

Wellington, C.L., Singaraja, R., Ellerby, L., Savill, J., Roy, S., Leavitt, B., Cattaneo, E., Hackam, A., Sharp, A., Thornberry, N., Nicholson, D.W., Bredesen, D.E., Hayden, M.R., 2000. Inhibiting caspase cleavage of huntingtin reduces toxicity and aggregate formation in neuronal and non-neuronal cells. J. Biol. Chem. 275, 19831-19838.

Wellington, C.L., Ellerby, L.M., Gutekunst, C.-A., Rogers, D., Warby, S., Graham, R.K., Loubser, O., van Raamsdonk, J., Singaraja, R., Yang, Y.-Z., Gafni, J., Bredesen, D., Hersch, S.M., Leavitt, B.R., Roy, S., Nicholson, D.W., Hayden, M.R., 2002. Caspase cleavage of mutant huntingtin precedes neurodegeneration in Huntington's disease. J. Neurosci. 22, 7862-7872.

Wenthold, R.J., Prybylowski, K., Standley, S., Sans, N., Petralia, R.S., 2003. Trafficking of NMDA receptors. Annu. Rev. Pharmacol. Toxicol. 43, 335-358.

Westphal, R.S., Tavalin, S.J., Lin, J.W., Alto, N.M., Fraser, I.D., Langeberg, L.K., Sheng, M., Scott, J.D., 1999. Regulation of NMDA receptors by an associated phosphatase-kinase signaling complex. Science 285, 93-96.

Wexler, N.S., Young, A.B., Tanzi, R.E., Travers, H., Starosta-Rubinstein, S., Penney, J.B., Snodgrass, S.R., Shoulson, I., Gomez, F., Ramos Arroyo, M.A., Penchaszadeh, G.K., Moreno, H., Gibbons, K., Faryniarz, A., Hobbs, W., Anderson, M.A., Bonilla, E., Conneally, P.M., Gusella, J.F., 1987. Homozygotes for Huntington's disease. 326, 194-197.

Wheeler, V.C., White, J.K., Gutekunst, C.A., Vrbanac, V., Weaver, M., Li, X.J., Li, S.H., Yi, H., Vonsattel, J.P., Gusella, J.F., Hersch, S., Auerbach, W., Joyner, A.L., MacDonald, M.E., 2000. Long glutamine tracts cause nuclear localization of a novel form of huntingtin in medium spiny striatal neurons in HdhQ92 and HdhQ111 knock-in mice. Hum. Mol. Genet. 9, 503-513.

White, R.J., Reynolds, I.J., 1996. Mitochondrial depolarization in glutamate-stimulated neurons: an early signal specific to excitotoxin exposure. J. Neurosci. 16, 5688-5697.

Wüllner, U., Young, A.B., Penney, J.B., Beal, M.F., 1994. 3-Nitropropionic acid toxicity in the striatum. J. Neurochem. 63, 1772-1781.

Wyszynski, M., Lin, J., Rao, A., Nigh, E., Beggs, A.H., Craig, A.M., Sheng, M., 1997. Competitive binding of alpha-actinin and calmodulin to the NMDA receptor. Nature 385, 439-442.

Wyszynski, M., Kharazia, V., Shanghvi, R., Rao, A., Beggs, A.H., Craig, A.M., Weinberg, R., Sheng, M., 1998. Differential regional expression and ultrastructural localization of alpha-actinin-2, a putative NMDA receptor-anchoring protein, in rat brain. J. Neurosci. 18, 1383-1392.

Wyttenbach, A., Carmichael, J., Swartz, J., Furlong, R.A., Narain, Y., Rankin, J., Rubinsztein, D.C., 2000. Effects of heat shock, heat shock protein 40 (HDJ-2), and proteasome inhibition on protein aggregation in cellular models of Huntington's disease. Proc. Natl. Acad. Sci. U.S.A., 97, 2898-2903.

Wyttenbach, A., Sauvageot, O., Carmichael, J., Diaz-Latoud, C., Arrigo, A.P., Rubinsztein, D.C., 2002. Heat shock protein 27 prevents cellular polyglutamine toxicity and suppresses the increase of reactive oxygen species caused by huntingtin. Hum. Mol. Genet. 11, 1137-1151.

Xia, H., Hornby, Z.D., Malenka, R.C., 2001. An ER retention signal explains differences in surface expression of NMDA and AMPA receptor subunits. Neuropharmacology 41, 714-723.

Xia, J., Lee, D.H., Taylor, J., Vandelft, M., Truant, R., 2003. Huntingtin contains a highly conserved nuclear export signal. Hum. Mol. Genet. 12, 1393-1403.

Xiong, Z.G., Raouf, R., Lu, W.Y., Wang, L.Y., Orser, B.A., Dudek, E.M., Browning, M.D., MacDonald, J.F., 1998. Regulation of N-methyl-D-aspartate receptor function by constitutively active protein kinase C. Mol. Pharmacol. 54, 1055-1063.

Yamamoto, A., Lucas, J.J., Hen, R., 2000. Reversal of neuropathology and motor dysfunction in a conditional model of Huntington's disease. Cell 101, 57-66.

Yanai, A., Huang, K., Kang, R., Singaraja, R.R., Arstikaitis, P., Gan, L., Orban, P.C., Mullard, A., Cowan, C.M., Raymond, L.A., Drisdel, R.C., Green, W.N., Ravikumar, B., Rubinsztein, D.C., El-Husseini, A., Hayden, M.R., 2006. Palmitoylation of huntingtin by HIP14 is essential for its trafficking and function. Nat. Neurosci. 9, 824-831.

Young, A.B., Greenamyre, J.T., Hollingsworth, Z., Albin, R., D'Amato, C., Shoulson, I., Penney, J.B., 1988. NMDA receptor losses in putamen from patients with Huntington's disease. Science 241, 981–983.

Yuen, E.Y., Jiang, Q., Feng, J., Yan, Z., 2005. Microtuble regulation of N-methyl-D-aspartate receptor channels in neurons. J. Biol. Chem. 280, 29420-29427.

Zeitlin, S., Liu, J.P., Chapman, D.L., Papaioannou, V.E., Efstratiadis, A., 1995. Increased apoptosis and early embryonic lethality in mice nullizygous for the Huntington's disease gene homologue. Nat. Genet. 11, 155-163.

Zeron, M.M., Chen, N., Moshaver, A., Lee, A.T.-C., Wellington, C.L., Hayden, M.R., Raymond, L.A., 2001. Mutant huntingtin enhances excitotoxic cell death. Mol. Cell. Neurosci. 17, 41-53.

Zeron, M.M., Hansson, O., Chen, N., Wellington, C.L., Leavitt, B.R., Brundin, P., Hayden, M.R., Raymond, L.A., 2002. Increased sensitivity to N-methyl-D-aspartate receptor-mediated excitotoxicity in a mouse model of Huntington's disease. Neuron 33, 849-860.

Zeron, M.M., Fernandes, H.B., Krebs, C., Shehadeh, J., Wellington, C.L., Leavitt, B.R., Baimbridge, K.G., Hayden, M.R., Raymond, L.A., 2004. Potentiation of NMDA receptor-mediated excitotoxicity linked with intrinsic apoptotic pathway in YAC transgenic mouse model of Huntington's disease. Mol. Cell. Neurosci. 25, 469-479.

Zheng, X., Zhang, L., Wang, A.P., Bennett, M.V., Zukin, R.S., 1999. Protein kinase C potentiation of N-methyl-D-aspartate receptor activity is not mediated by phosphorylation of N-methyl-D-aspartate receptor subunits. Proc. Natl. Acad. Sci. U.S.A. 96, 15262-15267.

Zhou, H., Li, S.H., Li, X.J., 2001. Chaperone suppression of cellular toxicity of huntingtin is independent of polyglutamine aggregation. J. Biol. Chem. 276, 48417-48424.

Zhu, J.X., Goldoni, S., Bix, G., Owens, R.T., McQuillan, D.J., Reed, C.C., Iozzo, R.V., 2005. Decorin evokes protracted internalization and degradation of the epidermal growth factor receptor via caveolar endocytosis. J. Biol. Chem. 280, 32468-32479.

Zoghbi, H.Y., Orr, H.T., 2000. Glutamine repeats and neurodegeneration. Annu. Rev. Neurosci. 23, 217-247.

Zuccato, C., Ciammola, A., Rigamonti, D., Leavitt, B.R., Goffredo, D., Conti, L., MacDonald, M.E., Friedlander, R.M., Silani, V., Hayden, M.R., Timmusk, T., Sipione, S., Cattaneo, E., 2001. Loss of huntingtin-mediated BDNF gene transcription in Huntington's disease. Science 293, 493-498.